Slaking characteristics of geomaterials in direct shear test

一面せん断試験による地盤材料のスレーキング特性の解明

Keshab Sharma

ケシャブ　シャーマ

September 2012

Slaking characteristics of geomaterials in direct shear test

一面せん断試験による地盤材料のスレーキング特性の解明

By

Keshab Sharma

ケシャブ　シャーマ

Supervisor: Associate Professor Takashi Kiyota

Co-supervisor: Professor Junichi Koseki

A Thesis submitted to Graduate School of Engineering, Department of Civil Engineering, The University of Tokyo for the partial fulfillment of the requirements for the degree of

Masters of Engineering

Department of Civil Engineering

Graduate School of EngineeringThe University of Tokyo

Japan

September 2012

ABSTRACT

Numerous slope stability and other geotechnical problems worldwide have been reported due to the presence of mudstones. Similarly, in the world, infrastructure developments have been extended to hillsides and mountainous areas because of population growth, economics needs and other constraints. Soft sedimentary rock named mudstone is the most often encountered geomaterials during the major construction works that are undertaken in those areas.

In the past decade, there has been a significant increase in knowledge with respect to the mechanics of geomaterials. Several fundamental issues have been solved, and important achievements have been made in certain areas. However, most of these achievements are either deal with rock or with soil because most of geotechnical engineers are generally used to viewing geomaterials either as soils whose behavior is highly susceptible to the fabric and water content of the intact material, or as a rock, with engineering behavior primarily controlled by fissures and joints. However, mudstones have two inherent properties: firstly, they are intermediate in behaviour between rock and soil, and secondly, they tend to transgress from rocklike to soil-like materials within relatively short time-frames. So, present experimental and theoretical methods used in geotechnical engineering practice are not inadequate for assessing the stability of mudstones. In general, the laboratory investigations on durability characteristics of mudstones are only made through the general slaking test. However, studies examining the effects of slaking on strength and deformation behaviour of mudstones are sparse.

This research began by investigating the landslides to explore the probability of slaking induced landslides in soft sedimentary rock formations. Significant numbers of landslide events were found to be occurred after moderate rainfall, sometimes followed by drought. Similarly, intensive review of the studies that have been previously undertaken to study the slaking of mudstones was done to ascertain the current state of knowledge regarding this process.

At the beginning of the experiment, the conventional slaking tests were performed to classify the tested material on the basis of slaking durability. In order to examine slaking effects on strength and deformation characteristics of crushed mudstone (Hattian Bala and Ishikawa), a series of direct shear tests were conducted on the crushed mudstone by

simulating cyclic wetting and drying under different stress conditions by using a modified direct shear apparatus. In addition, a series of the monotonic loading tests on dry and saturated specimens were also performed to compare strength and deformation characteristics with those of the cyclic wetting and drying creep test. Similar tests were also conducted on conventional granular material such as Chiba gravel and Toyoura sand and Glass beads for the comparison of stress-strain behaviour after saturation and cyclic wetting and drying with crushed mudstones. Sieve analysis was performed after each experiment and degradation index was used to quantify the particle crushing due to slaking.

The strength and deformation characteristics of crushed mudstones under dry, saturated and cyclic wetting and drying conditions were compared with standard granular soils such as Silica sand (Toyoura), crushed sand stone (Chiba gravel) and Glass beads as well. The saturated and the one with cyclic wetting and drying mudstone specimens exhibit largely different stress-displacement features from those for dry specimens while the difference in stress-strain-volume change behaviours between dry and saturated conditions is insignificant for both Toyoura sand and Chiba gravel

The effects of stress ratio, density of specimen, initial water content before wetting, slaking index and number of cyclic wetting and drying on slaking were investigated. It was concluded that the slaking induced shear displacement is the function of various factors such as stress ratio, density of specimen, initial water content before wetting, slaking index and number of cyclic wetting and drying. Drying induced slaking also observed when water content of the mudstone specimens became smaller than certain threshold value of water content.

Key Words: Direct shear; Slaking; Cyclic wetting and drying; Stress ratio; Particles crushing, Shear strength and deformation

.

ACKNOWLEDGEMENTS

First, I would like to express my deepest gratitude to Associate Professor Takashi Kiyota for his guidance, encouragement and assistance throughout the period of this research for Master's Thesis. I thank him for his seemingly infinite patience, and for always being there when I needed him the most. He always provided me unflinching encouragement and support in various ways. He not only guides for my research but also cares and helps me as my parents in my daily life in Japan.

I would like to thank my co-supervisor Professor Junichi Koseki for his valuable suggestion and inspiration. He gave me confidence to wrap the master thesis.

I am equally thankful to Professor Kazuo Konagai for his constant support and caring professor, always asking us if we had any problems.

I am extremely obliged Dr. Hiroyuki Kyokawa for his kind help and direction, which has helped me in conducting my research. He always helps me to learn more and more about soil mechanics. I am deeply indebted to my colleagues Daisuke Okuno and Wataru Munekata who kindly made me familiar to the direct shear apparatus.

I would like to thank Takesi Sato for his kind help to maintain of apparatus. I am obliged to Hiroko Takashaki and Toshihiko Katagiri for their devoted help and managing everything that I needed for my research.

I gratefully acknowledge Jina Lee for her crucial contribution from the beginning of my thesis and friendly behaviour. I would like to express my sincere thanks to all members of Kiyota and Konagai Laboratory for their direct and indirect co-operation, advices and help during the period of my Master's study and thesis work.

I am extremely obliged to Toru Asakura who took care of all the administrative matters during my stay. You are very kind and cooperatives. You always take care of foreign students and translate Japanese into English for convenience of us. I always miss you wherever I am.

Further appreciation is also extended to the Kishi laboratory, IIS, for providing the equipments to perform X-ray diffraction power test.

Many thanks to all the Nepalese colleagues of University of Tokyo for their cooperation and kind supports. I am very grateful for my two year at University of Tokyo, made possible by the scholarship funded by the Asian Development Bank. I would like to

acknowledge members of Foreign Student Office (FSO) for their help and cooperation before came to Japan as well during our life in Japan.

Finally, much appreciation goes to Mom and Dad, and the rest of my family as well relatives; their support and belief in me have always inspired me in my endeavors.

.

TABLE OF CONTENTS

CHAPTER 1

INTRODUCTION

1.1 General

Geomaterials are defined as any material from geological origin. Geomaterials are of enormous economic importance to the global construction industry. Similarly, in the world, infrastructure developments have been extended to hillsides and mountainous areas because of population growth, economics needs and other constraints. Soft sedimentary rock is the most often encountered geomaterials during the major construction works that are undertaken in those areas, involving deep excavations, cuts and fills etc. With this massive infrastructure development on such young and fragile geology, a large number people are being exposed to typical geotechnical failures which can be triggered by either earthquake or rainfall or both. Where large scale works are to be constructed on the soft sedimentary rock, it is necessary to understand the physical and mechanical properties of the mudstones underlying the foundations and to decide whether the ground is suitable for construction for long term. Similarly, we need to carry out the stability of the surrounding mudstones slope if any.

In the past decade, there has been a significant increase in knowledge with respect to the mechanics of geomaterials. Several fundamental issues have been solved, and important achievements have been made in certain areas. However, most of these achievements are either deal with rock or with soil because most of geotechnical engineers are generally used to viewing geomaterials either as soils whose behavior is highly susceptible to the fabric and water content of the intact material, or as a rock, with engineering behavior primarily controlled by fissures and joints. However, soft sedimentary rocks such as mudstone, shale etc. have two inherent properties: firstly, they are intermediate in behaviour between rock and soil, and secondly, they tend to transgress from rocklike to soil-like materials within relatively short time-frames. The behaviour of soft sedimentary rocks is totally dependent on their environment that it experiences. Among different types of soft sedimentary rocks,

mudstone is the most sensitive against to surrounding environment. So, the detailed knowledge on the change in behaviour of mudstones due to the surrounding environment is becoming essential in geotechnical engineering practice for sustainable development and better serviceability.

Because of the periodic fluctuation of ground water or reservoir level due to distinct seasonal changes, geomaterials often suffered from alternate cyclic wetting and drying. In case of mudstones, the successive cycles of wetting and drying generate a significant physical degradation that takes place in very short periods of time. This phenomenon known as slaking becomes seriously unfavorable for long term stability of natural and artificial slopes, settlement of embankments, bearing capacity of foundation and strength of pavement etc. The strength and deformation behaviour of such geomaterials becomes very complex as different factors such as the water content before wetting, the number successive cyclic wetting and drying, density of geomaterials and finally particles crushing largely affects the overall behaviour. So, many geotechnical problems specifically on mudstones have demonstrated that conventional methods typically used in geotechnical engineering practice are not adequate for stability analysis of such unique geomaterials.

1.2 Typical geotechnical problems

1.2.1 Landslide

In 1999, the Tsaoling landslide was triggered by the Chi Chi earthquake in Taiwan. However, the dip for the slip surface is too gentle (about 14^0) to generate a landslide, even if there were an earthquake tremor, because the angle of internal friction at the peak shear strength of landslide material (shale and sandstone) in normal condition is well enough to resist slide (Chigira et. al; 2003, Towhata et al., 2002;). Shale is weathered by slaking (Fig. 1.1), which is assumed to be one of the major causes of intermittent retrogressive development of the landslides.

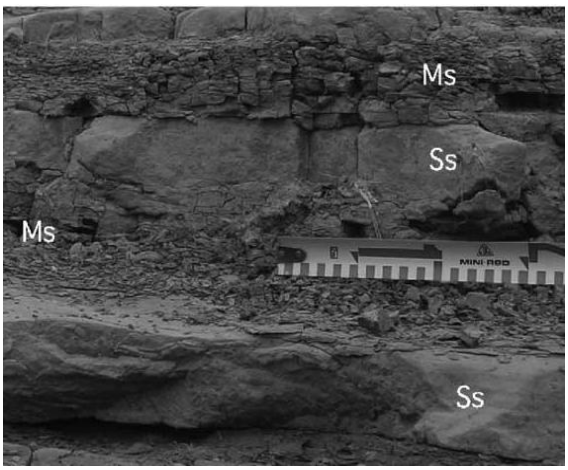

Fig.1.1. Slaking of the shale intercalated with sandstone which is fragmented but sandstone is not. (Chigira et. al., 2003)

Southwest China's Guizhou Province experienced its worst drought in this century in 2009/2010 as shown in Fig. 1.2. The drought had cut drinking water supplies to five million people, and more than two million animals. Similarly, sixty percent of agricultural land has been hit. A landslide occurred on 29th March, 2010 just after moderate rainfall (about 15 mm/day according to TRRM data) followed by the worst drought in a century (Fig. 1.3). Similarly, many more rainfall induced landslides occurred in 2010 in Guizhou Province, China. However, the intensity and amount of rainfall was not higher than average annual rainfall.

Photo: http://feww.wordpress.com/2010/03/18/worst-ever-drought-in-sw-china/

Fig.1.2. Dry Agriculture farm due to worst drought

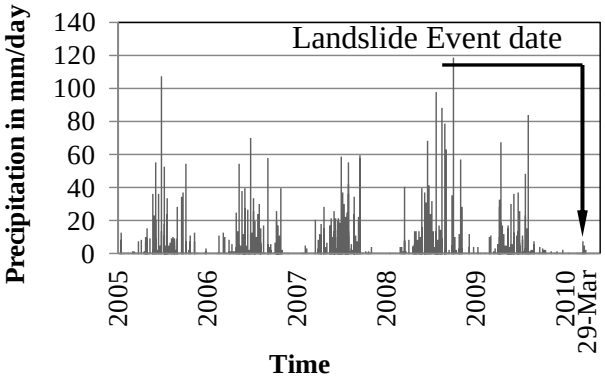

Fig. 1.3 Precipitation in Guizhou from TRMM

A large number of dry landslides occur every year. However most of these dry landslides are out of scope of researchers or the media. These dry landslides are of shallow depth and small in size. Because of their smaller size, generally no causalities and huge economic loss are encountered. That is why these landslides are out of scope of many researchers and media. An unexpected dry landslide occurred along the approach road to the Tamakoshi hydropower project, Dolakha, Nepal on 12th December, 2011 as shown in figure 1.4. According to Nepalese media, no rainfall occurred and no construction activities were done at that time in that landslide area. December is one of the driest months in context of Nepal (Fig. 1.5). The cause of this dry landslide is still under investigation.

1.2.2 Earth embankment and other structures

The Ataturk Dam, Turkey is the fourth largest clay cored rock-fill dam in the world. It was constructed in 1990. When the reservoir level started to rise, settlement problems started to occur along the crest reaching considerable level (Cetin et al., 2000). Both vertical and horizontal displacements are still taking place under more or less constant loading

conditions (Malla et. al., 2007). The vesicular basal rock used in the cross-section of the dam was found to be weathered as shown in Fig. 1.6. However, the displacement rates are gradually slowing down with time.

An earthquake of magnitude 6.5 occurred on 11th August 2009 in the Suruga Bay, Japan. A large number of collapses occurred along Tomei expressway (Fig. 1.7). Bulging of wall was also noticed before the earthquake possible due to the expansion of backfill materials. Variation of ground water level or percolation of water may have accelerated the slaking of backfill materials. Slaking reduced the strength of backfill materials and ultimately was found to be one of the major causes of the damage of Tomei Expressway (Takagi et al., 2010).

Fig.1.7. Collapsed highway embankment along Tomei expressway, Japan (Takagi et al., 2010)

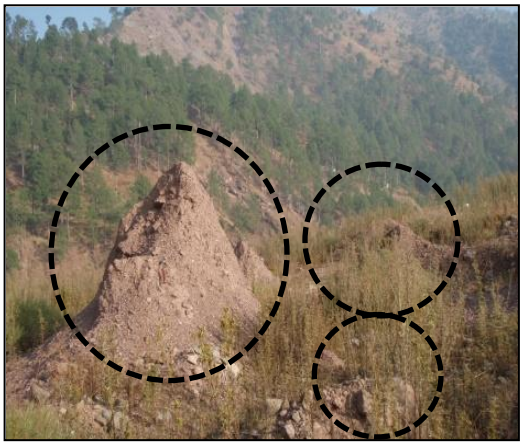

Fig. 1.8 Slaked Mudstone of Muree formation around the middle portion of landslides dam (Kiyota et al., 2011)

A huge landslide dam was formed by the 2005 Kashmir earthquake (7.6 Mw) in Pakistan. The dam was formed of mainly crushed mudstones and sandstones which can easily slake (Fig. 1.8). The dam was breached in 2010 just after moderate rainfall followed by drought (Sattar et. al., 2010; Kiyota et. al., 2011). These are only few representations of typical geotechnical failure. As already mentioned, it is quite understandable that the geotechnical analysis and design

Fig.1.6. Weathered vesicular basalt blocks used in the rock-fill section of dam (Cetin et al., 2000)

practice for ordinary geomaterials rely on experience obtained from past failures. Conventional simplified theories may not work well for such most abundant lithologies like mudstone.

1.3 Problem statement and its significance

Figure 1.9 shows the increment shear displacement of various geomaterials due to wetting under constant stress condition. From the Fig. 1.9, it is clearly seen that the impact of wetting upon shear displacement is more prominent in case of mudstones as compare to other geomaterials such as Sand stone (Chiba gravel) and Silica sand (Toyoura sand) etc. The shear displacement of Hattian Bala mudstone (HM) having a slaking index (JGS 2125-2006) of 1 and Ishikawa mudstone (IM) having a slaking index (JGS 2125-2006) of 3 is about 5 times and 70 times greater than Chiba gravel (CG) respectively, due to wetting under the same testing conditions. The details of Hattian Bala and Ishikawa mudstone will be explained in Chapter 4. Many other authors (Dick et. al., 1994) mentioned that mudstones deteriorate rapidly when subjected to changes in moisture content, which is responsible for triggering numerous slope stability problems, excessive settlements and other problems. Most of typical geotechnical problems described in previous section are related to the slaking of geomaterials. The low durability of certain mudstones, coupled with their physical breakdown due to slaking, is responsible for countless slope instability problems (Flemming et al., 1970, Regues et al. 1995), coal mine roof falls, shale embankment failures (Bragg and Zeigler 1975; Shamburger et al. 1975; Lutton 1977; Bragg and Zeigler 1978; Strohm 1978; Dick and Shakoor, 1992 and Bhattarai et al., 2007) and loss of bearing capacity of foundation (Mochizuki et al., 1985; Noda and Nishi, 1988).

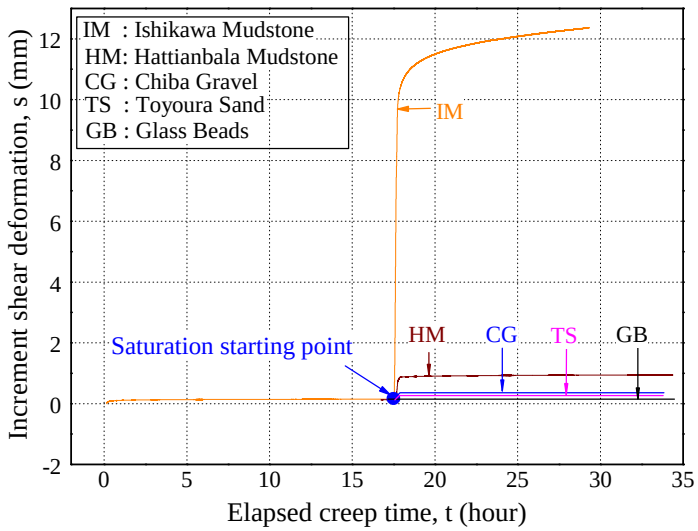

Fig. 1.9 Effect of slaking on creep deformation on different geomaterials with R= 0.3

The cyclic wetting and drying process is very common in many parts of the world due to distinct seasonal changes. Similarly, the global warming promotes a strong disturbance on the world-wide weather. Subjected to this impact, both the rainfall pattern and the environmental temperature in the mudstone areas are changing obviously. The number of high temperature days is increasing; the rainy season is gradually shortened. Thus, the mudstone area all over the world is now under a very serious situation which it has never been subjected to. After a drought has ended, and an intense rain has occurred, the new threat of slaking induced landslides becomes present, as the drought before the rainfall accelerates the slaking of mudstones. It is necessary for the long-term evaluation of the slopes to know how the stabilities of the mudstone slopes are changed in accordance with the slaking process.

Among the wide variety of geomaterials, mudstone is the most common group of the rock material found in the earth's crust, accounting for the majority of sedimentary rock types (Tucker, 1981 and Jakobsen and Johansen, 2000). It represents approximately two-thirds of the stratigraphic column and one-third of the total land area.

It is necessary to evaluate the durability of such rocks against wetting and drying, their effects on physical and mechanical properties, and ultimately the stability of the natural and cut slopes. Slaking of geomaterials was studied by many researchers (Terzaghi and Peck, 1948; Ladd, 1960; Nakano, 1967; Eigenbrod, 1972; Franklin and Chandra, 1972; Moriwaki 1974; Matsukura and Yatsu, 1982; Botts, 1986 and Yoshida et al., 1991). Nakano (1967) conducted a research on the breaking of tertiary mudstone with slaking and observed the changes in soil properties. Most of these researches are related with the change in physical properties such as density, particle size distribution etc of mudstone due to slaking, do not deal with mechanical properties. Only a few researchers tried to evaluate the impact of slaking on the mechanical properties of geomaterials. However testing conditions were different than reality. Because of the inherent properties of mudstone as described in 1.2, the understanding of the mechanism of soft sedimentary rocks like mudstones under cyclic environmental changes is still lacking.

Therefore, in order to predict the long term response of various natural slopes and other geotechnical structures, a better understanding of the strength and deformation characteristics of geomaterials undergoing cyclic wetting and drying induced deterioration (slaking) is essential. So, the author tried to achieve a better understanding of slakable geomaterials through this research.

1.4 Objectives and aims

A large number of methodologies have been developed for assessing slaking of geomaterials. The details of existing methodologies for testing the susceptibility to slaking are explained in chapter 3. The existing methodologies only describe physical appearance or mass loss due to slaking under no stress condition. Similarly, a rapid drying process under very high temperature is adopted. However, slaking typically occurs under stress conditions in the field. Similarly, the drying process is very slow and steady in the field. It can be seen that there is a large gap between the process involved in existing methodologies and the field conditions. So, existing methods do not provide adequate information regarding the effects of this slaking on the strength and stress-strain behavior of geomaterials in the field. The author has found virtually no literature involving systematic research on the effects of slaking under conditions of confinement.

Design and analysis of engineering structures, such as dams, highway embankments, foundations, slopes, and underground excavations etc. require shear strength parameters (cohesion, c and internal friction angle, Φ) of mudstones. Therefore, shear strength parameter for slakable geomaterials after certain cycles of wetting and drying are either scare or assumed. The relationship between the slaking index ratios with the strength parameters of slakable geomaterials is still under study. Similarly, to understand the geological hazards which may occur in the mudstone area after long drought, it is essential to fully understand the basic slaking characteristics of mudstone under constant stress conditions.

The main objectives of this research can be outlined as follow.

- To analysis the slaking characteristics of crushed mudstones in term of mechanical properties by simulating cyclic wetting and drying under constant stress conditions with a simple apparatus.
- To compare the strength and deformation characteristics of dry and saturated specimens with those of the cyclic wetting and drying test.
- To compare the slaking characteristics of different geomaterials having different slaking indexes.
- To explore probable slaking induced landslide by analyzing landslide event, geology and precipitation.

The slaking of geomaterials can be an important tool in simulating the long term behaviours of geomaterials experiencing cyclic wetting and drying phenomena. If the findings of this research are incorporated in conventional soil mechanics models, it can be very useful in the analysis of long term stability of natural slope, embankments and foundations on soft sedimentary rock formation.

1.5 Organization of Dissertation

Primarily due to the transitional nature of some geomaterials, a somewhat multidisciplinary knowledge base is necessary before one can fully understand the slaking characteristics of geomaterials. The author therefore conducted an extensive literary review concentrating on slaking induced geotechnical problems, factors affecting the slaking of geomaterials and laboratory observations of the slaking characteristics of geomaterials. One of the intentions of the author in writing this dissertation has been to present an insightful review of many of the problems associated with slaking of geomaterials and occurrence of possible slaking induced landslides. Considering the scope of work and objectives of this research, the dissertation is presented in six chapters to explain details of previous relative research, work don and the main outcomes of this research. A comprehensive layout of the dissertation is as follow.

Chapter 1 is an introduction to this dissertation which briefly explains the synopsis of this research. The typical geotechnical problems, objectives and aims as well as the scope of work and limitations are described to reveal the research curriculum.

In Chapter 2, the author collects and reviews rainfall induced slides events and classifies them on the basis of geology and precipitation intensity. Similarly, some basic concepts and mechanisms of rainfall induced landslides are also discussed here.

Chapter 3 gives a brief literature review on different aspects of slaking such as causes, mechanism and consequences. The understanding on the slaking mechanism and impacts of cyclic wetting and drying on physical properties of mudstones is presented in this chapter. Literature review on swelling and shrinkage of mudstone due to cyclic wetting and drying are also summarized. Finally, existing studies on the strength and deformation characteristics of slakable materials are also discussed.

The author has performed laboratory experiments involving direct shear tests on different geomaterials and glass beads that have undergone various cycles of wetting and drying under confinement. The experimental setups of these experiments are presented in

Chapter 4. The description of the physical properties of samples, their origins, general slaking tests and XRD tests are also included in this Chapter 4.

The time histories of creep deformation during cyclic wetting and drying of all tests are presented in details in Chapter 5. Results of the monotonic shear loading tests on dry and saturated specimens are also presented to compare the strength and deformation characteristics with those of the cyclic wetting and drying creep tests. The particles size distribution curve before and after each experiments are also incorporated in this chapter.

From the detailed test results presented in Chapter 5, the effects of slaking on shear strength and deformation are evaluated in Chapter 6. Similarly, a summary of slaking effect on different geomaterials under different stress ratios is also presented in this chapter.

Finally, the conclusions in Chapter 7 present a concise summary of the major points of the entire dissertation.

CHAPTER 2

CASE STUDY ON RAINFALL INDUCED LANDSLIDES

2.1 General

Landslides constitute a major threat to both lives and property worldwide especially in regions of residual soil subjected to heavy rainfall. In areas of steep terrain that experience prolonged intense rainfall events, the mass instability of soil slopes continue to affect large populations and cause economic loss. Especially, in mountainous areas, landslides are the second most destructive natural hazard after earthquakes (Runqiu, 2009; U.S. geological survey, 2000). The casualties and economic loss due to landslides increased greatly in the last century, and most of the landslides resulted from global climate change and human activities (Au, 1998). They are more frequent in young tectonic mountains such as the Himalayas of Nepal (Yamagishi et al., 2000; Lin et al., 2002; Bhasin et al., 2002), Rocky and Andes mountain chain in American continent (Parise and Wasowski, 1999; Collison et al., 2000; Mauritsch et al., 2000) hills of Japan and Taiwan.

Although slope failure may develop due to various factors such as earthquake shaking, loading of slope or removal of toe etc. Almost all traditional slope stability analyses incorporate the rainfall influence by changing the ground flow patterns with increasing pressure heads and often a rising ground table. For elongated slopes it is often assumed that the groundwater table is parallel to the slope surface and simple rises to reduce the stability of the slope.

Researchers working in various terrains have already observed and analyzed different mechanisms for rainfall induced landslides. Only a few researchers and non-scientific media have raised the issues of slope failure just after light/intense rainfall followed by drought mainly in mudstone formations. In these studies, the researchers (Spears and Taylor, 1971; Matsukura and Mizuna, 1986; Editorial, 2001 and 2007; Sadisun et al., 2003 and Qureshi et. al., 2009) conclude that slaking induced landslide initiation is a

complex problem involving the analysis of particle crushing due to slaking, suction force and unsaturated soil shear strength etc. However to date, an analytical formulation that incorporate the complete slaking phenomena and suction force within a traditional slope stability framework has not been developed. In the past, many studies (Spears and Taylor, 1971; Matsukura and Mizuna, 1986; Editorial, 2001 and 2007 and Qureshi et. al.2009) were conducted to investigate the weathering potential of rocks in relation to the slope stability problems, but still the understanding is not reproducible. Weathering studies, in practical assessment of slope failures, help to understand what stage the landscape has reached in the weathering process. In the field of geotechnical engineering, recognition of the weathered conditions of the slope is a critical issue in evaluating the slope failure hazards.

As already described in the Introduction Chapter, the global warming promotes a strong disturbance on the world-wide weather. Subjecting to its impact, both of the rainfall pattern and the environmental temperature in the mudstone area are obviously changing. The number of high temperature days is increasing; the rainy season is gradually shortened. Thus, the mudstone areas all over the world currently are in a very serious situation which it has never been subjected to. After a drought has ended, and an intense rain has occurred, the new threat of slaking induced landslides becomes present because the drought before rainfall accelerates the slaking of mudstones. It is necessary for the long-term evaluation of the slopes to know how the stabilities of the mudstone slopes are changed in accordance with slaking the process.

2.2 Infinite slope analysis

A slope that extends for a relatively long distance and has a consistent subsurface profile may be analysed as an infinite slope. The failure plane for this case is parallel to the surface of the slope and the limit equilibrium method can be applied readily.

a) Infinite slopes in dry cohesionless soil

A typical section or “slice” through the potential failure zone of a slope in a dry cohesionless soil is considered as shown in Fig. 2.1. All the forces acting on the slice are presented by free body diagram.

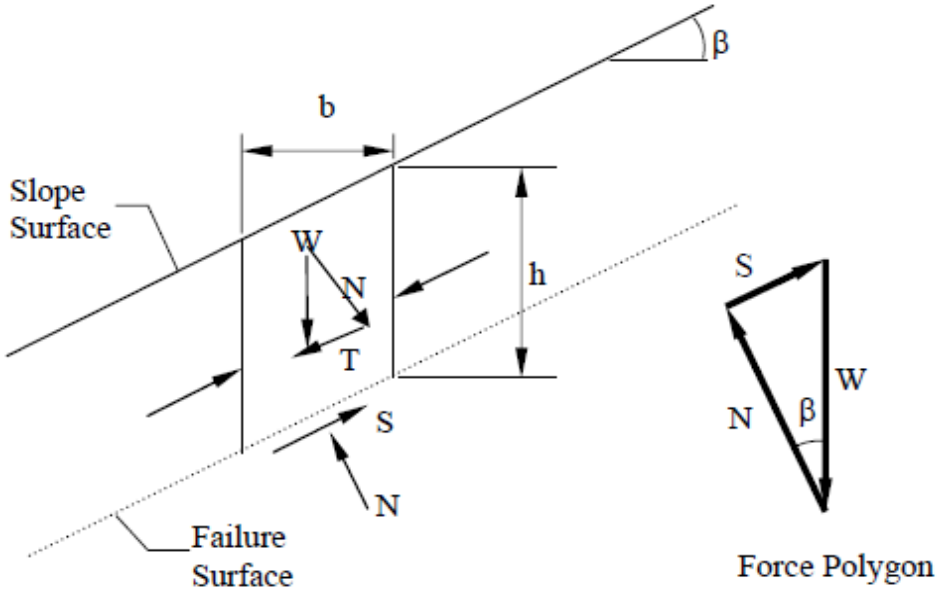

Fig.2.1. Infinite slope failure in dry sand with free body diagram of forces

The weight of the slice of having a unit length is given by;

$$W = \gamma b h \quad \ldots\ldots\ldots\ldots\ldots\ldots\ldots\ldots\ldots\ldots\ldots\ldots\ldots\ldots\ldots\ldots\ldots\ldots \quad (2.1)$$

Where, γ is the unit weight of the dry soil, b is the width of slice and h is height of slice as shown in Fig. 2.1

The normal (N) and tangential (T) force components of W acting on a slip surface with an β angle are determined as

$$N = W \cos\beta \quad \ldots\ldots\ldots\ldots\ldots\ldots\ldots\ldots\ldots\ldots\ldots\ldots\ldots\ldots\ldots\ldots\ldots\ldots \quad (2.2)$$

$$T = W \sin\beta \quad \ldots\ldots\ldots\ldots\ldots\ldots\ldots\ldots\ldots\ldots\ldots\ldots\ldots\ldots\ldots\ldots\ldots\ldots \quad (2.3)$$

The shear strength along the failure plane is given by:

$$S = N \tan\phi \quad \ldots\ldots\ldots\ldots\ldots\ldots\ldots\ldots\ldots\ldots\ldots\ldots\ldots\ldots\ldots\ldots\ldots\ldots \quad (2.4)$$

Where, ϕ is the angle of internal friction.

The factor of safety (FOS) is defined as the ratio of available shear strength to strength required to maintain stability. Thus, the FOS will be given by:

$$FOS = \frac{S}{T} = \frac{N \tan\phi}{W \sin\beta} = \frac{W \cos\beta \tan\phi}{W \sin\beta} = \frac{\tan\phi}{\tan\beta} \quad \ldots\ldots\ldots\ldots\ldots \quad (2.5)$$

From the equation (5), it is clear that the FOS is independent of the slope depth, h, and depends only on the angle of internal friction, ϕ and the angle of the slip surface, β. The slope is said to have reached **limit equilibrium** when $\phi = \beta$ and the FOS becomes 1.

b) Infinite slopes in cohesive soils with parallel seepage

If the seepage of a saturated slope in a cohesive soil is parallel to the surface of the slope as shown in Figure 2.2, the same limit equilibrium concepts may be applied to determine the FOS, which will now depend on the effective normal force (N'). In the saturated soil case, effective shear strength parameters, (c' and φ') are used.

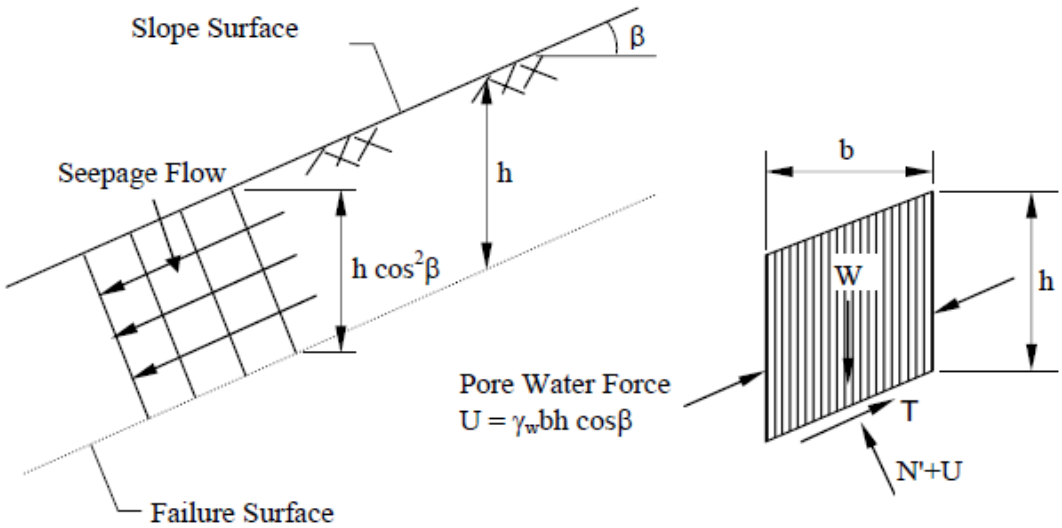

Fig.2.2. Infinite slope failure in a cohesive soil with parallel seepage with free body diagram of forces

From the Fig.2.2.Weight of slice (W) and he effective normal forces (N') are as following;

$$W = \gamma_{sat}\, b\, h \quad \text{.....} \quad (2.6)$$

$$N' = N - U = \gamma_{sat}\, b\, h \cos\beta - \gamma_{w}\, b\, h \cos\beta \quad \text{.....} \quad (2.7)$$

$$T = W \sin\beta \quad \text{.....} \quad (2.8)$$

Similarly, the pore water force acting on the base of a typical slice having a unit length.

$$U = \frac{b\,(\gamma_{w}\, h \cos^{2}\beta)}{\cos\beta} = \gamma_{w}\, b\, h \cos\beta \quad \text{.....} \quad (2.9)$$

Where, b is width of assumed slice, γ_{w} unit weight of water, h is any depth less than or equal to the depth of saturation and β is slope of slip surface.

The available shear strength, S, along the failure plane will depend on φ' and the effective normal force, N' =N-U, where N is the total normal force. The total shear strength, S is given by the following equation:

$$S = \frac{c'\,b}{\cos\beta} + (N - U)\tan\phi' \quad \text{..... (2.10)}$$

From the equation (2.10) and (2.8), the factor of safety (FOS);

$$FOS = \frac{S}{T} = \frac{S\ c'\ b/\cos\beta + (N - U)\tan\phi}{W\ Sin\beta} \quad \text{..... (2.11)}$$

From equation (2.8), substituting the value of W into equation (2.11) and simplifying the equation:

$$FOS = \frac{c' + (\gamma_{sat} - \gamma_w)\,h\cos^2\tan\phi}{\gamma_{sat}\,h\cos\beta\ Sin\beta} \quad \text{..... (2.12)}$$

For the case of a saturated cohesionless soil, c' = 0, Then the equation (2.12) becomes

$$FOS = \frac{(\gamma_{sat} - \gamma_w)\tan\phi}{\gamma_{sat}\ \tan\beta} \quad \text{..... (2.13)}$$

From equation 2.13 it is obvious that FOS is again independent of the slip surface depth, h. Similarly, in the case of cohesionless soil, it is seen from equation (2.11) that both strength parameters c' and φ' have a vital role in stability of slope.

Botts (1986) and Tovar and Colmenares (2011) found a more than 70 % reduction in the angle of internal friction (φ) of mudstone due to slaking. In addition, c was reduced by about 40 % after 4 cycles of wetting and drying. Similarly, Yoshida et al. (1997), Sadisun et al. (2003), Bhattarai et al. (2007), Youn and Tonon (2010), and many other researchers showed a significant reduction in shear strength parameters after a number of cycles of wetting and drying. According to Spears and Taylor; 1971, the shear strength parameters for the shallowest fissile mudstone and shale samples show a decrease in the angle of internal friction of up to 37 % and a drop in cohesion of around 93 %.

From the equations 2.5, 2.12 and 2.13, it is obvious that the slaking of mudstone could slope failure trigger. Similarly, Matsukura and Mizuna (1986) and Qureshi et al., (2009) explained that slaking has a great influence on the value of c and φ, which in turn determine the slope angle and of course, the stability of slopes.

However, drying is possible only up to shallow depths. So, slaking can induce shallow landslides (small scale) and the speed of landslide is very slow as compared to

heavy rainfall induced landslide. Because of these facts, slaking induced landslides may not cause any casualties and large economic loss. So, no media and researchers have focused on this type of disaster.

2.3 Landslide events collection

Thousands of rainfall induced landslides occur every year in the world. So, the number of landslide events considered in this research is almost negligible as compared to the total number of landslides which occur. The main objective of this chapter is to explore landslide events preceded by significant drought. These landslides may be due to slaking of soft sedimentary rocks.

In order to analyse a landslide in this research, the author tried to collect several primary elements and secondary elements to describe the event and landslide characteristic, when available. The both primary and secondary elements are:

Primary elements

1. Location details (town/village, province, and country etc.)
2. Time (event date and local time)
3. Trigger (rainfall pattern and rainfall intensity)
4. Geology

Secondary elements

5. Latitude and longitude
6. Type and relative size of the event (e.g., landslide, debris flow, mudslide, rock avalanche etc.)
7. Impact information (e.g., Casualties and economic loss etc.)

The primary and secondary elements for each landslide event were obtained mainly from landslide related paper (Kirschbaum et al., 2009; Huang and le, 2011 and more), online news media, and hazard databases, including: United States Geological Survey (USGS), Disaster management website, ministry of home affairs , Nepal, Landslide blogs, Global disaster data base, International Consortium on Landslides website, International Landslide Centre, University of Durham, other online regional and national newspaper articles and media sources. After identifying the landslide event, precipitation data and geological information were collected from Tropical Rainfall Measuring Mission (TRMM) and available geological map respectively, details of which are discussed later.

2.3.1 Geology

As previously mentioned, the location of landslide events in terms of latitude and longitude was also collected from different sources. The latitude and longitude were used to extract the geological information of landslides events from available geological map. Figures 2.3-2.5 show some typical geological maps of China, Africa and Nepal respectively which contain more than 50 groups of rock. However in order to analyse the landslide distribution using the rock type, similar types of rock, based on its formation and age have been grouped together, six groups of rock were obtained as follows as follows:

a) Granite with other intrusive rocks
b) Volcanic and plutonic rocks
c) Mudstone, sand, conglomerates and chert etc.
d) Metamorphic
e) Other (do not lie within the above mentioned categories or are a complex combination of these rocks)
f) Unidentified

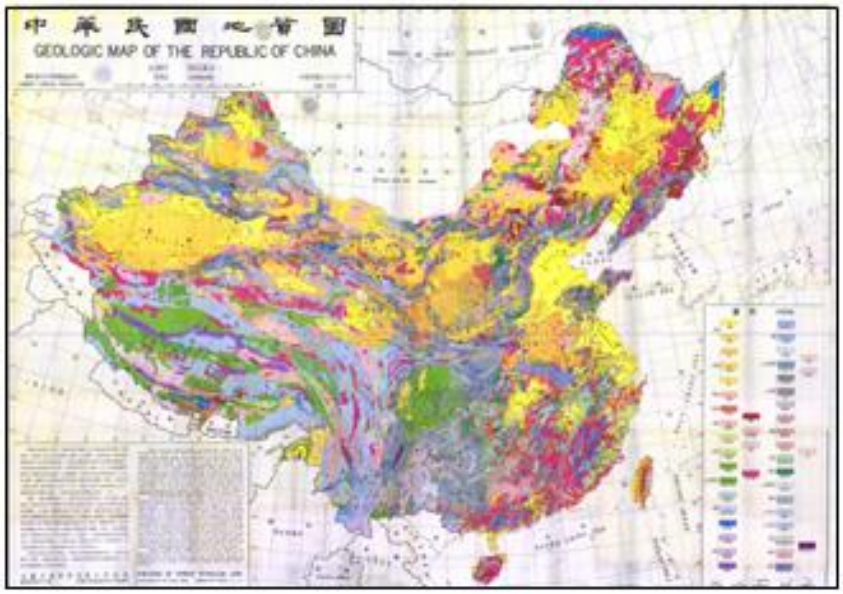

Fig. 2.3 Geological map of China

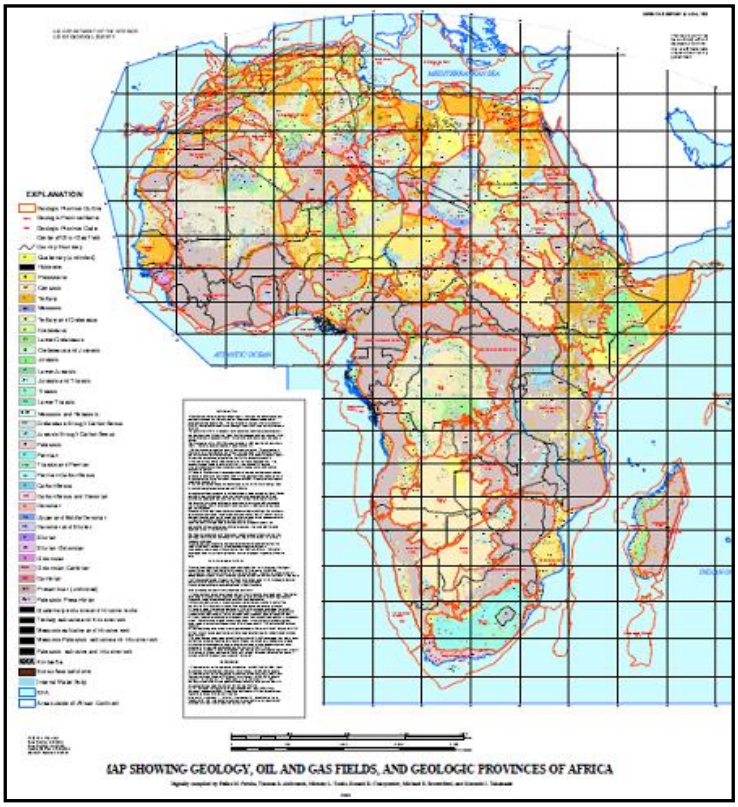

Fig. 2.4 Geology map of Africa region

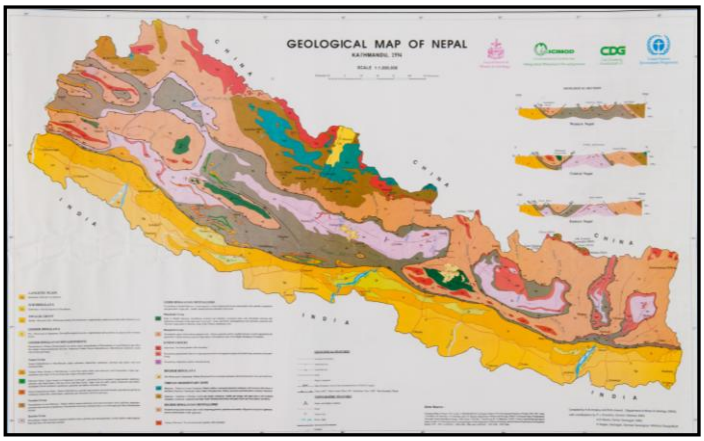

Fig. 2.5 Geological map of Nepal

2.3.2 Precipitation

The precipitation record of the landslide area, obtained from the Tropical Rainfall Measuring Mission (TRMM) satellite is shown in Fig. 8. The Tropical Rainfall Measuring Mission (TRMM) is a joint U.S.-Japan satellite mission to monitor tropical and subtropical precipitation and to estimate its associated latent heat. TRMM was successfully launched on 27 November 1997 from the Tanegashima Space Center in Japan. TRMM estimates the

rainfalls over tropical to subtropical regions with 0.25° x 0.25° resolution. Details of the algorithm can be found at http://trmm.gsfc.nasa.gov/3b42.html. Data are open to public via their website. Ground base validation or calibration with rain gauge data from corresponding landslide area is required to obtain more accurate precipitation data from TRMM (Wolff et al., 2005; Robinson et al., 2000 and Islam et al., 2010). This part of research is only for motivation or background of this research. Time constraint is also another major factor to use crude precipitation data from TRMM to analyze the rainfall induced landslide on the basis of precipitation intensity per day. Ground base validation or calibration with rain gauges data from corresponding sites should be done for detailed and further research on the same topic. Similarly, use of KBBI (Keetch-Byram Drought Index) or DDSLR (Dry Day Since Last Rainfall) is one of best tools to quantify the drought or dry days. A precipitation data set for at least 5 years before the landslide event was analysed in this studies. Figures 2.7-2.9 are some typical examples of precipitation patterns derived from TRMM.

Classification of rainfall intensity

The classification of rainfall intensity per hour or per day is a complex and difficult task. Rainfall intensities are classified from different points of view such as agriculture, flooding and landslides etc. Moreover, it largely depends on location and other climatic conditions. So, many countries and organizations develop their own classification assuming different threshold values. Table 1-3 show some typical rainfall intensity classifications used in India and China. As shown in the table, these thresholds vary considerably from one country to another, which means that it would be difficult to obtain a universal classification on the basis of the different thresholds.

Table 1 Rainfall intensity classification in India

S.N.	Intensity (mm/day)	Classification
1	<35 mm	Light rain
2	35-74.9 mm	Rather heavy rain
2	75-124.9 mm	Heavy rain
4	>125 mm	Very heavy rain

Table 2 Rainfall intensity classification in China

S.N.	Intensity (mm/day)	Classification
1	<10 mm	Light rain
2	10-25 mm	Moderate rain
2	25-50 mm	Heavy rain
4	50-100 mm	Heavier rain
5	>100 mm	Extremely heavy

For simplicity and uniformity, the author classified the rainfall intensity per day for this research. However, this classification is not based on any scientific logic.

Table 3 Rainfall intensity classification used in this research

S.N.	Intensity (mm/day)	Classification
1	<30 mm	Light rain
2	30-60 mm	Moderate rain
2	60-100 mm	Heavy rain
4	>100 mm	Very Heavy rain

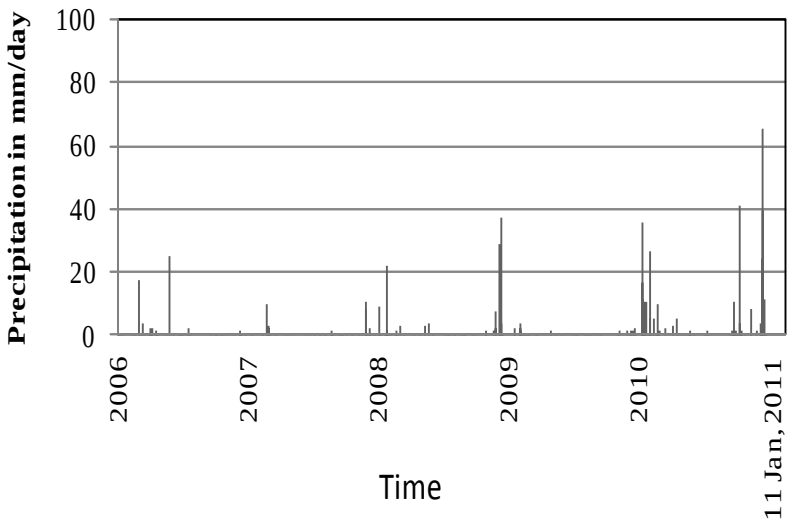

Fig. 2.6 Daily precipitation in Dana Point, Pacific coast highway, USA from TRMM

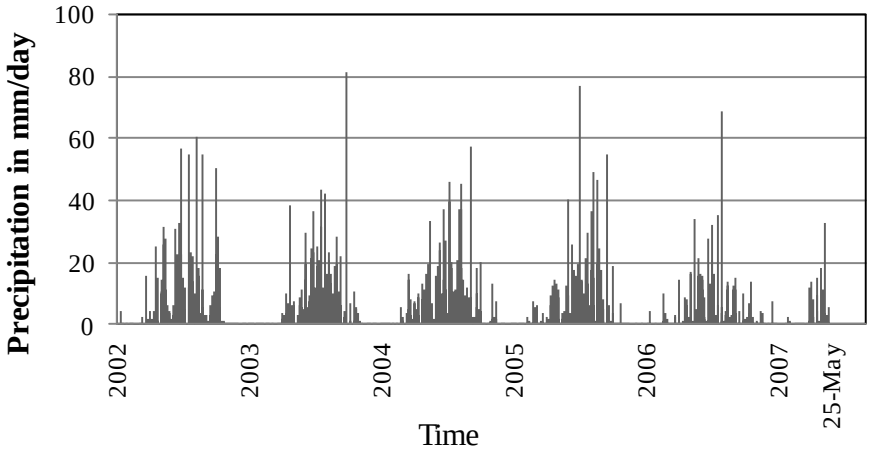

Fig 2.7 Daily precipitation in Flenglexiang, Sichuan Province, China from TRMM

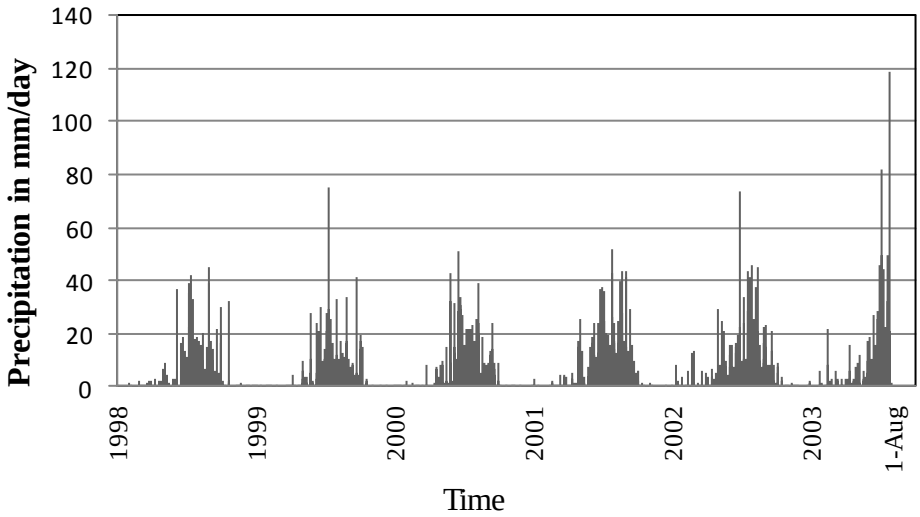

Fig. 2.8 Daily precipitation in Mankamana, Gorkha, Nepal from TRMM

2.4 Distribution of landslides

After analyzing the precipitation from the TRMM and geology from available geological maps of more than 300 random landslides event from all over the world, the following scenarios were found.

2.4.1 Geology

As mentioned in Chapter 2.2.1, in order to study the effect of rock type on landslide hazard, similar types of rock, based on their formation, were grouped together to obtain 6 groups.

Percentage of landslides occurring in each group is as follows. Group 1: (Granite with other intrusive rock such as basalt, andesine, diorite etc.) has a contribution of about 15 % on total landslide event. Group 2: (Volcanic and plutonic) is responsible for about 5 %. Group 3: (Mudstone, sand, conglomerates and chert etc.) represents largest proportion among other groups. About 40 % of landslides occurred on soft sedimentary rock formations i.e. Mudstone, sand, conglomerates and chert etc. Group 4: (Metamorphic rocks) is responsible for about 11 % of total rainfall induced landslides. Group 5: (Other: all the rock which not lie on group 1-4 and very complex geological formation to identify fall in this group) is responsible for 20 % of total rainfall landslides. Finally, Group 6: (Unidentified) corresponds to those landslides event with lack of geological information. The graphical representation of the landslide distribution on rock types is presented in Fig. 2.9

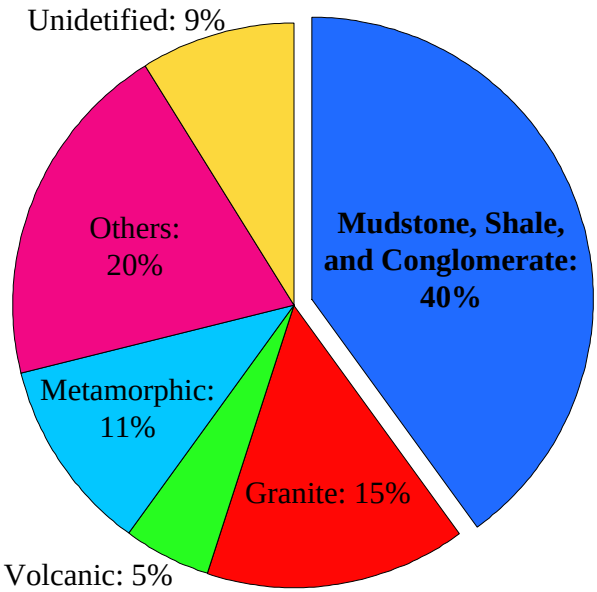

Fig. 2.9 Landslides classified by frequency occuring in each rock group

Safaei et al. (2002) also analyzed the distribution of 422 landslides in Mazandaran province, Iran. The author mentioned that more than 37 % of landslides are related to soft sedimentary rock formations. Similarly, Soralump et al. (2007) showed that about 44.69 % of total rainfall induced landslides in Thailand occurred in soft sedimentary rock formations. The output of this case study of rainfall induced landslides is very close to Safaei (2002) and Soralump et al. (2007). However the other author considered only a part of the world.

2.4.2 Precipitation

The main objective of this research is to evaluate the slaking characteristics of geomaterials. It is known that soft sedimentary rocks are highly prone to slaking susceptibility. That is why, the author tried to classify the rainfall induced landslides on soft sedimentary rock formation on the basis of rainfall intensity per day. However, the daily rainfall intensity is not the only influential factor for triggering landslides. The rainfall intensity per hour and rainfall duration etc should also be considered. As previously mentioned, due to various reasons only rainfall the intensity per day is considered. The classification of rainfall intensity is described in Chapter 2.2.2.

It is found that about half of rainfall induced landslides on soft sedimentary rock formations are triggered by moderate and light rainfall. About 17 % of landslides on soft sedimentary rock formations were triggered by light rainfall, while 30 % were caused by moderate rainfall. Similarly, the remaining half of landslides events were triggered by heavy and very heavy rainfall. The graphical representation of landslide distribution on the basis of rainfall intensity per day is presented in Fig. 2.10.

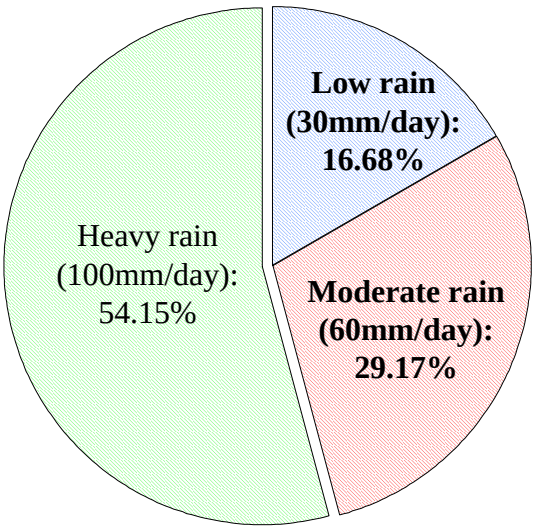

Fig. 2.10 Landslides classified by frequency occuring on the basis of rainfall intensity

Figure 2.11 shows the rank of rainfall intensity at the time of landslide event. About 42 % landslides were occurred due to the highest precipitation within five years duration. Conventionally, it is believed that the rainfall induced landslides cause by heavily rainfall. It is found that about 12 % rainfall induced landslides on soft sedimentary rock formations are triggered by lowest rainfall intensity. So, the traditional explanation for rainfall induced landslides is insufficient regarding the mechanism landslide due to lowest rainfall intensity. The term slaking should be introduced to define the mechanism and threshold of landslide initiation.

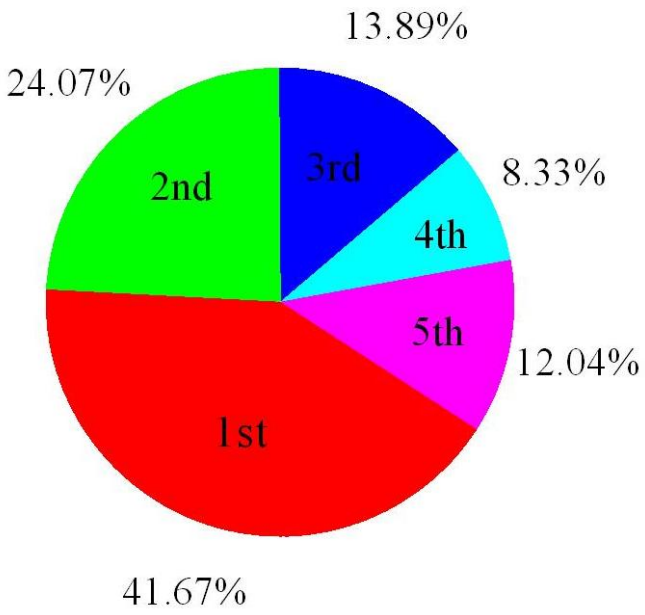

Fig. 2.11 Landslides classified on the basis of ranking of rainfall intensity at the time of landslide considering five years precipitation

2.5 Conclusions

Conventionally, it is believed that the rainfall induced landslides cause by heavily rainfall. Such a landslide event is analysed by susceptibility of hill slopes to generation of positive pressure heads under a saturated regime, in association with water storage capacity of regolith zone and/or subsurface water flow paths. However, about 50 % of total rainfall induced landslides in soft sedimentary rock were found to be occurred after moderate and light rainfall. So, the traditional explanation for rainfall induced landslides is insufficient

regarding the mechanism and threshold of landslide initiation. Some landslides most probably occur under an unsaturated regime, resulting only from a decrease in shear strength of the soil (Krahn et al., 1989; Terlien, 1997) especially in soft sedimentary rock formation due to slaking of mudstones. However, detailed field and laboratory investigations of landslide areas are necessary to inspect the subsurface structures and to obtain geotechnical properties of slope materials. Then, real mechanism of land even could be explained precisely.

CHAPTER 3

LITERATURE REVIWEW

3.1 General

As mentioned in the Introduction chapter, many researchers have been investigating the slaking behaviour of geomaterials, especially mudstones for many years. Considering the various aspects of slaking, this chapter provides a brief overview of the existing literature on slaking of geomaterials. Since the focus of this study is on the slaking behaviour of geomaterials and its effects on strength and deformation, research works published on various aspects of slaking of geomaterials, especially mudstone are reviewed here. Once the current level of knowledge has been examined, the direction of future research can be more easily determined and focused.

In this chapter, first, the mechanism by which the slaking is believed to occur will be investigated by studying various research papers on this subject, as well as summarizing how the slaking process will be defined. Cyclic wetting and drying as well as swelling and shrinkage are always associated with slaking or deterioration of mudstones, so previous research on the impact of cyclic wetting and drying as well swelling and shrinkage of geomaterials are also presented here. Finally, research papers on the strength and deformation characteristics of slakable materials are studied and few results of these papers are summarized here.

3.2 Slaking mechanism and process

The term '*slaking*' is defined as 'the softening or crumbling and disintegration of the geomaterials upon cyclic drying and wetting; specifically the breaking up of dried geomaterials or indurated soil when immersed in water or fully or partially saturated with water, or the breaking up of clay-rich sedimentary rocks when exposed to air or experienced drying (Nakano, 1967; Moriwaki, 1974; Surendra et al., 1981 and Vallejo et al., 1993). For the present study, slaking is defined as the softening or breakdown and dispersion of rocks,

especially mudstones, in response to alternate wetting and drying or even only in water immersion. Some mudstones at natural water content slake when immersed in water. Others when immersed will remain stable with regard to slaking. However, if these materials are first dried and then rewetted, drying induced slaking can occur. Nakano (1970) presented evidence that some materials will not slake as long as the water content remains above a certain threshold value.

Nakano (1967), Taylor (1988), Huppert (1988), Dick and Shakoor (1992), Moon and Beattie (1995), Bell et al. (1997), Koncagul and Santi (1999), Gokceoglu et al. (2000), Dhakal et al. (2002), Lashkaripour and Boomeri (2002), Lashkaripour and Ghafoori (2002) and among other researchers studied factors affecting the slaking or durability of different geomaterials such as mudstone, sandstone etc. According to those studies, the slaking of geomaterials depends upon many factors such as mineralogy, physical and chemical properties (fabric, porosity, mineral alignment, micro-fractures, density) and geology (lithology, cementation) etc. Sadisun et al. (2005) stated that the main factors controlling slaking are expandable clay minerals, non-clay minerals (pyrite) and soluble minerals. Santi and Koncagul (1996) proposed different modes of slaking of shale and the main cause for each type. Surface slaking, swelling slaking, body slaking and Dispersion slaking are the four modes of slaking which result from the presence of Calcium-illite/Calcium-kaolinite, Sodium-montmorillonite, Calcium-montmorillonite and Sodium-kaolinite respectively.

As already mentioned, many researchers have speculated on the slaking mechanism, few have carried out extensive investigations concerning these possible slaking mechanisms. According to them, slaking is a very complex process as it depends on many factors as mentioned above. Therefore, there is very little understanding of the slaking mechanism due to cyclic wetting and drying or even due to a single immersion. However, there are different mechanisms discussed in the geotechnical literature, each of which offers valuable insight into the slaking mechanism and process. There are two primary schools of thought for the slaking mechanism and process due to cyclic wetting and drying or even single emersion or prolonged drying.

a) Pore-air compression

Pore-air compression is the predominant slaking mechanism in mudstones composed primarily of non-expansive clay minerals such as kaolinite. Terzaghi (1936),

Moriwaki (1974), Bell (1992) and Vallejo et al. (1993) and many others researchers purposed a slaking mechanism in terms of pore-air compression.

In alternate drying and wetting, when mudstones become dry, air is drawn into macro-pores and a high suction pressure develops. This in turn results in increased shearing resistance of the individual fragments by virtue of the high contact pressures. The bulk of the voids are filled with air under extreme desiccation conditions (Figure 3.1).

When the rock is then rapidly immersed in water, water will be pulled into the each macro-pore, as a result of capillary forces developed due to suction, and the air that originally filled the micro-pores will be subjected to compression (Fig. 3.1b) Tensile failure of mineral skeleton along the weakest planes may occur as a result of which the significant

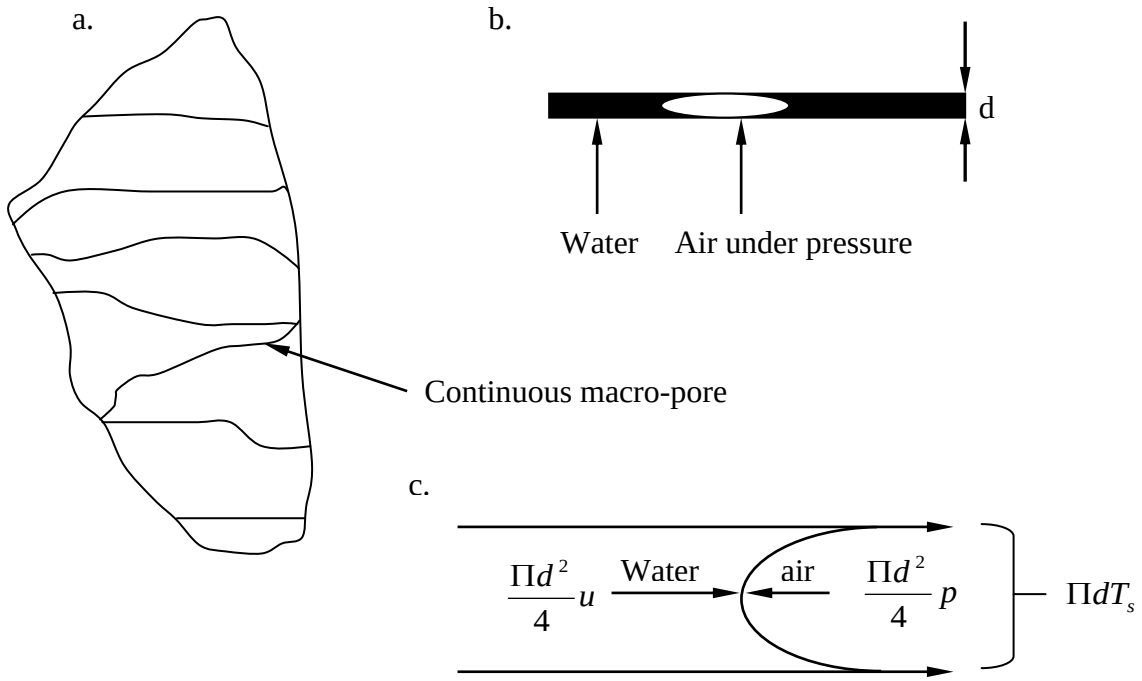

Fig. 3.1 Forces acting on the micro and macro pore in mudstone (Means and Parcher, 1963)

surface area to be exposed increases (Taylor and Spears, 1970). The air pressure developed in the macro-pores depends on the capillary pressures, which themselves are related to the surface tension of the water (Seedsman, 1986) and the pore radius (Vallejo, et al., 1993). The system of forces acting at the interface between the air and the water in a macro-pore is shown in Fig. 3.1c (Means and Parcher, 1963).

Considering equilibrium conditions, the relationship between pore pressure and pore diameter can be explained by the equations below.

$$\Pi d T_s - \frac{\Pi d^2}{4} p + \frac{\Pi d^2}{4} u = 0 \quad \text{…….... (3.2.1)}$$

Where, d is the diameter of the macro-pore, T_s is the surface tension of water acting on the meniscus, p is the air pressure inside the macro- pore and u is the pore water pressure.

From the equation 3.2.1, the following relationship can be obtained

$$p = u + \frac{4T_s}{d} \quad \text{…… (3.2.2)}$$

An analysis of the equation 3.2.2 shows that the air-filled pore air pressure, p in the macro-pore increases as the pore diameter, d decreases. Thus, the smaller the diameter of the macro-pore, the larger the pressure will be. In summary, slaking of mudstones by air compression will be more significant in those mudstones containing smaller micro-pores (Means and Parcher, 1963 and Vallejo et al., 1993). Youn and Tonon (2010) also summarized four different factors that affect the slaking of clay bearing rocks by pore air compression as following.

1) Air pressure entrapped in pore spaces and between clay particles
2) Osmotic swelling pressure of expandable clay minerals
3) Pre-existing fissures in rocks
4) Gradual removal of cementation by alternate wetting and drying

However, slaking by pore air compression is only possible, when the pressure build up occur rapidly (Seedsman, 1986). Low permeability and the presence of expansive clays may restrict the movement of the wetting front. Given enough cycles of drying and wetting, breakdown can occur as a result of air pressure. This process can reduce the mudstone into gravel-size particles (Bell, 1992). Bell (1992) explained failure occurring in consolidated and poorly cemented rocks in terms of swelling pressure and capillary suction pressure. This failure happens during the saturation process, when the swelling pressure, or internal saturation swelling pressure (σs), developed by capillary suction pressures, exceeds the tensile strength. Taylor (1988) attributed, slaking in less indurated mudstones, to a combination of increasing air pressure as water invades narrow capillaries, and tensile failure of weak inter-crystalline bonds due to drying induced pore water suctions. According to Moon and Beattie (195), pore-air pressure compression, release of residual stresses which exceeds the rock strength and the loss of cohesion of clay due to the absorption of water on

to the surfaces of clay may be important mechanisms applicable to the slaking of geomaterials. The reliability of this mechanism can be demonstrated by the absence of slaking when slake testing is performed under a vacuum.

b) Hydration of clay mineral

Nakano (1967) explained the mechanism of slaking process in terms of the hydrated clay mineral present within the rock structure. This is an important hypothesis to consider, primarily because clay mineral must be present within the rock for it to be slaked in this way. According to Nakano, the slaking/ weakening of mudstone is due to a kind of chemical dissolution mainly by the formation of hydrogen bond between originally adsorbed water molecule and newly adsorbed water molecule around clay particles (Fig. 3.2). It is

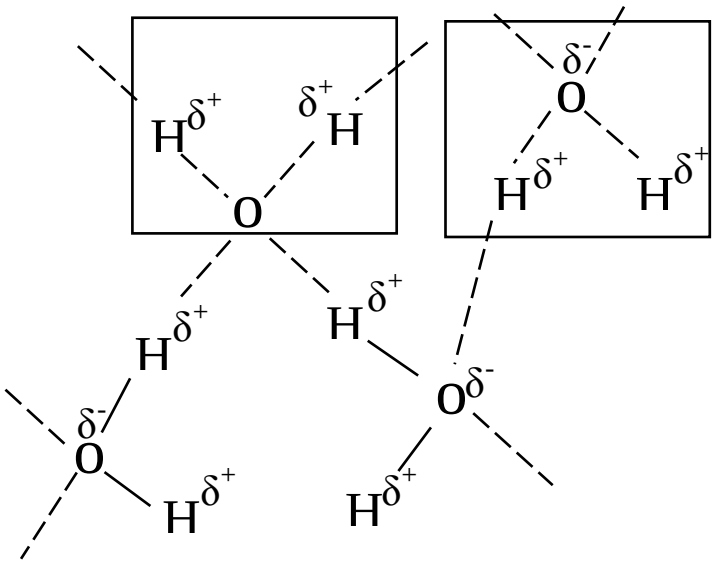

Fig. 3.2 Hydrogen bond between originally adsorbed and newly one water molecule (Nakano, 1967)

presumed that a part of the free Gibb's energy which evolved due to the hydrogen bond formation is used as a mechanical destructive energy in slaking. Similarly, when the water molecules are held around clay particles through the hydrogen bond, the basal spacing of expansive clay minerals like montmorillonite increases, causing strain in mudstone and destructing it.

Huggett (2003) and Scherer (2006) also explored the importance of clay mineral hydration in the weathering of rocks due to cyclic wetting and drying. Hugget and Scherer did not define the weathering of rocks due to cyclic wetting and drying as slaking. However, many authors refer to this process as slaking. As mentioned above, there are a number of

papers (Yatsu, 1988 and Hall and Hall, 1996) suggesting that clay mineral do not need be present for slaking of mudstones to occur. If these tests are correct, there must be another mechanism for the slaking of mudstone. This is not to say that idea behind slaking is incorrect. Indeed, there is overwhelming evidence that slaking does occur. Rather, it is important to consider the possibility that the clay mineral expansion does not tell the complete story; there is more to process for slaking.

3.3 Measurement of slaking

Several types of slake durability tests have been developed and used by researchers worldwide to assess the slaking susceptibility of geomaterials. Some tests are based on specific mechanisms of rock disintegration, resulting from physical breakdown by wetting and drying. Some tests are performed to measure the amount of tightly held surface, pore and capillary water, as an indicator of the resistance to slaking. Some tests are qualitative while some are semi-quantitative or quantitative.

The following slaking related tests will be discussed here:

1. Jar slake test (Vellejo et al., 1993 and USBR, 2006)
2. Slake durability test (Franklin and Chandra, 1972)
3. Slaking index test (JGS 2125-2006)
4. Slaking ratio test (NEXCO-100, 2006)
5. Rate of slaking (Morgenstern and Eigenbrod, 1974)
6. Wet-dry deterioration test (Withiam and Andrews, 1982)
7. Emerson crumb test (Emersion, 1967)
8. Water absorption ((Anwar et al., 2000)

1. Jar slake Test (Vellejo et al., 1993 and USBR, 2006)

The jar slake test is a simple and rapid test to evaluate the durability of weak rocks, such as mudstone. A rock piece about 50-100 grams, is oven-dried at a temperature 105° C for 24 hours before immersion in water. Rock deterioration pattern during the test is observed, and the slaking behaviors as well as the final state are recorded as a jar slake index (Ij) as classified in table 4. This test is performed to give a qualitative assessment of the rock's slaking characteristics after immersion.

Table 3.1 Jar Slake Ranking (Vellejo et al., 1993)

Jar Slake index (Ij)	Behaviour after immersion
1	Degrades to a mud
2	Breaks rapidly and totally reduces to flakes
3	Breaks slowly and forms few chips
4	Breaks rapidly and develops several fractures only
5	Breaks slowly and develops few minor cracks
6	No change

2. Slake durability test (Franklin and Chandra, 1972)

The slake durability of rocks is an important parameter when investigating the engineering behavior of a rock mass (Franklin and Chandra 1972; Onodera et al. 1974; Crosta 1998; Koncagul and Santi 1999; Gokceoglu et al. 2000; Dhakal et al. 2002; Singh et al. 2005), especially weak and soluble rocks such as shale, clay-bearing rocks, travertine and weak limestones, as it represents the degradability. The slake durability test, recommended by both the American Society for Testing and Materials (ASTM) (ASTM, 1996) and the International Society for Rock Mechanics (ISRM) (ISRM, 2007), is the most frequently performed test, originally developed by Franklin and Chandra(1972).

The test uses a steel drum with a 2-mm size mesh. Ten rock pieces are taken, each weighing 40–60 g, with a total weight of approximately 450–550 g. After oven-drying the sample at a temperature 105° C for 16 hours (until constant weight is achieved), it is placed in the drum with a 2 mm size mesh (Fig. 3.3) and the drum is sunk in water and rotated at 20 rpm for a period of 10 minutes. After this process, the material retained in the 2 mm mesh drum is collected and oven-dried at 105° C for 24 hours and then cooled for 20 minutes before recording the final weight after the first cycle. This procedure is repeated. The durability of rock is classified on the basis of Id2 as

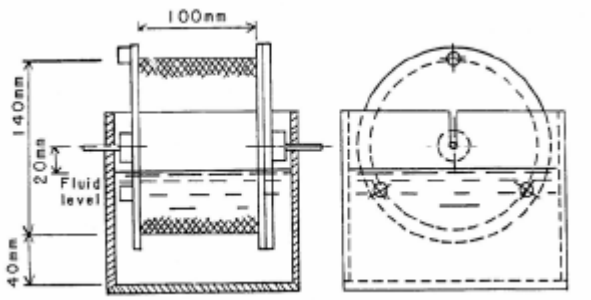

Fig. 3.3 Slake durability equipment (ASTM, 1992)

described in Table 3.2, where Id2 is the ratio of the dry weight remaining in the 2 mm mesh drum to the initial dry weight, expressed as a percentage. The standard method recognized by ASTM and ISRM is based on the two cycles of drying and wetting, however many researchers (Taylor, 1988; Moon and Beattie, 1995; Ulusay et al., 1995; Bell et al., 1997; Gokceoglu et al. 2000; Yagiz and Akyol, 2008 and Yagiz, 2010) recommend more cycles of wetting and drying to evaluate rocks of higher durability.

Table 3.2: Gamble's slake durability classification (Gamble, 1971)

S.N.	Group Name	% Id1 (Dry weight basis)	%Id2 (Dry weight basis)
1	Very high durability	>99	>98
2	High durability	98-99	95-98
3	Medium high durability	95-98	85-95
4	Medium durability	85-95	60-85
5	Low durability	60-85	30-60
6	Very low durability	<60	<30

Many researchers tried to develop a relationship between Id2 and strength parameters. Gemici (2001) established a relation between Id2 and point load strength as shown in Fig. 3.4. Sadisun et al. (2004) proposed a relation between important clay contents which play an important role in slaking and Id2 (Fig.3.5). The slaking index and smectite content relationship could be better used to subdivide the argillaceous rock into individual rocks. Yilmaz and Karacan (2005) performed the regression analyses between Id2 and void ratio (e) and the best-fitted relation was plotted for mudstone in doline formation. The test results in Fig. 3.6 have shown a very good correlation with the correlation coefficient (R) of 0.96. Yagiz (2010) established the relationships between the slake durability indices and modulus of elasticity (E), Uniaxial compressive strength (UCS) and shear velocity (Vp) etc for some carbonate rocks as shown in Fig. 3.7 and 3.8. It is very useful to estimate strength parameter from very simple and popular test like slake durability test. Gokceoglu et al. (2000) also performed a lot of experiments to find the relation between Id4 and uniaxial compressive strength. The outcomes of the experiments are as shown in Fig. 3.9.

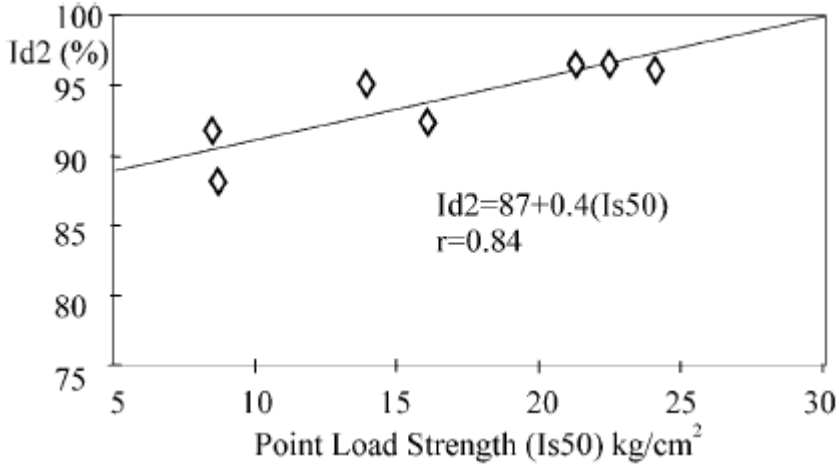

Fig. 3.4 Relation between slaking index and point load strength (Gemici, 2001)

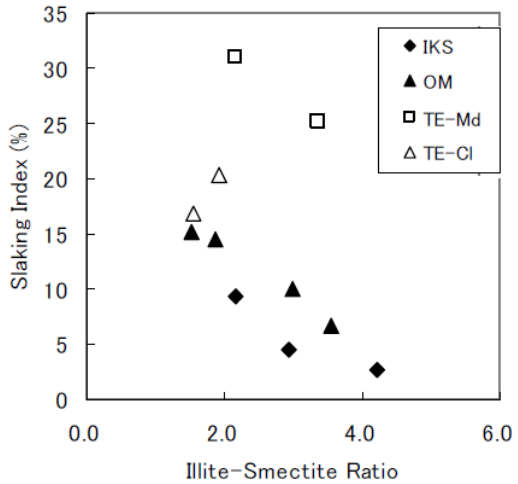

Fig 3.5 Relation between clay content and slaking index (Sadisun et al., 2004)

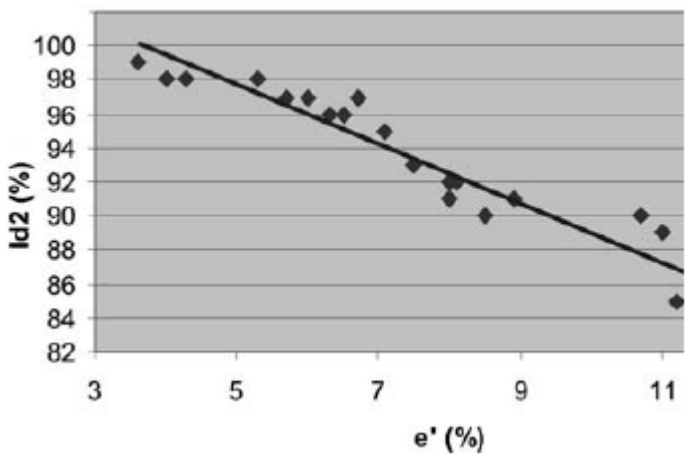

Fig. 3.6 Slake durability index versus effective porosity (Yilmaz and Karacan, 2005)

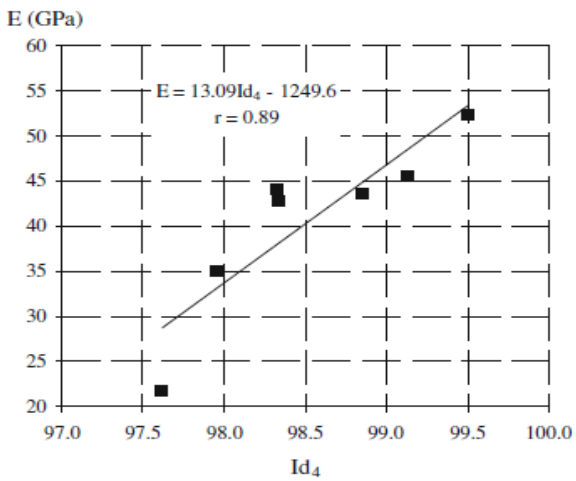

Fig. 3.7 Relationship between the E and Id4 (Yagiz, 2010)

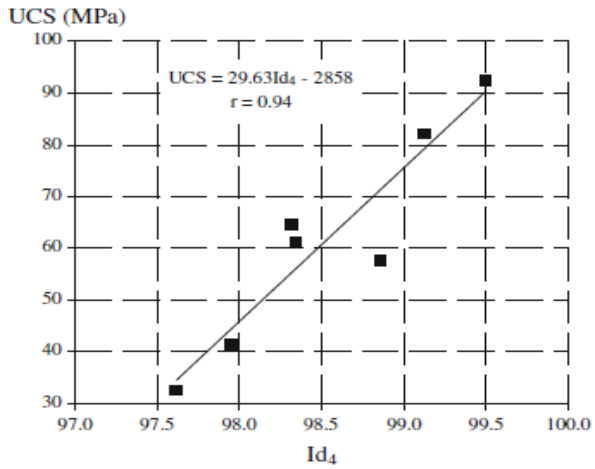

Fig. 3.8 Relationship between the UCs and Id4 (Yagiz, 2010)

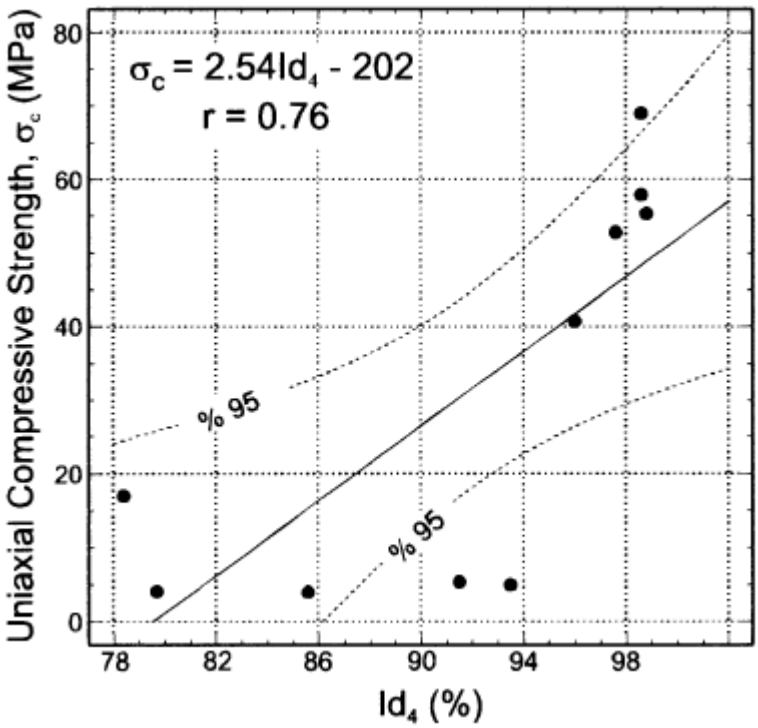

Fig. 3.9 Relationship between Id4 and Uniaxial compressive strength (sc) of the marls (Gokceoglu et al. (2000)

3. Slaking index test (JGS 2125 -2006)

The Slaking index test method is developed and adopted by Japanese Geotechnical society (JGS). The details of the Slaking index test are explained in Chapter 4.

4. Slaking ratio test (NEXCO- 100, 2006)

The Slaking index test method is developed and adopted by Nippon Expressway Corporation Limited (NEXCO). The details of the Slaking ratio test are explained in Chapter 4.

5. Rate of slaking (Morgenstern and Eigenbrod, 1974)

It consists of saturating the mudstone sample generally in a funnel with a filter paper for at least 2 hours. After 2 hours, free water is removed through the filter paper. Then, the rate and amount of water absorbed by the mudstone is determined. The rate and amount of water absorption can reflect porosity, void geometry and fractures. The slaked portion of the sample is separated and Atterberge limits of slaked sample are found, which implicitly reveal the proportion of clay size materials. Morgenstern and Eigenbrod, (1974) relate the degree of slaking to liquid limit as given in Table 3.3.

Table 3.3 Description of the degree of slaking (Morgenstern and Eigenbrod, 1974)

S.N.	Amount of Slaking	Liquid limit (%)
1	Very low	<20
2	Low	20-50
3	Medium	50-90
4	High	90-140
5	Very high	>140

6. Wet and dry deterioration test (Withiam and Andrews, 1982)

As in the slake durability test, this test also consists of several cycles of alternate wetting and drying. Wetting is carried out by soaking rock pieces in water or chemical solutions (e.g. sodium sulphate). The test is considered to involve a cyclic wet-dry process, the rate of water adsorption, and the rate of slaking (Withiam and Andrews, 1982). Both the sodium sulphate soundness test (ASTM D 5240-92) and the ASTM test of the durability of rock under wetting and drying conditions (ASTM D 5313-92) are classified as ‘wet-dry deterioration tests’.

Sodium sulphate soundness test (ASTM D 5240-92) involves the oven-drying of 5 rock lumps having a volume of 10 cm^3 and then immersed in a sulphate solution. This process completes one cycle. Five successive drying and immersion cycles are required to complete one Sodium sulphate soundness test (ASTM D 5240-92). This test is very popular for testing aggregates used in road pavement and concrete.

The percentage of soundness loss is calculated as follows:

$$Average\,soundness\,loss = \frac{Wi - Wf}{Wi}\,\%$$

Where, W_i = oven-dried cumulative mass of all rocks prior to testing, and W_f = oven-dried cumulative mass of the largest remaining pieces of all rocks after testing.

In case of wet and dry test (ASTM D 5313-92), at least 5 rock specimens are used, the size of which should be as possible but not less than 125 mm. Each specimen should be 64 mm thick and cut normal to bedding or any potential planes of weakness. The test consists of oven-drying the rock sample and placing the sample on a thin layer of sand in a container filled with water for a period of 12 hours. The sample is removed from water and then dried in an oven at a temperature of 60-70° C for at least 6 hours. The same process of wetting and drying should be repeated for 80 cycles. Like in the Sodium sulphate soundness test (ASTM D 5240-92), only the largest remaining piece of each rock specimen is used in the calculation. The resistance of the rock sample to the accelerated weathering can be evaluated. The percentage of loss is calculated as follows:

$$Average\,soundness\,loss = \frac{Wi - Wf}{Wi}\,\%$$

Where, Wi = oven-dried cumulative mass of all rocks prior to testing, and Wf = oven-dried cumulative mass of the largest remaining pieces of all rocks after testing.

The test is very useful for determining the durability of rock bed for erosion control and riprap testing. However, there is not any guideline to classify rocks on the basic of average soundness loss value.

7. Emersion crumb test (Emersion, 1967)

In this test, specimens from the field directly are immersed in water. Ingles and Metcalf (1972) recommended using good quality water. Slaking is observed first (slaking or no slaking), and subsequent dispersion (dispersion or flocculation) is observed in the finest slaked fragments. In this test, the slaking behaviour is defined by breakage of the specimen,

while the dispersion behaviour is derived from the diffusion of the soil particles over the specimen or covering the bottom of the beaker. The slaking behaviour of the specimens can be grouped into eight classes (Emerson, 1967).

8. Water absorption test (Anwar et al., 2000)

The rate and amount of water absorption also reveal the durability of rock (Anwar et al., 2000). Water absorption is thus also very important. The details of water absorption are explained in Chapter 4.

3.4 Swelling and Shrinkage of mudstones

Focusing on mudstones, a few researchers described the observed cyclic swelling and shrinkage behavior of mudstones or soft rocks. According to Seedsman (1993), when moisture in soil or rock decreases, air enters into the pores and when moisture returns by capillarity, air is captured and its pressure increases in the internal pores which lead to a higher swelling pressure. This higher swelling pressure leads to slaking. Suction pressure increases with the decrease in water content during the drying phase. Higher negative suction pressure causes the failure of weak crystalline bond of mudstones which also ultimately leads to particle breakage (slaking).

As described above, the slaking process relates to the swelling mechanism of the clay mineral, which is attributed to the ability of the rock to take up water between grains and in interlayer structures which causes the increase in volume (Moriwaki, 1974; Anwar et al., 2000). Similarly, many authors also relate the shrinkage to slaking (Nakano, 1970; Surendra et al., 1991; Vallejo et al., 1993 and Anwar, 2000). Swelling is a combination of physico-chemical reactions involving water and stress relief (ISRM, 1983).

Moriwaki (1974), Einstein (1996) and Youn and Tonon (2010) recognized that swelling (then slaking) in mudstones is caused by one or a combination of three mechanisms: mechanical (compressed entrapped air), osmotic and hydration of ion around the clay surface (Moriwaki, 1974; Einstein, 1996). According to ISRM (1983), Einstein (1996) and Doostmohammadi et al. (2008), the physico-chemical reaction with water is usually the major contribution to swelling but it usually takes place simultaneously with, or following, stress relief. As previously mentioned, the slaking of geomaterials is consequence of swelling and shrinkage. So, all factors affecting the slaking, of course, influence the swelling and shrinkage of geomaterials. These factors are mineralogy,

lithology, ground characteristics, hydrology, stress state and especially weathering conditions (Moriwaki, 1974, Pejon and Zuquette, 2002; Moosavi et al., 2006).

Gysel (1987), Einstein (1996), Barla (1999) and Hawlader et al. (2003 and 2005) explained the swelling behaviour of mudstones by only considering the first saturation period and neglects the shrinking stage due to the following drying season. Typically in the field, mudstones are subjected to cyclic wetting and drying with distinct seasonal change or with ground water variation or reservoir level changes etc. The research on cyclic wetting and drying induced swell-shrink behavior and its effect on the strength and deformation is thus very important. In reality, these types of research are very rare. For the soft rock containing expansive clays, many researchers such as Chen et al. (1985), Chen and Ma (1987), Subba Rao and Satyadas (1987) and also Basma et al. (1996) have addressed the problem of cyclic swelling and shrinking. It was inferred that when clays are repeatedly subjected to full swell, then desiccated to their initial water content, they gradually display less expansion. On the other hand, Osipov et al. (1987), Day (1994) and also Basma et al. (1996) showed that the swelling potential increases with the number of wetting and drying cycles when the samples are allowed to fully shrink up to a water content equal to or less than the shrinkage limit. These studies show the influence of the shrinking stage on the next swelling period. Zhang et al. (2010) performed free swelling tests on argillaceous (Cox) and clay stones (OPA) by wetting the samples with water vapor. He measured strains at a low relative humidity of *RH* = 23% and 100% relative humidity for

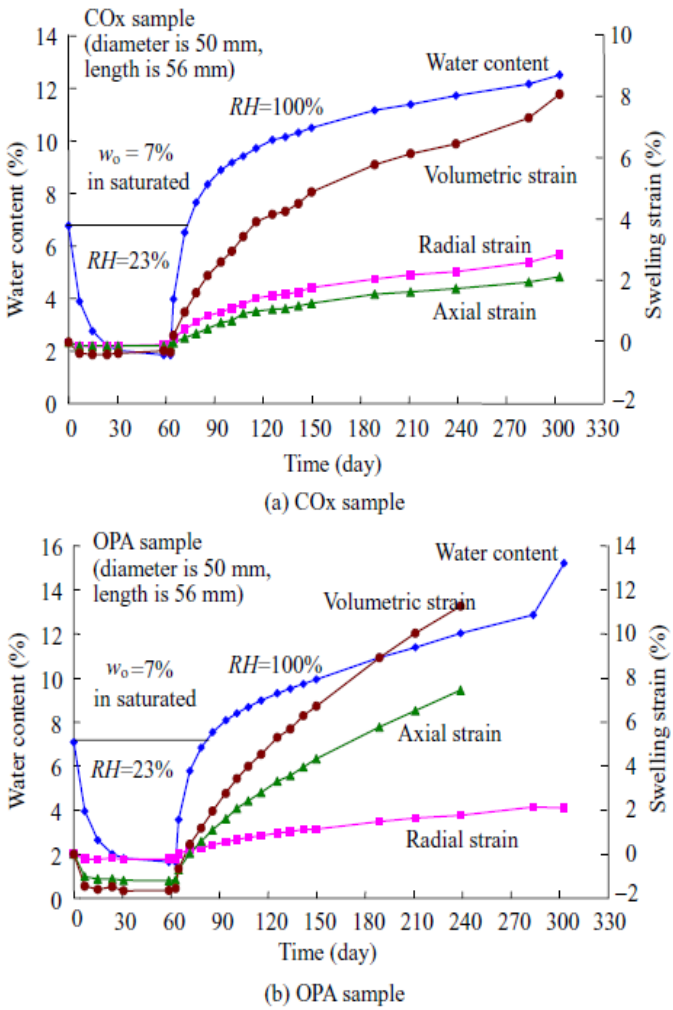

Fig. 3.10 Free swelling strains measured on COx and OPA samples (Zhang et al., 2010)

two months and eight months respectively. After reaching equilibrium during drying at *RH* = 23%, the remaining water contents in both samples became asymptotic at the water content about 1.7%, but the shrinkages behaviour are different (Fig. 3.10). A larger shrinkage of 1.6% was observed on the OPA sample with more clay content, about 5 times that of Cox sample with less clay content. The tests also showed that the mudstones can take up great amounts of water, over 14%–18%, much more than that of about 7% in natural and saturated states. The increase of water content yielded a large volume expansion up to 8% – 12%. More water uptake and volume expansion could be expected if wetting continued to reach equilibrium. Additionally, it is to be pointed out that the swelling of the sedimentary mudstones is pronouncedly anisotropic due to bedding planes. A larger swelling strain occurs in direction perpendicular to the bedding plane (Fig.3.10). The anisotropic swelling is so strong that it is able to break down the mudstones along the bedding planes. Figure 9 shows the pictures of the samples after swelling.

Huang et al. (1995) performed some cyclic wetting and drying tests on shales and approximated the relation between maximum swelling potential (i.e. maximum pressure and strain) between the first and the second test cycles. From the Fig. 3.11, it is seen that the maximum swelling pressure measured in the second cycle test decreased significantly, and the time needed to reach a peak pressure reduced as well.

Al-Shamrani and Al-Mhaidib (1999) performed a series of experiments to measure swelling under different confining stress conditions. Figure 3.12 shows that swelling decreases with the increase in confining pressure. According to many researchers swelling reveals the slaking of geomaterials. So, slaking of geomaterials may also be related to confining pressure. Similarly, the same authors did research on the influence of swelling on the shear strength of shale. It can be seen from Figure 3.13 that the amount of swell has a significant

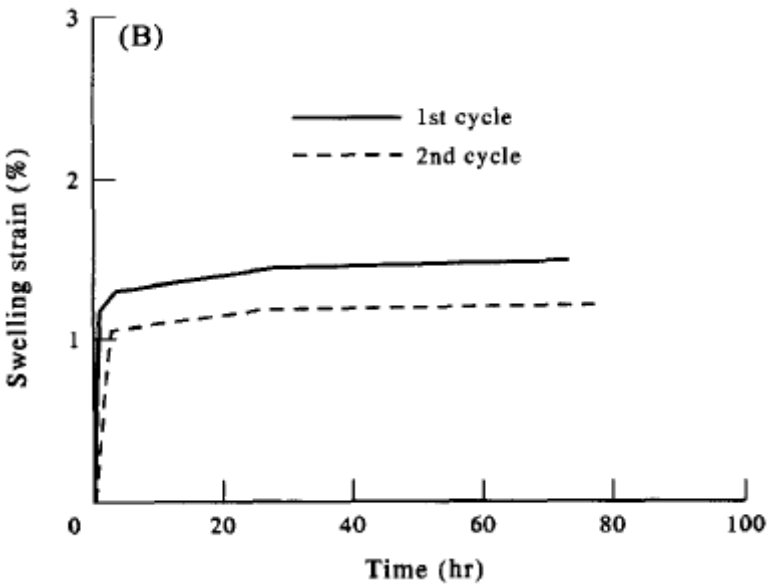

Fig. 3.11 swelling strain in the first cycle and second cycle wetting of shale (Huang et al. (1995)

influence on the shear strength of shale. For instance, shear strength decreases by about 50% when the shear was initiated at a swell percent of 25% of the ultimate vertical swell.

Fig. 3.12 Relation between confining pressure and swelling (Al-Shamrani and Al-Mhaidib, 1999)

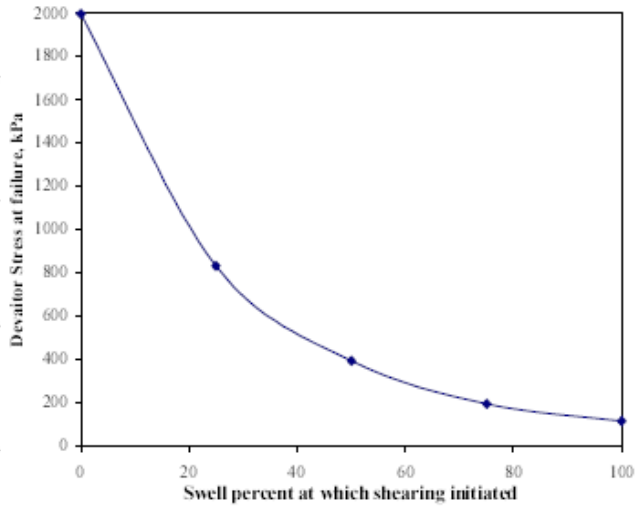

Fig. 3.13 Deviator stress at failure versus swelling in percent for shale samples (Al-Shamrani and Al-Mhaidib, 1999)

Furthermore, the shear strength is approximately 10% of the shear strength of the non-swelled soil when the sample was sheared after reaching the ultimate vertical swell.

Pejon and Zuquette (2002) described the impact of cyclic wetting and drying on the swelling behavior of mudrocks. They demonstrated that accumulated maximum axial swelling strain of different mudrocks varied according to the number of wetting and drying cycles. From the Fig. 3.14, the trend of increasing swelling strain with the cycles is seen clearly. However, samples air-dried to constant weight experienced bigger and faster swelling than the samples air-dried to natural moisture content after each wetting cycle (Fig. 3.15a and b). The texture, structure, clay content, bulk density, specific gravity, dry density, initial moisture content, initial void ratio, porosity, degree of saturation, methylene blue value (vb), cation exchange capacity

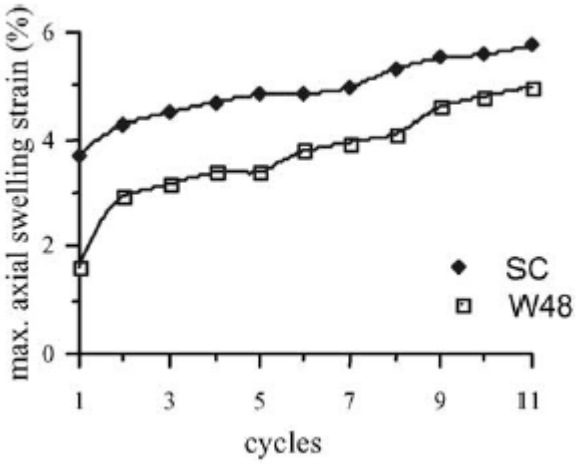

Fig. 3.14 Maximum swelling strain with respect to wetting and drying cycles (Pejon and Zuquette, 2002)

(CEC), clay activity index (Acb), carbonate content and mercury porosity are effective parameters for swelling rate (Pejon and Zuquette , 2002)

Anwar et al. (2000) conducted the free swelling and slaking tests to examine the behavior of swelling of 24 specimens which consisted of sandstone, shale, coaly-shale, sandy-shale and mudstone. All these specimens showed similar trend in swelling, in which sandstones were less than 1 % but shales were in the order 2- 12 %. From the Fig. 3.16a, it

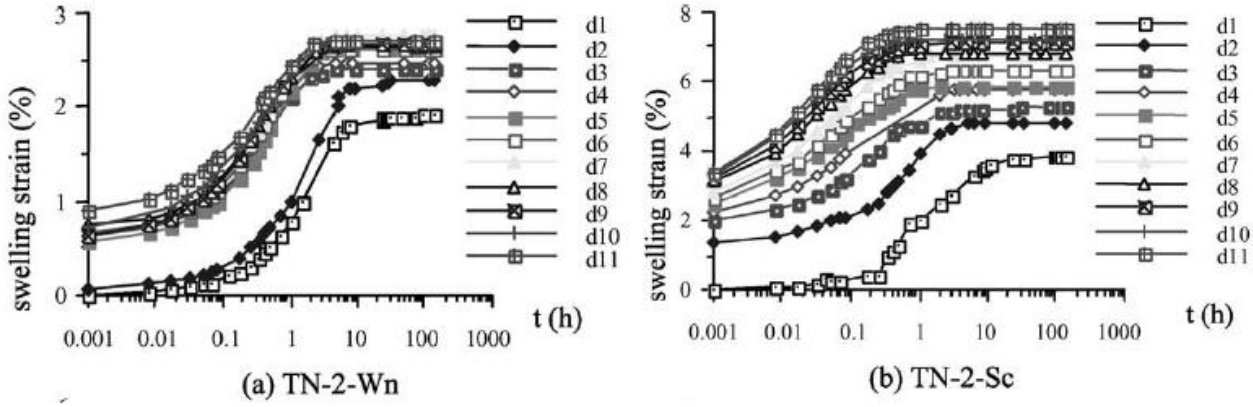

Fig. 3.15 Swelling strain of samples after being dried to (a) natural moisture in air (b) completely dried (Pejon and Zuquette, 2002)

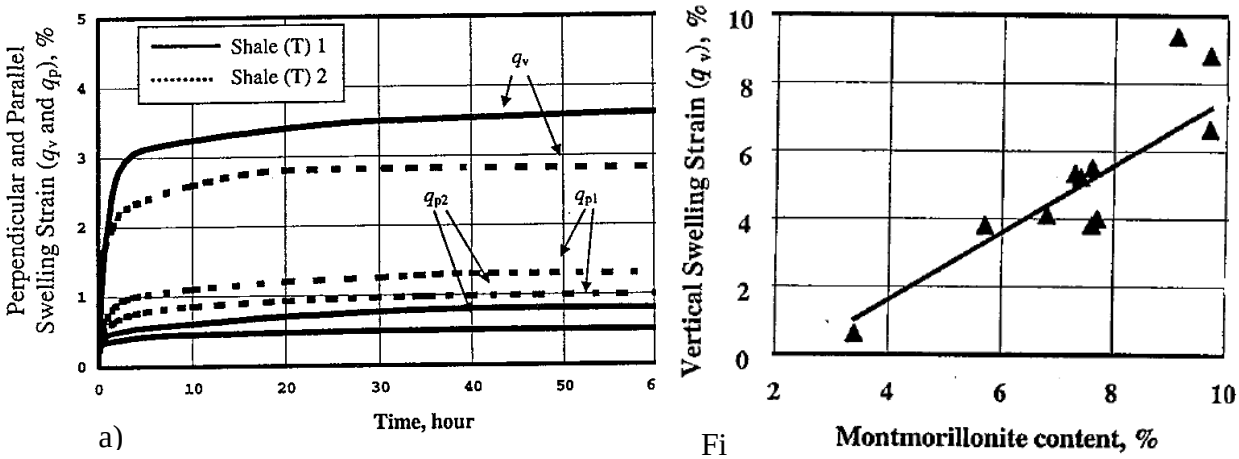

Fi

Fig. 3.16 a) time histories of swelling b) effect of Montomorilonite on swelling strain (Anwar et al., 2000)

is seen that the largest swelling occurred in the initial stage, and then it was followed by slow growth of the expansion. It showed that the mudstones are highly prone to swelling which ultimately lead to slaking. Similarly he found that the expandable clay mineral content may effect upon the swelling strain as shown in Fig. 3.16 b. This fact is significant in the slaking process.

Doostmohammadi et al. (2007) performed some cyclic swelling tests under oedometric condition on mudstone samples. The swelling pressure of the samples was measured in the axial direction over the time. The maximum swelling pressure increased with each cycle (Fig. 3.17). The increasing rate of swelling pressure was decreased after the third cycle and it finally reached an almost steady state.

As Al-Shamrani and Al-Mhaidib (1999) presented, Lee et al. (2002) also concluded that the larger the confining stress, the smaller the swelling strain is (Fig. 3.18). The swelling strain may approach zero at higher confining stress.

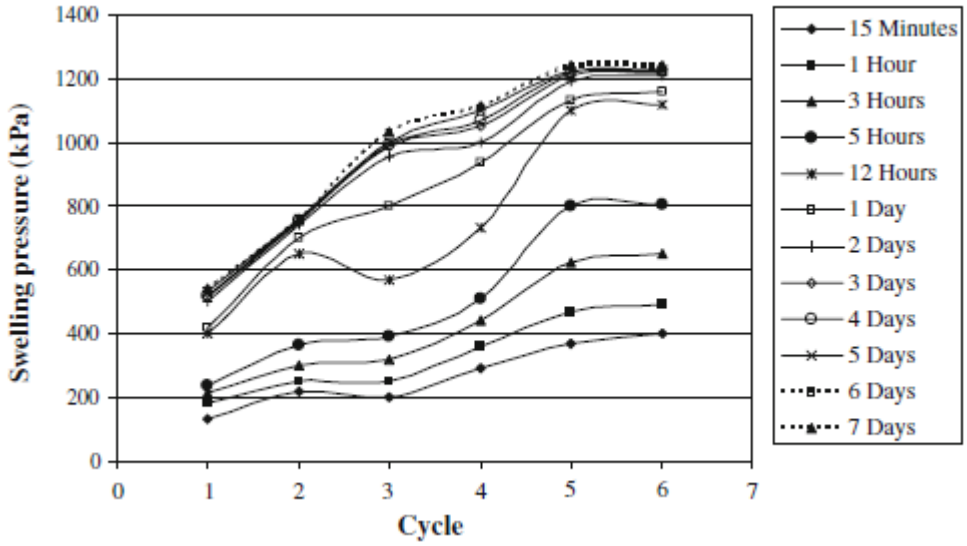

Fig. 3.17 The trend of swelling pressure in equal times of cycles (Doostmohammadi et al., 2007))

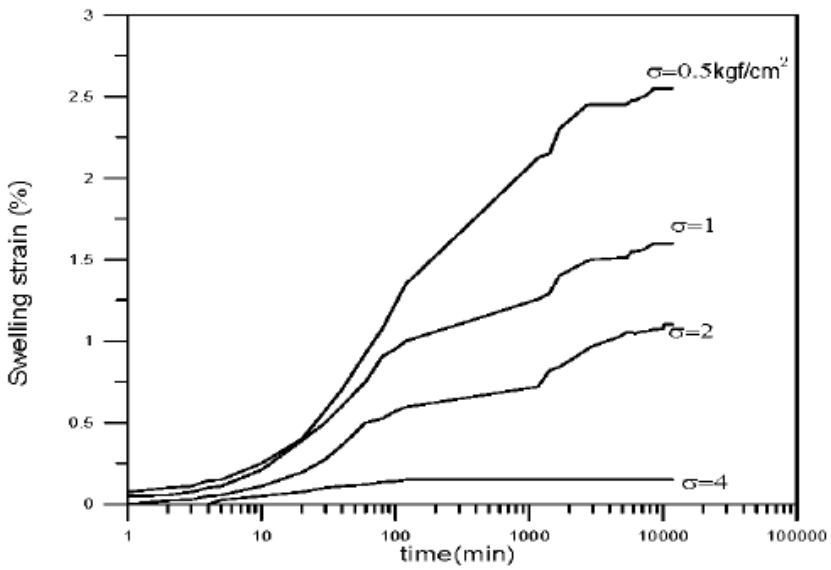

Fig. 3.18 Swelling strain under different confining stress (Al-Shamrani and Al-Mhaidib (1999)

3.5 Effect of wetting and drying on the properties of geomaterials

Many researchers have been seeking to evaluate the effect of cyclic wetting and drying on geomaterials. Most of their studies are done on soft sedimentary rock i.e. mudstone etc. Some studies related to cyclic wetting and drying have already been discussed in previous chapter. Table 3.4 provides the list of some researches done in laboratory simulating wetting and drying process. The material used, methodology adopted and outcomes of these researchers are also mentioned in Table 3.4. Of course, each research mentioned in Table 3.4 was done by individual research groups. However, these research studies have some similarity from different perspectives. Laboratory studies can initially be grouped on the basis of objectives, methodology adopted and final outputs.

Franklin and Chandra (1972); Gokceoglu et al. (2000); Sri-in and Fuenkajorn (2007) and Erguler and Ulusay, (2009) performed cyclic wetting and drying experiments to find the slake durability index, which is used to evaluate the slaking susceptibility of mudstone. The details of the slaking durability index were described in Chapter 3.3. Rocks containing higher carbonate are less susceptible to disintegration during cyclic wetting and drying. Similarly, rock containing higher amount of clays can easily undergo disintegration due to cyclic wetting and drying. Hall and Hall (1996); Nicholson (2001); Kanyaya and Trenhaile (2005); Wells et al. (2005); Gonzalez and Scherer (2006) and Subner and Loubser (2008) applied a large number of cyclic wetting and drying cycles. The wetting period is relatively very short as compared to the drying period. All these experiments were conducted under isolated environmental conditions. Actually these experiments were conducted to study the mechanism of wetting and drying. Hall and Hall (1996) investigated the relationship between the way in which the rock types received moisture and the changes in the internal structure of the rock. He found that the large number of cyclic wetting and drying has a significant influence on particle crushing even in case of hard rock rather than mudstone. Gonzalez and Scherer (2006) tried to develop a relationship between the number of cycle and the volume change (swelling) of specimen. Similarly, Pradini et al. (1996) also conducted the cyclic wetting and drying test to develop the relationship between the number wetting and drying cycle and volume change (swelling). Gradual increase in swelling over the time was observed. Matsukura and Yatsu (1982) and Huang et al. (1995) also monitored the swelling of geomaterials due to cyclic wetting and drying. They found that the swelling

of geomaterials largely depends on the clay mineral and its type. Dick et al. (1994); Gokceoglu et al. (2000); Pezen and Zuquette (2002) and Tovar and Colmenares (2011) simulated cyclic wetting and drying and analyzed the mineralogical composition by using XRD or SEM. Dick et al. (1994) found strong relationship between slaking and clay content. Pezen and Zuquette (2002) found considerable breakdown of soft rock even if rock has low clay content. Tovar and Colmenares (2011) showed that cyclic wetting and drying generates the alternation and destruction of the rocks and an increase in void ratio. Okamoto et al. (1984) found considerable change in both physical and mechanical properties of mudstone after certain number of cyclic wetting and drying. The authors also concluded that change in both physical and mechanical properties of mudstone depends on the degree on dryness before immersion. Same results were described by Doostmohammadi et al. (2009). Hachinohe et al. (1999) tried to evaluate the behaviour of geomaterials due to cyclic wetting and drying in natural condition. Hachinohe et al. (1999) concluded that weathering rates decrease logarithmically over time rather than linearly. Botts, 1998 found increase in fissures in shale after cyclic wetting and drying leading to the decrease in shear strength. Canton et al. (2001) conducted cyclic wetting and drying tests on consolidated mudstone. Canton et al. (2001) showed increase in both water absorption and porosity.

Table 3.4 List of various studies on Effect of wetting and drying on the properties of geomaterials

S.N.	Author	Material	Experiment procedure	Measured parameter	Obtained results
`	Franklin and Chandra, 1972	Mudstones	Alternate wetting and drying cycles	Mudstones disintegration i.e. Slake durability index	Slake durability index
2	Okamoto et al., 1984	Neogene mudstone cylinder 50 mm dia. and 20-100 mm height	Physical and mechanical test, Absorption test and Swelling pressure measurement under simulating cyclic wetting and drying	Change in physical and mechanical properties, absorption, swelling and slaking characteristics	All measured parameters are dependent on the degree of dryness of the specimen, and do not vary evenly according to drying time and temperature
3	Matsukura and Yatsu, 1982	shale and Tuff cube of one edge about 50 cm	Naturally dried for six month at room temperature before experiment, during experiment 9 hours dried in vacuum desiccators and 15 hours submerged in distilled water	Swelling pressure, percentage of mass loss, Mass loss of different shale and tuff	Slaking rate depends on different kinds of the clay mineral contained in the rocks
4	Dick et al., 1994	Mudrocks	slake durability test and XRD	Slake durability index and mineralogical content	Showed a strong relationship between percent expandable clays and slake durability index for clay stones
5	Huang et al., 1995	Shale cube	2 cycles wetting and drying carried out at different temperature	Maximum swelling pressure	Percent of expandable clays and slake durability index for clay stones

6	Hall and Hall, 1996	Sandstones/dolerite block	145 cycles of wetting and drying carried out using different method	Change in sample dry mass and water absorption	Significant influences on crushing of particles
7	Pardini et al., 1996	Smetitic mudrocks block	3 cycles by Non-contact laser profiling (3 days wetting and 12 days drying)	Bulk density and Surface micro-topography variations	Minimal effect on bulk density and surface micro-topography
8	Botts, 1998	Clay shale cylinder	Slake durability test (only one cycles, 0-28 days drying)	Fissure measurement of slaking under confining pressures and application of critical state model	Up to 80 % of rock strength decreased even after 1 cycles of wetting and drying
9	Hachinohe et al., 1999	Sandstones and mudstones core	Weathering profile observed in the field by using needle penetrometer	Residual strength ratio	Weathering rates decrease logarithmically over time rather than linearly
10	Gokceoglu et al., 200	Marls, clay stone and sandstones etc	4 cycles of wetting and drying by multiple slake durability testing	Uniaxial compression test and Mineralogy by XRD	Durability of clay-bearing rocks correlates well with amount of expandable clay content
11	Nicholson, 2001	Lime stones and chalk	40, 80 cycles wetting and drying on different rocks (12 hours wetting and 6-10 hours drying), Salt weathering test	Weight loss, fracture density, effective porosity and mercury intrusion porosimetry	Change in effective porosity and amount of water for saturation
12	Canton et al. 2001	mudstones blocks	5, 10 and 20 cycles of wetting and drying using sand bath	Total mineralogy, Micro-morphology, salt chemistry	Increase in both water absorption capacity and porosity

13	Pezen and Zuquette, 2002	French mudrocks core	11 cycles wetting and drying (duration of wetting and drying depended on moisture level) and SEM measured	Grain size and pore size distribution, Ion exchange capacity and mineralogical composition	Considerable breakdowns of particles even if rock has low mineral content
14	Kanyaya and Trenhaile, 2005	Basalts/Sandstones/Argillite cores and cubes	700-930 cycles wetting and drying using tidal simulator in laboratory environment	Rate of down wearing in the field by MEM	Down wearing rates decrease with elevation
15	Wells et al., 2005	Schist cube	5000 cyclic wetting and drying simulated tropical climate (5 minute wetting and 67 minute drying)	Particle crushing and moisture content	Significant changes in rock morphology
16	Gonzalez and Scherer, 2006	Portland brownstone plate	30 minute wetting and 60 minute drying applied by automatic machine	Ratio of wet and dry modulus and free swelling ratio	Gradual increase in swelling over time
17	Subner and Loubser, 2008	Sandstones block	52 cycles wetting and drying using different moisture amplitude (2-6 min wetting and 48 hours drying)	Change in sample dry mass, change in water absorption, porosity and saturation coefficient	Moisture amplitude has not significant impact on degree of slaking/weathering that takes place over an intermediate time period
18	Doostmohammadi et al., 2009	Mudstones cylinder 50 mm dia. and 20 height	Simulating cyclic drying and wetting in Swelling pressure test apparatus	Swelling strain of mudstones under different dead pressure with respect to number of cyclic wetting and drying	Swelling potential of mudstones is quite different when the water content of the sample changes periodically as opposed to the case where the sample is under constant water content

19	Tovar and Colmenares, 2011	Argillaceous Rocks	Drying and wetting cycle (120 hours for each wetting and drying), Fluorescence test and SEM test	Change in shear strength and mineralogical composition	Drying and wetting cycles, generate alternation and destructuration of the rocks, increase void ratio; are main causes of shear strength reduction
20	Gokceoglu et al., 2000	Seven rock cube (sedimentary, volcanic and metamorphic)	Multiple-cycle slakes durability testing, X-ray diffraction (XRD) analysis before and after durability test and Uniaxial compression testing.	Slake durability, mineralogical composition	High values of durability from the rock usually corresponds their higher carbonate contents. Decrease in SDI after 3 or 4 cycles
21	Sri-in and Fuenkajorn, 2007	sedimentary, and metamorphic with different clay	6 cycles of drying and wetting (24 hours at 105 ^{0}C for drying and 24 hours in 24 ^{0}C water)	Slake durability index, change in internal angle of friction and weight loss	usually correspond to their higher carbonate seems a better way to increase the number of cyclic wetting and drying
22	Erguler and Ulusay, 2009	Clay bearing rocks block (30*30*40 cm)	1 cycle drying and wetting(24 hours at 105 ^{0}C for drying and 24 hours in water), XRD diffraction	Slake durability index, disintegration index tests, slake durability rating (SDR) and Mineralogical constituent	The comparison between the disintegration index values of the laboratory specimens and the samples from the same outcrops exposed to atmospheric conditions for 1 year showed close agreement.

After reviewing the existing literature of research studies upon the effect of wetting and drying on properties of geomaterials, a number of conclusions can be drawn. As mentioned in the Introduction chapter, almost all cyclic wetting and drying related research on geomaterials are done under atmospheric pressure condition (no stress condition). However, geomaterials in the field are subjected to the cyclic wetting and drying under confining stress conditions. Similarly, the rate of drying is very rapid and very high temperature is applied as compared to natural temperature. The effect of rapid drying and very high temperature is neglected. The impact of duration for drying and wetting is also not taken into consideration in almost all research. ASTM, JGS and some other authors developed standard procedures for evaluating the impact of cyclic wetting and drying on geomaterials. However, it is found that only few researchers followed the standard procedure. So, the outputs of these researches cannot be easily compared to one another, making it difficult for all the information gathered to be integrated into one cohesive whole. The experiments were conducted in isolation. It means only a small part of the rock is considered under laboratory environment which may totally differ from real weather or environment. It is understood that weathering processes do not act in isolation. It is not only important to understand the response of each individual process, but also how all the different processes interact with one another to cause the observed effect.

In spite of such limitations, most of the existing methodologies of cyclic wetting and drying are very simple. The results obtained from these experiments will largely help to evaluate the response of geomaterials under cyclic wetting and drying.

3.6 Strength and deformation characteristics of slakable materials

Botts (1986) did both theoretical and experimental assessments of the effects of slaking on the engineering behavior of clay shales. He found the drastic decreases in strength resulting from slaking as shown in Fig. 3.19. Figure 3.19 shows the axial stress-axial strain-volume change relationships for the Pierre shale specimens tested under 207 kPa (30 Psi) confining pressure. Here in the figure, 30/4-23 corresponds to the test performed under 30 Psi confining pressure simulating 4 days of drying and 23 days of wetting and so on. Drying times for these samples varied from 0 to 28 days. These results

show that the shear strength of Pierre shale samples is significantly decreased with longer drying times.

Comparison of sample 30/4-1A and 30/4-23 indicate that shear strength is reduced with longer wetting time; however drying times seem to be the most influential factor. As observed in sample 30/28-3, the peak strength of the Pierre shale has been reduced by 80 % to a value very near the residual strength of unaltered samples with only a single cycle of drying and wetting. Similarly, Young's Modulus was found to be almost constant for samples with similar drying times, but greatly reduced with increased drying time. Young's Modulus of Elasticity varied from about 193,000 kPa for virgin Pierre shale to 34,000 kPa for samples which had undergone 28 days of drying (i.e. an 80 % increase in sample compressibility with slaking). In contrast, as seen in Figure 3.19, the volume change (the ratio of axial strain to volumetric strain) remained almost constant for all samples, regardless of the degree of softening.

Tovar and Colmenares (2011) performed a series of direct shear test on fresh argillaceous rock and argillaceous rocks experiencing number of cyclic drying and wetting. Figure 3.20 shows the reduction in maximum shear strength and allows us to observe the effect of wetting and drying cycles. He found that drying and wetting cycles have a significant effect on the shear strength, decreasing the angle of friction and increasing the intercept of the envelope with the passage of wetting and drying cycles as shown. The shear strength reduction was significant (70 %) after 4 cycles of wetting and drying cycles.

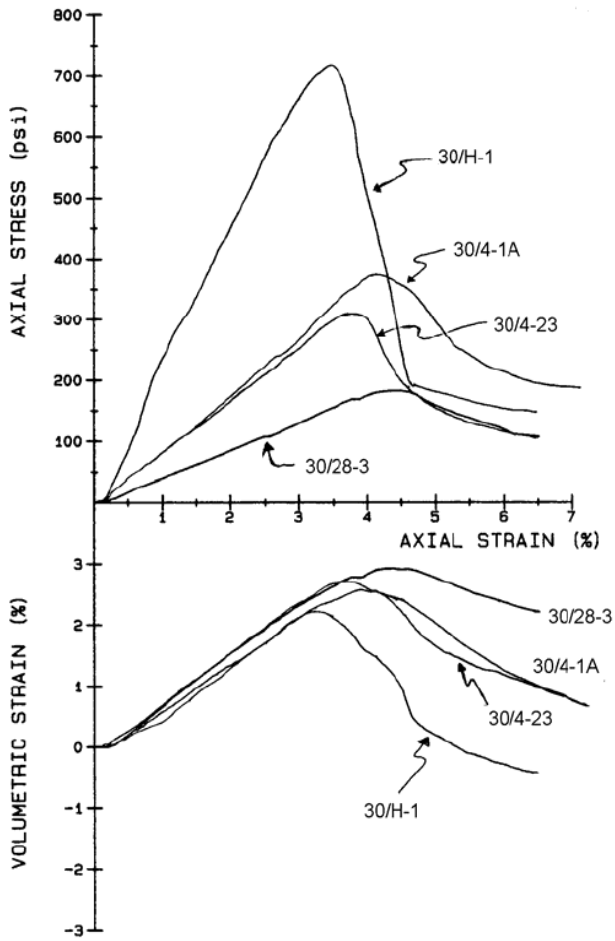

Fig 3.19 Comparative stress-strain plots showing drastic softening of Pierre shale after slaking (Botts, 1986)

Bhattarai et al. (2007) investigated the shear properties of fresh mudstone, remolded mudstone and mudstone after one and four cycles of drying and wetting. He reported that

significant reductions in peak shear strength were observed after both one cycle and four cycles of wetting and drying. The shear strength of the specimens after four cycles of wetting and drying was very close the shear strength of the fully softened specimen as shown in Fig. 3.21.

Figure 3.22 shows the shear stress–shear displacement–volume change relationships for the specimens made of mudstones aggregates. It is seen that for all the applied vertical stress, the immersed specimens give smaller peak shear stress than those without immersion. Reduction in shear stress seems larger for a smaller applied vertical stress. The inclination of shear stress–shear displacement curve in the early stage of shearing, though not clearly seen, also seems to decrease due to immersion. Regarding the volume change, it is noticed that for a vertical pressure of 80 kPa, the specimen without immersion exhibits a dilatant behavior but that the immersed specimen loses such dilative nature. For applied vertical pressures of 320 and 640 kPa, the volumes of the specimens without immersion are contractive and immersion does not cause much difference.

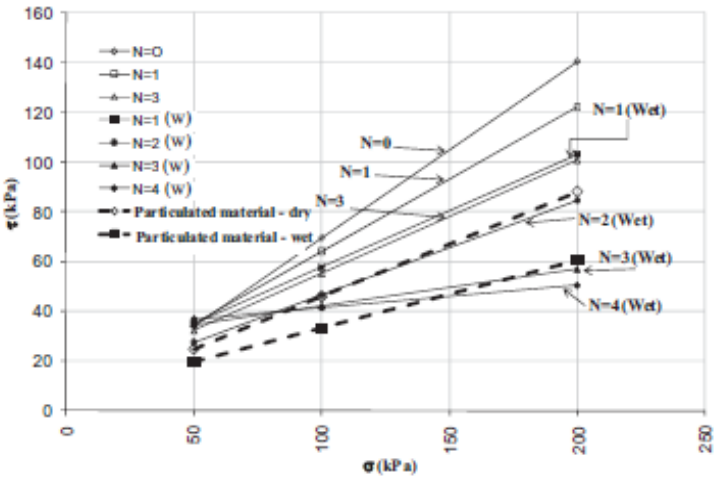

Fig.3.20. Mohr-Coulomb envelopes for wetting and drying cycles (N) applied (Tovar and Colmenares, 2011)

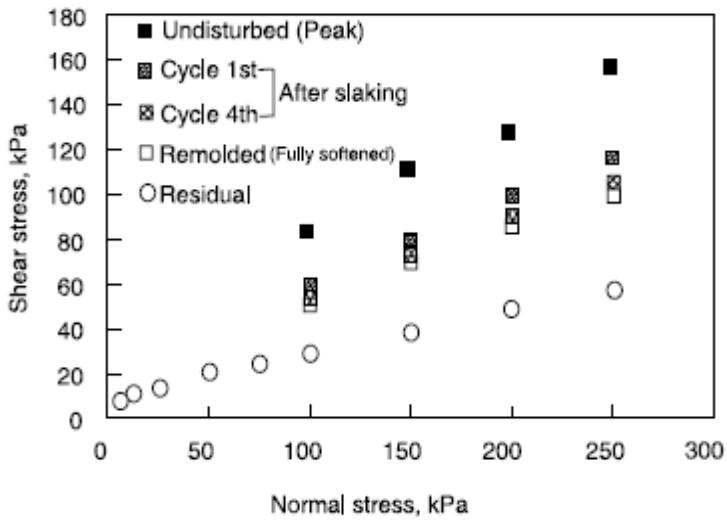

Fig.3.21. Shear strength envelopes for fresh, slaked and remolded mudstone specimen (Bhattarai et al., 2007)

The effect of water content on the creep behaviour of soft rock was studied by Jongpradist and Horii (2007). Drained triaxial creep tests of specimens with 80%, 40% and 10% saturation degree were performed at the same stress state. The graph of the axial creep strain as a function of time is shown in Fig. 3.23. The magnitude and rate of axial creep strain at the same loading time is largest when the saturation degree is 80% and decreases as the saturation degree decreases. Furthermore, creep leads to failure at about 800 minutes in the case of 80% saturation degree, while this phenomenon is not observed during the tests with 40 % and 10 % saturation. This means that creep of soft rock is more significant with the increase of water content. Yoshida et al. (1997) computed the strength envelope for mudstone shown in Figure 3.24 along with its variation with time due to softening. It shows that the stable slope now will be change to unstable with the elapsed of time. This example illustrates the deterioration of mudstone due to softening, especially weathering.

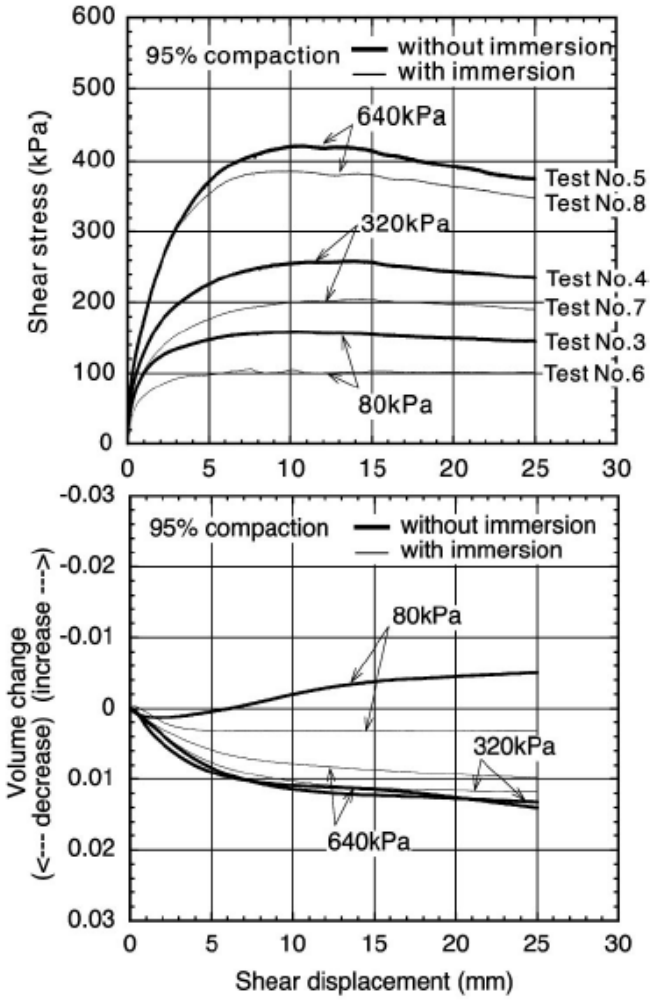

Fig. 3.22 Shear stress–shear displacement–volume change relationships (Yoshida et al., 2004)

Chen (1997) performed uniaxial compressive tests on Gutingken mudstone, Taiwan under different water contents. Obviously, the author found that the uniaxial compressive decreases with increase in water content (Fig. 3.25). According to Fig.3.25, when the water content increases from 0% to 9-10%, the uniaxial compressive strength of Gutingken mudstone

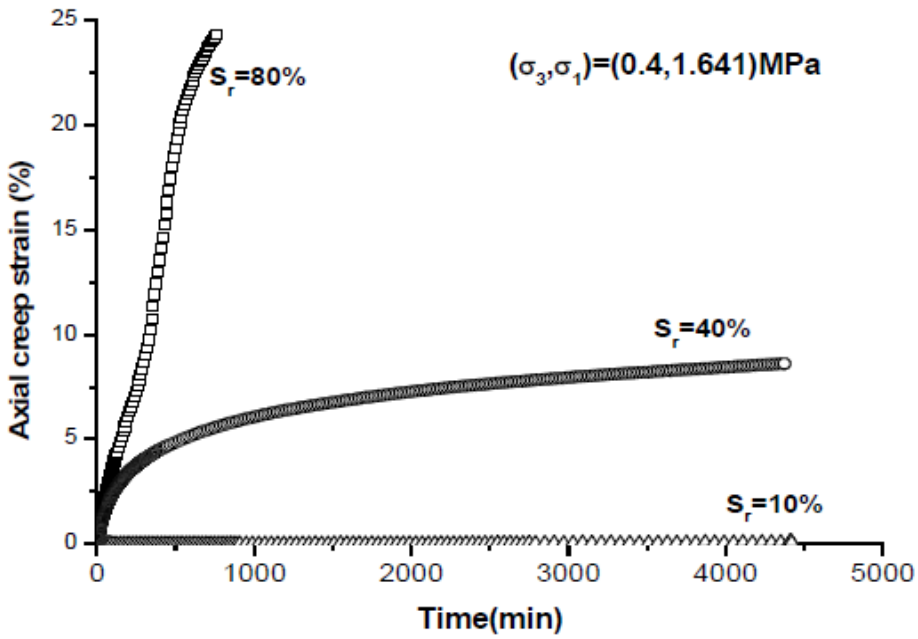

Fig. 3.23 Results of creep test with different saturation degree at the same stress (Jongpradist and Horii (2007))

reduces from 39.6 MPa to 3.5 MPa, and the failure strain increases from 1.42% to 2.5%. Figure 3.26 shows that the loosely packed specimens composed of crushed mudstones (US1 and US2) begin to settle immediately after being submerged in water. On the other hand, densely packed specimens (US3, D1 and D2) do not show any settlement. The specimen D2 composed of dry crushed mudstones exhibits relatively very small swelling instead of compression after saturation with water (Nakano et al., 1998).

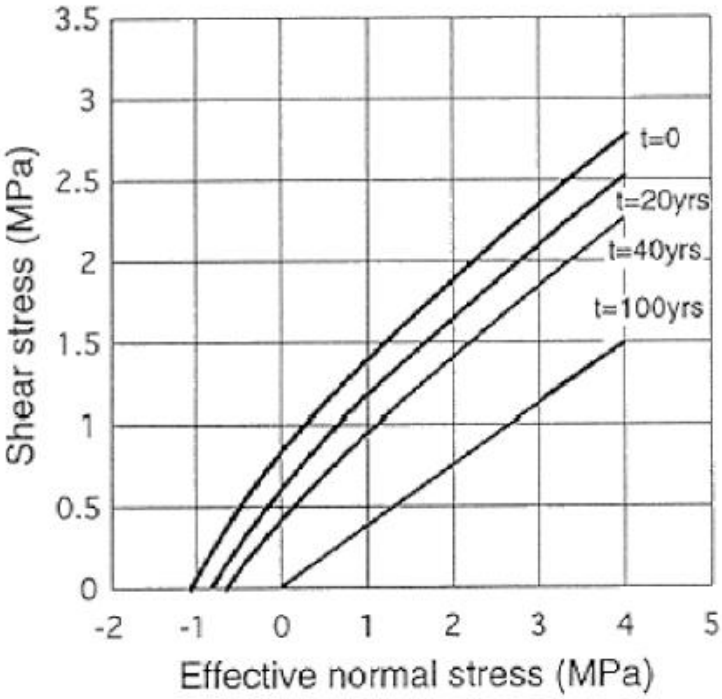

Fig. 3.24 Results of creep test with different saturation degree at the same stress state (Yoshida et al., 1997)

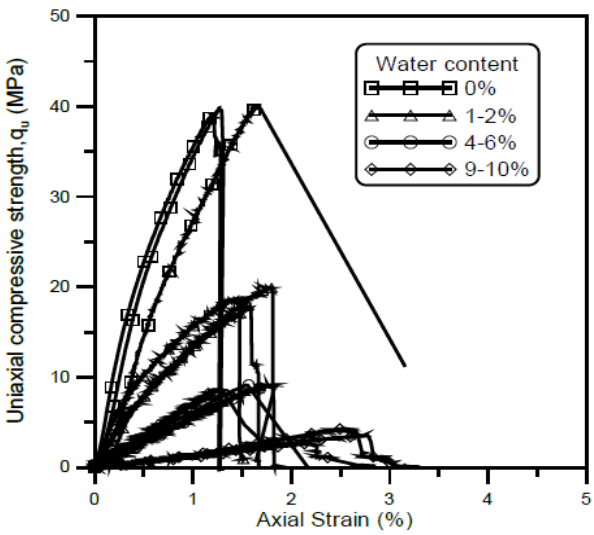

Fig. 3.25.Uniaxial compressive tests under different water contents (Chen, 1997)

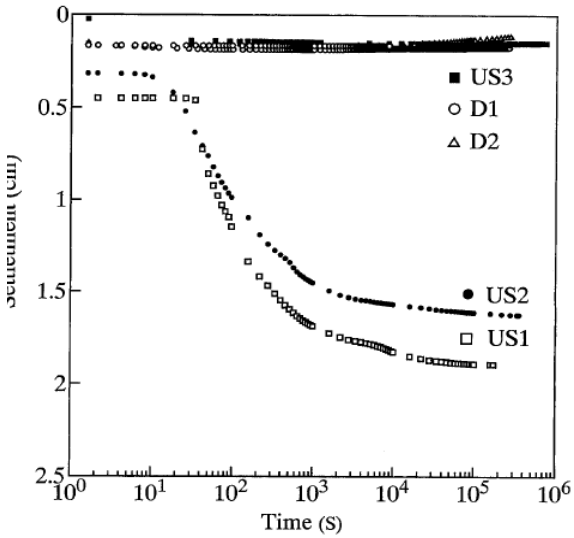

Fig. 3.26 Settlement behaviour after submergence (Nakano et al., 1998)

The effect of drying and wetting on the engineering properties was investigated in terms of peak deviator stress and elastic modulus under triaxial conditions by Youn and Tonon (2010). Figure 3.27a shows stress–strain curves of the four tested clay-bearing rocks in fresh conditions and Fig. 3.27b shows the stress–strain curves after one cycle of drying and wetting. By comparing the stress–strain curves in Fig. 3.27a and b for the same material, it is readily recognizable how sharply the elastic modulus decreased after the drying–wetting cycle.

Mechanical anisotropy of compositionally layered shale may be weak, given a relatively weak preferred orientation of illite (or other phyllosilicates). Ibanez and Kronenberg (1993) found that the strength of soft rock largely depends on the orientation of bedding plan with respect to the load applied (Fig. 3.28). The strengths of shale samples compressed parallel, perpendicular, and at 45 ° to bedding are strongly dependent on confining pressure applied on it (Fig. 3.29).

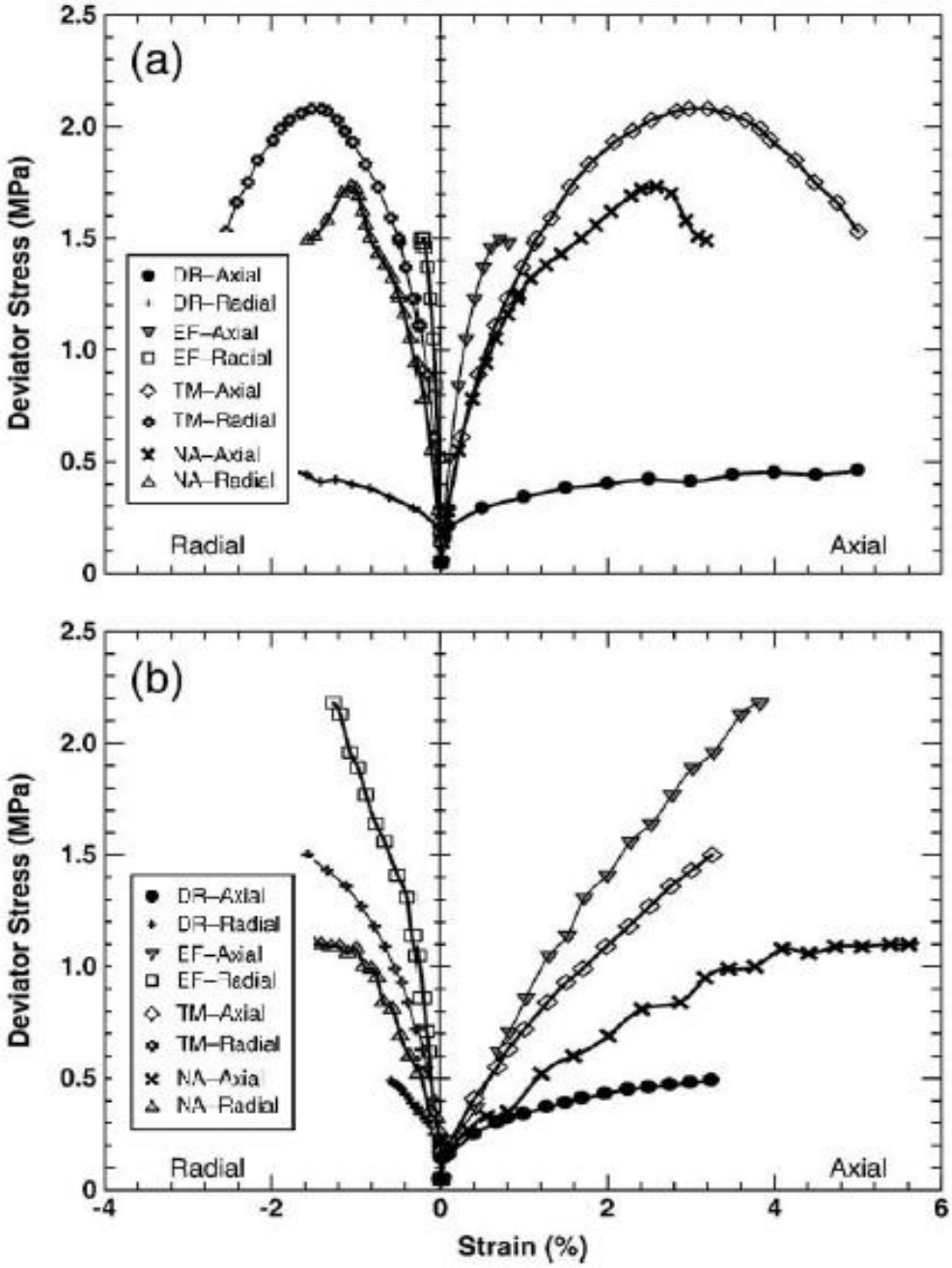

Fig. 3.27 Stress–strain curves: (a) fresh material (b) after 48 h of air-drying for Del Rio Clay (DR), Eagle Ford Shale (EF), Taylor Marl (TM), and 24 h of air-drying for Navarro Shale (NA) (Youn and Tonon, 2010)

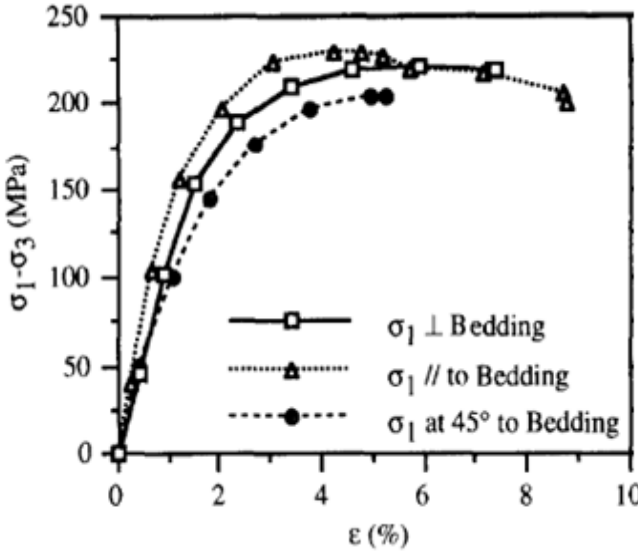

Fig.3.28. Stress-strain curves for shale samples compressed perpendicular, parallel and at 45 ° to bedding (Ibanez and Kronenberg, 1993)

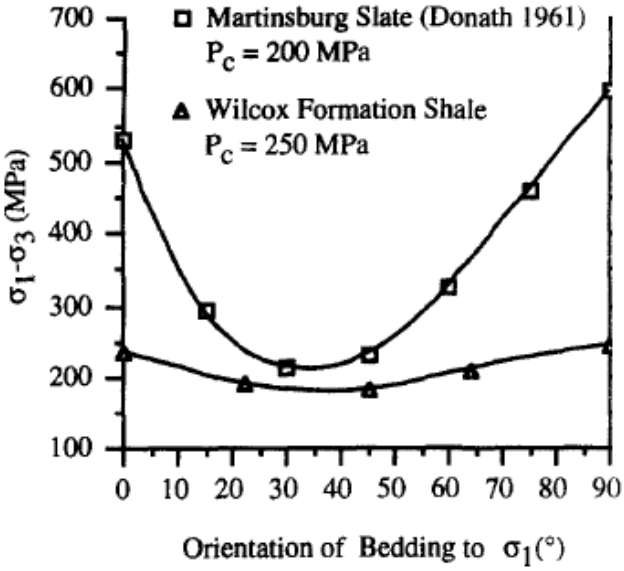

Fig.3.29. Comparison of the weakly defined strength anisotropy of the Wilcox formation shale with that of Martinsburg slate (Ibanez and Kronenberg, 1993)

3.7 Conclusions

After the literature review, it is clear that mudstones are problematic geomaterials. The current tests for slaking susceptibility all involve measuring the effects of wetting and drying cycles under unconfined conditions. It is clear that these methods do not provide adequate information regarding the effects of this slaking on the strength and deformation behavior of clay shale in the field. The author has found virtually no literature involving research on the effects of slaking on strength and deformation under confining stress condition as in real field. So, the effects of slaking and reduction of strength and deformation characteristics of mudstones is still a key concern for geotechnical engineer.

CHAPTER 4

EXPERIMENTAL SETUP

4.1 General

This chapter describes the selected material, its physical properties and origin, samples preparation procedure, particle size distribution and general slaking test. Similarly, the reason behind the choice of this particular material and apparatus, loading conditions and the general experimental procedure are also presented in this experimental setup section.

4.2 Materials

As discussed in Chapter 1, a lot of geotechnical engineering problems have been observed in soft sedimentary rock formations mainly in mudstones. The term “mudstones” refers to the fine-grained, siliciclastic sedimentary rocks (claystones, mudrocks, siltstones, and shales) in which more than 50% of the particles are smaller than 0.06 mm in size (Folk et al., 1970; Grainger, 1984 and Dick and Shakoor, 1992). The mudstones undergo both mechanical and physical weathering due to cyclic wetting and drying which could lead to a drastic loss of strength and stiffness, instability of natural slopes and excessive settlement of embankments. The intension of using crushed mudstone is to accelerate the slaking rate in the laboratory and also for necessary adjustments to the size of direct shear box.

Fig. 4.1 Hattian Bala mudstone

Fig. 4.2 Ishikawa mudstone

Fig.4.3 Chiba gravel

Four types of geomaterials shown in Figure 4.1-4.4 were used for evaluating slaking characteristics of geomaterials from different parts of Japan and Pakistan. Out of these four geomaterials, two materials are mudstones from Pakistan and Ishikawa, Japan. The remaining two materials were Chiba gravel (Chiba gravel) and Toyoura sand (Silica sand) which are very popular granular materials for geotechnical experiment. Only few a experiments were performed on Chiba gravel and Toyoura sand to compare their strength and deformation characteristics with that of crushed mudstones. Similarly few tests on completely non slakable material (Glass beads) were also carried out to compare slaking characteristics with geomaterials (Fig. 4.5). Out of these materials, crushed mudstone from Hattian Bala, Pakistan was used as main material for this research.

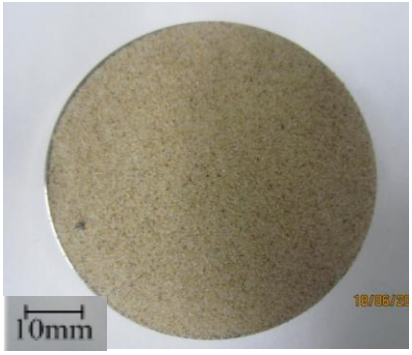

Fig. 4.4 Toyoura sand

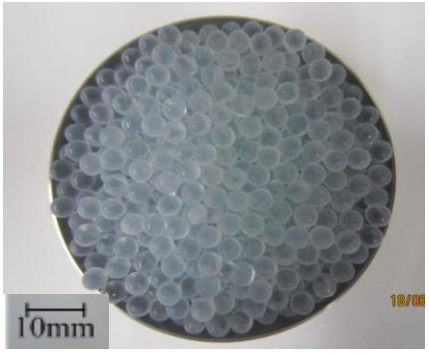

Fig. 4.5 Glass beads (4 mm dia.)

4.2.1 Sampling site

a) Hattian Bala mudstone

The Hattian Bala mudstone used in this investigation was obtained from the earthquake induced landslide dam, formed by the 2005 Kashmir earthquake, which is located southeast of Muzaffarabad, Pakistan (Fig 4.6 and 4.7). The earthquake induced landslide dam was suddenly breached on 9th February, 2010 just after moderate rainfall preceded by drought. Slaking of mudstone was assumed to be one of the major causes of the failure (Sattar et. al., 2010, Kiyota et. al., 2011).

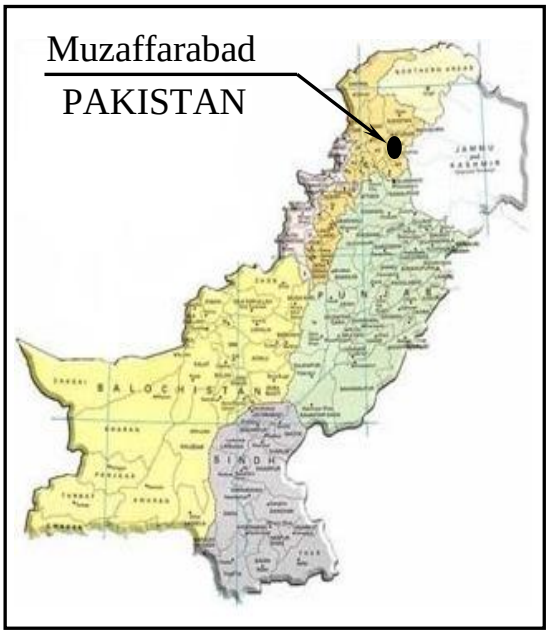

Fig. 4.6 Location of sampling site for Hattian Bala mudstone

The site is geographically located approximately 34.14800° North latitude and 73.722183° East longitude (Fig. 4.6). From a geological point of view, the source area is formed of Miocene aged Murree formation (Dunning et al., 2005 and Mirza et. al., 1996 etc.), composed of alternate layers of mudstone and sandstones with minor intercalations of limestone and conglomerates indicating its fluvial deposition environment. The fine grained mudstones are mostly deep red in color (Fig.4.1), being indicative of high iron contents. Kiyota et al. (2010) and Aziz et al. (2010) also used Hattian Bala mudstones for their research.

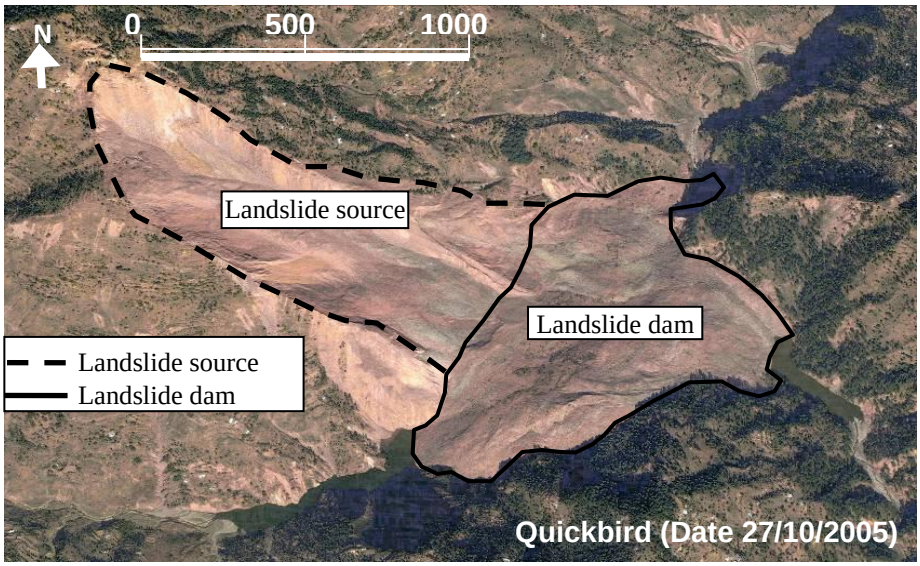

Fig. 4.7 Quick Bird view (27th Oct. 2005) of Hattian Bala landslide dam (Kiyota et al., 2011)

b) Ishikawa

The mudstone blocks collected form Ishikawa as shown in Fig. 5.8 was later crushed in the laboratory to specific particles sizes as a necessary adjustment to the apparatus dimension.

The site is geographically located approximately 36.4610° North latitude and 136.6251° East longitude. From a geological point of view, the source area is Sedimentary rock formation formed during middle-upper Miocene epoch.

Fig. 4.8 Mudstone extracted from Ishikawa, Japan

Fig. 4.9 Location map of Ishikawa

c) Chiba gravel

Chiba gravel is crushed well-graded angular sandstone from a quarry in Chiba, Japan. It is a very common granular geomaterial used in geotechnical laboratories in Japanese universities.

d) Toyoura sand

Toyoura sand originates from weathered granite in Toyoura, Yamaguchi prefecture, Japan. It has been extensively used as a standard material in geotechnical laboratory experiments in Japan for the last two decades e.g. Qui et al. (2000) and Wu et al. (2008), in direct shear test, Tatsuoka et al. (1986) in Plane strain compression (PSC), Goto (1986), in triaxial compression (TC) etc.

4.2.2 Physical properties of test materials

The particle size distribution (PSD) curves and physical properties of the crushed mudstones, Chiba gravel, Toyoura sand and Glass beads are presented in Fig 4.10- 4.14. However, the particle size distribution (PSD) and physical properties of crushed mudstones do not match each other because of the effect of manual crushing, the large volume of samples among other factors. The details of other physical properties such as density, void ratio etc are mentioned in Chapter 5 and 6. The effects of particle side distribution on strength and deformation (Igwe et. al., 2007; and Iwasaki and Tatsuoka, 1997) are neglected

in this research. The index properties were determined by following JGS standards. SI is the slaking index of material (details about SI are discussed in Chapter 3), Gs is the specific gravity of solids, D_{50} represents average particles size, Uc corresponds to the coefficient of uniformity (ratio of D_{60} and D_{10}) and F_C is percentage of particles finer than 2 mm sieve for coarser material and for finer material i.e. Toyoura sand, F_C is percentage of particles finer than 0.75 mm sieve.

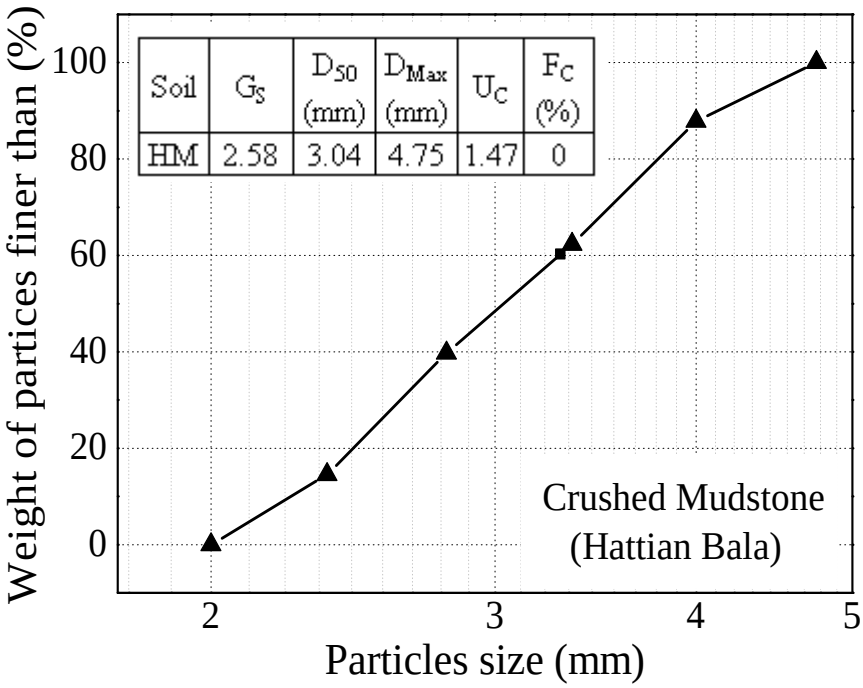

Soil	G_S	D_{50} (mm)	D_{Max} (mm)	U_C	F_C (%)
HM	2.58	3.04	4.75	1.47	0

Fig. 4.10 Physical properties and particles size distribution of the test materials from Hattian Bala, Pakistan

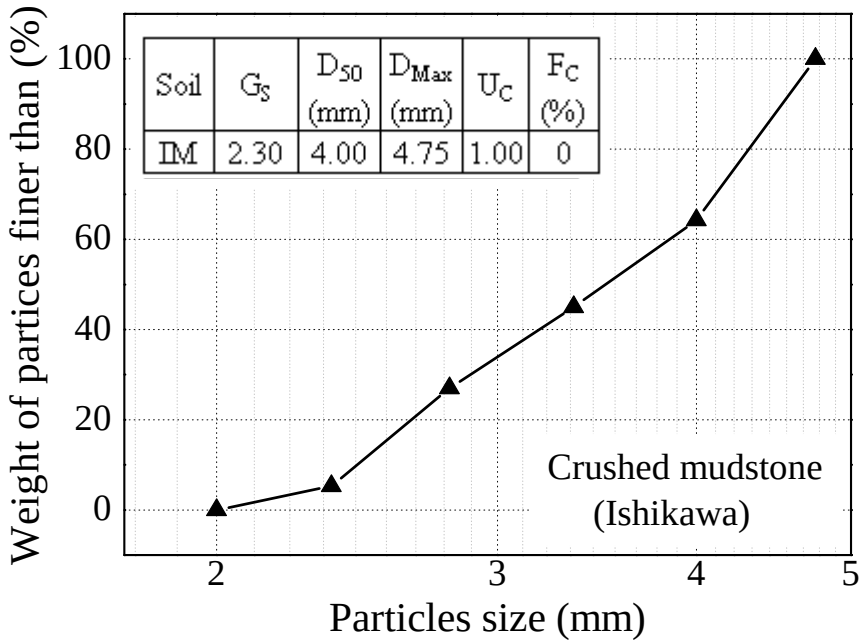

Fig. 4.11 Physical properties and particles size distribution of the test materials prepared by crushed soft rocks from Ishikawa, Japan

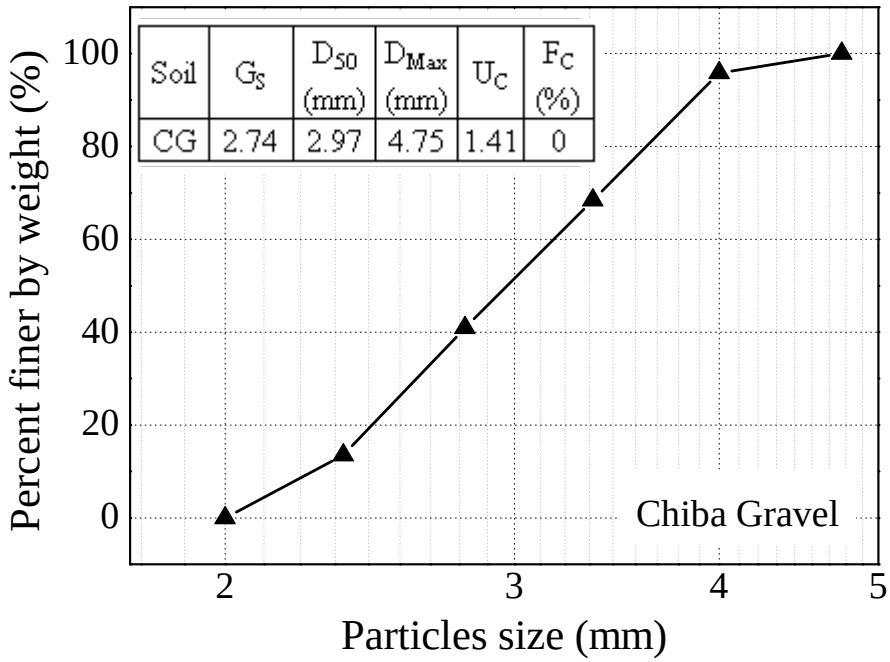

Fig. 4.12 Physical properties and particles size distribution of Chiba gravel

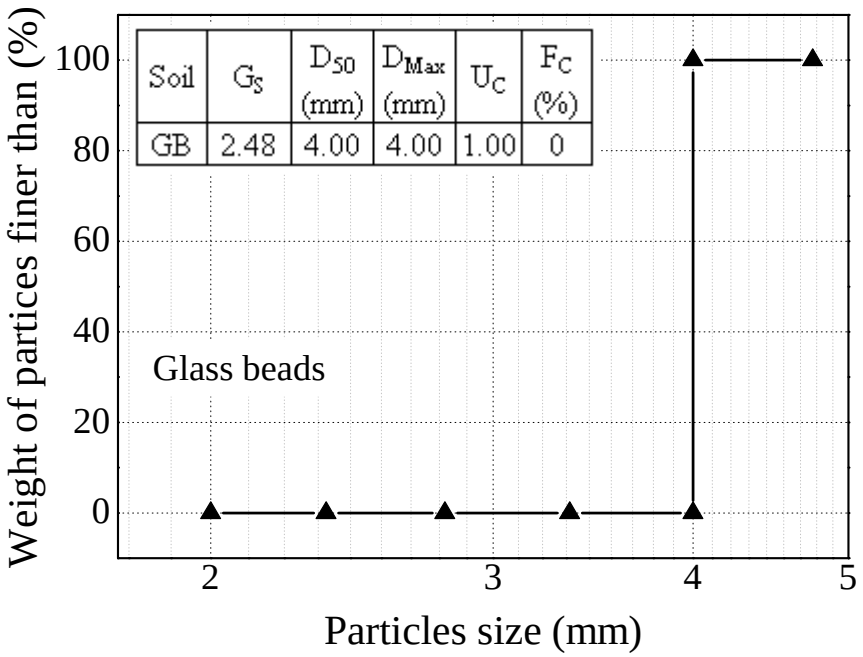

Fig. 4.13 Physical properties and particles size distribution of the test materials (Glass beads)

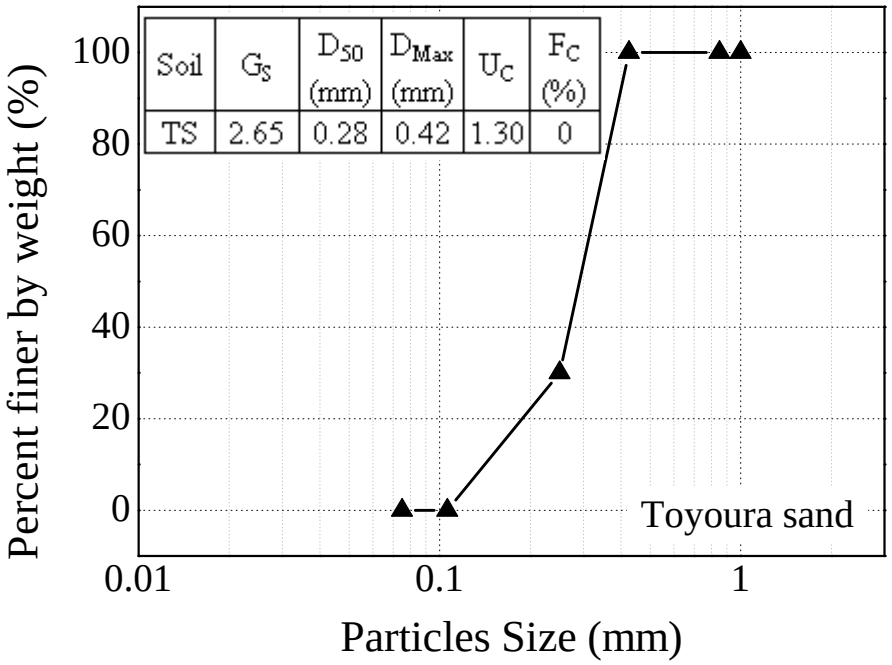

Fig. 4.14 Physical properties and particles size distribution Toyoura sand

4.2.3 General slaking test

a) Slaking index (JGS-2125)

In order to obtain the slaking index of the specimens, accelerated rock slaking tests (JGS 2125-2006) on crushed mudstone (Hattian Bala and Ishikawa), Chiba gravel and Glass beads were conducted.

In this test, there pieces of rock lumps which had approximately a volume of 50 cm^3 were taken (Fig 4.15). Each piece of the test sample was placed in a separate container and was oven-dried at a temperature of 40^0C. The distilled water was poured subsequently into the container until the specimen was fully immersed (approximately within 1 minute). The specimen was immersed for 24 hours. This represents one cycle. Specimens were then subjected to the same treatment during 3 successive cycles. To find the Slaking index of tested material, all samples were then described in terms of crack development and any disintegration that might occur as listed in Table 4.1 provided by JGS- 2125. Sadisun et al. (2002 b) also proposed a similar slaking classification. Photographs were taken before and after immersion.

Fig. 4.15 Fresh specimen before slaking test (Hattian Bala mudstone)

Table 4.1 Slaking classes (JGS 2125-2006)

Class	0	1	2	3	4
A					
	There is no change.	Orginially shape remains with a few craks	Many cracks appear, specimen is divided into some fragments, and original shape can be recognized	Whole body has crumbled; however not muddy. Original shape cannot be recognized	Whole body is muddy.
B					
	There is no change.	Original shape remains with a few cracks or with light circumferential disintegration.	Cicrumference has crumbled and it is diffucult to recognize orginal shape.	Cicumference has crumbled completely and separated into many particles. Orginial shape cannot be recognized.	Whole body is sandy

A: Typical states for mudstone of fine-grained tuff B: Typical state for siltstone, sand stone or coarse-grained tuff

b) Static slaking test (Santi, 1998 and Sadisun et al., 2002b)

The procedure of a static slaking index test is quite similar to the dry–wet cyclic slaking test. In this test, six pieces of parent rock which were taken had a mass between 100 and 150 grams as shown in Fig. 4.16. Each piece of the test sample was then placed in a separate beaker and oven-dried to a constant mass at 105^0 C. The oven dried rock pieces were cooled at room temperature. The distilled water was then poured into the beakers so that the rock pieces were covered by at least 10 mm of water. After about 24 hour of immersion, the samples were washed with water on a 2 mm standard sieve (No. 10 sieve). The material retained on the sieve was then put again into the beaker, decanted and oven-dried to a constant mass. The weight of the mass retained on 2 mm (no. 10 sieve) was recorded. The percentage of loosened sample to initial oven dried mass is calculated and recorded as a slaking index value (Is) for that cycle, or it can be defined by the following equation.

$$I_S = \frac{W_x - W'_x}{W_x} \qquad \text{.....} (4.1)$$

Where, W_x = total initial mass of oven dried material; W_x' = total mass oven dried material retained on the 2.00 mm sieve

Fig. 4.16 Six set of specimens for static slaking test of Ishikawa mudstone

On the basis of I_s value after one cycle, the slaking susceptibility of geomaterials is evaluated as Table 4.2.

Table 4.2 Class value of I_{s1}

S.N.	I_{s1}	Slaking susceptibility
1	0-2 %	Very low
2	2-10 %	Low
3	10-25 %	Medium
4	25-50 %	High
5	50-85 %	Very high
6	85-100 %	Extremely high

c) Slaking ratio (NEXCO- 100, 2006)

In this test, three sets of specimens of rock lumps were taken. Each set had a mass of 3 kilograms. The specimens were prepared by removing lumps finer than 19 mm and larger than 37.5 mm. Each set of specimens was kept in the oven until a constant was obtained at 105 ^{0}C. The oven dried rock lumps were cooled at room temperature. The distilled water was then poured into the pan so that the rock pieces were covered by at least 10 mm of water for 24 hours (Fig. 4.17). This represents one cycle and specimens were subjected to the same treatment during 5 successive cycles.

Fig. 4.17 Wetting of the Mudstone specimen in water during a slaking ratio test (Hattian Bala mudstone)

Then, the samples were washed with water on a 9.5 mm standard sieve. The material retained on the sieve was then put again into the oven and dried to a constant mass. The weight of mass retained on 9.5 mm was recorded. The percentage of retained sample on 9.5 mm sieve to initial oven dried mass is calculated and recorded as a slaking ratio value (Sr) for that cycle, or it can be defined by the following equation.

$$Sr = \frac{W_x - W'_x}{W_x} \quad \ldots\ldots\ldots\ldots\ldots\ldots\ldots\ldots\ldots\ldots\ldots\ldots \quad (4.2)$$

Where, W_x = total initial mass of oven dried material; W_x' = total mass oven dried material retained on the 9.00 mm sieve

d) Water absorption test

Slaking of mudstones due to cyclic wetting and drying is influenced by their ability to absorb water (Saffet, 2000; Erguler and Ulusay, 2009 and Cao et. al., 2006 etc.). Absorbed water is the water that, during submergence, fills the void spaces present in mudstones. However, because of the fact that most mudstones contain a certain amount of clay minerals which can adsorb water during submergence, absorption measurements usually also include a certain amount of adsorbed water. Water absorption was determined using a slightly modified procedure form of ASTM method C 97 (ASTM, 1987). The test requires submerging three sets of dried mudstones samples in water with each sample weighing at least 20-30 grams (Fig 4.18). To reduce the slaking of the tested samples, the absorption test was initiated at the natural water content of the samples. After 48 hours, the samples were removed from the water, surface dried, and weighed. The saturated samples were then oven dried at 105° C for 24 hours and then weighed. The percent absorption was calculated as follows:

$$Water\ absorption = \frac{W_w - W_d}{W_d}\ \% \quad \ldots\ldots\ldots\ldots\ldots\ldots\ldots\ldots \quad (4.3)$$

Where, W_w is saturated weight of samples and W_d is dry weight of samples.

The average value calculated from three sets of samples was defined as the water absorption of crushed mudstones.

Fig 4.18 Three sets of pycnometers inside the vacum to release air from the pores (Ishikawa mudstone)

4.2.4 Specimen preparation

As already mentioned, Slaking characteristics of crushed mudstones (Hattian Bala and Ishikawa) are analyzed in this study. There are two main reasons for selecting crushed mudstones. Firstly, the soils or rocks with in a slip layer of landslides are generally in a crushed state. Secondly, it greatly increases expose (surface) area of mudstones which will accelerate the slaking process in the laboratory. Moreover, the proper ratio of the shear box length to the mean particles size should be maintained (Jewell and Worth, 1987).

Both Hattian Bala mudstones and Chiba gravel are naturally crushed geomaterials. But, Ishikawa mudstones were needed to be crushed to a specific grain size for the preparation of the direct shear test specimen. Manual crushing with a wooden hammer was carried out. Both naturally and artificially crushed mudstones were sieved to retrieve particles finer than 4.75 mm and larger than 2 mm. The basic physical and index properties of tested materials were determined.

4.2.5 Sieve analysis

The crushed mudstones used in this study are comprised of grains which are susceptible to disintegration due cyclic wetting and drying. As described in the chapter 3.3,

the effect of slaking due to cyclic wetting and drying on crushed mudstones can also be quantified by determining particles degradation after a certain number of cyclic wetting and drying. The mechanical properties of granular materials are strongly dependent on the particle size distribution (Igwe et. al., and Iwasaki et. al., 1977). It is necessary to quantify the particles disintegration due to wetting and drying induced by using a proper index to analyse the slaking characteristics of geomaterials. In order to quantify particles disintegration due to slaking, sieve analyses were performed both before and after experiment

Particles crushing and degradation index

Generally, the amount of fines (F_C) measured after the experiment indicates the extent of particles crushing. However, overall changes in particles sixe distribution cannot be described adequately using a single aperture, such as a 2 mm sieve because it only calculates the amount of particles becoming finer than 2 mm sieve size. Therefore, the fragment size distribution approach was used in this study to better define the particle disintegration. The sieves used for particles size distribution included the following sizes: 4.75, 4.0, 3.35, 2.80, 2.36 and 2.0 mm. According to the fragment size distribution approach (Erguler and Shakoor et. al., 2009; Aziz et. al., 2010), a degradation index, I_D is defined on the basis of area under particles size distribution curve before and after experiment as shown in Fig. 4.19a. Many researchers have used different kinds of indexes for particles disintegration like grading index, I_G (Wood et al., 2008) and relative breaking index, Br (Einav et. al., 2007). Here, degradation index, I_D has been developed from these previous studies (Aziz et. al., 2010).

Figure 4.19b shows the advantages of I_D upon F_C to measure particles crushing during the experiment. For the same value of F_C different index, I_D values and shape of particles size distribution curved can be observed. There, degradation index, I_D can be used over all particles crushing for a given samples better than F_C. The particles size distribution curves of all specimens before and after experiment under different test conditions are presented in the Chapter 5.

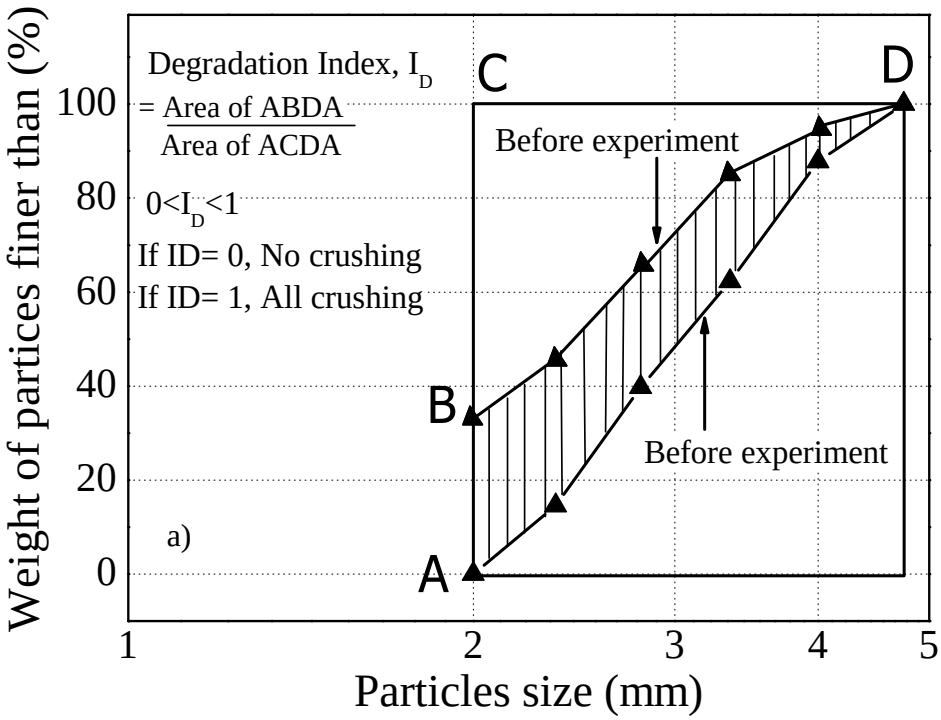

Fig 4.19 Definition of the degradation index, I_D

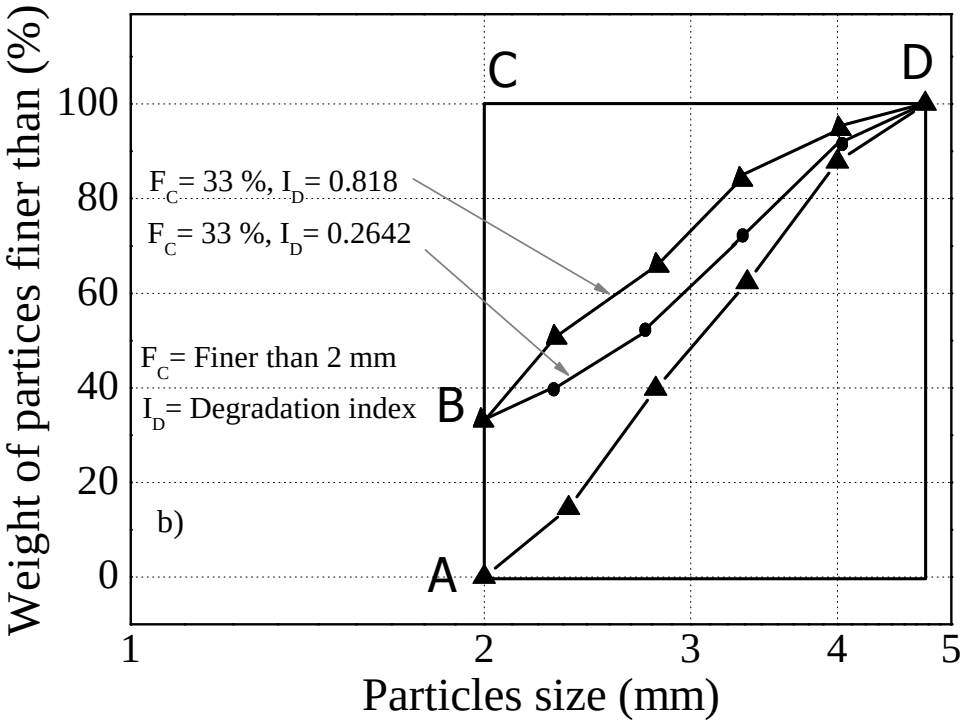

Fig. 4.19 Effect of shape of particles size distribution curve on the degradation index

4.2.6 X-Ray diffraction

X-ray diffraction analysis is the standard method for identifying clay mineralogy. The analysis provides semi-quantitative determinations of the various mineral constituents. The analysis was performed using a two-theta X-ray diffractometer. All analyses were conducted using a copper K-alpha source, equipped with a monochrome filter. Initial scans covered from 2 degrees to 60 degrees two-theta. Oriented ceramic-tile type mounts of each sample were prepared using the 2- micron (0.002 mm) and smaller size particles (Fig 4.20). This technique required mixing 10 to 20 grams of powder mudstone sample that passed sieve # 200 with 2 % sodiumhexametaphosphate and distilled water. The 2-micron size was selected because it is the optimum size for separating the clay minerals from the non-clay mineral components (Grim, 1969). This arrangement of x-ray scanning enabled the identification of clay mineral species according to characteristic basal diffraction peak positions, peak areas and relative intensities. The scans also provided the basis for estimating the quantity of each clay mineral species, according to a semi-empirical method developed by many researchers. Hattian Bala and Ishikawa mudstones were used for X-ray diffraction analysis.

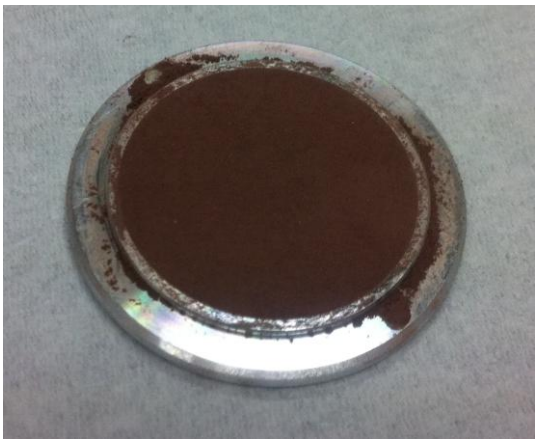

Fig. 4.20 Sample preparation for X-Ray Diffraction (Hattian Bala mudstone)

4.3 Modified direct shear apparatus

In the last few decades an enormous growth in the development of numerical tools likes FEM, DEM etc. for complex geotechnical engineering analysis has been achieved. The use of such tools demands advanced experiments to obtain the experimental characterization of the mechanical behavior of materials and to simulate the field condition as accurate as possible. Laboratory testing has provided the lifeblood for advances in modern geotechnical engineering. There are a number of advantages that laboratory testing offers; the sample and the failure modes can be observed physically which may help to understand anomalies and explain variations in the test results, index tests of the same material can be performed on

the same specimens, stresses can be directed towards the actual stress path, drainage condition can be controlled and stress, strain and pore water pressure can be measured from low strain to failure. Experiments are the only means by which cause and effect can be established. It has already been noted that an experiment differs from non-experimental methods in that it enables us to study cause and effect because it involves the deliberate manipulation of one variable, while trying to keep all other variables constant. However, there are some drawbacks to laboratory experiment. In the laboratory, it is almost impossible and expensive to prepare exact specimen with the structure and fabric as in the field. All samples are disturbed to some extent, which affects their strength and stiffness. A good quality laboratory requires a variety of specialized equipment and technicians with the training and skills to properly use that equipment. Despite these drawbacks, there are an increasing number of ways that laboratory testing can contribute to geotechnical practice.

For this research, modified direct shear apparatus was used for evaluating slaking characteristics of geomaterials. The details of modified direct shear apparatus are discussed later.

4.3.1 Application of direct shear

Direct shear test is simple in principle, quick and inexpensive. It is used especially to determine the shear strength of both cohesive as well as non-cohesive soils. Direct shear provides essential design parameters in the stability analysis of slope failures or foundation where lateral displacements are involved in the soil mass (Hanzawa, 1992). The advantages and disadvantages of direct shear tests are given below.

Advantages of direct shear testing are as follows:

- The test is relatively inexpensive and quick to perform. It is also easier to interpret the results.
- Rapid drainage can be achieved due to smaller thickness of sample.
- It has been found that soil parameters ϕ and c obtained by direct shear testing are nearly as reliable as triaxial values obtained by triaxial testing. Typical values obtained with the direct shear test are 1 to 2 degrees larger than values obtained with the triaxial test.
- It is good for measuring residual strength values.

Disadvantages or limitations of the direct shear test (Holtz and Kovacs, 2003) are as follows:

- Failure occurs along a predetermined failure plane which may not be weakest plane.
- Non-uniform distribution of shear stress along the failure surface. Initial failure occurs at the corners and ends of the box, and propagates towards the center.
- Area of sliding changes as the test progresses.
- There is an uncontrolled rotation of principal planes and stresses that occurs between the start of the test and failure.

4.3.2 Outline of apparatus

A number of factors are to be considered in the design of a direct shear apparatus (DSA). Indeed, the DSA has a number of inherent drawbacks as already mentioned, mostly originating from inevitable non uniform stress and strain condition associated with a progressive failure in the potential (horizontal) shear zone. Numerical analyses of the deformation and failure of granular material in direct shear by finite element method (FEM) or more recently by DEM showed that the principle axes of distributed contact force and initial rupture zone may first develop diagonally, not horizontally from the specimen edges (Cui et al., 2006).

To minimize the effects of these inherent drawbacks and to match as much closely a "quasi-simple shear" mode in the potential horizontal shear zone, attempts have been made to optimize the direct shear apparatus design by modifying the conventional type (Jewell et al., 1987; Shibuya et al., 1997; Lings et al., 2004). After Shibuya et al. (1997) and Wu et al. (2008), Fig. 2-3 summarizes the different types of DSA: the conventional direct shear apparatus can be categorized into Type A (ASTM D3080-90) while Type B and Type C refer to modified one in the Fig. 4.21.

The major problems with the conventional one concern: a) the rotation of the upper box; b) the side wall frictions. That is, the normal load is applied to the centre of the top loading platen that is not fixed against rotation. As a consequence, when subjected to lateral shearing, the distribution of normal stress along the central horizontal shear plan becomes inevitably biased (so does the shear stress) to maintain the equilibrium of moment within the specimen , which results in a more progressive mobilization of the shear strength along the central horizontal plan. The vertical load applied at the top loading platen becomes

different from the value acting on the shear plan. This is because of vertical friction acting along the inner walls of upper shear box caused by the volume changes of the specimen is due to the free vertical movement of the upper shear box. To minimize the above mentioned problems in the modified direct shear apparatus (Type B and C in Fig. 4.21), the top loading platen is fixed against rotation. Similarly, to minimize the effect of side wall friction in Type C (the one which was used in this research), the vertical load should be measured at the bottom of the lower shear box (No. 6 in Fig. 4.22) (Shibuya et al., 1997).

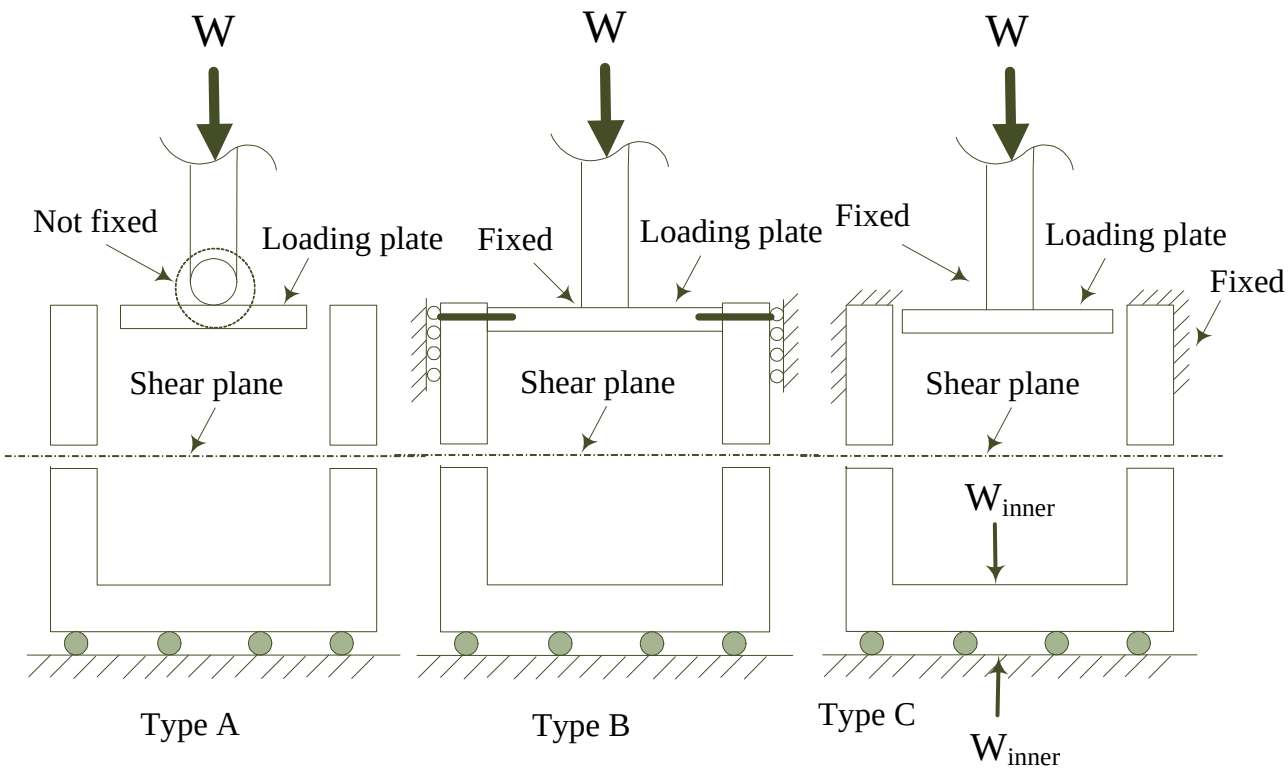

Fig. 4.21 Different type of Direct shear box (Shibuya et al., 1997; Wu et al., 2008)

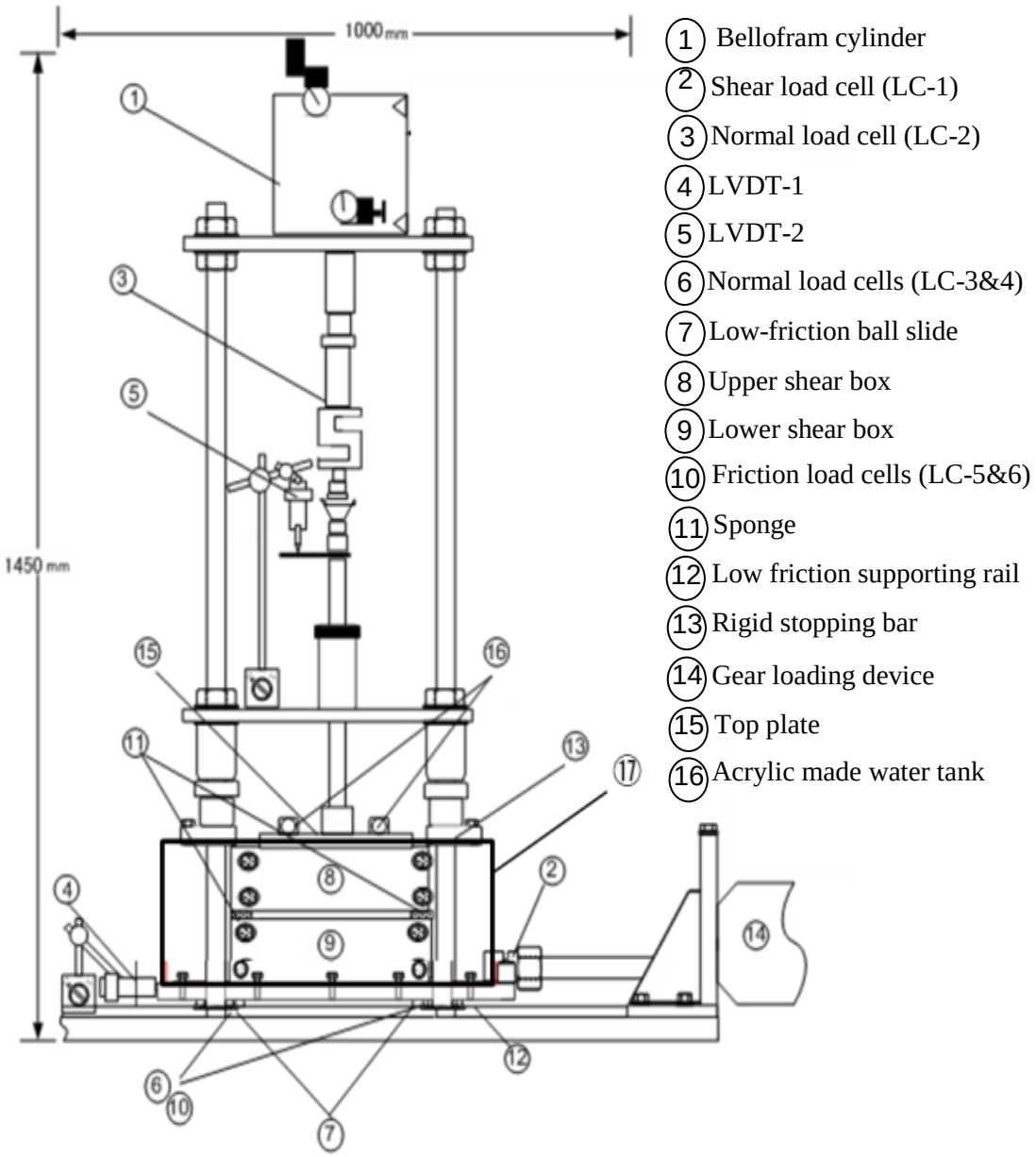

Fig. 4.22 Schematic diagram of modified direct shear apparatus

4.3.3 General description of the apparatus

(1) Shear box

It consists of two metal boxes i.e. upper and lower shear box (No. 8 and 9 in Fig. 4.22) with smooth inner walls. Shear box has inside dimension 20 cm* 20 cm* 10.8 cm. Jewell and Worth (1987) proposed that the proper ratio of shear box length to the mean particle size should be in the range 50-280. According to this criterion, the current shear box dimension is suitable for testing specimen with a mean particle size (D_{50}) up to 4 mm.

However, the size of this shear box is too large as compare to the conventional one. So, the ratio of shear box length to mean particles size derived from conventional shear box may not be appropriate for this large modified shear box.

The lower box (No. 9) moves on a low-friction supporting rail (No. 12). The upper box (No. 8) is fixed by means of two rigid bars (No. 13) to prevent both vertical and horizontal displacements. A piece of sponge tape (No. 11) is glued to the upper periphery of the lower box to prevent sand from spilling out from the opening during shearing as well as to prevent the inside volume of shear box from increasing because of shear displacement so that the volume change occurring in the specimen is due solely to the dilation or contraction of sand.

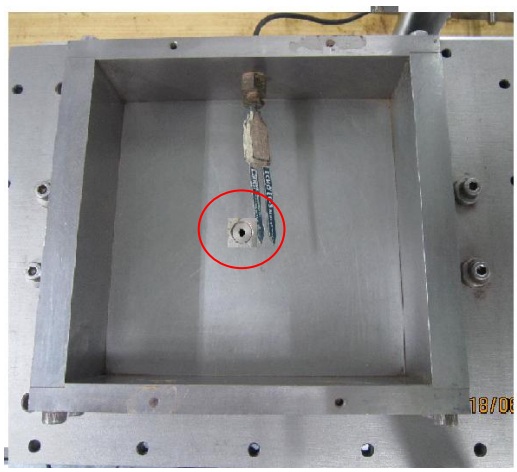

Fig. 4.23 Hole on the bottom of shear box

A suitable prescribed opening (as described later) can be set up in between the lower and upper boxes by inserting an appropriate number of spacers. A hole is provided on the bottom of shear box (Fig. 4.23) to facilitate the supply of water to saturate the specimen and also for removing water from the specimen.

(2) Vertical loading system

Vertical load is applied through air cylinder (No. 1). Normal load cell (No. 3) is used to measure applied upper load. The apparatus has a possible feedback control on normal load to impose any prescribed stress path in the shear stress-normal stress space. The vertical movement of the top shear box is not free; the vertical load applied at the top loading platen becomes different from the value acting on the shear plane due to the vertical friction acting along the inner walls of the top shear box caused by the volume changes of the specimen. To measure the exact loading on the shear plane with respect to the side wall friction, Normal load cells (No. 6) are used to measure the vertical load at the bottom of the lower shear box. Rate of consolidation can be controlled in an automated way.

(3) Shear loading system

The shear load is applied by a high precision gear loading system controlled by servo-motor (Fig. 4.24). The working mechanism of loading system is explained briefly here. The rotation of gear No. 2 is ensured by an A-C analog motor (No. 13) through the speed reduction gear (No. 1). The gear No. 2 is continuously rotating in the same direction while transmitting the rotation to the two bevel gears No. 3 and 4, where two bevel gears No. 3 and 4 are rotating in fixed but in opposite direction. Similarly, the rotation is transmitted to the shaft and loading piston either by one of the Electro-magnetic clutches (EMCs) (No. 6 and 7) depending on the direction of shaft. When one EMC is connected, the other one is unconnected and vice-versa, depending on the applied loading direction. In this way, by using the gear loading device, the direction of shaft rotation can be reversed without problems of backlash. However, in this research, only the loading condition was used i.e. only forward rotation of shaft. Moreover, the displacement can be precisely controlled with an accuracy of 1 μm in an automated way. It can smoothly switch displacement between different loading and displacement stages i.e. load control loading phases, or between load relaxation stages or between sustained loading and constant displacement rate loading etc. Similarly, it can change the displacement rate stepwise or gradually by a prescribed factor by removing/ adding an appropriate number of speed reduction gears. The above mentioned two functions are primordial to evaluate viscous properties of geomaterials accurately.

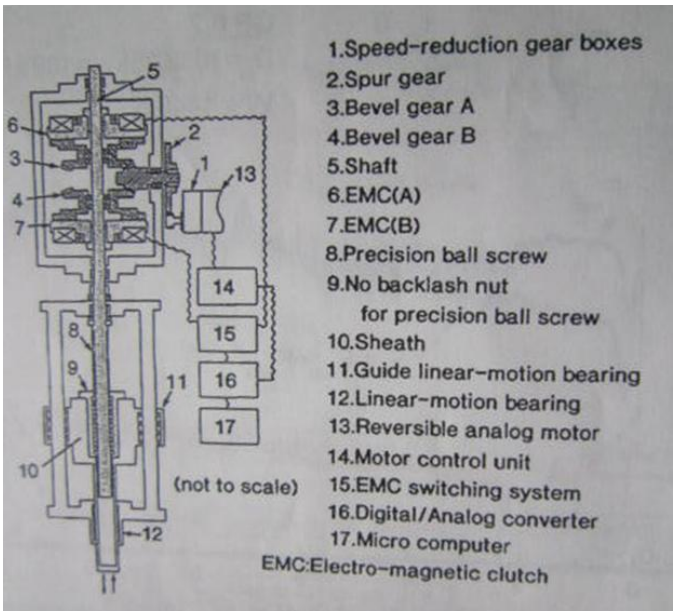

Fig. 4.24 High precision gear loading device (Tatsuoka et al., 1994) used to apply shear load (No. 13 in Fig 4.22)

The importance of all these features in order to obtain reliable data of direct shear tests on granular material was demonstrated by Shibuya et al. (1997), Qui et al. (2000) and Wu et al. (2008). More details of the apparatus are given by Duttine et al. (2008, 2009).

Finally, in this study, another improvement was made concerning the instantaneous measurement of water content of specimen inside shear box. A moisture sensor was inserted

into the lower shear box (Fig. 4.24) to measure the water content of specimen inside shear box. The details of the moisture sensor are presented in 4.3.3..

4.3.4 Moisture sensor

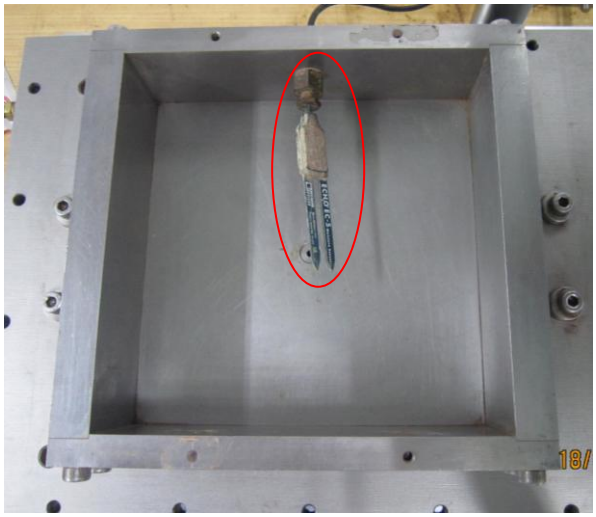

Fig. 4.25 Moisture sensor inserted inside shear box

Decagon's ECH2O (EC-5) sensor (Fig. 4.26) was used to measure the water content of the specimen inside the shear box. It is a very simple and compatible instrument for the direct shear box. Decagon's ECH2O (EC-5) sensor measures the volumetric water content of the soil by measuring the dielectric constant of the soil, which is a strong function of water content. However, not all soils have identical electrical properties. Due to the variations in soil bulk density, mineralogy, texture, salinity and surrounding environment, the dielectric constant of soil is no constant. The manufacturer, Decagon recommends that ECH2O (EC-5) sensor users conduct a soil-specific calibration for best possible accuracy in volumetric water content measurements. An independent researcher (Czarnomski et al., 2005 etc.) found that resolution, precision and repeatability of ECH2O (EC-5) sensors are excellent.

Fig. 4.26 Moisture sensor

To minimize the possible data errors as well as to a develop relationship between water content by weight (w) and displayed Raw value (R in mv), the calibration of moisture sensor under same conditions as in experiment was carried out. ECH2O (EC-5) calibration generally followed the general procedure for calibrating capacitance sensors outlined by Starr and Paltineanu (2002). Calibration graph of ECH2O (EC-5) sensor for Hattian Bala

and Ishikawa mudstones are shown in Fig. 4.27 and 4.28 and data are summarized in Table 4.3 and 4.4 respectively.

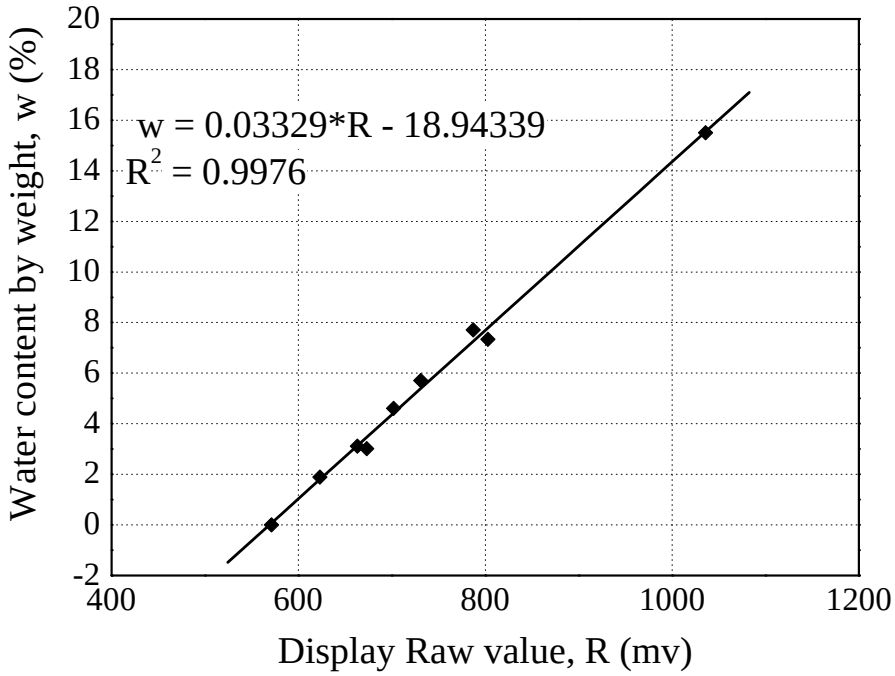

Fig. 4.27 Relationship between water content, W and display raw value, R (Hattian Bala)

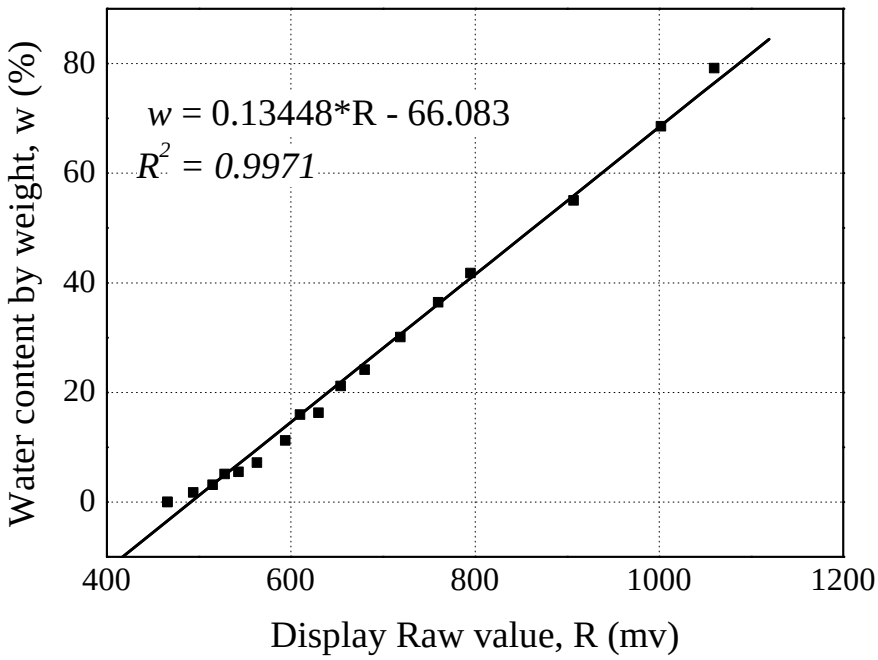

Fig. 4.28 Relationship between water content, W and display raw value, R (Ishikawa)

Table 4.3 Calibration of Moisture sensor for Hattian Bala mudstone

S.N.	Sensor out put		Container mass (g)	Sample volume (cm^3)	Wet soil mass + container (g)	Dry soil mass + container (g)	Mass & Volume of water (cm^3)	Dry soil mass (g)	Soil bulk density (g/cm^3)	Water content by mass of soil (%)	Average Water content by mass of soil (%)	Volumetric water content (cm^3/cm^3)	Average Volumetric water content (m^3/m^3)
	m^3/m^3	Raw constant, R											
0	0	571										0.000	
1	0.091	673	29.06	52.177	110.01	107.64	2.37	78.58	1.506	3.016	3.013	0.045	0.045
			29.23	52.177	109.33	106.99	2.34	77.76	1.490	3.009		0.045	
2	0.202	803	29.12	52.177	115.24	109.7	5.54	80.58	1.544	6.875	7.335	0.106	0.113
			29.04	52.177	114.92	108.71	6.21	79.67	1.527	7.795		0.119	
3	0.408	1036	29.04	52.177	119.9	110.76	9.14	81.72	1.566	11.185	15.51	0.175	0.243
			29.2	52.177	121.5	109.61	11.89	80.41	1.541	14.787		0.228	
			28.27	52.177	125.02	111.51	13.51	83.24	1.595	16.230		0.259	
4	0.049	623	29.06	52.177	111.41	109.93	1.48	80.87	1.550	1.830	1.887	0.028	0.029
			29.14	52.177	111.96	110.38	1.58	81.24	1.557	1.945		0.030	
5	0.083	663	29.35	52.177	107.92	105.52	2.4	76.17	1.460	3.151	3.119	0.046	0.047
			29.15	52.177	112.68	110.14	2.54	80.99	1.552	3.136		0.049	
			29.53	52.177	111.09	108.66	2.43	79.13	1.517	3.071		0.047	
6	0.116	702	29.28	52.177	111.08	107.42	3.66	78.14	1.498	4.684	4.614	0.070	0.070
			29.42	52.177	111.16	107.56	3.6	78.14	1.498	4.607		0.069	
			29.33	52.177	113.19	109.54	3.65	80.21	1.537	4.551		0.070	
7	0.14	731	27.47	50.941	111.11	106.56	4.55	79.09	1.553	5.753	5.708	0.089	0.088
			27.74	50.941	111.8	107.29	4.51	79.55	1.562	5.669		0.089	

			27.91	50.941	108.38	104.04	4.34	76.13	1.494	5.701		0.085	
8	0.188	787	28.32	50.941	114.15	108.14	6.01	79.82	1.567	7.529	7.709	0.118	0.121
			28.19	50.941	114.6	108.35	6.25	80.16	1.574	7.797		0.123	
			28.03	50.941	113.29	107.12	6.17	79.09	1.553	7.801		0.121	

Table 4.4 Calibration of Moisture sensor for Ishikawa mudstone

S.N.	Sensor out put		Container mass (g)	Sample volume (cm^3)	Wet soil mass + container (g)	Dry soil mass + container (g)	Mass & Volume of water (cm^3)	Dry soil mass (g)	Soil bulk density (g/cm^3)	Water content by mass of soil (%)	Average Water content by mass of soil (%)	Volumetric water content (m^3/m^3)	Average Volumetric water content (m^3/m^3)
	m^3/m^3	Raw constant, R											
1	0	466								0.000	0	0.000	0.000
2	0.006	494	29.12	52.177	66.14	65.5	0.64	36.38	0.697	1.759	1.76	0.012	0.012
			29.04	52.177	66.23	65.59	0.64	36.55	0.701	1.751		0.012	
3	0.03	563	29.04	52.177	67.95	65.444	2.506	36.40	0.698	6.884	7.20	0.048	0.051
			29.2	52.177	67.85	65.3	2.55	36.1	0.692	7.064		0.049	
			28.27	52.177	68.04	65.32	2.72	37.05	0.710	7.341		0.052	
4	0.039	594	29.06	52.177	69.24	65.12	4.12	36.06	0.691	11.425	11.20	0.079	0.078
			29.14	52.177	69.4	65.42	3.98	36.28	0.695	10.970		0.076	
5	0.055	630	29.35	52.177	71.21	65.37	5.84	36.02	0.690	16.213	16.28	0.112	0.112
			29.15	52.177	71.2	65.33	5.87	36.18	0.693	16.224		0.113	
			29.53	52.177	71.21	65.34	5.87	35.81	0.686	16.392		0.113	

6	0.073	654	29.28	52.177	72.15	65.43	6.72	36.15	0.693	18.589	21.15	0.129	0.146
			29.42	52.177	73.25	65.39	7.86	35.97	0.689	21.852		0.151	
			29.33	52.177	73.95	65.6	8.35	36.27	0.695	23.022		0.160	
7	0.111	719	27.47	52.177	75.85	65.3	10.55	37.83	0.725	27.888	30.08	0.202	0.217
			27.74	52.177	76.55	65.42	11.13	37.68	0.722	29.538		0.213	
			27.91	52.177	77.74	65.43	12.31	37.52	0.719	32.809		0.236	
8	0.256	1060	28.32	52.177	94.13	65.54	28.59	37.22	0.713	76.814	79.17	0.548	0.565
			28.19	52.177	94.92	65.34	29.58	37.15	0.712	79.623		0.567	
			28.03	52.177	95.75	65.43	30.32	37.4	0.717	81.070		0.581	

4.4 Direct shear test procedure

4.4.1 Initial setting and loading

Experimental setup was done carefully as following.

1. A 10 mm think sponge was glued to the upper periphery of the lower shear box (Fig. 4.29). The upper box along with the appropriate number of spacers was also installed on lower shear box (Fig. 4.30). The two boxes were tightly maintained by temporary bolts to avoid any movement of the boxes during the specimen preparation and compaction (Fig. 4.30).
2. The moisture sensor was inserted into the lower shear box. The position of the moisture sensor was carefully maintained (Fig. 4.24).
3. A porous stone was laid at the bottom of lower shear box. In addition, filter paper was also laid on the porous stone as shown in Fig. 4.31. The porous stone was used only for saturated and cyclic wetting and drying experiments.
4. The specimen was divided into 7 sub-layers to obtain uniform compaction and to prevent from particles segregation. Crushed mudstone was slowly poured from negligible height (See fig. 4.32). The specimens were not thoroughly compacted to prevent from particle breakage and to simulate the natural condition in the slope. However, a wooden parallelepiped was used (See Fig. 4.33) to carefully compact each layer of the specimen to achieve the prescribed height, if each layer height was found more than prescribed value.
5. After the final layer, the specimen was carefully leveled. Filter paper was first laid and the porous stone was laid later. But, in case of the drying monotonic loading test, the final layer was completed by placing a surrounding cardboard mould to collect the surplus crushed mudstones. After light compaction, the top end of the specimen was carefully leveled by sliding a sharp metal bar to remove the excessive crushed mudstone towards the cardboard mould. The cardboard was removed and specimen was covered by filter paper (Fig. 4.34).
6. The specimen density was calculated from the mass in shear box. The difference between the initial (before experiment) calculation, and the final calculation (after specimen preparation) was very small.

7. The DS box was slowly translated under the vertical piston. The upper box was attached to rigid bars and rigid bars were tightly attached to the vertical bars of the apparatus using nuts and bolts (Fig. 4.35).
8. The load piston of the gear loading device was temporarily connected to the shear box frame to prevent the sliding of the lower shear box. The vertical piston with loading plate was lowered by manually decreasing the air pressure in the cylinder until it reached very close to the specimen.
9. The temporary bolts used to connect the lower and the upper shear box, and the spacer used to maintain a fixed gap between upper and lower shear boxes were removed very carefully.
10. The load piston of the gear loading device which was temporarily connected to shear box frame to prevent sliding of lower shear box, was disconnected from the shear box frame.

Fig. 4.29 Attached sponge to the lower periphery of the upper shear box

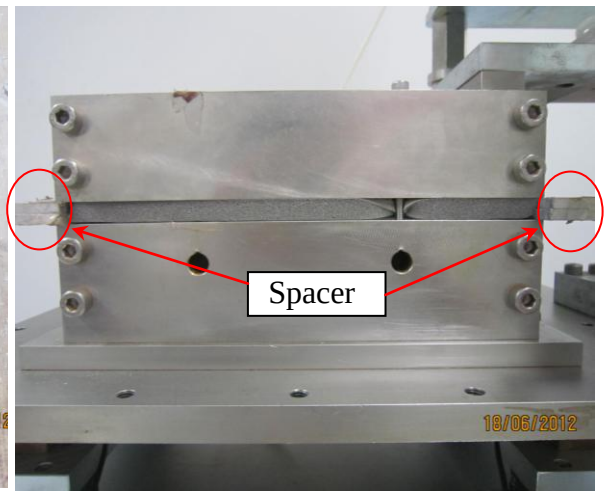

Fig. 4.30 Assembled upper and lower shear box with prescribed spacing

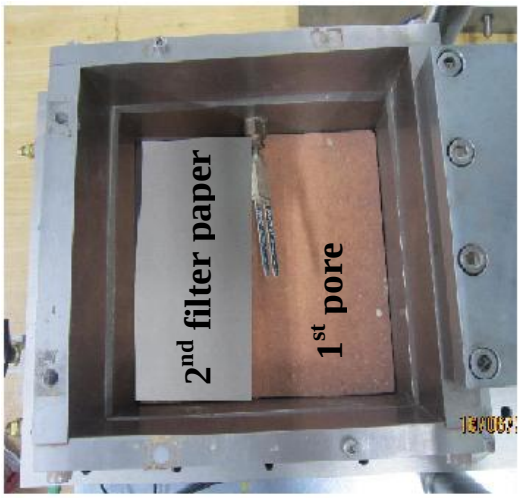

Fig. 4.31 Pore stone and filter paper

Fig. 4.32 Deposition of materials of prescribed

Fig. 4.33 Compaction of specimen

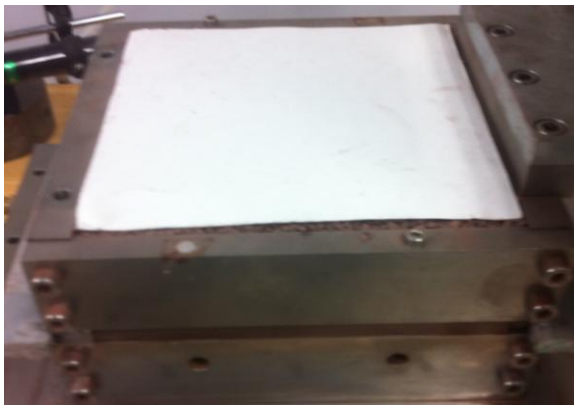

Fig. 4.34 Covering specimen after final

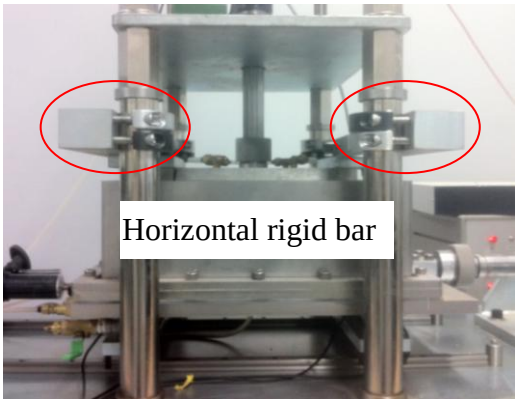

Fig. 4.35 Final setting before loading applied

11. The connection between the vertical piston and the top cap was checked and made tight. Then, all load cells and both horizontal and vertical LVDTs (Linear

variable differential transducer) were checked and calibrated. Starting from this stage, the readings of vertical LVDT and vertical LCs (load cell) were recorded (in a before consolidation process (b4con) file.)

12. Then, the vertical piston was lowered by manually decreasing the air pressure in cylinder. An initial pre-load of about 80 N was usually applied. This pre-load was of negligible influence on vertical deformation and consolidation.
13. The vertical LVDT (No. 5 in Fig. 4.22) was positioned and initialized.
14. Consolidation was started gradually at a typical rate of 1 kPa per minute until the normal stress (σ_v) reached the nominally prescribed value. The Typical normal stress reached at the end of consolidation for the tests performed in this study was 5 kPa. As the vertical displacement rate was recorded, it could be checked that the vertical displacement rate became almost null and that the vertical compression eventually stopped after several minutes.

In this study, the loading process during the test consisted of three stages as shown in Fig. 4.36

Initial loading

Before the start of initial loading, the following steps were done:

1) Connect the load piston of the gear loading device to the DS box frame.
2) Turn on the motor control unit and servo-control unit.
3) Setup the horizontal LVDT (No. 4 in Fig. 4.23)
4) Reset the reading of all displacement transducers and friction load cells to zero.
5) Arrange the settings in computer according to prescribed stress ratio or stress path (Fig. 4.32). The loading process is fully automated. All the different steps of loading history (stress path, Fig. 4.36) can be simply written in a text file that can be directly implemented from the program interface by using computer as follows:
    a. Monotonic loading at a constant vertical stress starting/ending at a given shear stress or shear displacement. (In this experiment, initial shear stress was applied up to R* σ_v, σ_v = 5 kPa)

b. Anisotropic loading (both shear and vertical loading) starting/ending at given shear stress/ vertical (In this experiment, shear stress was applied up to R* σ_v, σ_v = 50 kPa).
c. Sustained loading stage starting at a given shear stress level for a specified time period,
d. Constant acceleration test for a specified time period until a given shear displacement rate and starting at a given shear stress or shear displacement

6) Both shear stress, τ, and vertical stress, σ_v, were applied to the dry specimen gradually keeping their ratio, R (=τ /σ_v, σ_v=50 kPa), constant. The value of R represents the inclination of slopes. The shearing process is then fully automated. In this research, the value of R was used as 0.3, 0.5 and 0.7 which are equivalent to 16.7^0, 26.56^0 and 34.99^0 slopes respectively. Similarly, the value of σ_v was fixed to 50 kPa. The value of σ_v depends on the thickness of the overburden soil or depth of the slip surface etc. As mentioned in Chapter 2, the slaking induced landslides are generally shallow depth landslides. So, to represent the condition of shallow landslides the value of 50 kPa was used for σ_v.

Creep loading (with cyclic wetting and drying)

The Sustained loading stage was started at a given shear stress level for a specified time period. The Time period depends on the type of materials used and the nature of experiment.

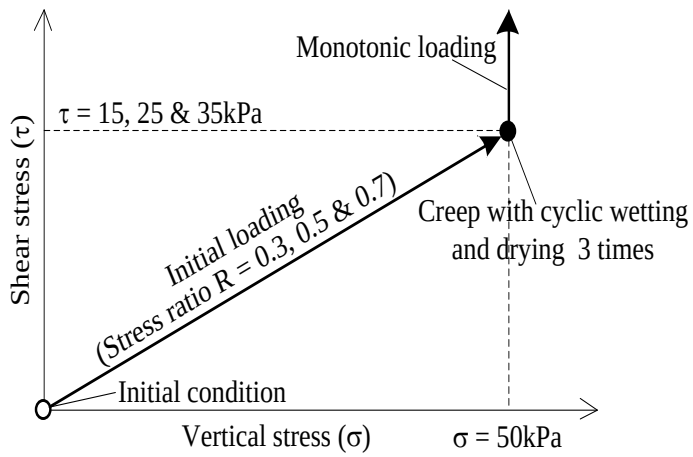

Fig.4.36 Stress path

1) In case of dry monotonic loading (ML) tests, after the prescribed τ and σ_v (= 50 kPa) values were reached, sustained loading was continue until the stabilization of both shear and vertical deformations was achieved. It took several hours for the stabilization of both shear and vertical deformations.

2) In case of other tests simulating cyclic wetting and drying, after the stabilization of both shear and vertical deformations, a prescribed number of cyclic wetting and drying was carried out under constant stress conditions. Details of wetting and drying process are discussed later.

Monotonic loading

After creep loading (with prescribed cyclic wetting and drying), finally a monotonic shear loading was applied at a constant rate of s (0.2 mm/min) to evaluate the stress-strain characteristics of geomaterials under constant stress condition (σ_v = 50 kPa) until the specimen's residual stage was reached.

4.4.2 Wetting

A large container (Fig. 4.37) was added to the direct shear apparatus for water pounding to saturate the specimen through the sides of the shear box. Similarly, two cylinders were used as shown in Fig 4.38 to maintain proper water head for smooth supply of water inside the specimen. One cylinder was used to supply water inside the specimen through the hole (Fig. 4.23) provided on the bottom of the shear box while another cylinder was used to supply water outside the shear box. In addition, one small tank was also used for continuous supply of water to both cylinders as shown in Fig. 4.23.

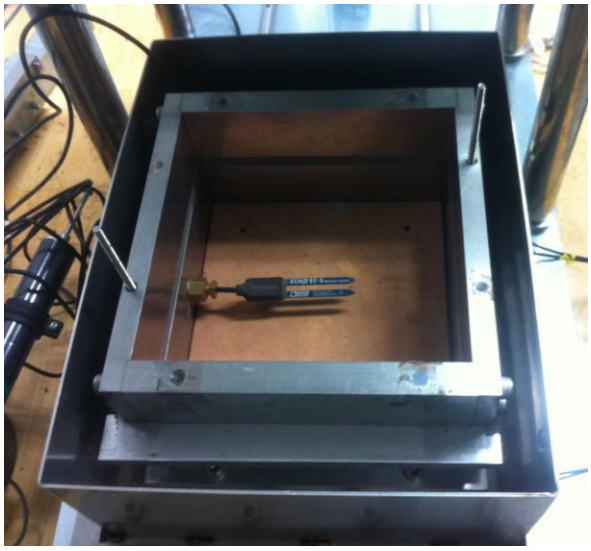

Fig. 4.37 Large container to saturate the specimen inside shear box

First the water was supplied in a large container (outside of shear box) up to about 10 mm height. Then, the wetting was carried out by pouring the distilled water from the bottom of the lower shear box. When the water level reached the opening level inside the specimen, water was supplied to the large container again up to the level higher than the opening to prevent the outflow of mudstones particles from the shear box. Again, the water was supplied from the bottom of the shear box until the specimen was fully immersed. The water flow should be controlled carefully not to scour the specimen during wetting. It took about 30 min for wetting the specimen.

The wetting process always started after stabilization of both shear and vertical displacements due to either the loading or drying processes. Similarly, the water content during drying should also be almost constant before starting a new wetting process.

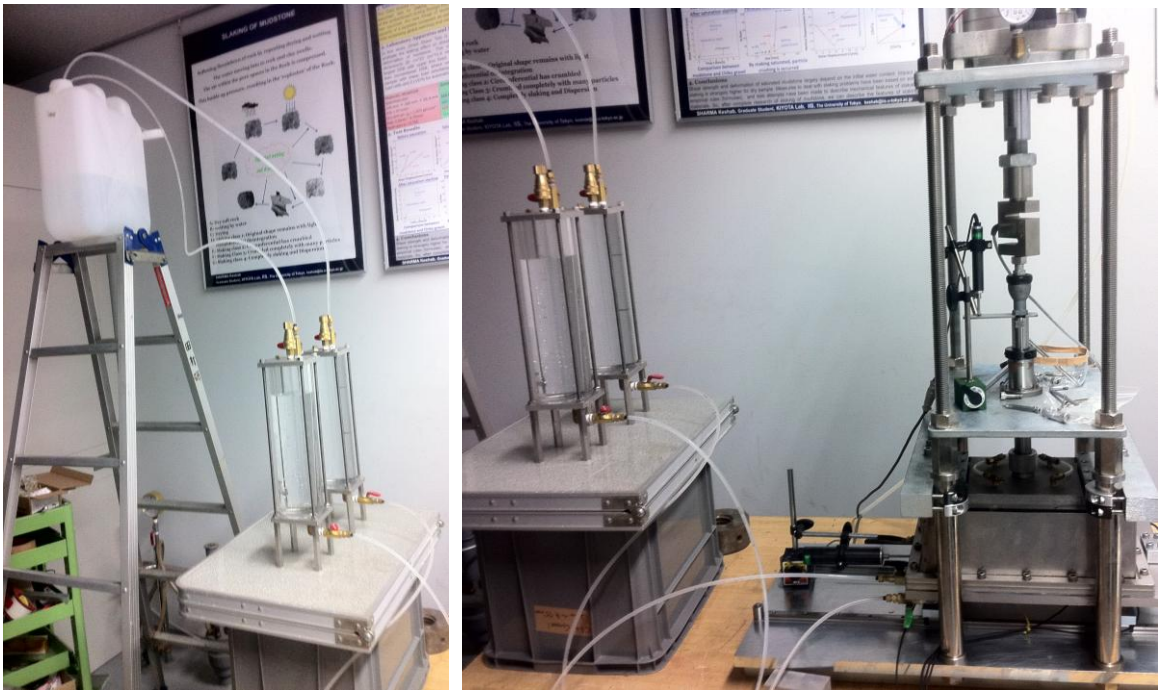

Fig. 4.38 Experimental setup to saturate specimen inside the shear box

4.4.3 Drying

When both shear and vertical displacements due to immersion led to stabilize, water was drained out through the pipes connected to the holes at the bottom of the shear box and outside of the shear box (in between wall of large container and shear box). When gravitational water was drained out almost completely, the dry air was pumped from the bottom of the shear box by using a dry pump (Fig. 4.39). Gravitational water is free water moving through the soil by the force of gravity. It is largely found in the macro-pores of soil and it drains rapidly through the water table in all soils except the most compacted ones. The shear box was covered by silica gel (Fig. 4.40) as shown in Fig. 4.41. Both the shear box and water containers were also covered by a vinyl sheet to control the humidity around the shear box as shown in Fig.4.42, while room temperature was maintained at 30^0 C. The water content of the specimen was measured frequently using a moisture sensor through the Pro-Check. The room temperature and humidity were monitored as shown in Fig.4.41.

Fig. 4.39 Dry air pump to supply dry air

Fig. 4.40 Silica Gel

Fig. 4.41 Shear box covered by silica gel and temperature and humidity measurement

Fig. 4.42 covered by vinyl sheet

CHAPTER 5

TEST RESULTS

5.1 General

To describe the slaking effects on the strength and deformation characteristic as well as particles crushing of mudstones, a series of direct shear tests with other preliminary experiments were conducted. Similar tests were also conducted on conventional granular material such as Chiba gravel and Toyoura sand. Non-slakeable Glass beads was used for few tests as well.

This chapter presents the preliminary data obtained from the slaking test and the main experimental results obtained from the direct shear tests. Materials properties, test conditions, procedures, and stress paths were explained in details in the preceding chapters. All the test results are summarized in the main body of the dissertation. The results presented in this chapter will be helpful in comparison slaking characteristics of non-conventional geomaterials obtained from crushed soft rocks (Hattian Bala and Ishikawa mudstone) with the non-slakable conventional materials (Chiba gravel, Toyoura sand and Glass beads).

Along with the properties of various test materials used in this study, the effect of the slaking index, density of the specimen, water content before wetting and stress ratio are the key parameters for explaining and comparison of the test results. Similarly, the influences of the cyclic wetting and drying on the physical and mechanical properties of various geomaterials used in this study will be discussed in the succeeding chapter.

5.2 General slaking test

5.2.1 Slaking index test

In order to obtain the slaking index of the specimens, accelerated rock slaking tests (JGS 2125-2006) on crushed mudstones (Hattian Bala and Ishikawa), Sand stone and Glass beads were conducted.

a) b)

Fig. 5.1 Hattian Bala mudstone piece a) before slaking test b) after slaking test with minor cracks

a) b)

Fig. 5.2 Ishikawa mudstone piece a) before slaking test b) Crumbled mudstone after slaking test

a) b)

Fig. 5.3 Sand stone a) before slaking test b) after slaking test (Kiyota et al., 2011)

As described in Chapter 4.2.3, JGS 2125-2006 guideline identifies slaking classes of the sandstone and the mudstone specimens with respect to time during the first drying-wetting cycle. Figures 5.1, 5.2 and 5.3 show the overall changes of the mudstone and sand stone specimens before and after completing the tests (i.e. after the three drying-wetting cycles).

Small cracks and small bubbles appeared on surfaces of the Hattian Bala mudstone specimens 30 minutes after the first pouring while the Ishikawa mudstone specimens converted into number of fragments. The Hattian Bala mudstone specimens however did not exhibit any further changes during the subsequent wetting/drying cycles, and their shapes were kept intact (estimated slaking class = 1). However, the Ishikawa mudstone specimen crumbled and original shape could not recognized after the three drying and wetting cycles (estimated slaking class = 3).

Similarly, Sandstone specimens showed little sign of slaking (estimated slaking class = 0), while small cracks and small bubbles appeared on surfaces of the mudstone specimens 30 minutes after the first pouring. The slaking index of Glass beads specimens were also evaluated and found as level 0.

5.2.2 Static slaking test

In order to obtain the slaking index value of the specimens, Static slaking test (Santi, 1998 and Sadisun et al., 2002b) on crushed mudstones (Hattian Bala and Ishikawa), were conducted.

The slaking index values of the specimens obtained were as follows:

Table 5.2 Static slaking test (Hattian Bala)

Specimen No.	Initial dry weight, gm	After experiment (retained weight on 2 mm sieve), gm
1	120.35	120.05
2	141.46	140.73
3	149.01	148.89
4	127.35	127.34
5	129.81	129.61
6	134.26	134.26
	802.24	800.88

The static slaking index of Hattian Bala mudstone was found as 0.17.

Table 5.2 Static slaking test (Ishikawa)

Specimen No.	Initial dry weight, gm	After experiment (retained weight on 2 mm sieve), gm
1	120.35	117.25
2	141.46	136.58
3	149.01	145.38
4	127.35	124.36
5	129.81	124.98
6	134.26	130.58
	802.24	779.13

The static slaking index of Hattian Bala mudstone was found as 2.88.

Higher static slaking index value indicates the higher vulnerability to slaking.

5.2.3 Slaking ratio test

In order to obtain the slaking ratio of the specimens, slaking ratio test (NEXCO- 100, 2006) on crushed mudstones (Hattian Bala and Ishikawa) were conducted.

The slaking ratios of the specimens obtained were as follows:

Table 5.3 Slaking ratio test (Hattian Bala)

Specimen No.	Initial weight, gm (19 mm - 37.5 mm)	After experiment (retained weight on 9.5 mm sieve), gm
1	3000	2895.25
2	3000	2902.65
3	3000	2919.26
	9000	8717.16

The slaking ratio of Hattian Bala mudstone was found as 96.85.

Table 5.4 Slaking ratio test (Ishikawa)

Specimen No.	Initial weight (gm) (19 mm - 37.5 mm)	After experiment retained on 9.5 mm sieve
1	3000	40.5
2	3000	50.12
3	3000	59.78
	9000	150.4

The slaking ratio of Hattian Bala mudstone was found as 1.67.

Higher slaking ratio indicates the durability of mudstone to slaking.

5.2.4 Water absorption

Slaking of mudstones due to cyclic wetting and drying is influenced by their ability to absorb water (Saffet, 2000; Erguler and Ulusay, 2009 and Cao et. al., 2006 etc.). Absorbed water is the water that, during submergence, fills the void spaces present in mudstones.

In order to obtain the water absorption value of the specimens, water absorption test (ASTM method C 97) on crushed mudstones (Hattian Bala and Ishikawa) were conducted.

The water absorption of the specimens obtained was as follows:

Table 5.5 Water absorption (Hattian Bala)

Container no.	Weight of container, W_1 (gm)	Weight of dry sample and container, w_2 (gm)	Weight of saturated sample and containers, w3 (gm)	Water absorption, W %
1	29.18	105.15	103.59	2.05
2	29.22	104.38	102.85	2.04
3	29.16	103.85	101.95	2.54
		Average water absorption, W %		2.21

Table 5.6 Water absorption (Ishikawa)

Container no.	Weight of containers, W1 (gm)	weight of dry sample and container, w2 (gm)	Weight of saturated sample and container, w3 (gm)	Water absorption, W %
1	29.28	74.65	47.52	59.80
2	29.32	73.26	45.98	62.08
3	28.53	69.58	43.25	64.14
		Average water absorption, W %		62.01

Higher water absorption value indicates the higher vulnerability to slaking.

5.3 Direct shear test with cyclic wetting and drying

Stress-strain-volume change characteristics from monotonic direct shear tests on crushed mudstone (Hattian Bala and Ishikawa) as well as other materials (Chiba gravel, Toyoura sand and Glass beads) at constant vertical stress (σ_v=50 kPa) under dry, saturated and cyclic wetting and drying conditions are presented this section. The test results obtained from the cyclic wetting and drying under constant creep loading will be interpreted and discussed to examine their behaviour on natural slope or when used as construction materials for embankments. All these tests were performed under strain controlled conditions at constant

relatively slow rate 0.2 mm/min to a maximum shear displacement of 15 mm. The basic properties of tested materials are listed in Table 5.7.

Table 5.7 Basic properties of tested materials

S.N.	Sample	Stress ratio during creep, R	Initial density (g/cm^3)	Initial void ratio(e)	Density before ML ((g/cm3)	Test condition during creep and ML
1	PreM001	0.3	1.482	0.741	1.508	Creep[1)] & ML[3)]
2	PreM002	0.5	1.529	0.688	1.549	Creep[1)] & ML[3)]
3	PreM003	0.7	1.553	0.661	1.577	Creep[1)] & ML[3)]
4	PreM005	0	1.563	0.651	1.573	Creep & ML under dry condition
5	PreM006	0	1.553	0.662	1.561	Creep & ML under dry condition
6	PreM007	0.5	1.558	0.655	1.567	Creep & ML under dry condition
7	PreM008	0.7	1.556	0.658	1.565	Creep & ML under dry condition
8	PreM009	0.3	1.478	0.746	1.491	Creep & ML under dry condition
9	PreM010	0.3	1.479	0.744	1.518	Creep (dry and wetting) & ML[3)]
10	PreM011	0.5	1.529	0.688	1.549	Creep (dry and wetting) & ML[3)]
11	PreM013	0.7	1.529	0.688	1.569	Creep (dry and wetting) & ML[3)]
12	PreG014	0.3	1.558	0.656	1.589	Creep[1)] & ML[2)]
13	PreG015	0	1.584	0.577	1.604	Creep & ML under dry condition
14	PreG016	0.5	1.599	0.561	1.598	Creep (dry and wetting) & ML[3)]
15	PreM017	0.8	1.593	0.568	Creep failure	Creep (dry and wetting) & ML[3)]
16	PreG018	0.5	1.529	0.688	1.596	Creep & ML under dry condition

17	PreG019	0.5	1.589	0.572	1.595	Creep (dry and wetting) & ML[3)]
18	PreG020	0.3	1.587	0.573	1.613	Creep & ML under dry condition
19	PreG021	0.3	1.589	0.572	1.601	Creep (dry and wetting) & ML[3)]
20	PreM022	0	1.587	0.573	0.672	Creep & ML under dry condition
21	PreM023	0.5	0.662	2.474	0.692	Creep & ML under dry condition
22	PreM024	0.5	0.683	2.366	Excessive displacem ent	Creep (dry and wetting) & ML[2)]
23	PreM025	0.3	0.678	2.392	0.687	Creep & ML under dry condition
24	PreM026	0.3	0.68	2.384	0.724	Creep (dry and wetting) & ML[3)]
25	PreM027	0.3	0.68	2.38	0.713	Creep[2)] & ML[3)]
26	PreM028	0.5	0.68	2.38	1.54	Creep[2)] & ML[3)]
27	PreM029	0.5	1.529	0.688	1.558	Creep & ML under dry condition
28	PreM030	0.5	1.536	0.68	1.587	Creep (dry and wetting) & ML[3)]
29	PreC010	0.5	1.566	0.648	1.542	Creep & ML under dry condition
30	PreC011	0.5	1.529	0.792	1.536	Creep (dry and wetting) & ML[3)]
31	PreT050	0.5	1.529	0.792	1.536	Creep & ML under dry condition
32	PreT052	0.5	1.549	0.709	1.555	Creep (dry and wetting) & ML[3)]

1) Creep with cyclic wetting and drying for 3 times, 2) Creep with cyclic wetting and drying for 2 times 3) ML under saturated condition

5.3.1 Hattian Bala

In this study, three cycles of wetting and drying were carried out on Hattian Bala mudstone specimens under three different anisotropic consolidation conditions to analysis the deformation and strength characteristics due to slaking by using a modified direct shear apparatus. A series of the monotonic loading tests on dry and saturated specimens were also performed to compare strength and deformation characteristics with those of the cyclic wetting and drying creep test. As already described, the slaking index (JGS 2132) of the mudstone was evaluated as level 1, while the slaking ratio (NEXCO-110, 2006) was 96.85 %. Similarly, the index properties of Hattian Bala mudstone were explained in Chapter 4.

Figure 5.4-5.7 show the typical instantaneous response of creep deformations and water content of the specimen during the wetting and drying cycles for three specimens; PreM003, PreM002 and PreM001. PreM002, PreM003 and PreM001 experienced three cycles of wetting and drying while PreM028 experienced only one and half cycles. The time t= 0 corresponds to the start of creep loading. For all specimens, the creep shear and vertical displacements converged on constant values after several hours of initial loading.

Each cyclic wetting and drying creep test took about one month to complete. Influence of wetting in the first cycle upon shear displacement appears to be significant for all specimens (Fig. 5.4a -5.7a). For the second wetting processes, the increment of shear displacements are relatively small, almost 1/10 times the increment of shear displacement in the first wetting (Fig. 5.4a-5.6a). But, in case of PreM001, the increment of shear displacement during second wetting is almost negligible (Fig. 5.6a). Similarly, for the third wetting processes, the increments of shear displacements are equal to zero for all specimens. Nakano et al. (1998) and Panabokke and Quirk (1956) reported that the slaking level of clay aggregates became higher as the initial water content of the specimen became lower. Therefore, it can be understood that the maximum displacement was observed during the first wetting because the specimen in this study was prepared by oven-dried crushed mudstone.

In addition, from Fig. 5.4a- 5.6a, the creep shear displacement caused by wetting seems to be decreased with progress of cycle, almost zero during the third wetting, even the water content of specimens before wetting is relatively lower about 0.7 %. This may be attributed to the specimen densification due to previous wetting and drying processes (Nakano et al., 1998).

Figure 5.4b-5.7b show considerable vertical displacement that occurred in each wetting step. This expansive behavior of crushed mudstone would consist of two phases, swelling caused by water absorption of expansive clay mineral and dilatancy due to shearing. Expansion of clay minerals also cause cracking in the grains which ultimately lead to disintegration. Cardoso and Alonso, 2009 also explained swelling induced particles disintegration in mudstones. However, expansive clay mineral like montmorillonite of smectite group was not found clearly from X-ray diffraction (XRD) analysis of Hattian Bala mudstones.

The vertical displacement, however, in case of R= 0.3, is almost negligible except in the first wetting because of having higher water content (more than 3 %) of specimen before the second and third wettings (Fig. 5.6).

Figure 5.4-5.7 also show that water content decreases gradually during the first and second drying processes. Initially, no appreciable creep deformation is found to occur at higher water contents. When the water content becomes about 2.5 %, both vertical and shear displacements occur progressively with water loss and finally tend towards an asymptotic value at water content of about 0.8 %. However, in case of PreM003, the water content decreases gradually during drying process but become almost constant when water content is about 3 %. No response of drying process upon both shear and vertical displacement is found in PreM003 (Fig. 5.6).

One of the noticeable behaviors observed in these experiments is a quite large creep deformation during the drying processes (Fig. 5.4-5.7). Slaking phenomena cause loss of intra-particles cementation and tensile failure of the weakly crystalline bonded granular materials due to drying induced pore water suctions. (Czerewko and Cripps, 200; Moropoulou et al., 2004; Karoglou et al., 2005; Soe et al., 2010). Reduction of pore water which lead to shrinkage and disaggregation of fabric especially around discontinuities during dry process. Consequently, such an evolution of soil grains produces rounded particles with relatively high sphericity and smooth circumference which sequentially decreases the interlocking behaviour (angle of internal friction) of granular medium. Particles slides on each other during shrinkage causing shear deformation simultaneously. The strength and stiffness gained during drying process are opposing to the further increase in shear displacement with drainage and evaporation of pore water which lead to shrinkage and disaggregation of fabric especially

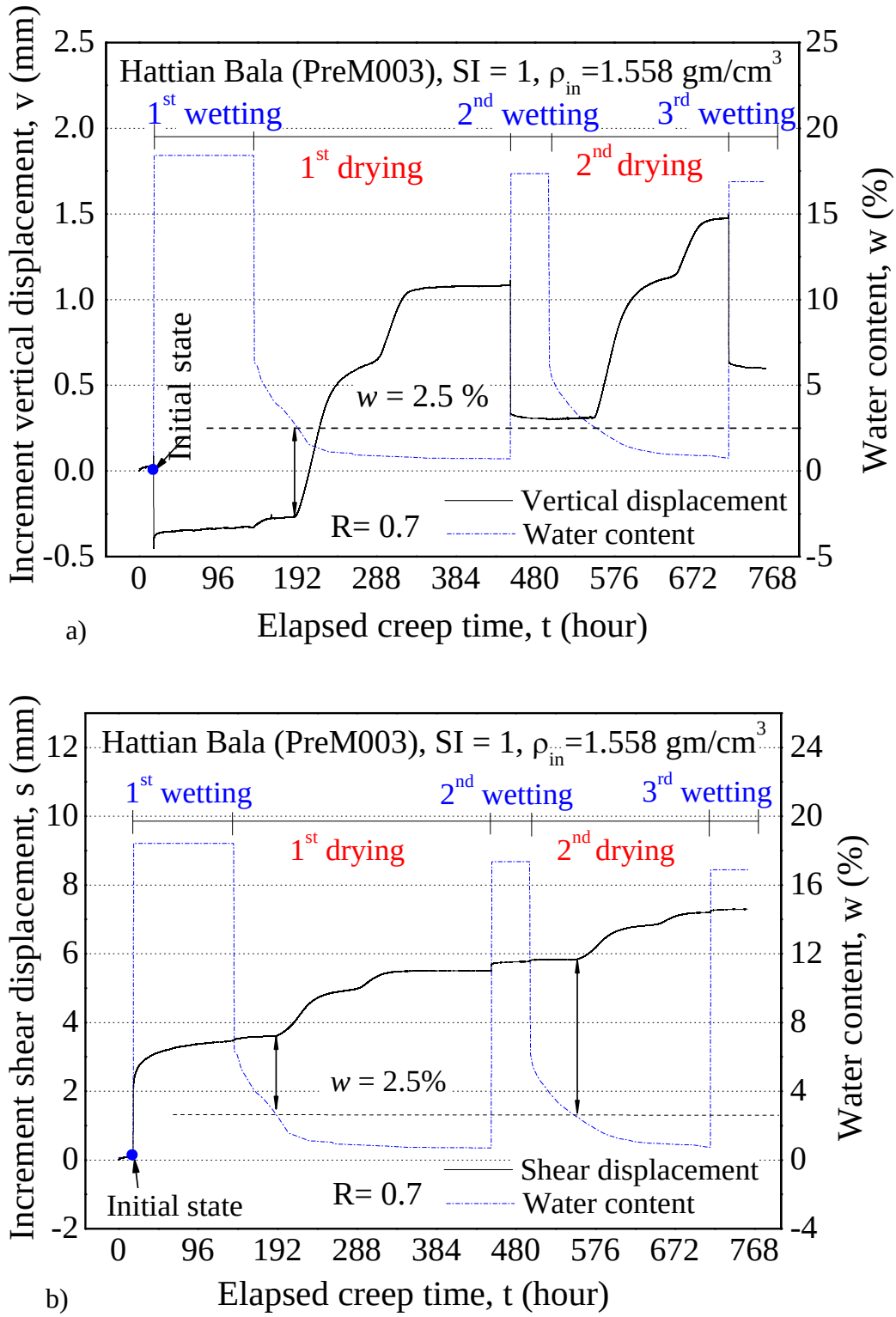

Fig 5.4 Time histories of water content, shear and vertical displacement (a) shear (b) vertical content under cyclic wetting and drying for 3 times for R= 0.7 (PreM003)

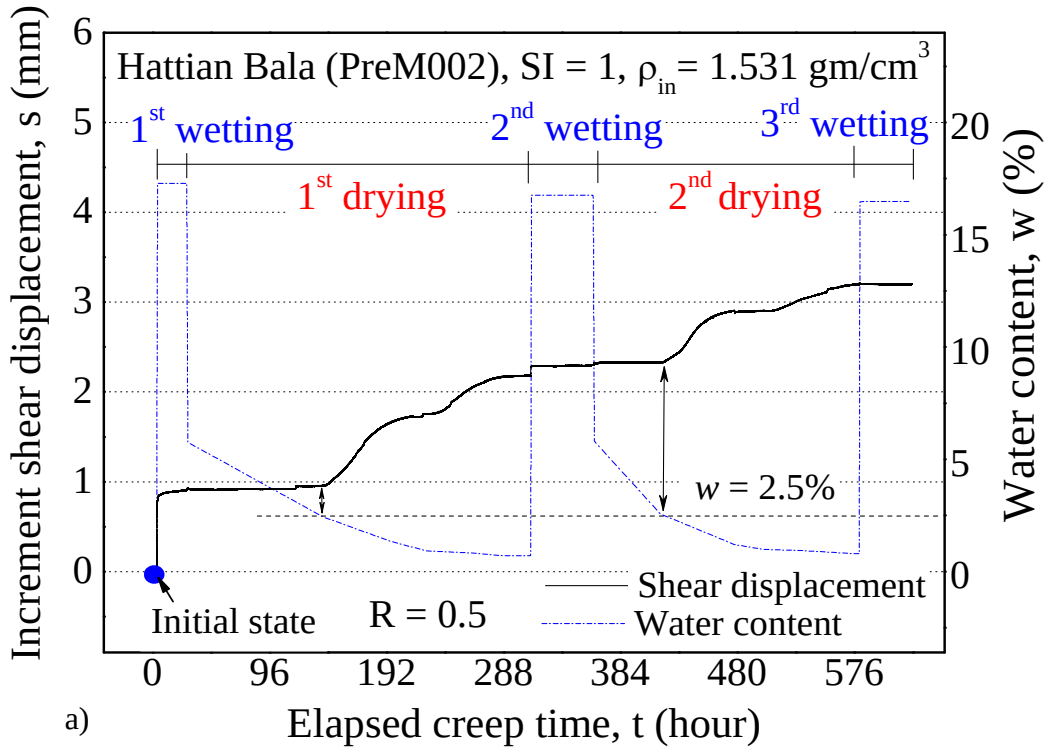

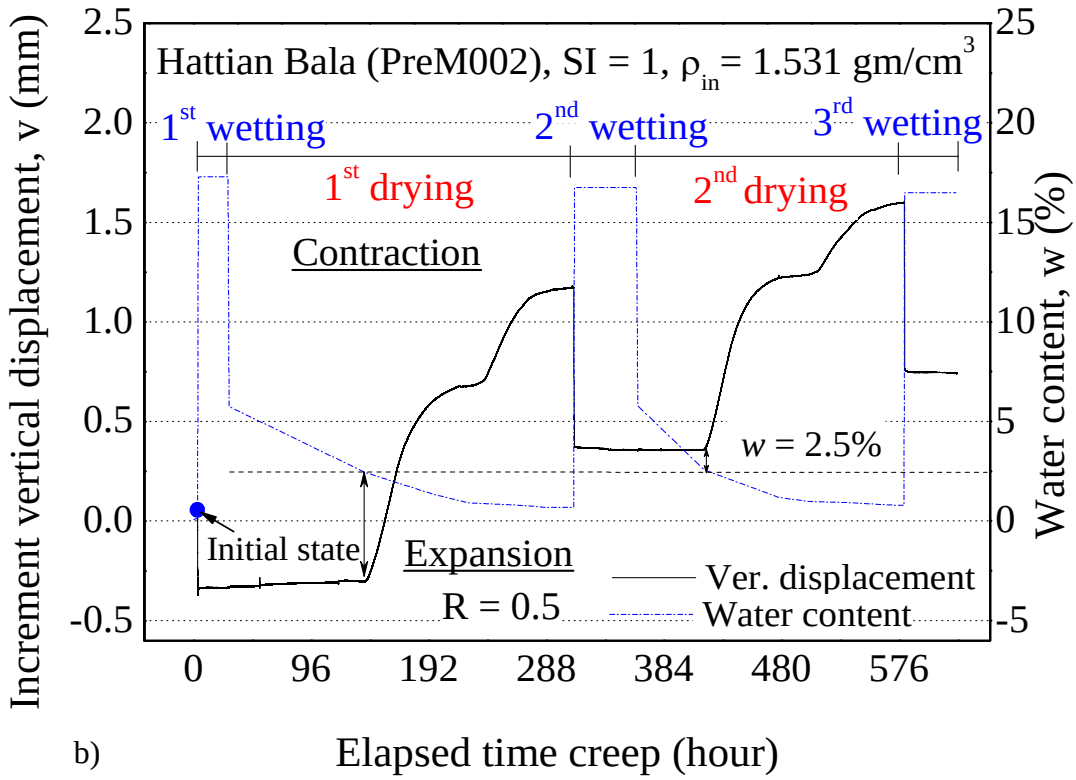

Fig 5.5 Time histories of water content, shear and vertical displacement (a) shear (b) vertical content under cyclic wetting and drying for 3 times for R= 0.5 (PreM002)

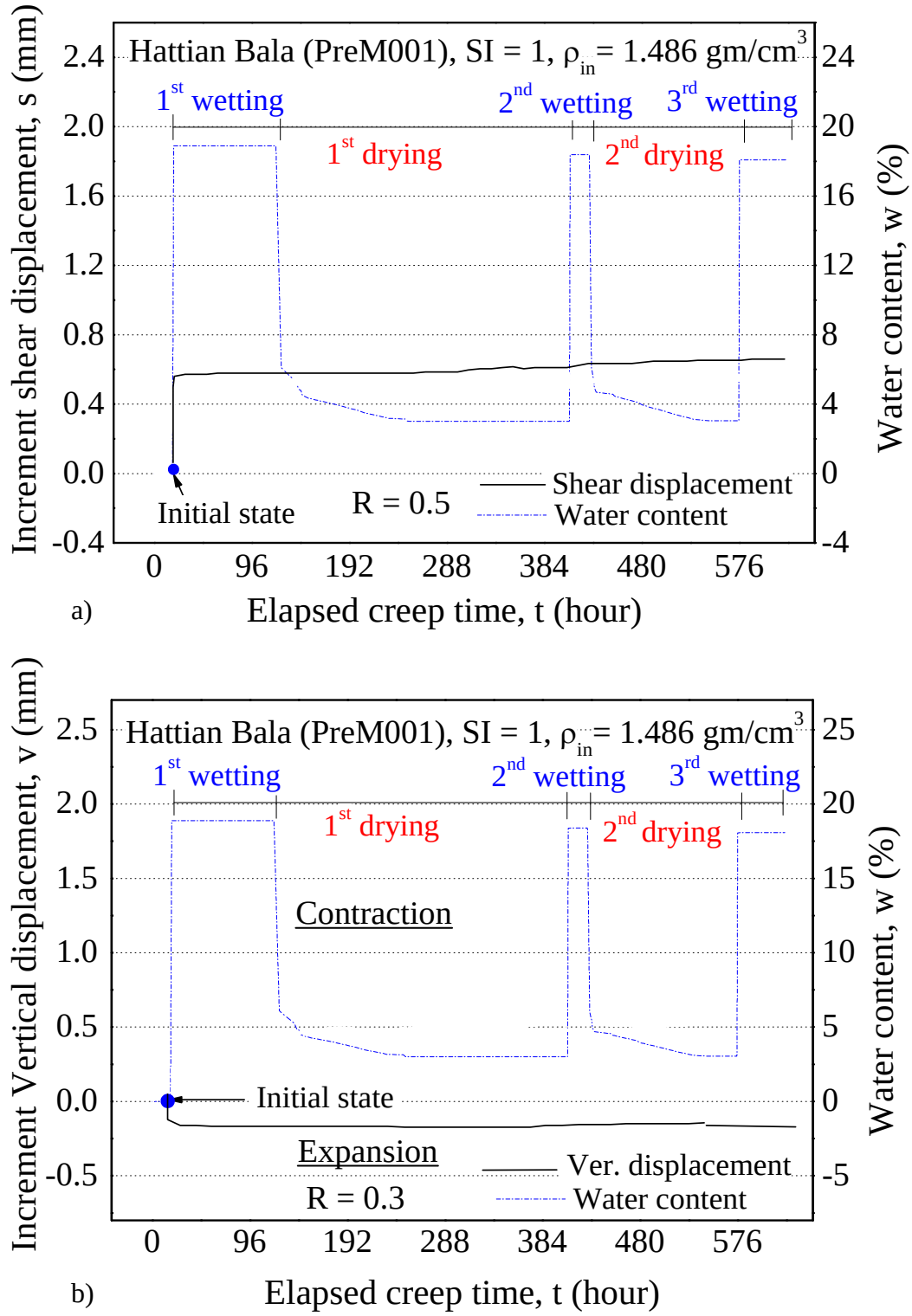

Fig 5.6 Time histories of water content, shear and vertical displacement (a) shear (b) vertical content under cyclic wetting and drying for 3 times for R= 0.3 (PreM001)

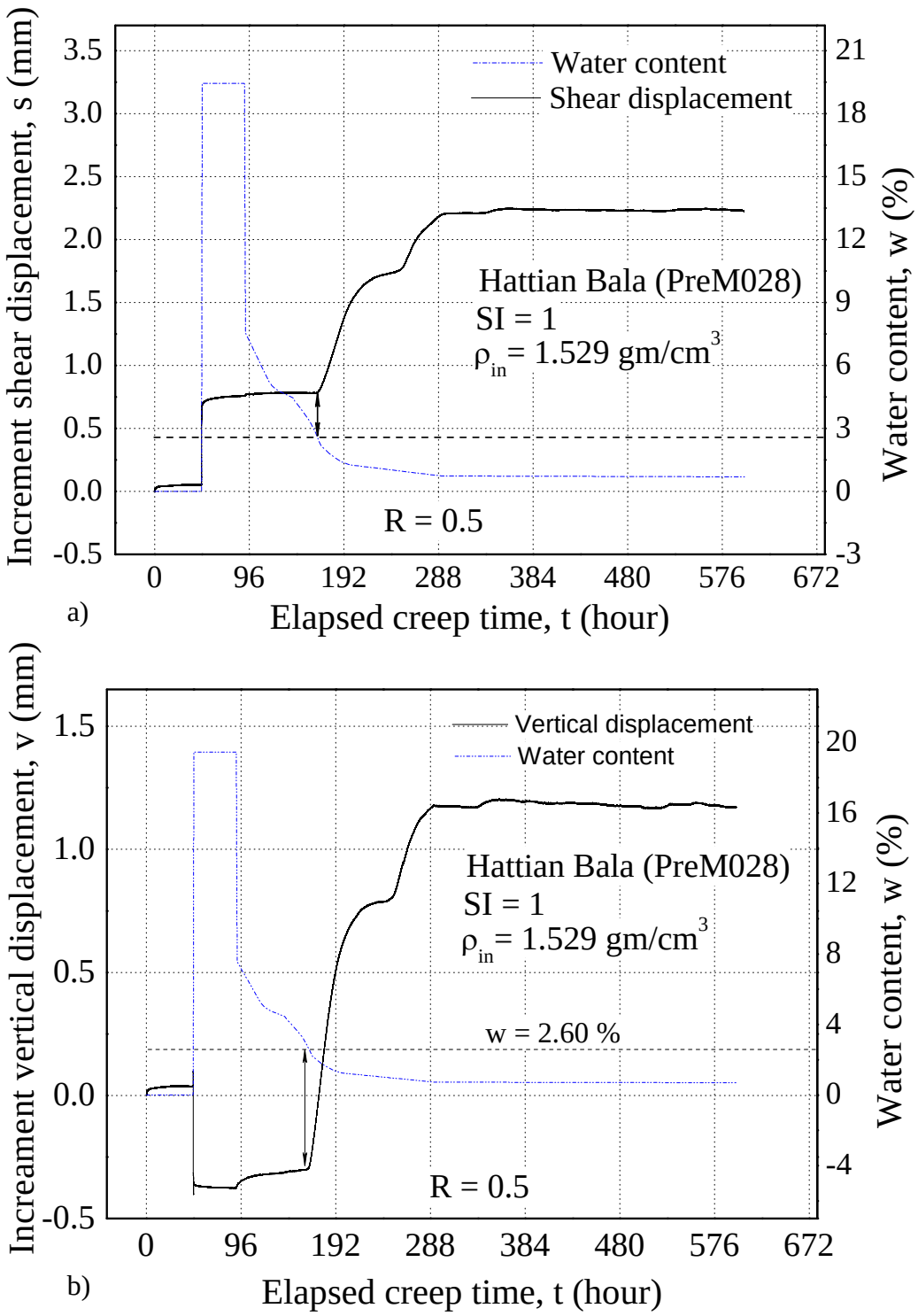

Fig 5.7 Time histories of water content, shear and vertical displacement (a) shear (b) vertical content under cyclic wetting and drying for 2 times for R= 0..5 (PreM028)

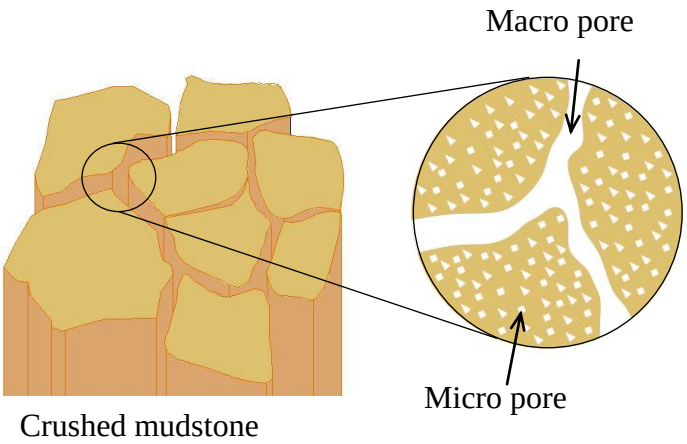

Fig. 5.8 Macro and micro pores system

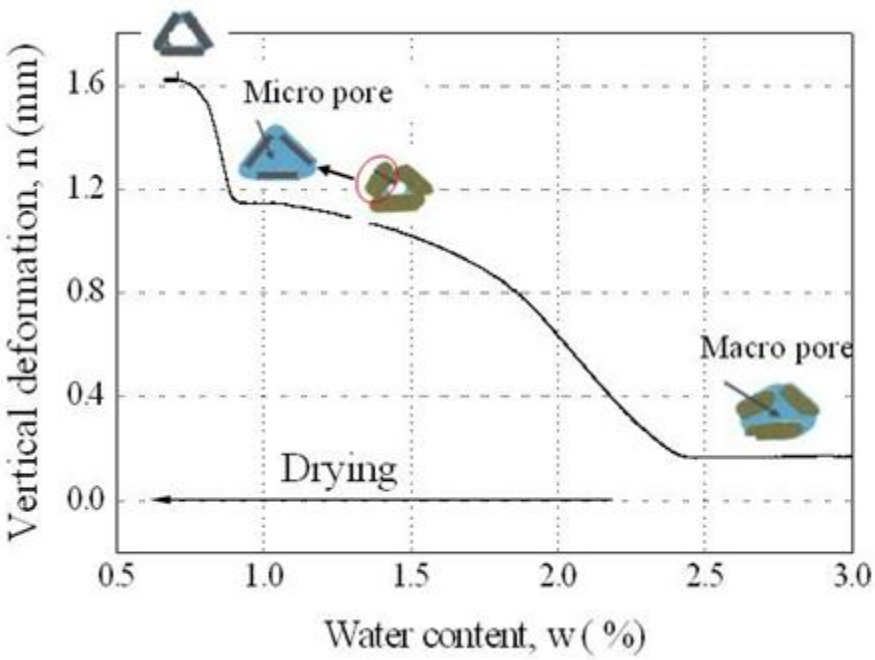

Fig. 5.9 Relationship between water content and drying induced vertical deformation (Braudeau et al. 2004)

around discontinuities. Therefore the drying induced deformation of crushed mudstones is very complex which could be challenging and crucial importance for strategic geotechnical structures.

As seen from the Fig. 5.4, 5.5 and 5.7 both shear and vertical displacement during drying are composed of two well defined curvilinear parts. Figure 5.8 shows schematic sketch of crushed mudstone particles which consist of two pore systems, inter (macro) and intra-primary (micro) porosity (Asaoka et al., 1997; Nakano et al., 1998 and Braudeau et al. 2004). It was assumed that water leaves the crushed mudstones from the inter-pedal (macro) pores causing shrinkage of inter-pedal (macro) pores (first part of curvilinear). When the inter-pedal (micro) pores empty out, intra-primary (micro) pores begin to shrink, losing its water content (second part of curvilinear) as shown in Fig. 5.9.

Figures 5.10 -5.15 show the shear stress-deformation-volume change relationship for the all dry, saturated and the one with cyclic wetting and drying history specimens. Here "volume change" denotes the ratio of shear and vertical displacement, and its negative value indicates dilation. The specimens of PreM001, PreM002 and PreM003 were subjected to the alternative step of loading history including three cycles of alternative wetting and drying while the specimens PreM0010, PreM011 and PreM013 were subjected to alternative step of loading including saturation only. Similarly, PreM007, PreM008 and PreM009 were subjected original loading history mentioned in Chapter 4. The time t=0 corresponds to the start of initial loading (anisotropic consolidation).

As described in previous chapter, initially, both shear stress, τ, and vertical stress, σ v, were applied to the dry specimen gradually keeping their ratio, R (= τ/σ_v, σ_v = 50 kPa), constant. Figures 5.10a, 5.12a and 5.14a show stress-strain behaviours under stress ratios 0.7, 0.5 and 0.3 respectively, where stress ratios 0.7, 0.5 and 0.3 are equivalent to slope ground having 35^0, 27^0 and 17^0 inclination respectively. The shear displacements from the origin, O to A (Fig. 5.10a, 5.12a and 5.14a) correspond to the initial loading. It shows that large shear deformation was obtained when stress ratio, R (= τ/σ_v) is high.

When both shear and vertical displacements due to initial loading had reached an almost constant value, the first wetting was carried out by supplying distilled water. This creep loading process represent a situation that slope ground is saturated by rain fall under constant stress condition. The shear displacements from A to B (Fig. 5.10a, 5.12a and 5.14a) are the combination of three probable phenomena such as creep, slaking and wetting induced displacement under constant loading. In addition, different deformation response was observed

for consecutive specimens under similar condition during initial loading and saturation of various specimens. This is possibly due to the irregular rearrangement of soil particles during specimen preparation, particles disintegration of some grains and or different collapsing/swelling direction upon saturation

As already mentioned, three specimens PreM001, PreM002 and PreM003 were subjected to three cycles of wetting and drying under constant loading. So, the shear displacements from B to C (Fig 5.10a, 5.12a and 5.14a) represent the cyclic wetting and drying induced displacement.

The segments A to D (Fig 5.10a, 5.12a and 5.14a) of the dry specimens are the stress-strain relationship during monotonic shear loading under constant stress (σ_v = 50 kPa) condition. Similarly, the portions B to D are the stress-strain relationship during monotonic loading under constant stress (σ_v = 50 kPa) for the saturated specimens while the segments C to D represent the stress- strain behaviours during monotonic loading after three cycles of wetting and drying.

Figure Fig 5.10b, 5.12b and 5.14b show the shear deformation-volume change relationship for all specimens under three different stress conditions. All specimens showed contractive behaviour during initial loading. In addition, all specimens exhibit swelling behaviours during first wetting. PreM002 and PreM003 undergo shrinkage during the drying step and swelling in the wetting step as aforementioned (Fig 5.10b and 5.12b). However, shear deformation- volume change relationship is not clearly visible during the cyclic wetting and drying for the specimen PreM001 under stress ratio 0.3 (Fig. 5.14b).

Finally, all specimens under stress ratio 0.7 and 0.5 exhibited dilative behavior during monotonic shear loading. However, it is seen that the residual state is no longer unique. For the specimens under stress ratio 0.3, it is noticed that for the specimens with dry condition exhibited a dilative behavior but that the saturated and the one with three cycles of wetting and drying specimens loses such dilative nature. The volumes of full saturated specimens are contractive nature.

Similarly, Figures 5.16 shows the shear stress-deformation-volume change relationship for the specimen (PreM028) experienced one complete cycle of wetting and drying and monotonic shear loading was applied under dry condition. PreM028 was also subjected to the

alternative step of loading history including one cycle of alternative wetting and drying. The time t=0 corresponds to the start of initial loading (anisotropic consolidation).

As described in previous paragraphs for other test, the shear displacements from the origin, O to A (Fig. 5.16a) correspond to the initial loading maintaining stress ratio 0.5. When, the both shear and vertical displacement due to initial loading became almost constant, the wetting was carried out as explained in Chapter 4. The segment A-B (Fig. 5.16a) probably is the results of creep, slaking and wetting induced displacement under constant loading during one complete cycle of wetting and drying. Then, the monotonic loading was applied to evaluate stress-strain characteristics of Hattian Bala mudstone under dry condition after one complete cycle of wetting and drying.

Figure 5.16b shows the shear deformation-volume change relationship during monotonic loading. The specimen (PreM028) showed contractive behaviour during initial loading. In addition, it exhibited swelling behaviour during wetting while shrinkage behaviour during drying process. Finally, it exhibited dilatative behaviour during monotonic shear loading under dry condition after one complete cycle of wetting and drying.

Figures 5.11, 5.13, 5.15 and 5.17 show the relationship between the shear stress ratio, R, the shear displacement, *s*, together with the associated volume change (i.e. the vertical displacement, *v*) for the Hattian Bala mudstone specimen. The values of *s* and *v* were set at zero at the beginning of monotonic loading. In addition, the values of friction angles, φ_d, (assuming apparent cohesion c_d =0) at peak strength were also indicated in these figures. The saturated and the one with cyclic wetting and drying mudstone specimen exhibit largely different stress-displacement features from those for dry specimen. The specimens were prepared at low initial density therefore peak and residual stress state (strain softening) even in dry conditions are not clearly visible. The initial stress-strain response becomes stiffer under both saturated and cyclic wetting and drying tests as compared to dry tests. This is probably due to aging and viscous effects on granular material because saturated and the one with cyclic wetting and drying test specimens experienced relatively longer creep loading (Prisco and Imposimato, 1996; Tatsuoka et al., 2000 and 2001; Nawir et al., 2002). So, both clear peak stress ratio and post peak stress softening appeared from monotonic shear loading on both saturated and the one with cyclic wetting and drying test conditions.

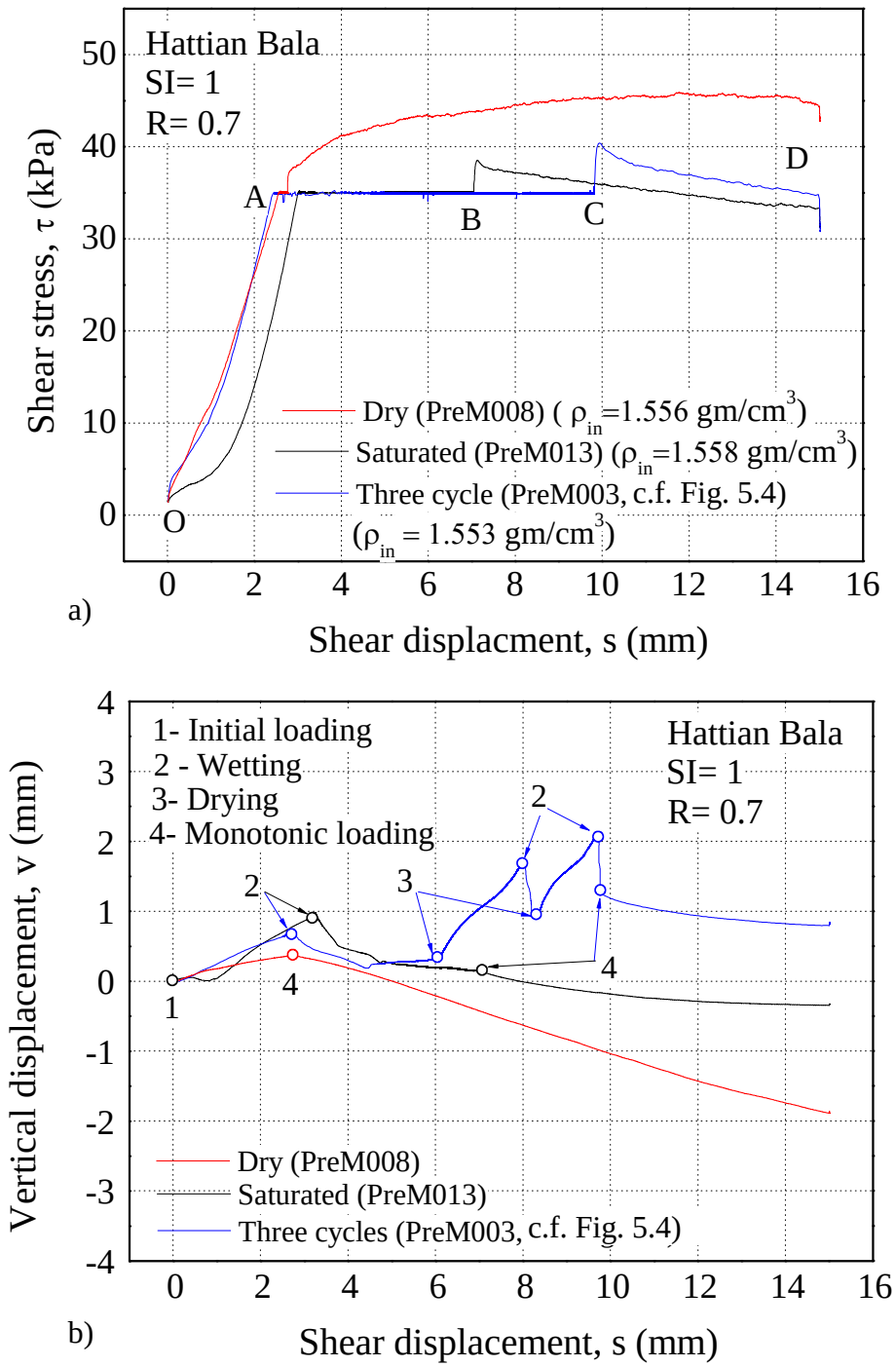

Fig 5.10 a) stress-deformation b) volume changes characteristics under R= 0.7 during experiment (Hattian Bala mudstone)

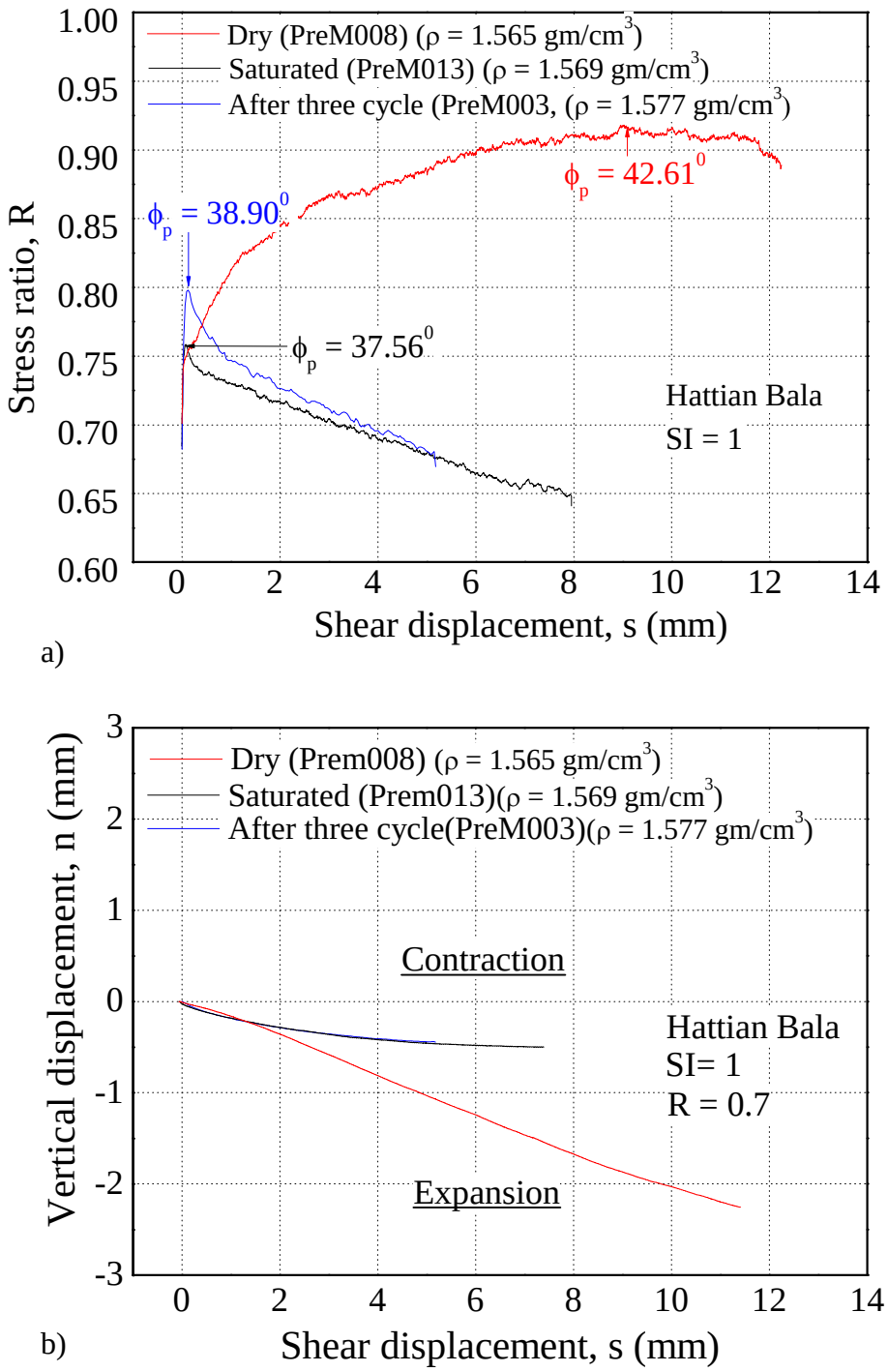

Fig. 5.11 Effect of slaking on a) stress-deformation b) volume changes characteristics of Hattian Bala mudstone specimen under R= 0.7

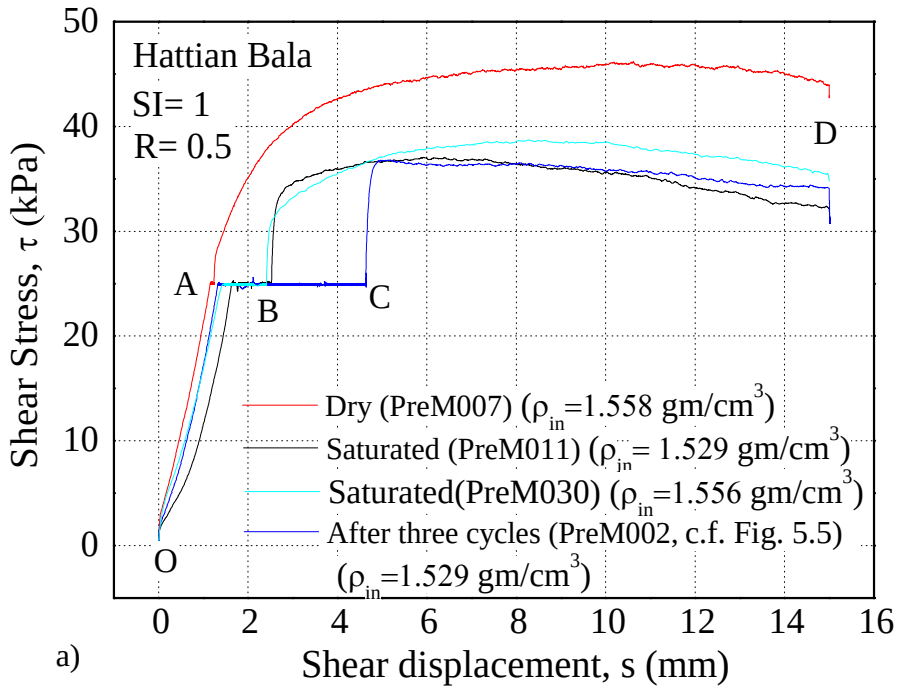

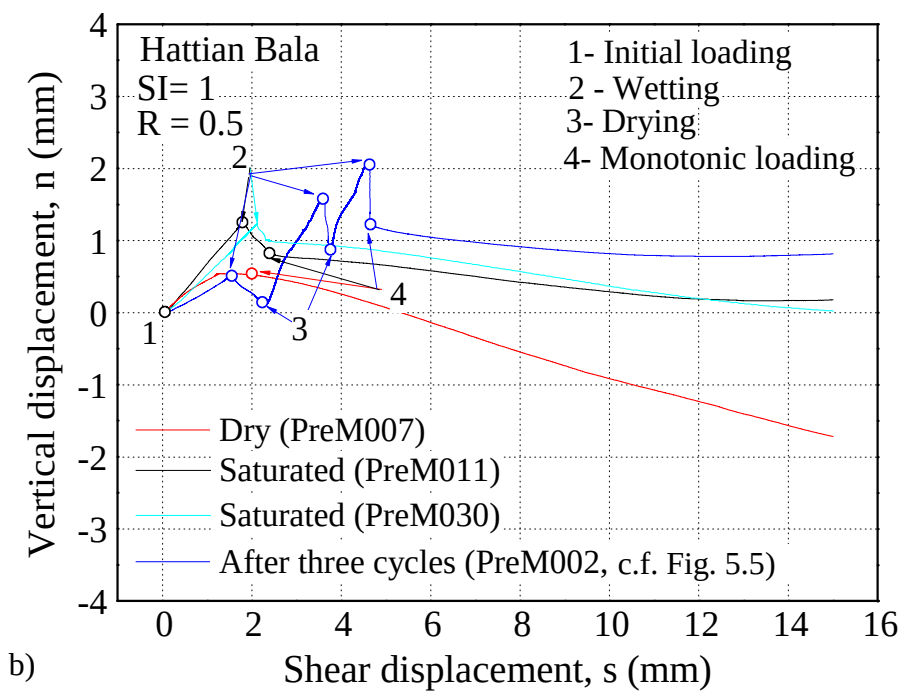

Fig 5.12 a) stress-deformation b) volume changes characteristics under R= 0.5 during experiment (Hattian Bala mudstone)

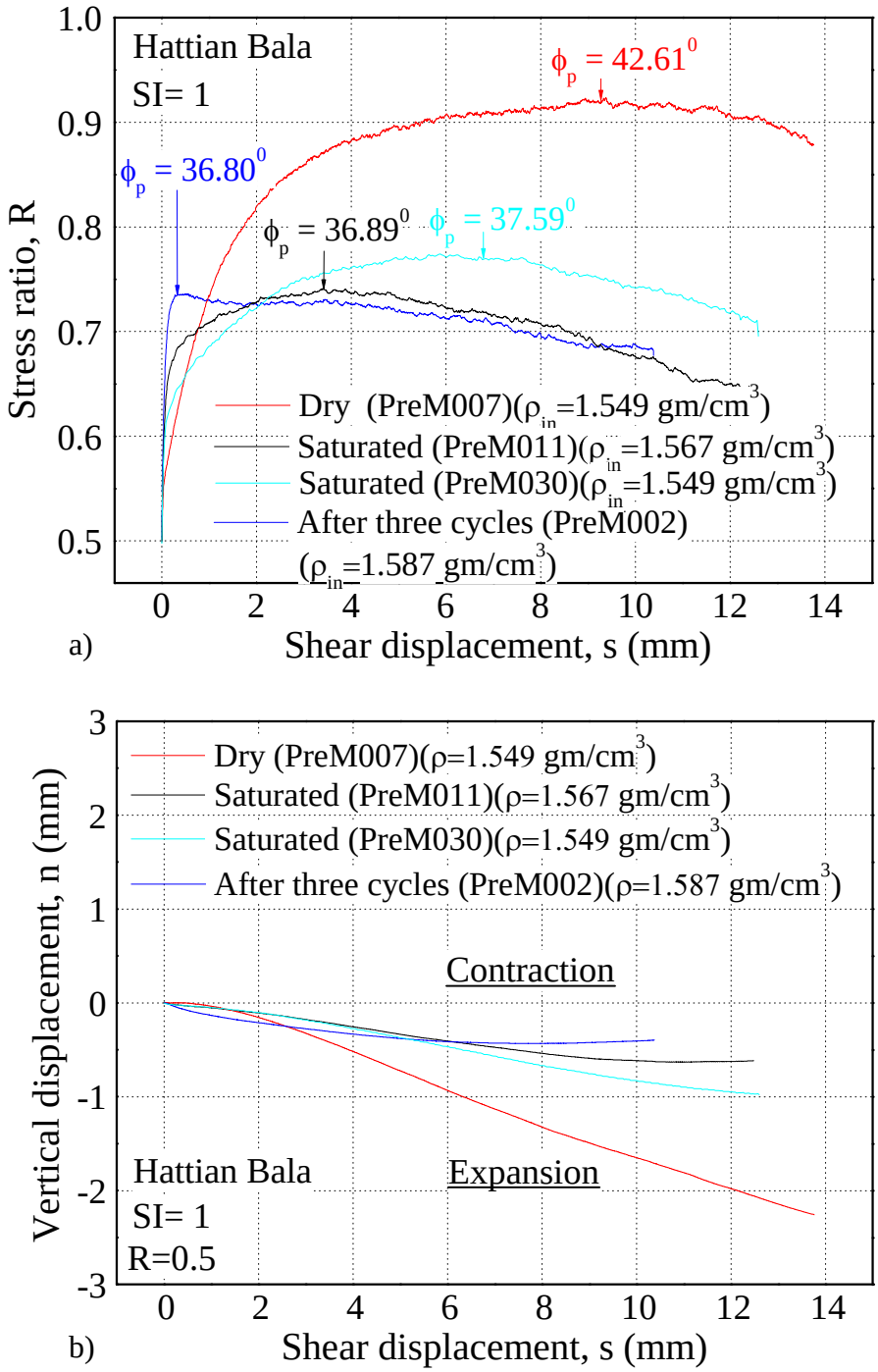

Fig. 5.13 Effect of slaking on a) stress-deformation b) volume changes characteristics of Hattian Bala mudstone specimen under R= 0.5

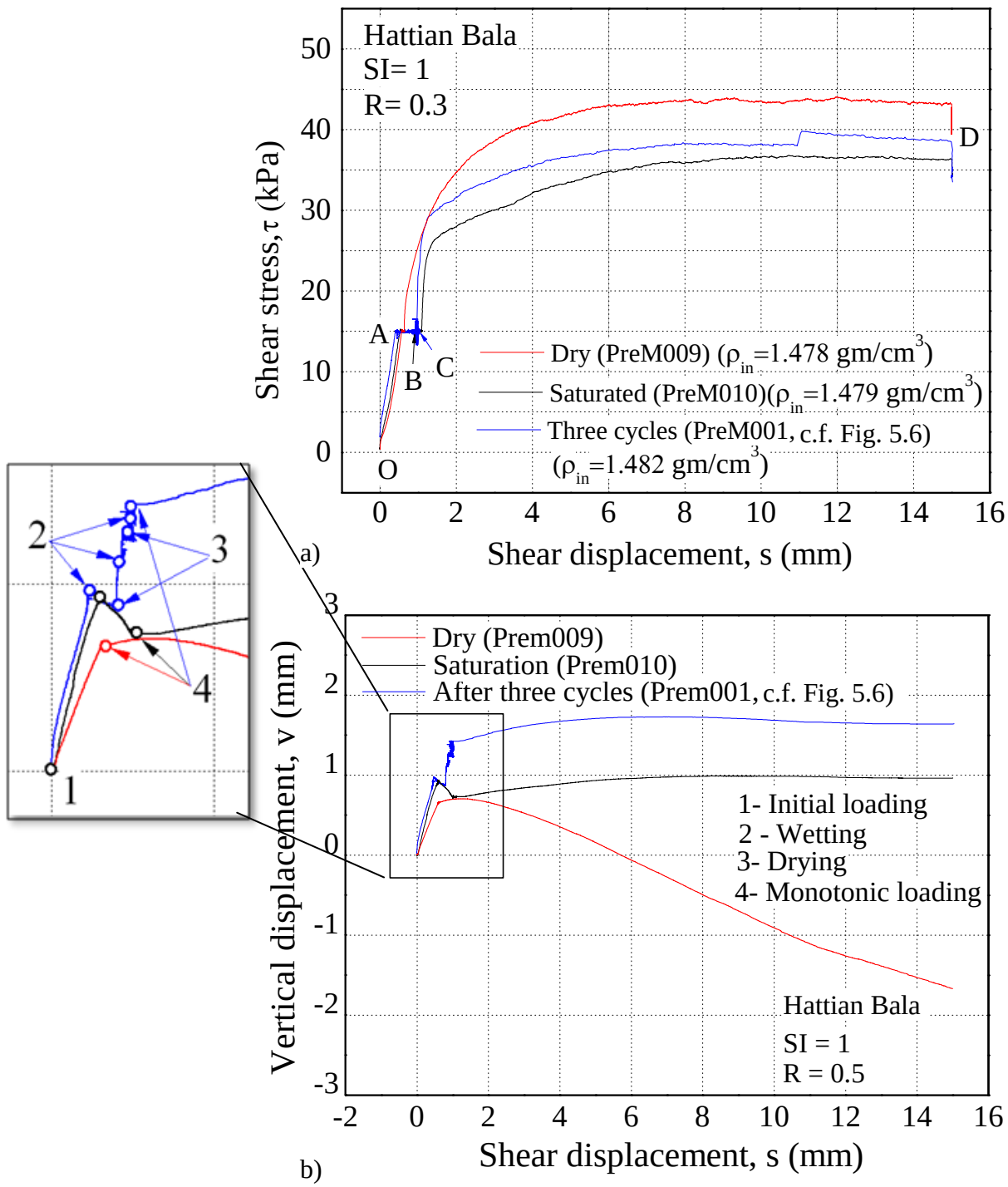

Fig 5.14 a) stress-deformation b) volume changes characteristics under R= 0.3 during experiment (Hattian Bala)

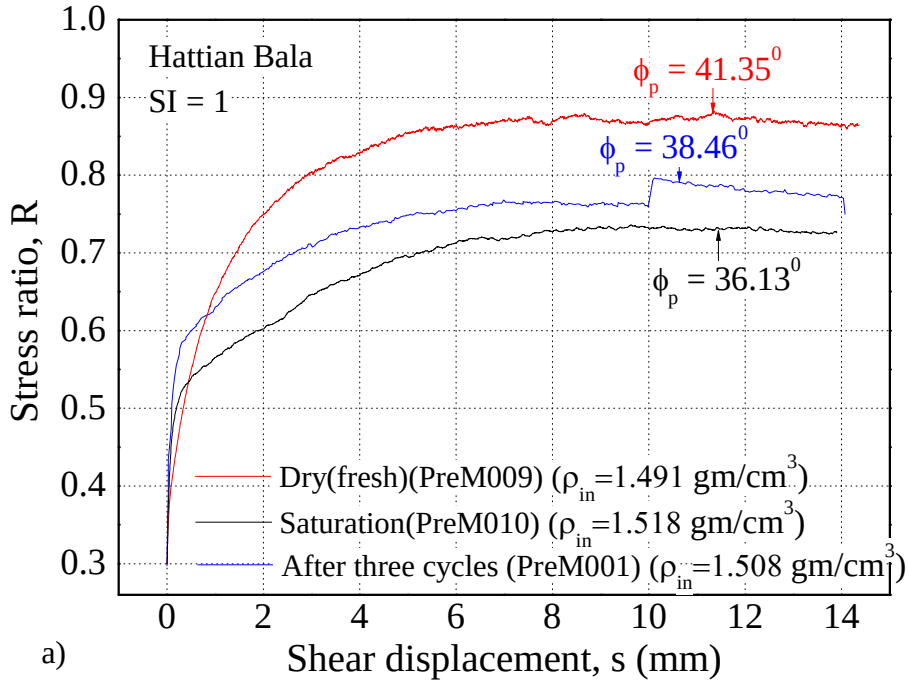

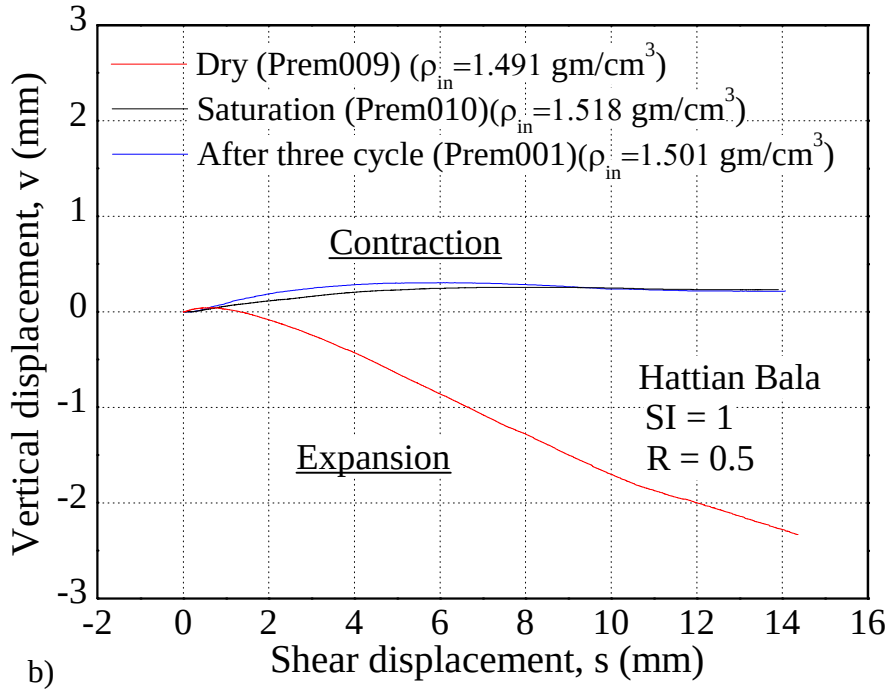

Fig. 5.15 Effect of slaking on a) stress-deformation b) volume changes characteristics of Hattian Bala mudstone specimen under R= 0.3

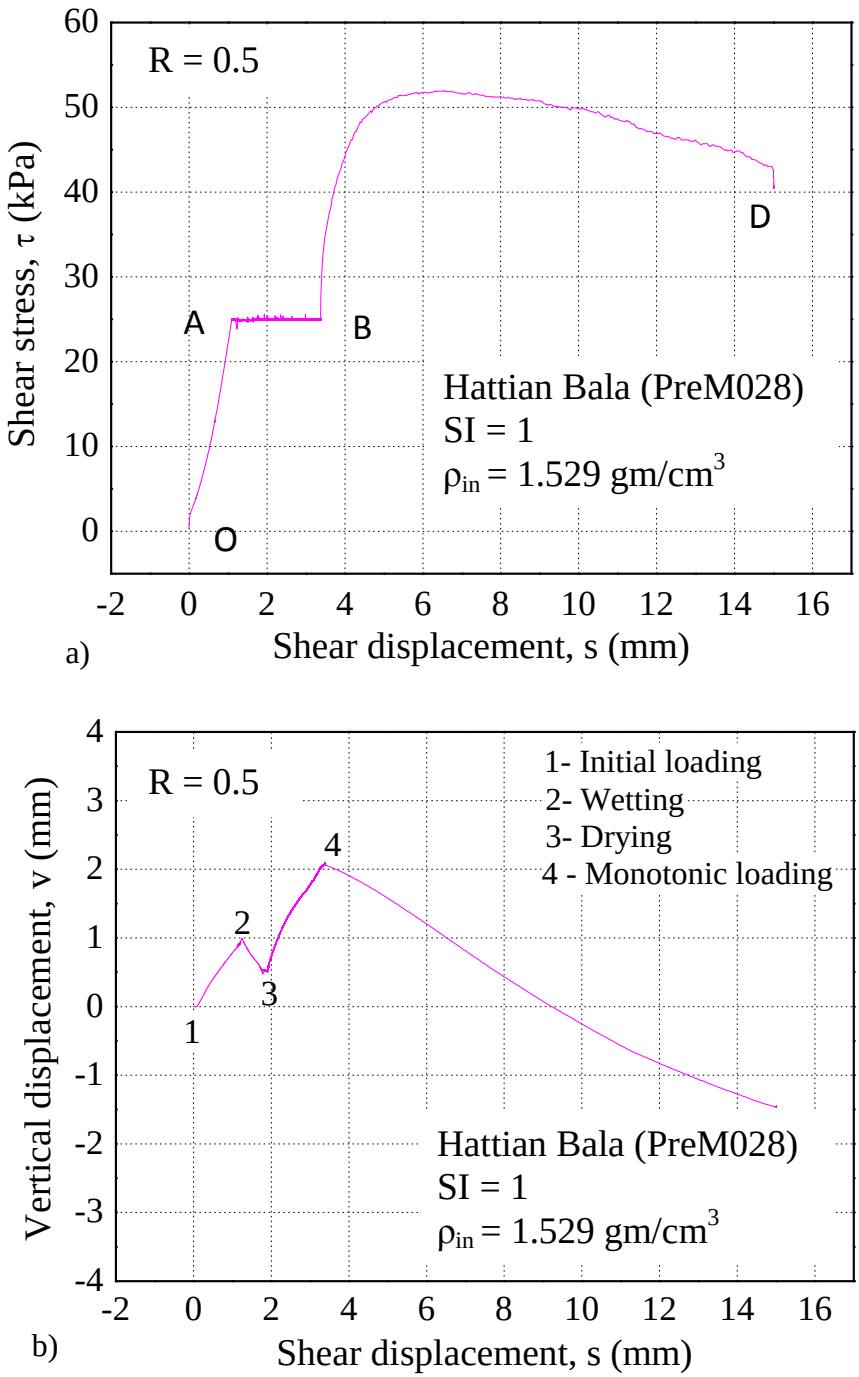

Fig 5.16 a) stress-deformation b) volume changes characteristics under R= 0.5 during experiment (Hattian Bala mudstone)

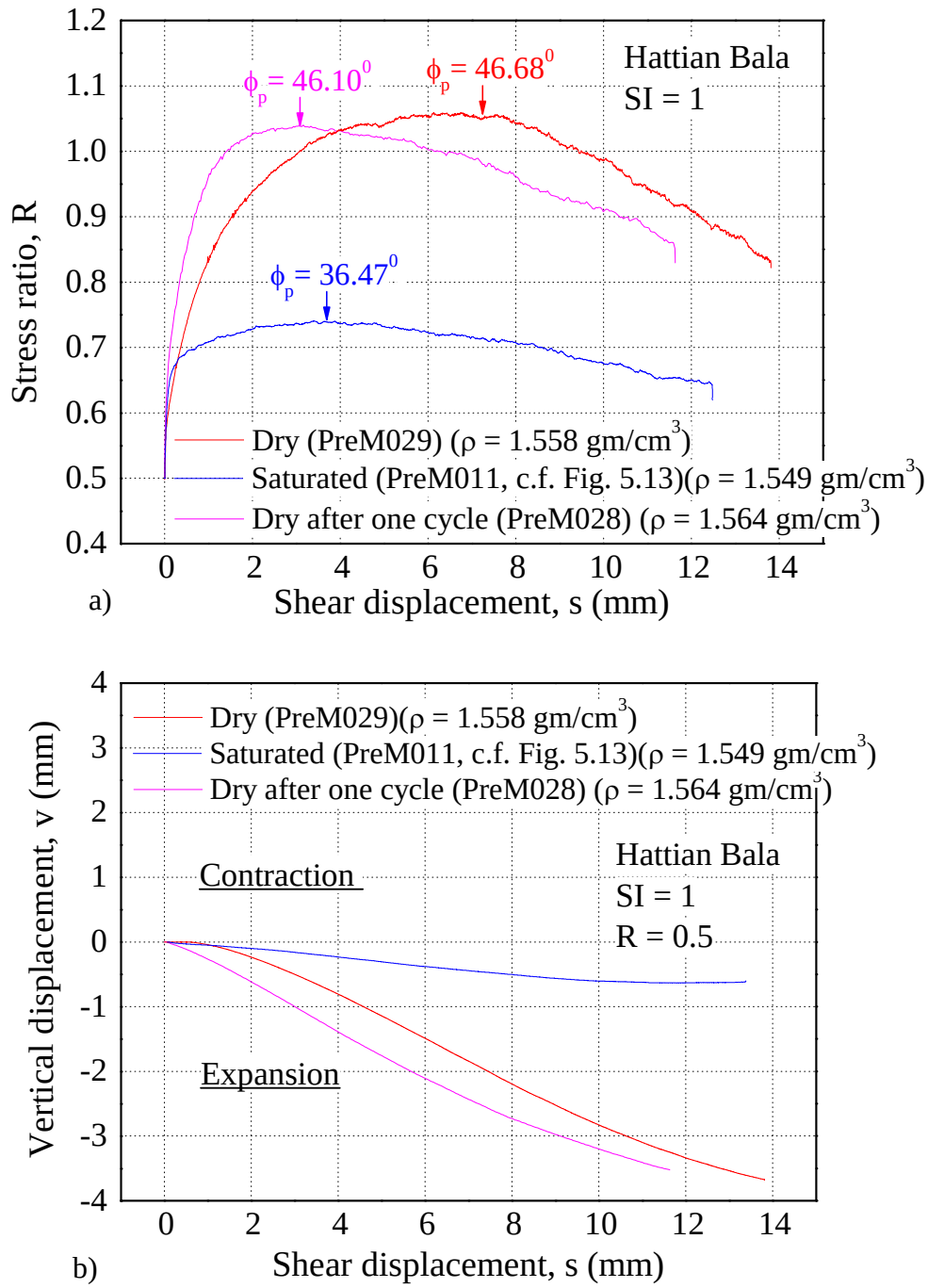

Fig. 5.17 Effect of slaking on a) stress-deformation b) volume changes characteristics of Hattian Bala mudstone specimen under R= 0.5

It is quite clear that the peak stress ratio of the specimens experienced three cycles of wetting and drying is higher than that of saturated specimens. This may be attributed to the specimen densification due to previous wetting and drying processes and aging and viscous effects due to relatively longer creep loading as compared to saturated specimen. In case of PreM030 (saturated test) and PreM002 (cyclic wetting and drying test) which had almost same density, the peak stress ratio of PreM030 (saturated test) is higher than PreM002 (cyclic wetting and drying test) even if PreM002 experienced longer creep time (Fig. 5.13a). The peak shear strength of the saturated and the one with cyclic wetting and drying test specimens is reduced by about 25 % as compared to the dry test specimens. So, it is concluded that the stress-strain response of crushed mudstones show higher peak stress ratio under dry condition with enormous decrease in peak shear stress after saturation essentially due to slaking induced particles disintegration.

As already discussed, all specimens except PreM001 and PreM010, under the three different condition exhibited dilative behavior during monotonic shear loading (Fig. 5.11b, 5.13b and 5.15 b). However, it is seen that the residual state is no longer unique. Generally, the position of residual state is unique under constant stress. The position of residual state varies with the degree of saturation. Monotonic shear loading was applied under fully saturated condition after one and three cycles of wetting and drying; there is a considerable difference in the position of residual states. So, this result indicates that particles crushing due to cyclic wetting and drying causes the difference in position of residual state. The PreM001 and PreM010 exhibited dilatative behaviour followed by contraction. This is attributed to the relatively low density of the specimen before monotonic loading (see Table 5.1).

Fig. 5.17 shows the stress-strain-volume change behaviour of three specimens namely; PreM029, PreM011 and Prem028. The specimen PreM029 correspond to dry and fresh (without any cyclic wetting and drying in laboratory) specimen. The specimen PreM011 was subjected to wetting under constant load condition, while the PreM028 subject to one complete cycle of wetting and drying. From the figure, it is quite clear that the reduction in peak shear strength during wetting is almost recovered during drying phase. However, there is small reduction is peak shear stress after one complete cycle of wetting and drying as compared to fresh specimen. Similarly, density, aging and viscous effects are neglected. The specimen with

one complete cycle of wetting and drying specimen experience relatively large creep time as compared to fresh specimen. This may be one of the reasons to recover the peak shear stress again. However, the resistivity to the slaking of Hattian Bala mudstone is also high. In general, it is concluded that the slaking effect on strength parameters due to cyclic wetting and drying is not found significant for the Hattian Bala mudstone specimen.

5.3.2 Ishikawa mudstone

The influence of the slaking on the mechanical properties and particle disintegration by simulating two cycles of wetting and drying under constant sustained loading were investigated.

Figure 5.18 shows the typical instantaneous response of creep deformations and water content of the specimen during the wetting and drying cycles for the Ishikawa mudstone specimens; PreM027. The time t= 0 corresponds to the start of creep loading. For all specimens, the creep shear and vertical displacements converged on constant values after several hours of initial loading.

Each cyclic wetting and drying creep test took about one month to complete. Influence of wetting in the first cycle upon shear displacement appears to be significant for the Ishikawa mudstones specimens (Fig. 5.18a). Similarly, significant positive vertical displacement (about 3 %) found during saturation process. Positive value of vertical deformation is taken as contraction. The vertical displacement of Ishikawa mudstone specimens during saturation being positive is indicative of slaking induced disintegration of soil particles as well as collapse of relatively open structure of these materials having high initial void ratios. For the second wetting processes, the increment of shear displacement is insignificant as compared to increment shear displacement during first wetting. However, substantial negative vertical displacement occurs during second wetting processes while the vertical displacement during first wetting was positive (Fig. 5.18a).

Figure 5.18 also shows that water content decreases gradually during drying processes. Initially, no appreciable creep deformation is found to occur at higher water contents. When the water content became about 62 %, both vertical and shear displacements occur progressively with water loss and finally tend towards an asymptotic value at water content of about 12 %.

As in the Hattian Bala mudstone specimen, both shear and vertical displacement during drying are composed of two well defined curvilinear parts.

The observations made in first wetting are in strong agreement with a study by Neves and Pinto (1988) on prediction of collapse settlement due to saturation rock-fill, mainly in embankment dams. Therefore, it is inferred that slaking induced deterioration of soil grains which ultimately leads to enormous compression upon sustained loading can be critical for the embankments constructed with crushed mudstones, for soil structure interaction of foundation placed on such soils as well as progressive slope failures.

Shear displacement caused by wetting seems to be decreased with progress of cycle, almost zero during the second wetting. This may be attributed to the specimen densification due to previous wetting and drying processes (Nakano et al., 1998) and relatively higher water content about 12 % before second wetting (Nakano et al., 1998 and Panabokke and Quirk, 1956).

The vertical displacement of Ishikawa mudstone during second wetting is contrary to the vertical displacement during first wetting (Fig. 6.6b) Considerable negative vertical displacement (expansion) occurred during second wetting. This is attributed to the densification of specimen during previous wetting and drying.

Relatively large creep deformation during the drying processes was observed which is similar to the Hattian Bala mudstones specimens.

Shear stress-deformation-volume change relationship for the all dry, saturated and the one with cyclic wetting and drying history specimens are shown in Fig. 5.19 and 5.20. Here “volume change” denotes the ratio of shear and vertical displacement, and its negative value indicates dilation. The specimens of PreM027 was subjected to the alternative step of loading history including two cycles of alternative wetting and drying while the specimens PreM026 was subjected to alternative step of loading including saturation only. Similarly, and PreM009 were subjected original loading history mentioned in Chapter 4. The time t=0 corresponds to the start of initial loading (anisotropic consolidation).

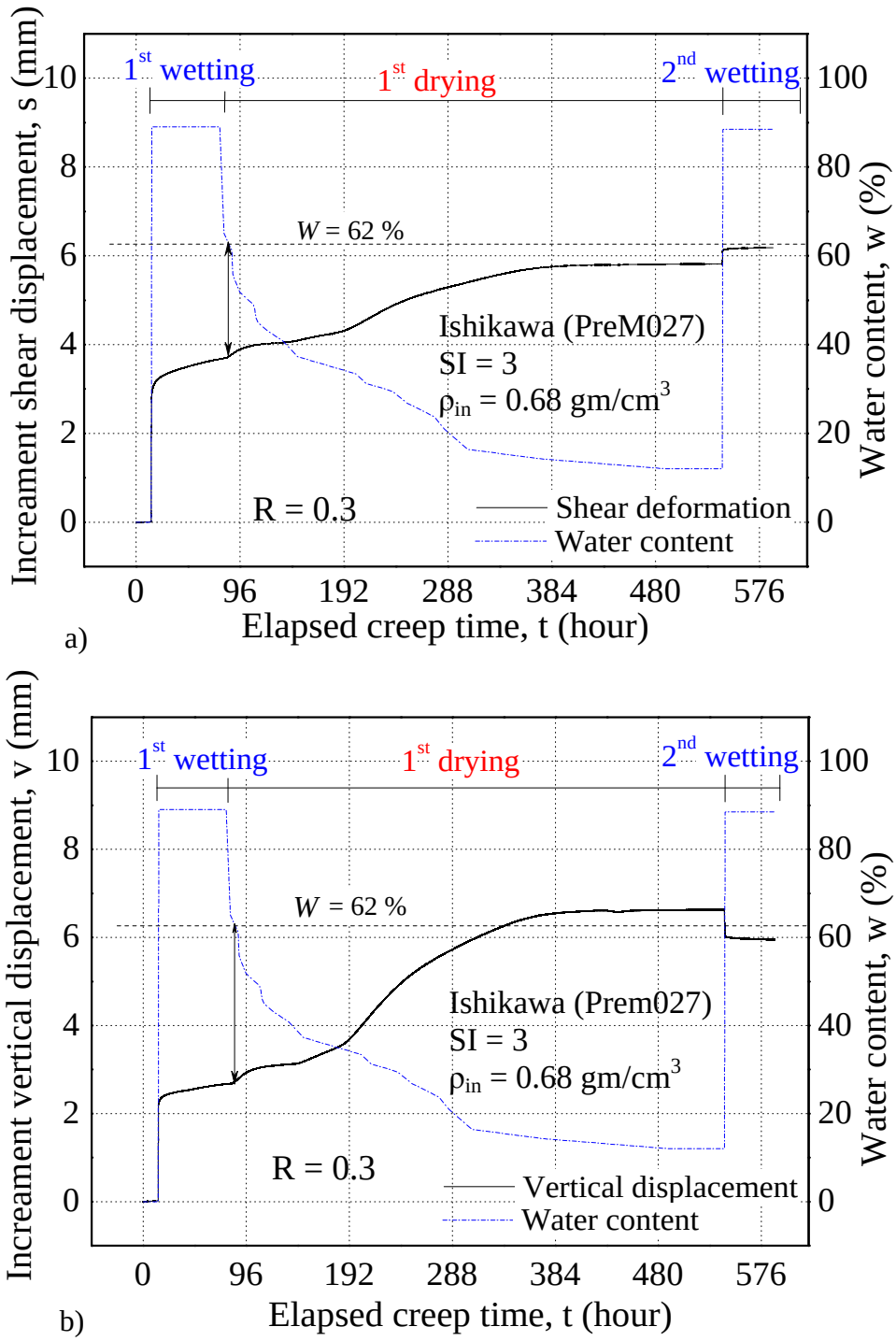

Fig 5.18 Time histories of water content, shear and vertical displacement (a) shear (b) vertical content under cyclic wetting and drying for 2 times for R= 0.3 (PreM027)

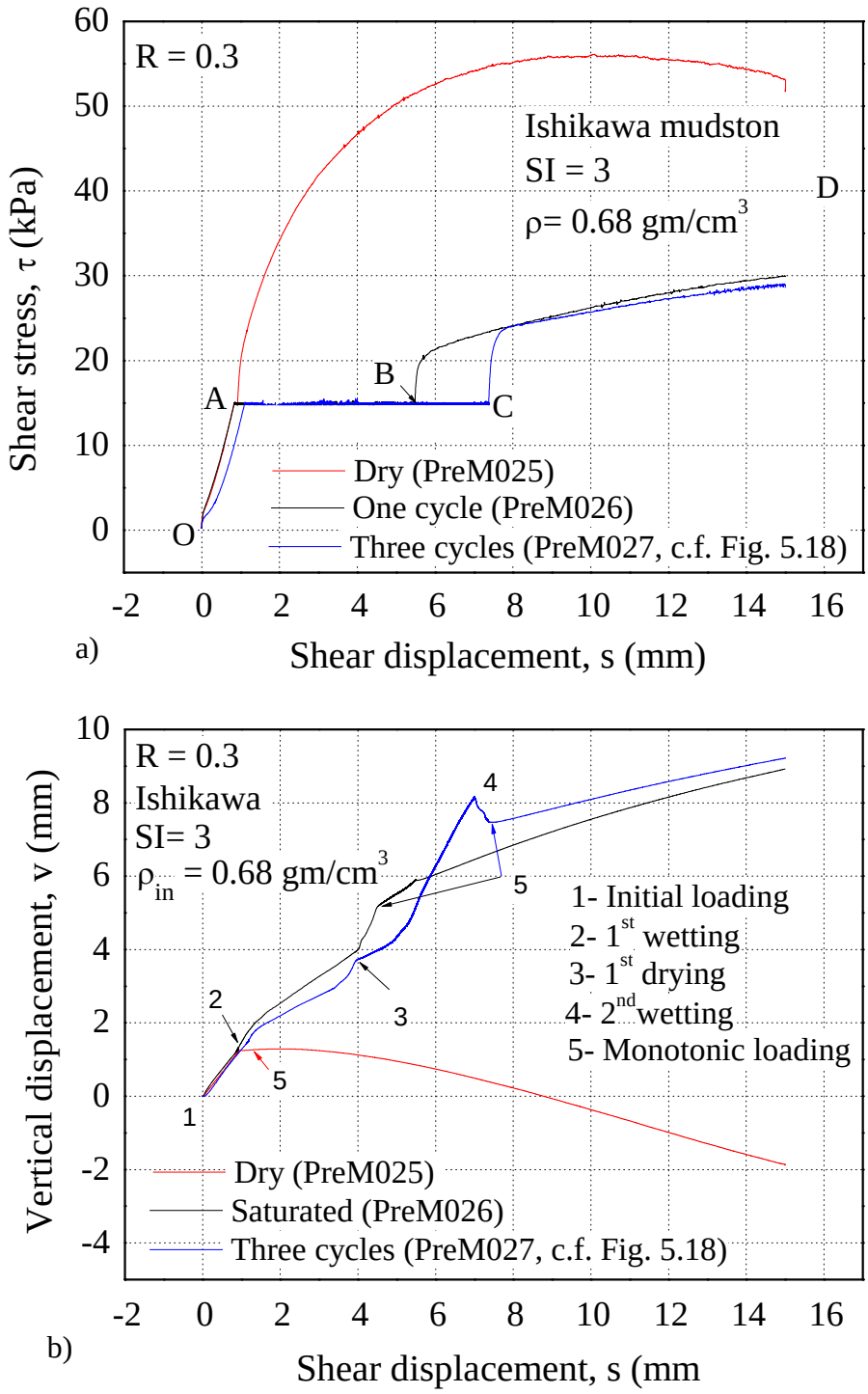

Fig 5.19 a) stress-deformation b) volume changes characteristics under R= 0.3 during experiment (Ishikawa mudstone)

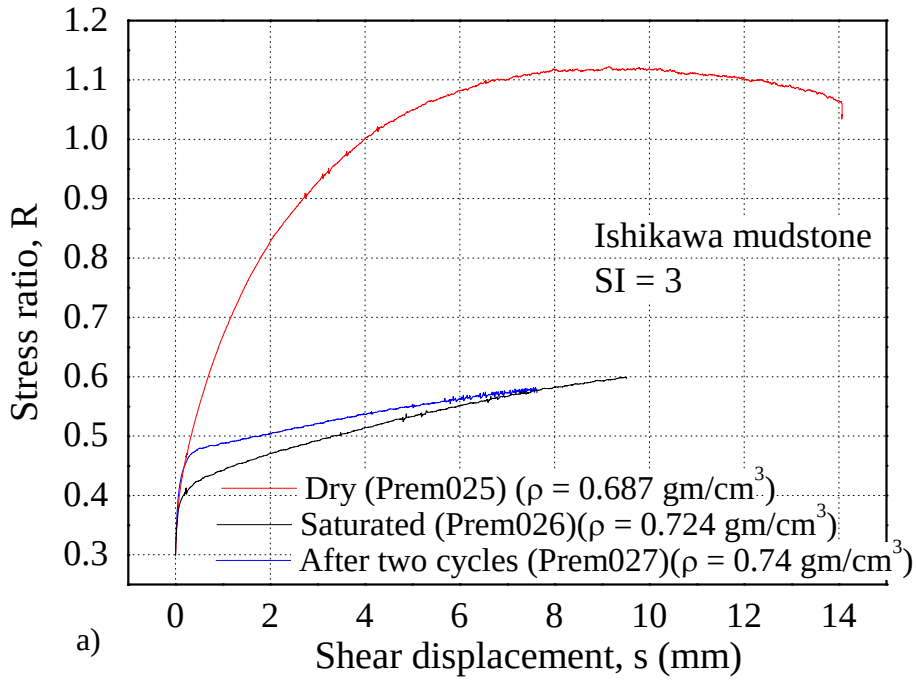

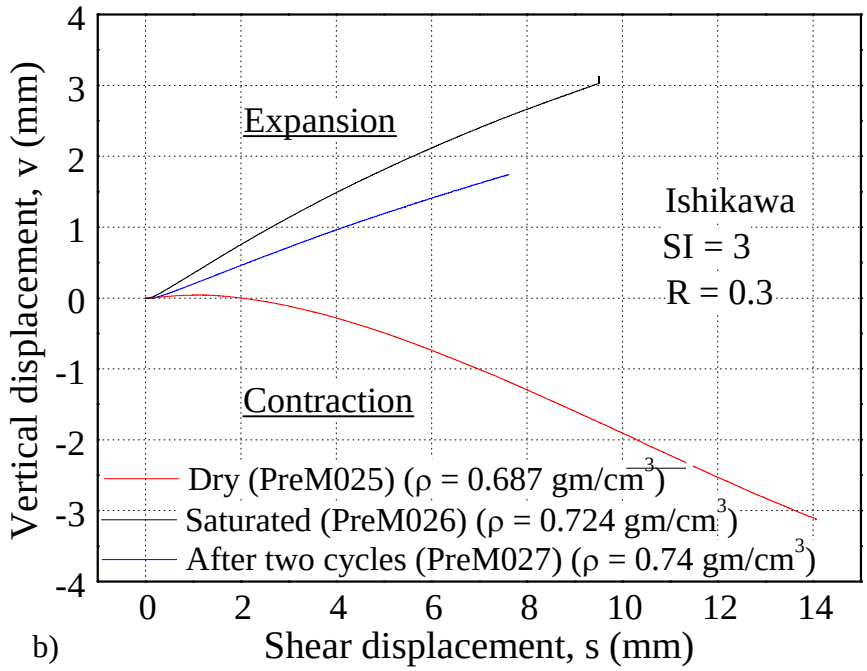

Fig. 5.20 Effect of slaking on a) stress-deformation b) volume changes characteristics of Ishikawa mudstone specimen under R= 0.3

Figure 5.19a shows stress-strain behaviours of Ishikawa mudstone dry, saturated and the one with cyclic wetting and drying specimen. As described in previous chapter, initially, both shear stress, τ, and vertical stress, σ v, were applied to the dry specimen gradually keeping their ratio, R (= τ/σv, σv = 50 kPa), constant. For the Ishikawa mudstone specimens, the creep load was applied maintaining stress ratio equal to 0.3 which is equivalent to slope ground with 17^0 inclinations. The shear displacements from the origin, O to A (Fig. 5.19a) correspond to the initial loading.

When both shear and vertical displacements due to initial loading had reached an almost constant value, the first wetting was carried out by supplying distilled water. This creep loading process represent a situation that slope ground is saturated by rain fall under constant stress condition. The shear displacements from A to B (Fig. 5.19a) are the combination of three probable phenomena such as creep, slaking and wetting induced displacement under constant loading. In addition, different deformation response was observed for consecutive specimens under similar condition during initial loading and saturation of various specimens. This is possibly due to the irregular rearrangement of soil particles during specimen preparation, particles disintegration of some grains and or different collapsing/swelling direction upon saturation

As already mentioned, the specimen PreM027 was subjected to two cycles of wetting and drying under constant loading. So, the shear displacements from B to C (Fig 5.19a) represent the cyclic wetting and drying induced displacement. The segments A to D (Fig 5.19a) of the dry specimens are the stress-strain relationship during monotonic shear loading under constant stress (σ_v = 50 kPa) condition. Similarly, the portions B to D are the stress-strain relationship during monotonic loading under constant stress (σ_v = 50 kPa) for the saturated specimens while the segments C to D represent the stress- strain behaviours during monotonic loading after three cycles of wetting and drying.

Figure 5.19b shows the shear deformation-volume change relationship for all specimens under different conditions. All specimens showed contractive behaviour during initial loading. In addition, the positive vertical displacement (contraction) was found during the first wetting. PreM027 exhibited shrinkage behaviour during the drying process with increase in shear displacement. The vertical displacement of Ishikawa mudstone during second wetting is

contrary to the vertical displacement during first wetting. Considerable negative vertical displacement (expansion) occurred during second wetting.

Stress-strain-volume change characteristics from monotonic direct shear tests on crushed mudstone specimens of Ishikawa material at constant vertical stress (σ_v=50 kPa) under dry, saturated and cyclic wetting and drying conditions are presented in Fig. 5.20.

Figures 5.20 show the relationship between the shear stress ratio, R, and the shear displacement, *s*, together with the associated volume change (i.e. the vertical displacement, *v*) for the Ishikawa mudstone specimen. The values of *s* and *v* were set at zero at the beginning of monotonic loading. In addition, the values of friction angles, φ_d, (assuming apparent cohesion c_d =0) at peak strength were also indicated in these figures. The saturated and the one with cyclic wetting and drying mudstone specimen exhibit largely different stress-displacement features from those for dry specimen. In case of saturated (PreM026) and the one with cyclic wetting and drying (PreM027) specimen, neither clear peak stress ratio nor post-peak stress softening appeared and the R-s curve converged monotonously (Fig. 5.20a). Consequently, the stress level at which significant plastic (or irreversible) deformation develops (i.e. the start of yielding or yield stress) is different between these two specimens. The peak shear strength of the saturated and the one with cyclic wetting and drying test specimens is reduced by about 45 % as compared to the dry test specimens. Relatively large inherent void ratios, e (2.3), slaking induced disintegration during wetting and particle rearrangement of weak soil grains are the most responsible factors for significant reduction in peak shear strength during wetting.

The dry specimen (PreM025) exhibited the dilative behaviour during monotonic shear loading while the saturated and the one with cyclic wetting and drying specimen (PreM026 and PreM027) continued to exhibit contractive behaviour (5.20b). Such stress-displacement characteristics are true to typical soft soils, indicating that the slaking process causes the examined mudstone material to disintegrate and therefore changes its mechanical features remarkably. The test, which experienced two cycles of wetting and drying (PreM027), seems stiffer than the saturated one. This may be attributed to the specimen densification during previous wetting and drying processes and aging and viscous effects due to relatively longer creep loading as compared to saturated specimen (Prisco and Imposimato, 1996; Tatsuoka et al., 2000 and 2001; Nawir et al., 2002).

Ishikawa mudstone showed relatively higher slaking index (level 3) and very small slaking ratio, which indicate highly susceptible to slaking. Similarly, large shear displacement and volumetric compression during saturation of crushed mudstones (Ishikawa) as well as a drastic loss of strength parameters upon submergence are revealed in this study. It is concluded that the observed soil behaviour can be critical for the slope stability. In addition, it can be critical for the embankments constructed with similar materials and bearing capacity of the place on such soft sedimentary rocks having higher slaking index or ratio.

5.3.3 Glass beads

The slaking index (JGS 2132) of the Glass beads was evaluated as level 0, while the slaking ratio (NEXCO-110, 2006) was 100 %. Similarly, the index properties of Glass beads were explained in Chapter 4. The influences of cyclic wetting and drying on Glass beads were evaluated by simulating two cycles of wetting and drying under constant sustained loading.

Figure 5.21 shows the typical instantaneous response of creep deformations of the Glass beads specimen (PreG0014) during the wetting and drying cycles. The time t= 0 corresponds to the start of creep loading. For all specimens, the creep shear and vertical displacements converged on constant values after several hours of initial loading.

The water was supplied to the Glass beads specimen after 5 hours creep loading. The Influence of wetting in the first cycle upon both shear and vertical displacement appears to be negligible (Fig. 5.21). Then, after 18 hours of creep loading under saturated condition, the water was removed from the specimen. The water content of the specimen decreased gradually and became almost zero after 4 days. As in the wetting, the influences of drying upon both shear and vertical displacements were not noticed. Similarly, for the second wetting processes, the increments of shear and vertical displacements were again almost zero.

Figure 5.22 and 5.123 show stress-strain-volume change behaviours of Glass beads under both dry and saturated conditions for the stress ratio 0.5. As described in previous chapter, initially, both shear stress, τ, and vertical stress, σ_v, were applied to the dry specimen gradually keeping their ratio, R (= τ/σ_v, σ_v = 50 kPa) constant. The shear displacements from the origin, O to A (Fig. 5.22a) corresponds to the initial loading. When both shear and vertical displacements due to initial loading had reached an almost constant value, the saturation was

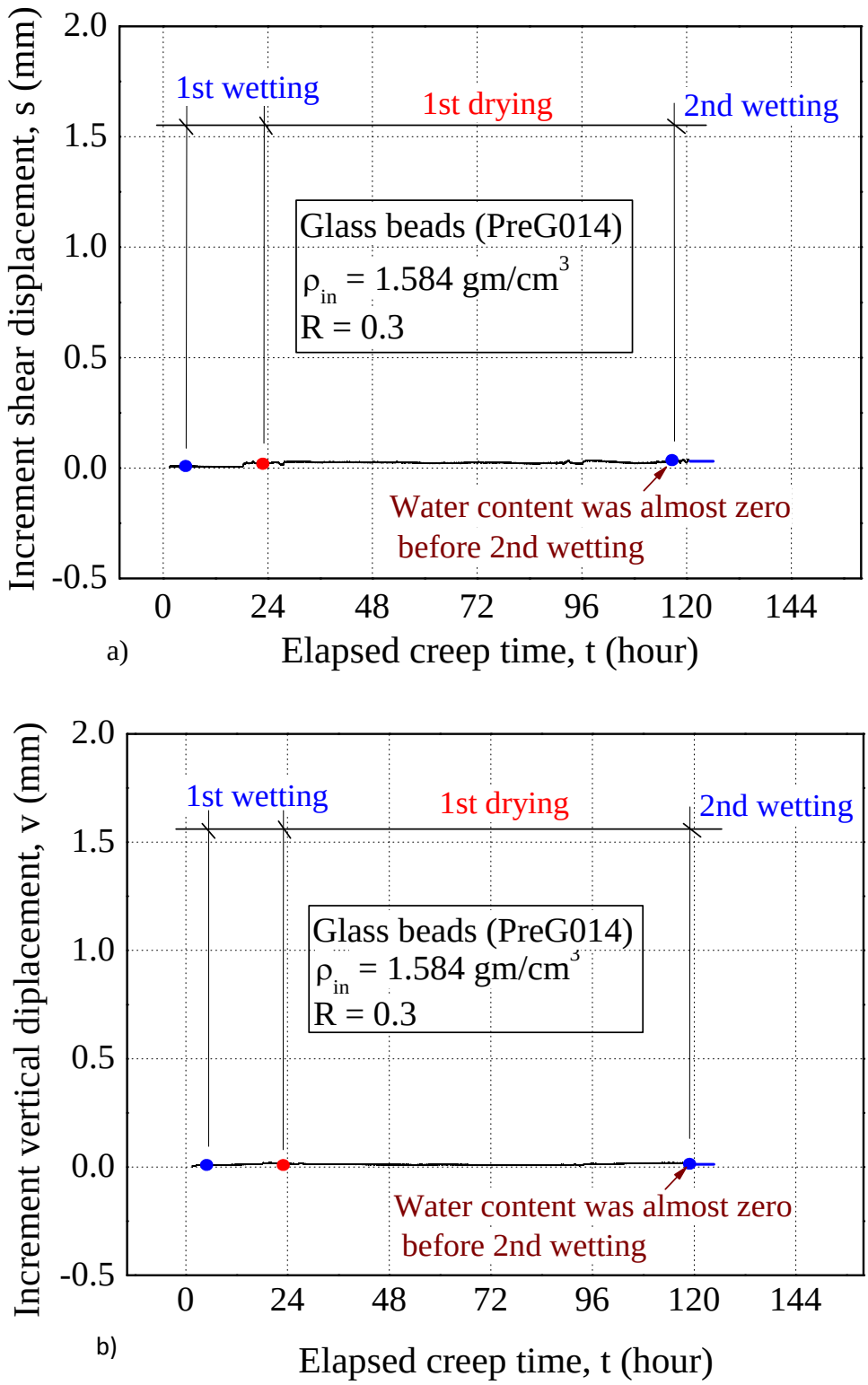

Fig 5.21 Time histories of water content, shear and vertical displacement (a) shear (b) vertical content under cyclic wetting and drying for 3 times for R= 0.3 (PreG014)

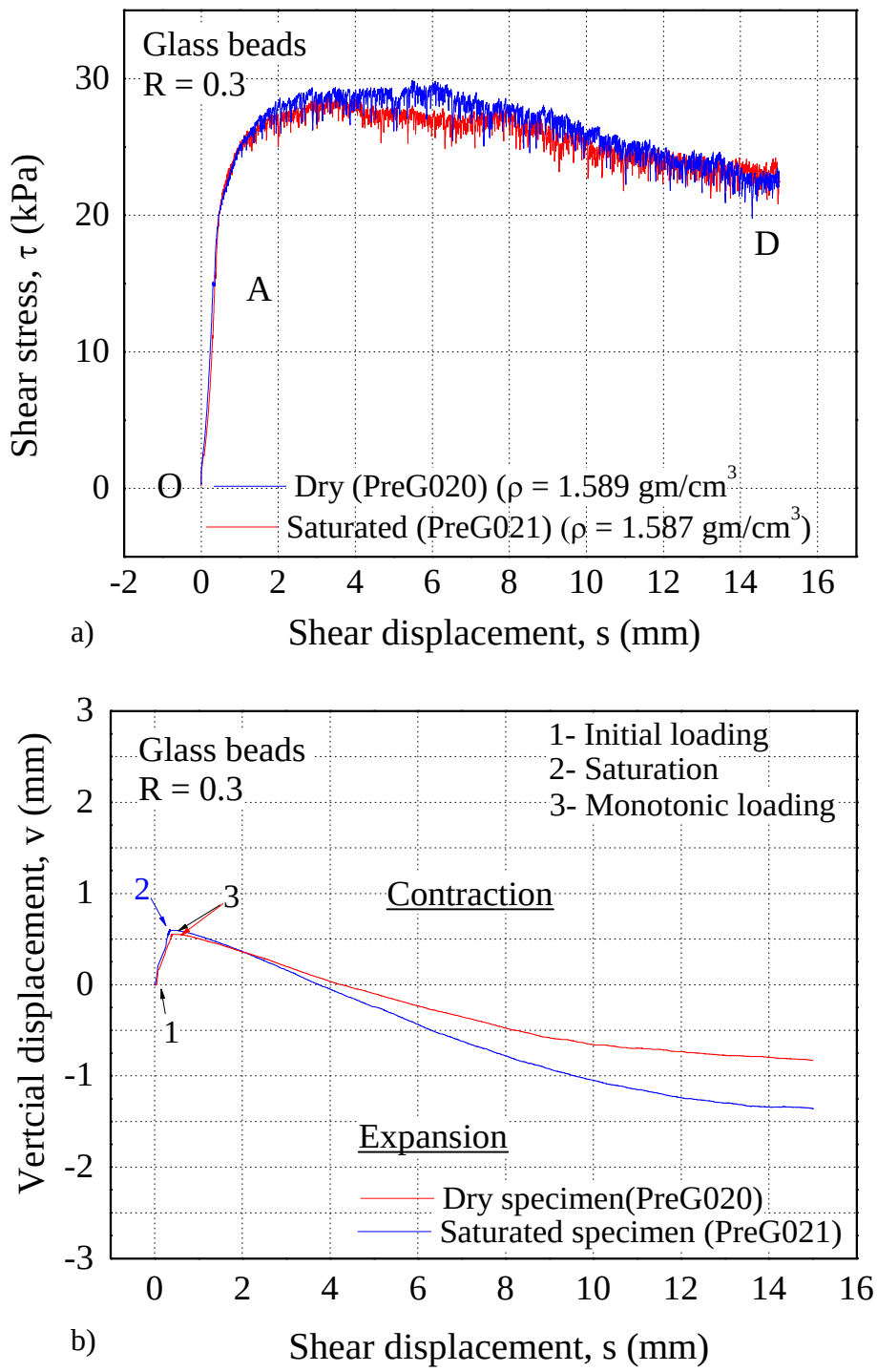

Fig 5.22 a) stress-deformation b) volume changes characteristics under R= 0.3 during experiment (Glass beads)

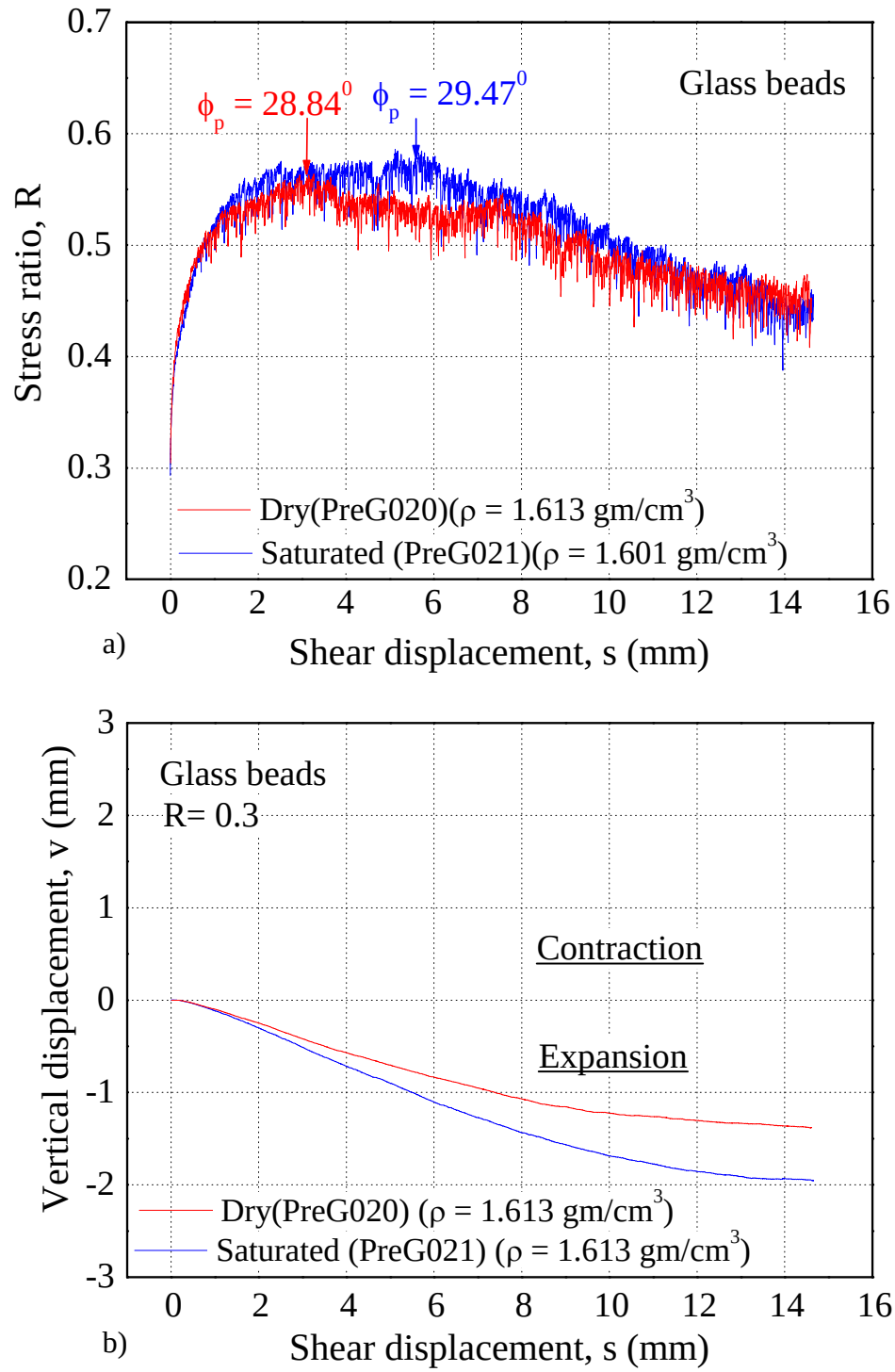

Fig. 5.23 Effect of saturation on a) stress-deformation b) volume changes characteristics of Glass beads specimen under R= 0.3

carried out by supplying distilled water from the bottom of shear box. This creep loading process represent a situation that slope ground is saturated by rain fall under constant stress condition. The segments A to D (Fig 5.22a) of the specimens are the stress-strain relationship during monotonic shear loading under constant stress (σ_v = 50 kPa) condition..

Figure 5.22b shows the shear displacement-volume change relationship for both specimens under dry and saturated conditions under stress ratio 0.5. Both specimens showed contractive behaviour during initial loading while these specimens exhibited dilative behavior during monotonic shear loading.

It can be seen from the Fig. 6.23a that the difference in stress-strain behaviours between dry and saturated conditions is insignificant under different stress condition for the Glass beads specimen. Clear peak and residual stress states or strain softening under dry as well as saturated conditions are observed. It is certainly due to the durable (non slakable) nature of grains which are unaffected by the presence of water.

However, the volume change behaviour during monotonic loading under saturated condition is different than that of dry condition (5.23b). Strangely, the saturated specimens showed more dilative behaviour as compared to dry specimen during monotonic loading. So, details investigation by using other apparatus like Tri-axial test is required to explain the volume change behaviour of glass beads under dry and saturated conditions.

5.3.4 Chiba gravel and Toyoura sand

The influences of saturation on sand stone specimens (Chiba gravel) and silica sand (Toyoura sand) were evaluated by applying water to the dry specimens under sustained loading condition.

Figure 5.23 and 5.24 shows the typical instantaneous response of creep deformations of the Chiba gravel (PreC011) and Toyoura sand (PreT052) specimens during saturation. The time t= 0 corresponds to the start of creep loading. For all specimens, the creep shear and vertical displacements converged on constant values after several hours of initial loading. The water was supplied to the specimens after 17 hours creep loading. The Influence of saturation upon both shear and vertical displacement appears to be negligible (Fig. 5.23 and 5.24).

Figures 5.25 and 5.26 show stress-strain-volume change behaviours of Chiba gravel and Toyoura sand under both dry and saturated conditions respectively. As described in previous

sections, initially, both shear stress, τ, and vertical stress, σ_v, were applied to the dry specimen gradually keeping their ratio, R (= τ/σ_v, σ_v = 50 kPa) constant. The shear displacements from the origin, O to A (Fig. 5.25a and 5.26a) correspond to the initial loading. When both shear and vertical displacements due to initial loading had reached an almost constant value, the saturation was carried out by supplying distilled water from the bottom of shear box. This creep loading process represent a situation that slope ground is saturated by rain fall under constant stress condition. The segments A to D (Fig 5.25a and 5.26a) of the specimens are the stress-strain relationship during monotonic shear loading under constant stress (σ_v = 50 kPa) condition.

Figures 5.25b and 5.26b show the shear displacement-volume change relationship of the specimens under dry and saturated conditions. Both specimens showed contractive behaviour during initial loading while these specimens exhibited dilative behavior during monotonic shear loading.

It can be seen from the Fig. 5.27 and 5.28 that the difference in stress-strain-volume change behaviours between dry and saturated conditions is insignificant for both Toyoura sand and Chiba gravel. Clear peak and residual stress states or strain softening under dry as well as saturated conditions are observed. It is certainly due to the durable (non-slakable) nature of grains which are unaffected by the presence of water. The smaller value of degradation index (ID) and Fines content (F_C) (Table 5.12 and 5.13) after the experiments also indicates the durability of grain. However, some differences in stress-strain-volume change behaviours could be noticed between dry and saturated test even though the difference is very small. The presence of pore water in saturated conditions can cause small variations in the soil skeleton and might be possible reason of negligible difference in stress-strain-volume change behaviours between dry and saturated tests. In general, it can be said that the slaking effect on stress-strain change behaviour of conventional granular materials is almost negligible. The specimens were prepared at high initial density therefore, volumetric expansion (positive dilatancy) during monotonic loading (shearing) for the Toyoura sand and Chiba gravel specimens was observed. The shear and vertical displacements during wetting were also found to be insignificant.

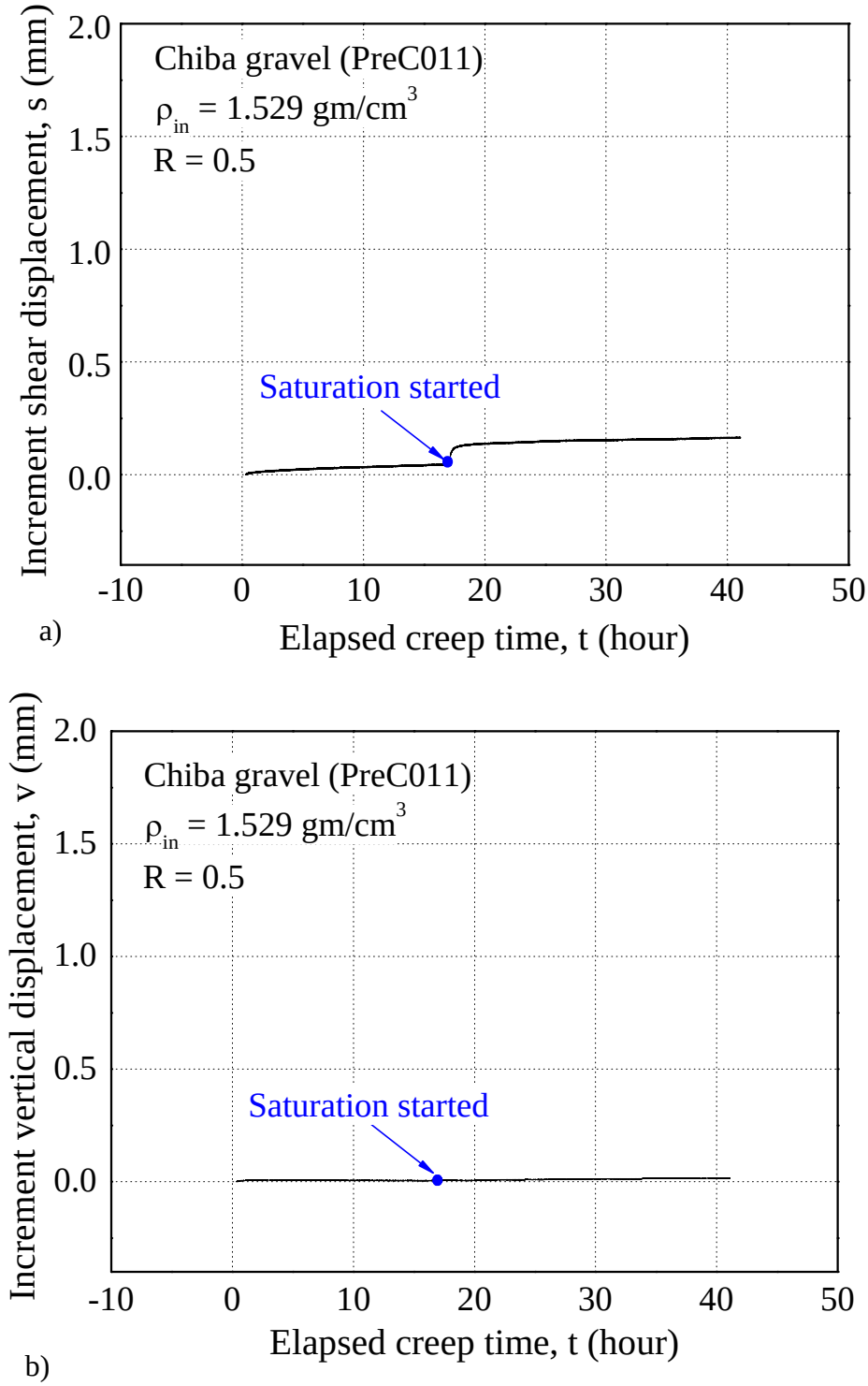

Fig 5.23 Increment a) shear b) vertical displacement during wetting under R = 0.5 (Chiba gravel)

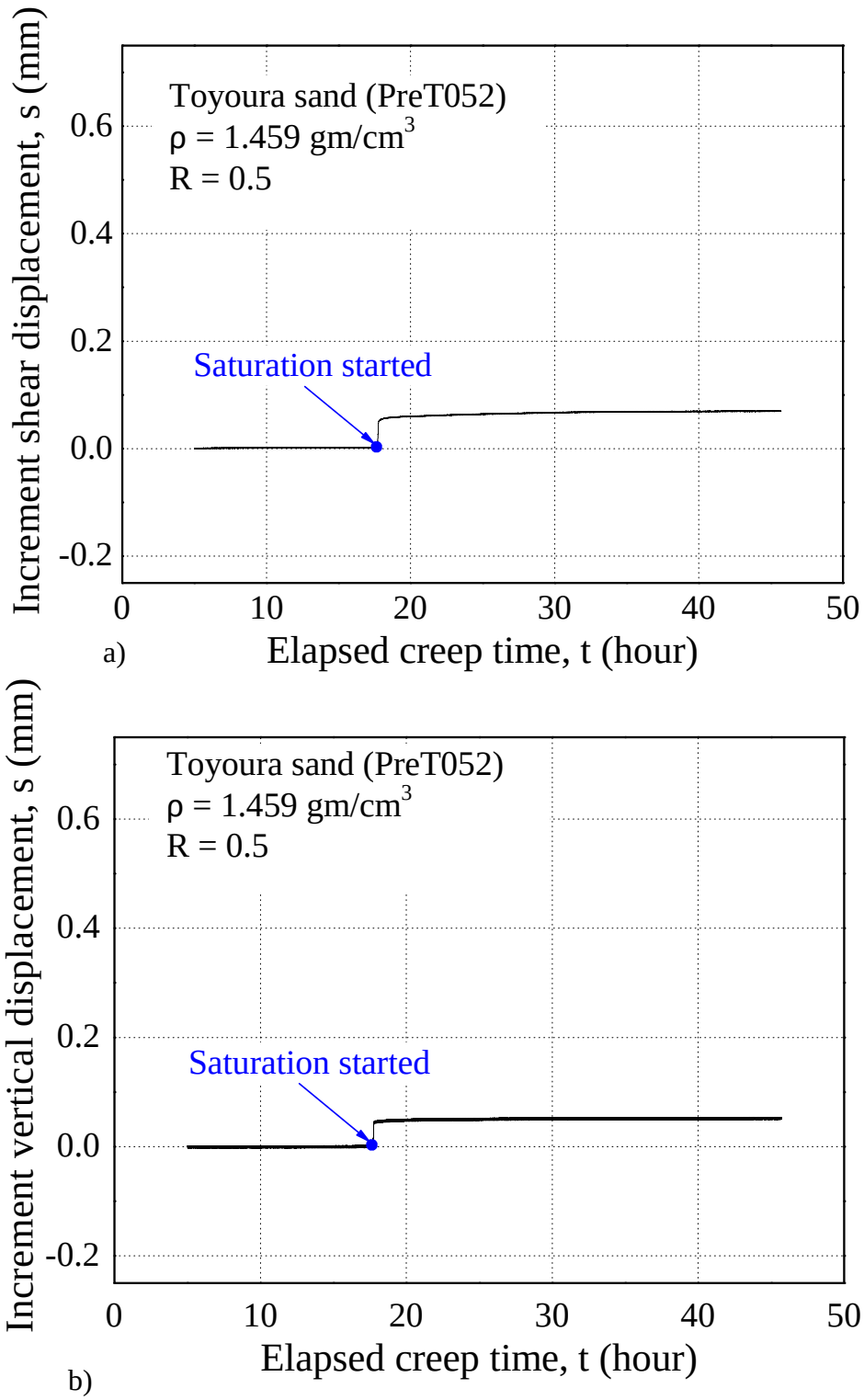

Fig 5.24 Time histories of shear and vertical displacement (a) shear (b) vertical displacement under R= 0.5 (Toyoura sand)

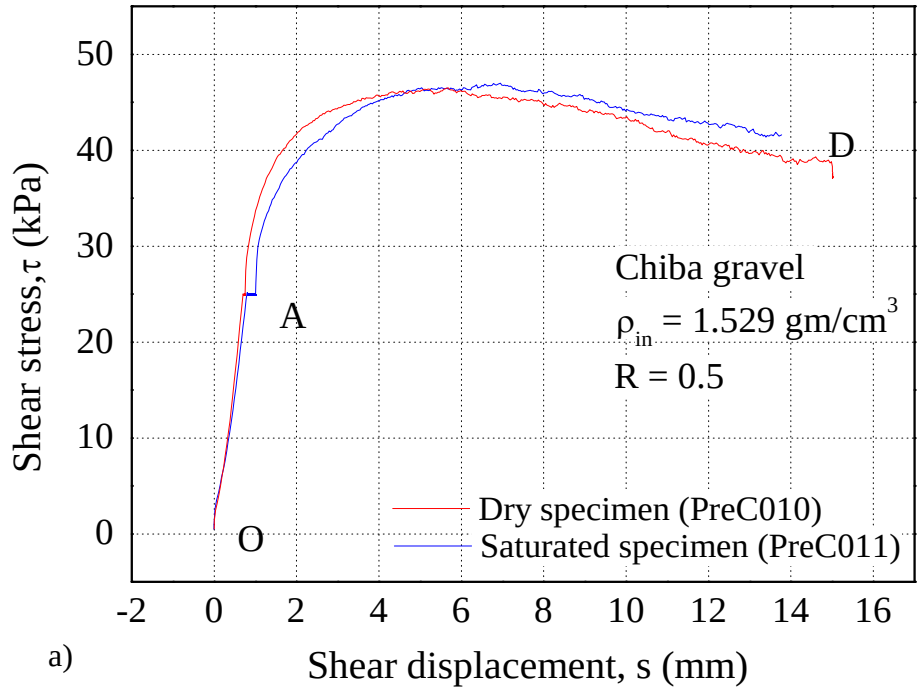

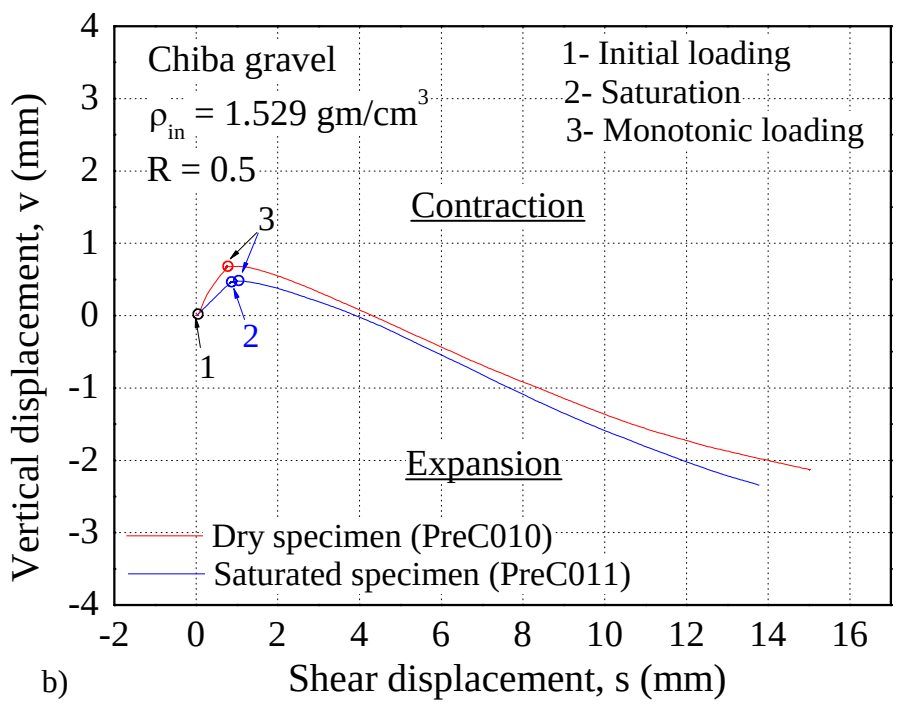

Fig 5.25 a) stress-deformation b) volume changes characteristics under R= 0.5 during experiment (Chiba gravel)

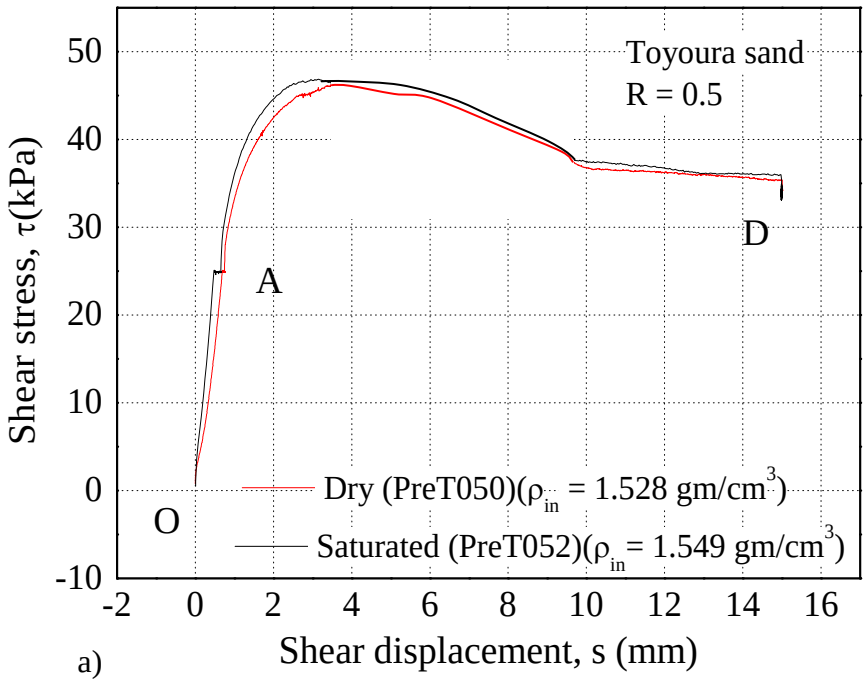

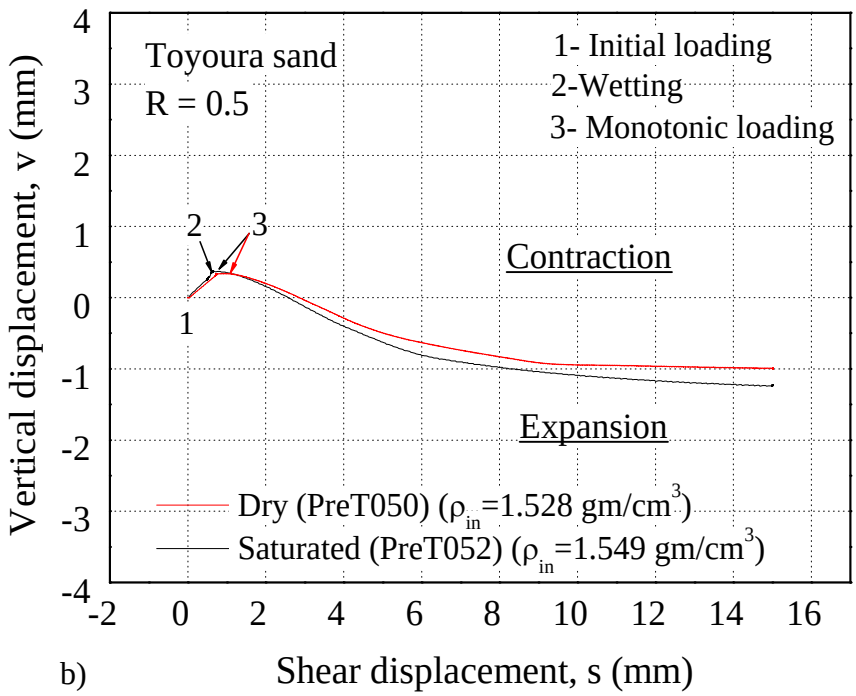

Fig 5.26 a) stress-deformation b) volume changes characteristics under R= 0.5 during experiment (Toyoura sand)

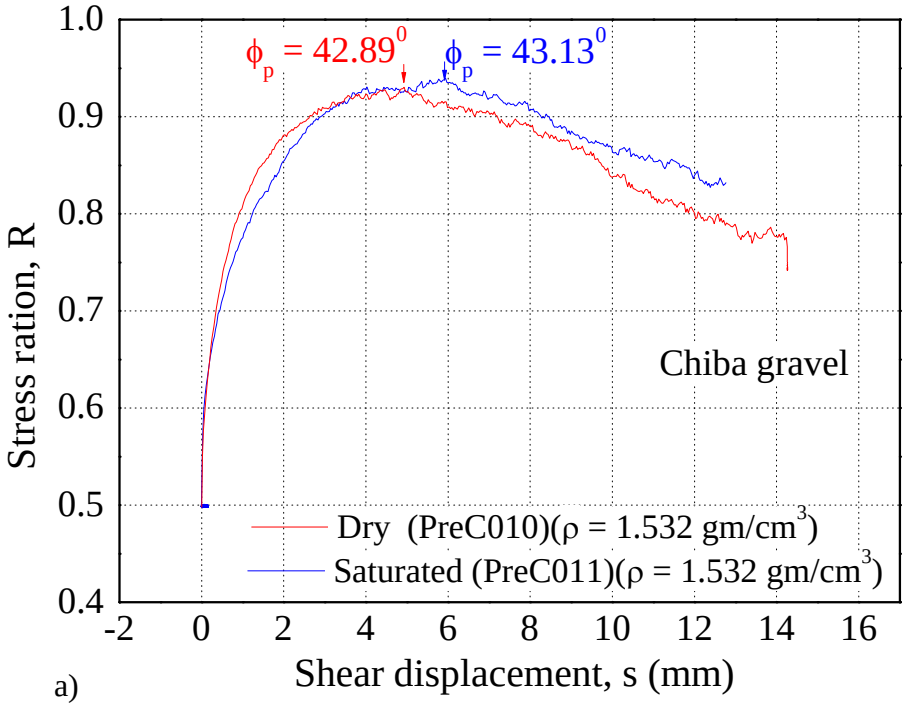

a)

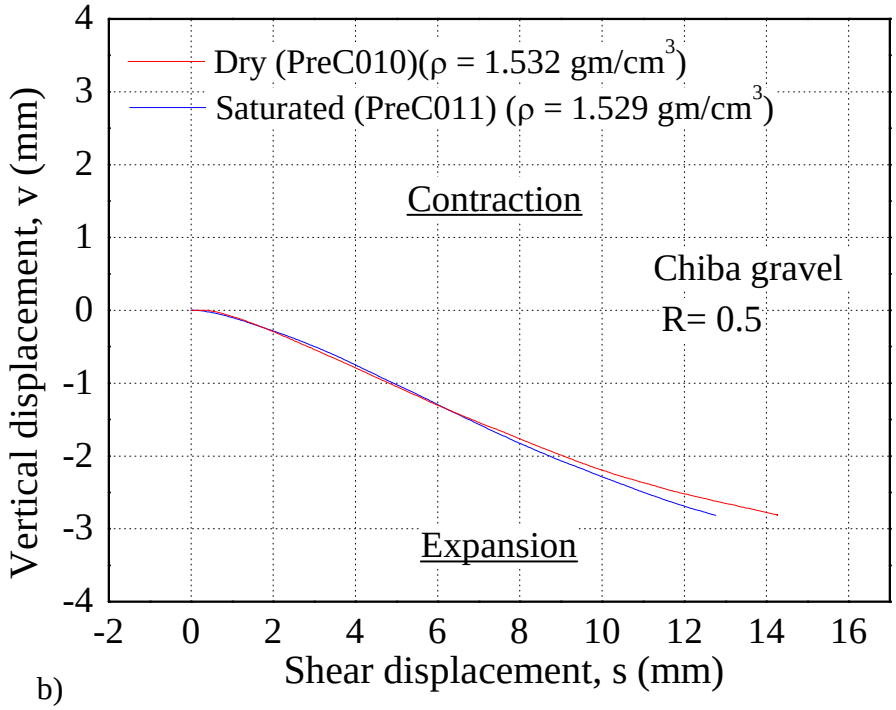

b)

Fig 5.27 a) stress-deformation b) volume changes characteristics under R= 0.3 during experiment (Glass beads)

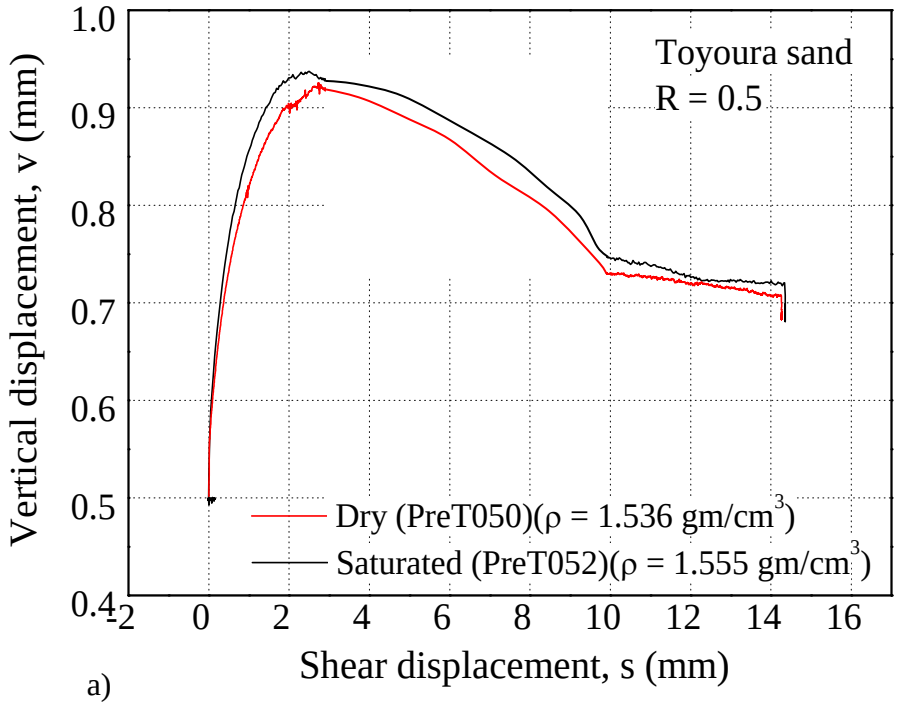

a)

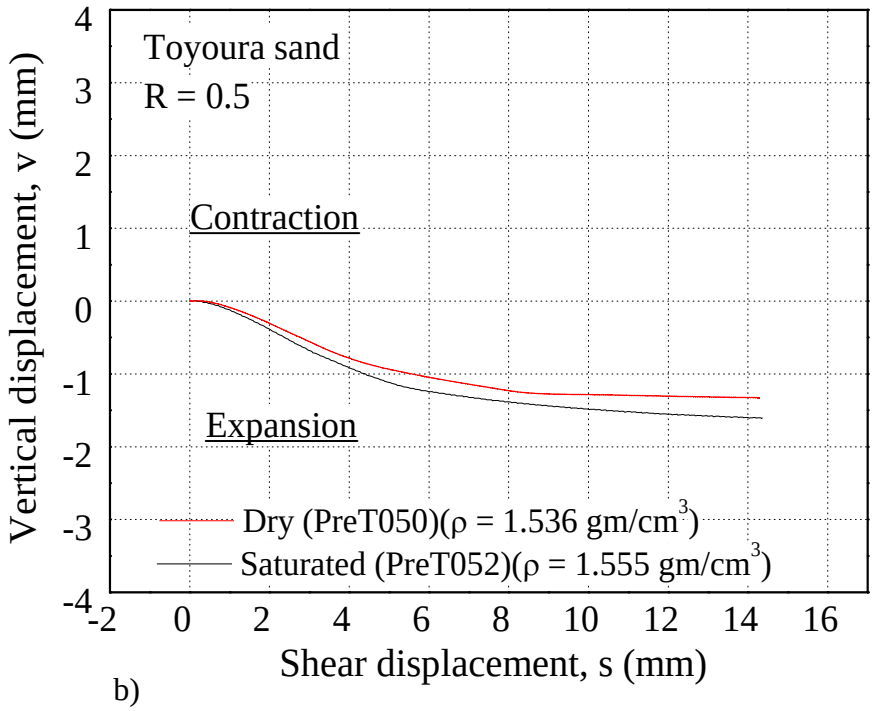

b)

Fig 5.28 a) stress-deformation b) volume changes characteristics under R = 0.3 during experiment (Toyoura sand)

From these discussion and the test results presented in this section, it is concluded that the stress-strain behaviour and volume change characteristics of Toyoura sand and Chiba gravel during monotonic shear loading are unaffected by presence of water i.e. no slaking effect on Chiba gravel and Toyoura sand. Similarly, Fioraqvante and Capoferri (1997), Wichtmann et al. (2005) and Youn et al. (2008) have reported negligible influence of saturated and dry condition on strength and stiffness as well as volume change characteristics of conventional granular materials consisting of durable grains.

5.4 Particle crushing and Degradation index

The mechanical properties of crushed mudstones are strongly affected by the slaking induced deterioration because the conventional soil mechanics parameter like angularity, mean grain size and grain size distribution etc., of crushed mudstones are no more constants. Therefore, the particles size distribution under working conditions should be known to assess the effects of deterioration on mechanical behaviour of the material. The index used in this study for quantification of slaking induced disintegration of crushed mudstones which is somehow related to slaking behaviour of crushed mudstones, was explained in Chapter 4. The slaking susceptibility of each mudstone upon saturation or cyclic wetting and drying can be quickly assessed by comparing the degradation index (I_D) and fines contents (F_C) at the end of dry, saturated and the one with cyclic wetting and drying tests.

Particle size distribution (PSD) curves are essential for qualitative and quantitative measurement of slaking susceptibility. Fineness (F_C) and degradation index (I_D) also useful for quantitative comparison of stress-strain response and volume change characteristics between dry, saturated and the one with cyclic wetting and drying conditions of various crushed mudstones (Aziz, 2010). Considering importance of degradation index (I_D), the particles size distributions of all the specimens before and after experiments were determined.

The particle size distribution (PSD) curves for the dry, saturated and the one with cyclic wetting and drying specimens tested under same stress ratio are presented in the same graphs. The Fig. 5.16 shows the particles size distribution (PSD) curves for the dry, saturated and the one with three cycles of wetting and drying Hattian Bala mudstones specimens tested under stress ratio 0.7.

The particle size distribution (PSD) after dry test for Hattian Bala mudstone shows some disintegration with average fines (finer than 2 mm) content and degradation index of 1.65 % and 0.06 respectively(Fig. 5.16). This is essentially due to crushing of relatively weak particles under vertical stress and monotonic shear loading.

Similarly, particles are crushed due to immersion and cyclic wetting and drying. It can also be defined as slaking induced disintegration. After experiment, it is seen that about 7.7 % particles by mass become finer than 2.0 mm after the saturated test, where as in the case of cyclic wetting and drying test 10.55 % particles by mass become finer than 2.0 mm respectively. Similarly, the degradation indexes were 0.12 and 0.16 for saturated and cyclic wetting and drying test (Fig 5.16).

Figure 5.17 shows the particles distribution curves (PSD) after the dry, saturated and the one with cyclic wetting and drying test for Hattian Bala mudstone specimen under stress ratio 0.5. About 1.5 %, 5.24 % and 8.24 % particles by mass become finer than 2.0 mm after dry, saturated and cyclic wetting and drying test. The degradation indexes after dry, saturated and cyclic wetting and drying tests were about 0.07, 0.11 and 0.15 respectively.

The particles distribution curves (PSD) for the tests under stress ratio 0.3 are presented in the Fig. 5.18. The average fineness (finer than 2 mm) content after each experiment is also mentioned in the same figure. Figure 5.19 shows the particles distribution curves (PSD) after the dry, saturated and the one with two cycles of wetting and drying test for Ishikawa mudstone. The particle size distribution (PSD) after dry test for Ishikawa mudstone shows some disintegration with average fines (finer than 2 mm) and degradation index of 3.92 % and 0.07 respectively. This is basically due to crushing of relatively weak particles under vertical stress and monotonic shear loading as in the Hattian Bala mudstone. After saturated and two cycles of wetting and drying tests, about 25.68 % and 27.28 % particles by mass were found finer than 2 mm which were probably due to slaking of crushed mudstone. Similarly, the degradation indexes after saturated and the one with cyclic wetting and drying tests were about 0.40 and 0.42 respectively.

Finally, the Fig. 5.20 show the particles distribution curves (PSD) after one complete cycle of wetting and drying for the Hattian Bala mudstones specimen (PreM028). Average

fines (finer than 2 mm) content and degradation index of the spacemen after one complete cycles of wetting and drying are 7.13 % and 0.13 respectively (Fig. 5.16).

The degradation index (I_D) and fines contents (F_C) of Hattian Bala, Ishikawa and Chiba gravel specimens after experiments are summarized in Table 5.8-5.13. Ishikawa mudstone with slaking index as level 3 showed (Table 5.10 and 5.11) the highest slaking induced disintegration with an average I_D and F_C of 0.4 and 25.68 % respectively after single immersion. Hattian Bala mudstone with slaking index as level 1, consisting of relatively durable grains, showed the least effects of slaking on particles crushing with an average value of I_D and F_C of 0.15 and 9 % respectively (Table 5.8 and 5.9). Similarly, Chiba gravel with slaking index as level 0, consisting of durable grains, showed almost no effect of slaking on particles crushing (Table 5.8 and 5.9). The degradation index (I_D) and fines contents (F_C) can be compared with slaking index (SI) and slaking ratio. So, from the above results, it is cleared that the material having relatively lower slaking index (SI) or higher slaking ratio shows higher degradation index (I_D) and fines contents (F_C).

In addition, Particles size distribution (PSD) after cyclic wetting and drying test for the both Ishikawa and Hattian Bala mudstone specimens also showed some more disintegration of particles as compared to saturation test, which is basically due to particles crushing (slaking) during cyclic wetting and drying. However, the differences of degradation index (I_D) and fines contents (F_C) between saturation test and cyclic wetting and drying test is relatively small. Panabokke and Quirk (1956) reported that the disintegration of clay aggregates became higher as the water content of the specimen before wetting became lower. Therefore, it can be understood that the maximum particles crushing occurred during the first wetting because the specimen in this study was prepared by oven-dried crushed mudstones.

Moreover, small deterioration of grains under dry conditions is also observed in each specimen, basically due to the crushing of relatively low durable grains under normal stress as well as shearing action. Most of deterioration of grains in the tests took place during saturation and partially during drying stages before shearing. To verify the above conclusion, the particles size distribution analyses of crushed mudstones (Hattian Bala) freely submerged in water (under atmospheric pressure only) were also carried out. It can be observed that the

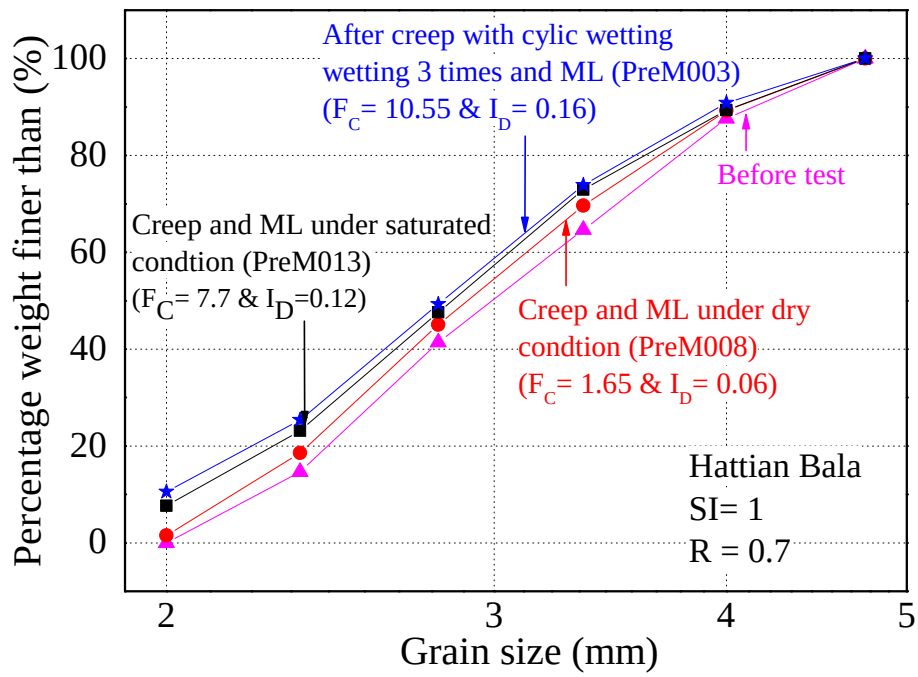

Fig 5.29 Particles size distribution curves of PreM008, Prem013 and PreM003 after dry, saturated and cyclic wetting and drying test under R= 0.7 (Hattian Bala)

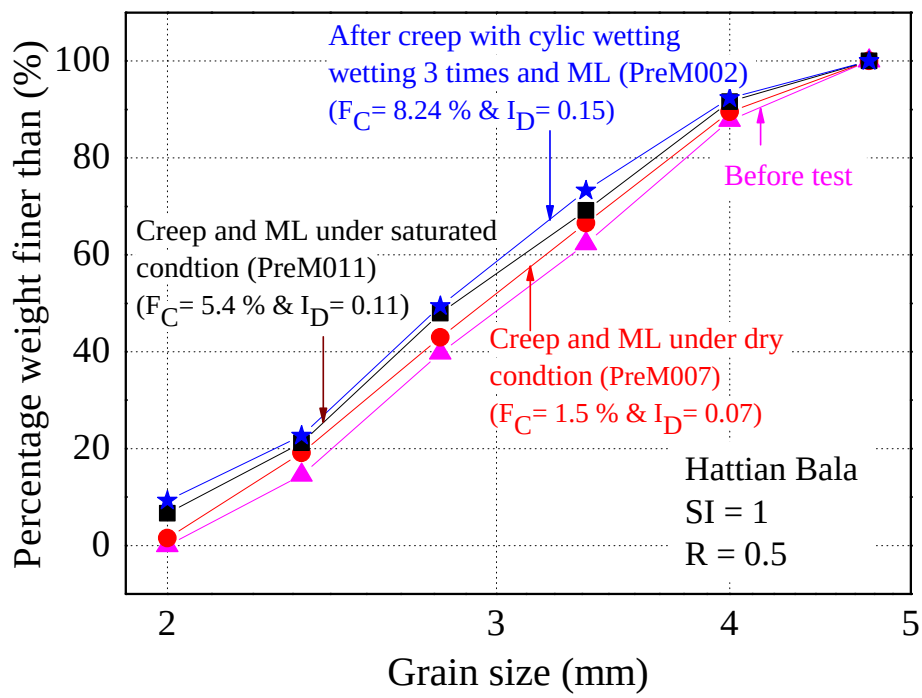

Fig 5.30 Particles size distribution curves of PreM007, Prem011 and PreM002 after dry, saturated and cyclic wetting and drying test under R= 0.5 (Hattian Bala)

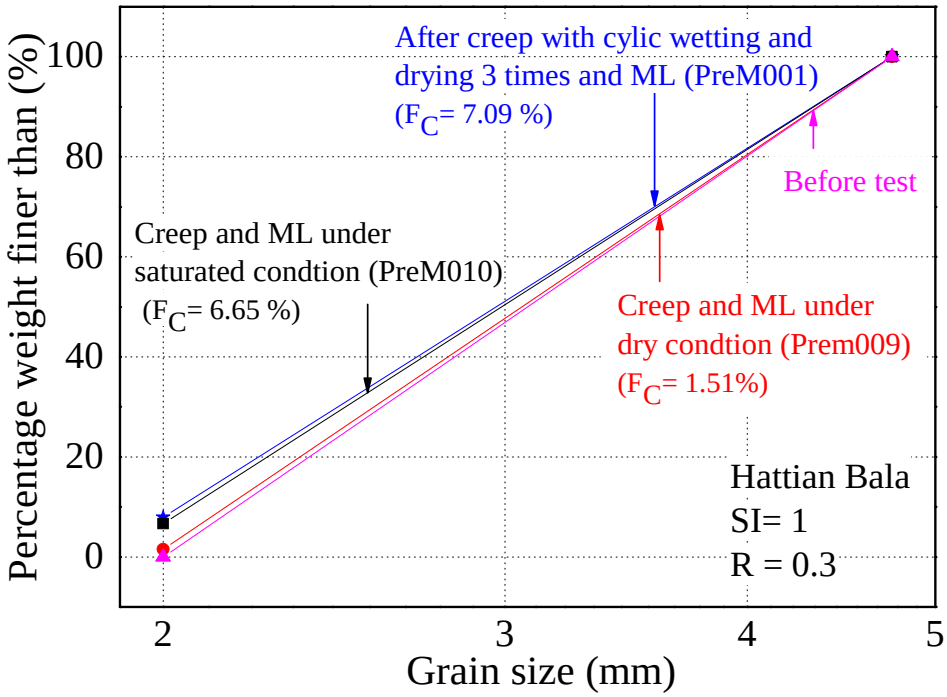

Fig 5.31 Particles size distribution curves of PreM009, Prem010 and PreM001 after dry, saturated and cyclic wetting and drying test under R= 0.3 (Hattian Bala)

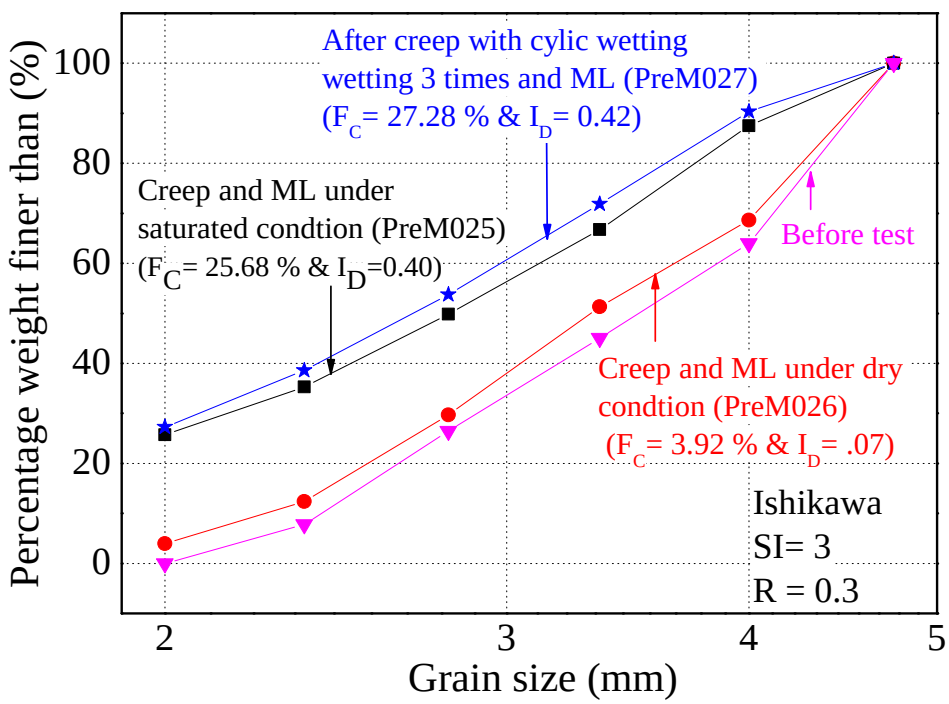

Fig 5.32 Particles size distribution curves of PreM025, Prem026 and PreM027 after dry, saturated and cyclic wetting and drying test under R= 0.3 (Ishikawa)

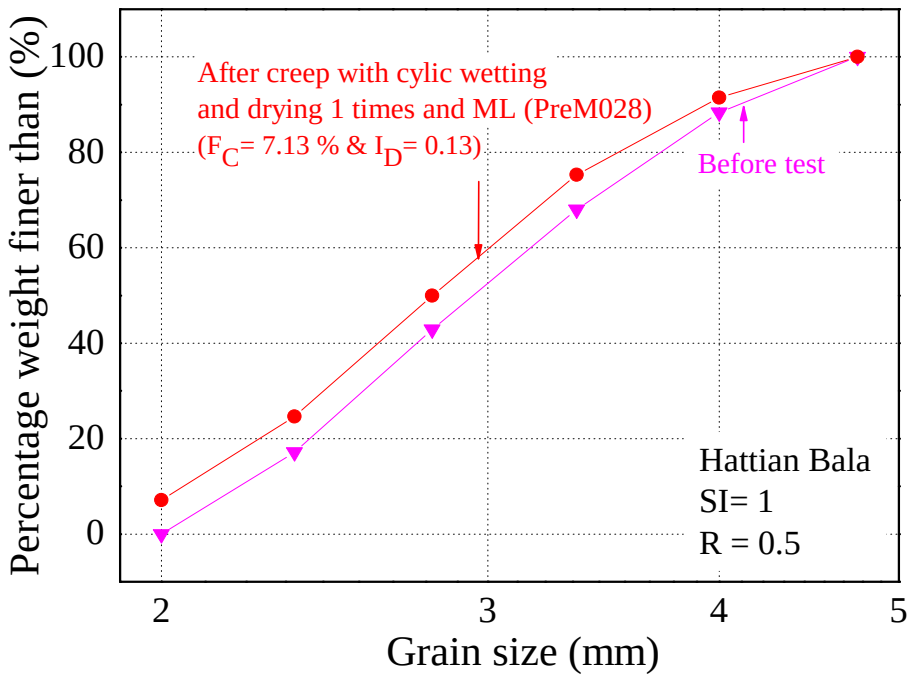

Fig. 5.33 Particles size distribution curves of PreM028 after one complete cycle and dry monotonic loading (R= 0.5)

increment of fines at no stress conditions are comparable to values observed for saturated monotonic shear tests (Fig. 5.34).

Similarly, the increment of fines during drying also observed during this experiment. The test PreM028 was conducted by applying monotonic loading applied under dry condition after one complete cycle of wetting and drying. The degradation index (I_D) and the Fines content is slightly higher than saturation tests (Table 1 and 2). The increment of degradation index and Fines contents in PreM0028 test indicates the drying induced slaking. Thus, it is inferred that the slaking phenomena causes surface deterioration of soil particles during drying and splitting along the weak planes which primarily completes during saturation stage (Czerewko and Cripps, 2001).

From the test results of Hattian Bala and Ishikawa mudstones, it can be observed that degradation index (I_D) of a given crushed mudstones has a clearly dependency on slaking characteristics of geomaterials. It can be concluded that higher the slaking index or lower slaking ratio reveal the drastic loss of strength during saturation and increase in disintegration index (I_D).

Table 5.8 Degradation index (I_D) of Hattian Bala mudstone specimens

Test condition	Stress ratio, R		
	0.7	0.5	0.3
Dry	0.06	0.07	0.06
Saturated	0.12	0.11	0.12
1 Cycle	-	0.13	-
3 Cycles	0.16	0.15	-

Table 5.9 Fineness contents (F_C) of Hattian Bala mudstone specimens

Test condition	Stress ratio, R		
	0.7	0.5	0.3
Dry	1.65	1.5	1.51
Saturated	7.7	5.4	6.65
1 Cycle		7.13	
3 Cycles	10.55	8.24	7.09

Table 5.10 Degradation index (I_D) of Ishikawa mudstone specimens

Test condition	Stress ratio, R		
	0.7	0.5	0.3
Dry	-	0.08	0.07
Saturated	-	-	0.4
Cyclic	-	-	0.42

Table 5.11 Fineness contents (F_C) of Ishikawa mudstone specimens

Test condition	Stress ratio, R		
	0.7	0.5	0.3
Dry	-	3.8	3.52
Saturated	-	0	25.68
Cyclic	-		27.28

Table 3.12 Degradation index (I_D) of Chiba gravel specimens

Test condition	Stress ratio, R		
	0.7	0.5	0.3
Dry	-	-	.01
Saturated	-	-	.01

Table 4.13 Fineness contents (F_C) of Chiba gravel specimens

Test condition	Stress ratio, R		
	0.7	0.5	0.3
Dry	-	-	0.2
Saturated	-	-	0.32

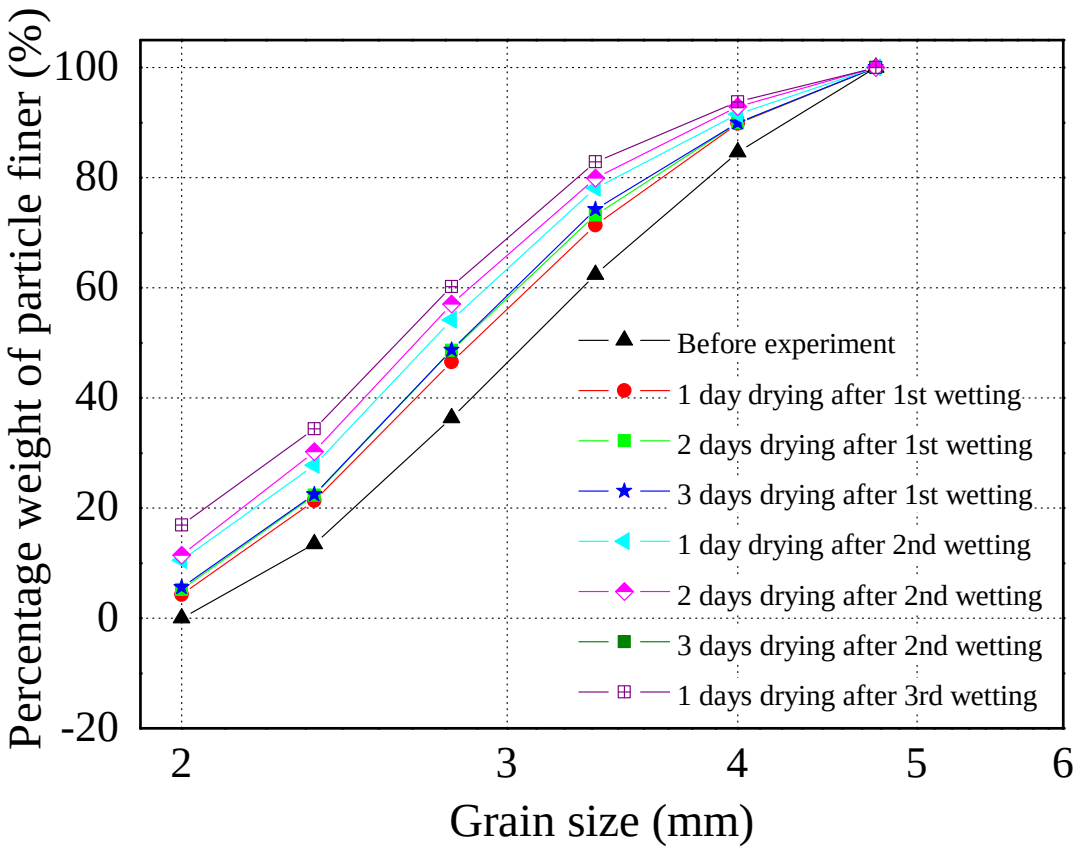

Fig. 5.34 Particle size distribution distributions curves of Hattian Bala mudstones after submerge in water

Finally, the phenomena of slaking induced particle crushing discussed in this research is contrary to the conventional studies of stress-induced particles crushing performed by Hardin (1985), Feda (2002), Einav (2007), Kikumoto et al. (2010) and many others.

5.5 X-ray Diffraction (XRD) power test

X-ray diffraction power test was used in order to determine the mineralogy of the rocks. Based on the results of the XRD analysis of Hattian Bala mudstones specimen, the Hattian Bala mudstone specimen demonstrated that the specimen generally comprised clay minerals, calcium and silicate. It is believed that the Calcium hiders the slaking of mudstones. It behaves as cementing materials. Similarly, the Ishikawa mudstones specimen showed Lithium Gallium silicate.

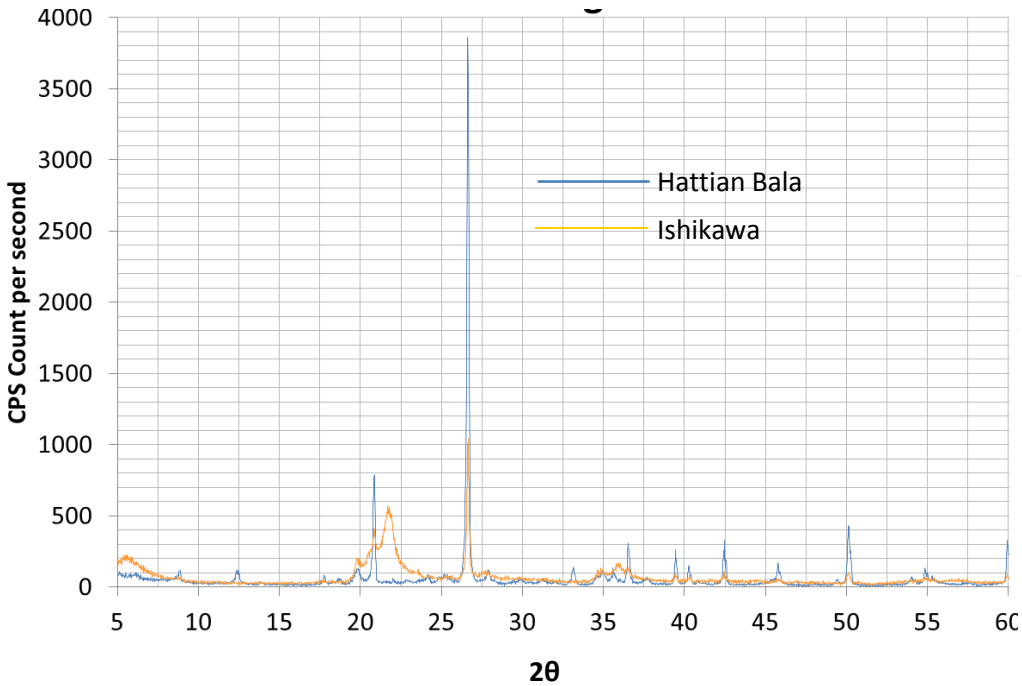

Fig. 5.35 X-ray diffraction result of Hattian Bala and Ishikawa mudstones

CHAPTER 6

RESULT ANALYSIS AND DISCUSSION

6.1 General

To describe the slaking effects on the strength and deformation characteristic as well as particles crushing of mudstones, a series of direct shear tests with other preliminary experiments were conducted. Similar tests were also conducted on conventional granular material such as Chiba gravel and Toyoura sand. Non-slakeable Glass beads specimens were used for few tests as well.

Along with the properties of various test materials used in this study, the effect of the slaking index, density of the specimen, water content before wetting and stress ratio will be discussed in this chapters. Similarly, the influences of the cyclic wetting and drying on the physical and mechanical properties of various geomaterials used in this study are discussed in this chapter.

6.2 Effect of stress ratio (R)

In this study, three cycles of wetting and drying were carried out on Hattian Bala mudstone specimens under different stress ratio to analysis the deformation and strength characteristics due to slaking by using a modified direct shear apparatus. Similarly, two cycles of wetting and drying were carried out on Ishikawa mudstones and Glass beads specimens under stress ratio 0.3. The test results obtained from the cyclic wetting and drying under constant creep loading will be interpreted and discussed to examine their behaviour on natural slope or when used as construction materials for embankments etc.

The results obtained from the cyclic wetting and drying tests are summarized in Fig. 6.1 and 6.2, showing increment values of creep shear and vertical displacement at each stress ratio, R. The wetting-induced maximum creep shear deformation of 3.4 mm was observed at R= 0.7 during the first wetting (see Fig. 4a) from the Hattian Bala mudstone specimen. Wetting-induced creep failure was observed at *R*= 0.8 on the same material.

Similarly, Kiyota et al. (2011) also reported that wetting-induced creep failure was observed at R= 0.8 under σ_v= 100 kPa on the same material as the one in this study. Therefore, it seems that the creep shear displacement during wetting increases with increase in the value of R, which would indicate high risk of slaking-induced instability at steep slopes.

The vertical displacement, however, in case of R= 0.3, is almost negligible except in the first wetting because of having higher water content (more than 3 %) of specimen before the second and third wettings. The vertical displacement in the wetting is affected by stress ratio, R values during creep shear loading and the progress of wetting and drying cycles.

As shown in Fig. 6.1, the creep shear displacements during drying increase with the increase in the value of stress ratio, R. However, in the case of R= 0.3, the lowest water content during the drying step is quite larger (about 3 %). This may be reason for relatively small creep displacement during the drying process at R= 0.3.

Figure 6.2 shows the relationship between stress ratio, R and reduction in peak angle of internal friction due to wetting. From the figure it is clearly seen that the reduction in peak angle of internal friction due to wetting is independent of stress ratio, R.

As already mentioned in previous chapter, the degradation index was evaluated after each experiment under different stress condition. The amount of particles crushing due to slaking is independent of stress ratio, R (Fig. 6.3).

Similarly, the results obtained from the cyclic wetting and drying tests on Ishikawa mudstone specimens are summarized in Fig. 6.2, showing increment values of creep shear and vertical displacement at stress ratio 0.3. The wetting-induced maximum creep shear deformation of 3.9 mm was observed at R= 0.3 during the first wetting (see Fig. 6.2a). Wetting-induced creep failure was observed at *R*= 0.5 on the same material. Therefore, it seems that the creep shear displacement during wetting increases with increase in the value of R, which would indicate high risk of slaking-induced instability at steep slopes.

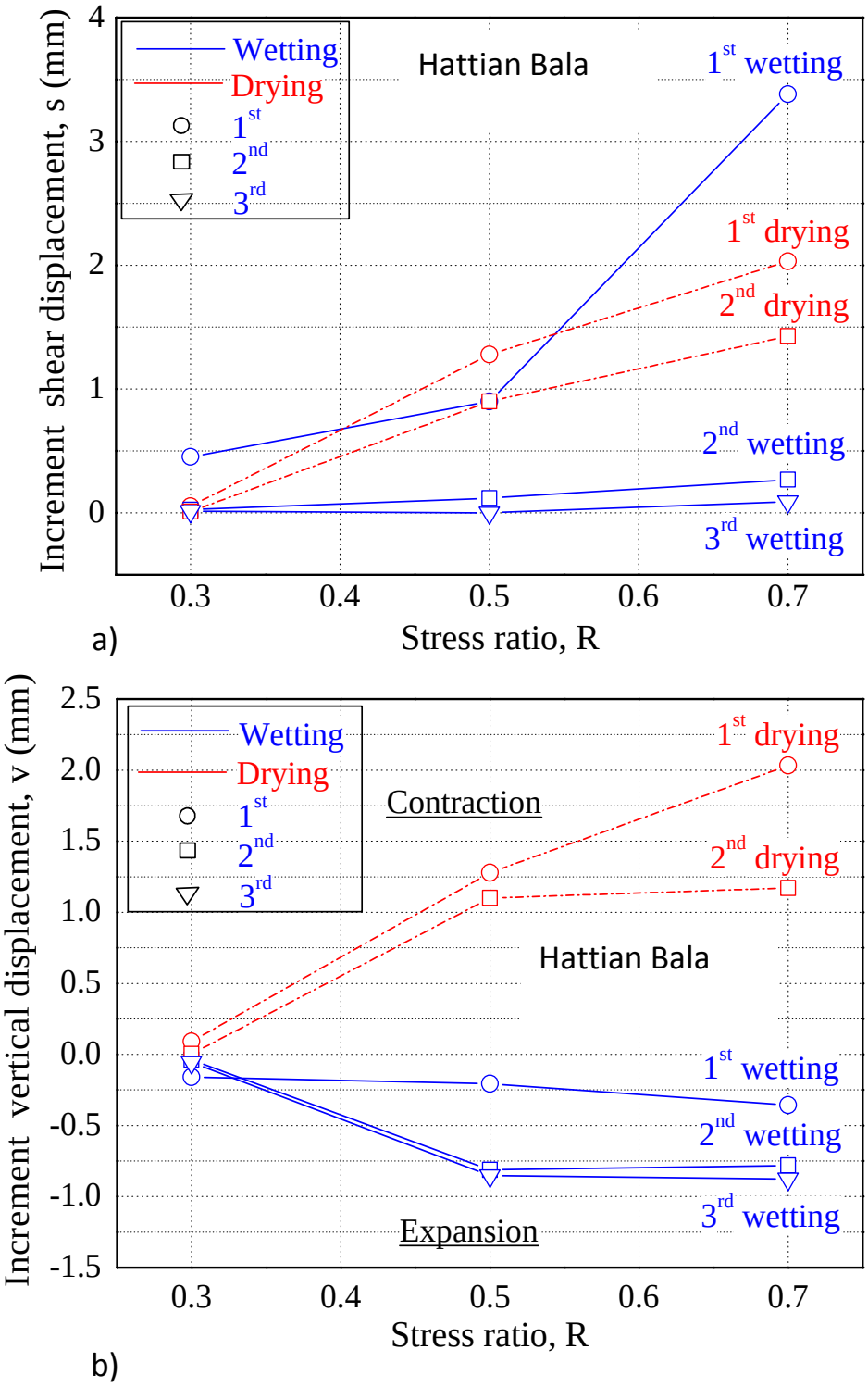

Fig. 6.1 Increment value of creep a) Shear b) Vertical displacement at each stress ratio, R

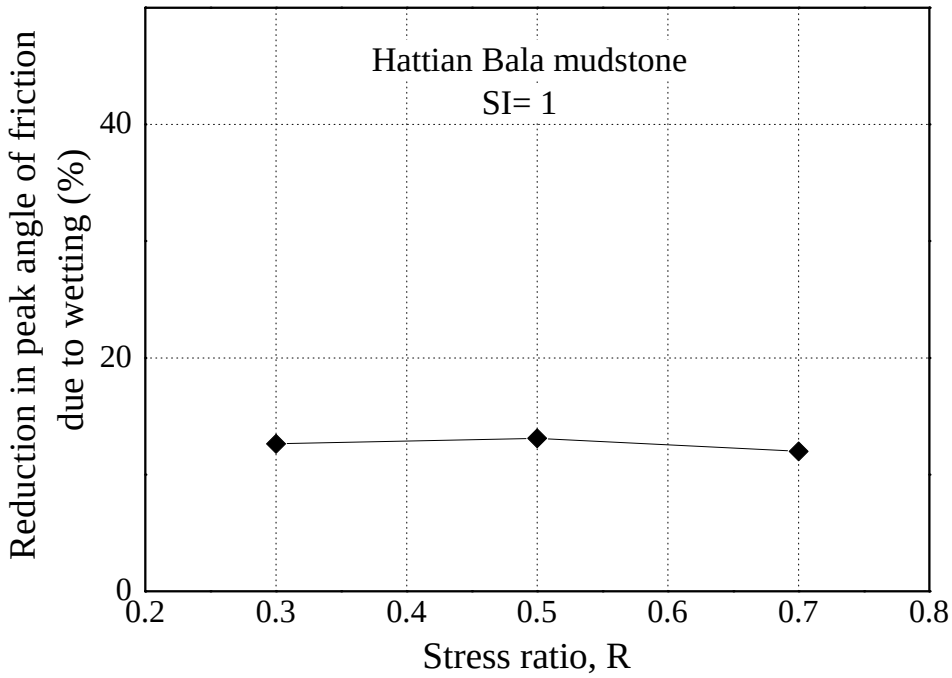

Fig. 6.2 Relationship between R and change in peak angle of internal friction

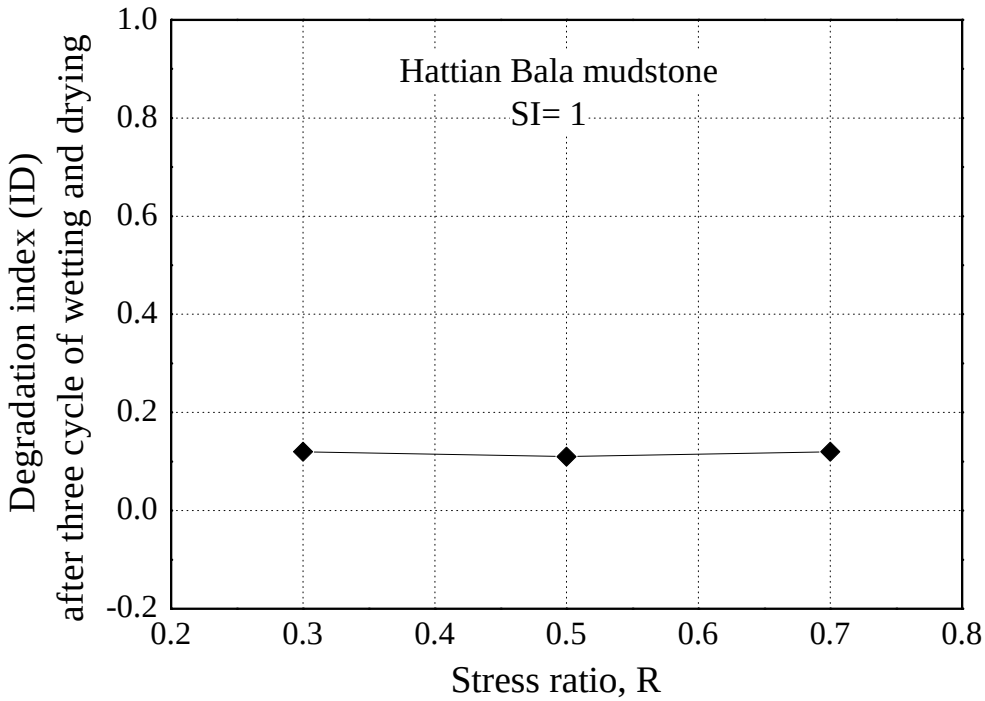

Fig. 6.3 Relationship between R and change in peak angle of internal friction

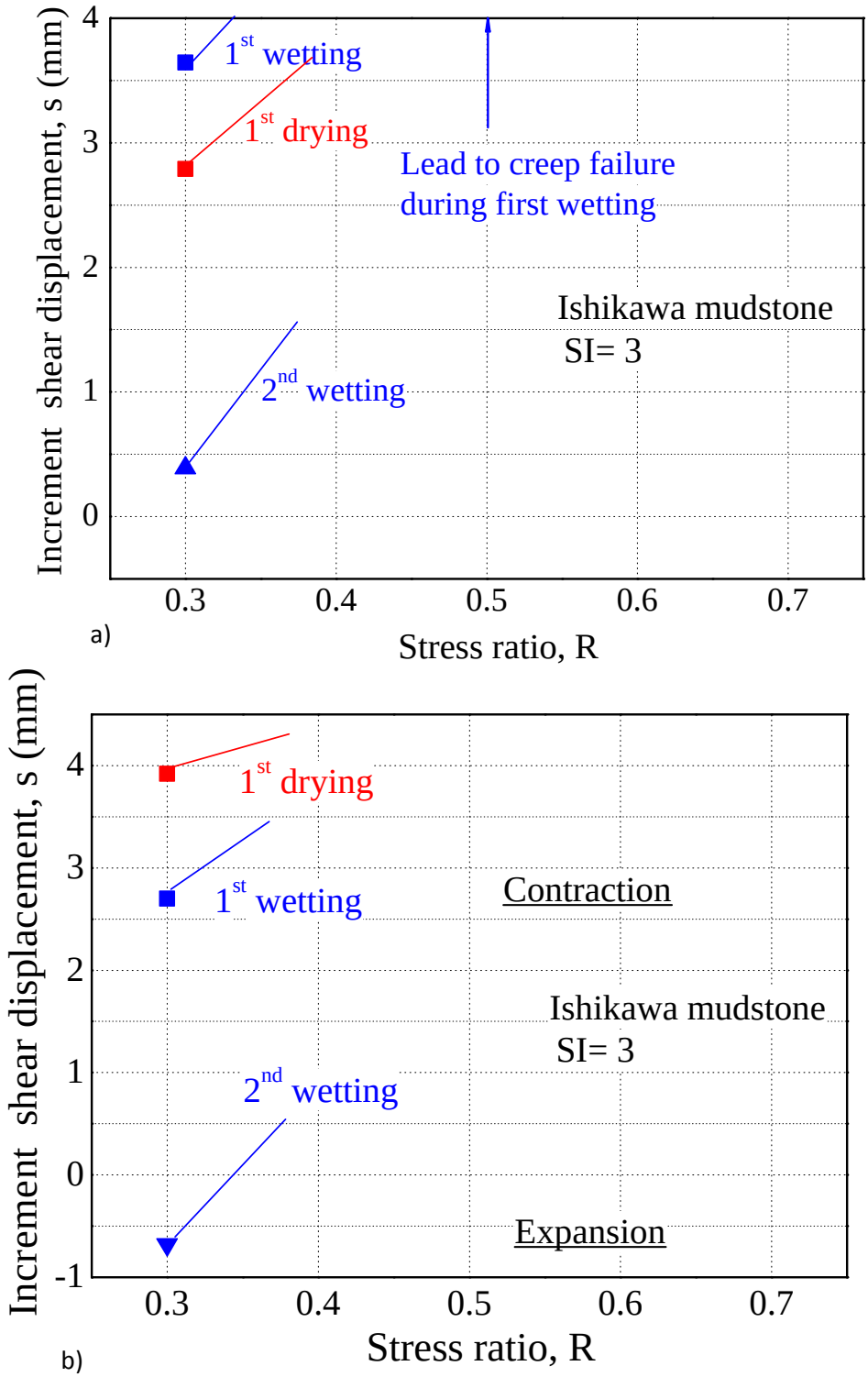

Fig. 6.4 Increment value of creep a) shear b) vertical displacement at each stress ratio, R

6.3 Effect of water content before wetting

The creep shear displacement during first wetting was significant under each stress ratio. However, the creep shear displacement caused by wetting seems to be decreased with progress of wetting and drying cycle (Fig. 6.1a). The water content before each wetting was not same. The Figures 6.5 and 6.6 show the relationship between water content before wetting and wetting induced shear and vertical displacement respectively. The shear displacement during wetting became higher as the water content before wetting of specimen became lower (Fig. 6.5). Nakano et al. (1998) and Panabokke and Quirk (1956) also reported that the slaking level of clay aggregates became higher as the initial water content of the specimen became lower. Therefore, it can be understood that the maximum displacement was observed during the first wetting because the specimen in this study was prepared by oven-dried crushed mudstone. The lowest water content during drying step is quite large (about 3 %) in case of R= 0.3. This may be reason for almost negligible creep shear displacement during the second wetting process at R = 0.3 (Fig. 6.1a).

Similarly, in case of Ishikawa mudstone specimens, the creep shear displacement during second wetting is relatively very small because of higher water content (about 12%) before wetting.

The vertical displacement is almost negligible when water content before wetting is more than 3 % (Fig. 6.6). The vertical displacement during wetting also became higher when water content before wetting became lower. However, the vertical displacement of oven dried specimen (water content about 0 %) during wetting is seemed to be smaller as compared to the vertical displacement occurred during wetting when water content before wetting was about 1 % (Fig. 6.7). This may be due to dilatancy effect due to significant shear deformation occurred when oven dried specimens are used. Collapse of weak grains during first wetting also causes reduction in negative vertical displacement during first wetting.

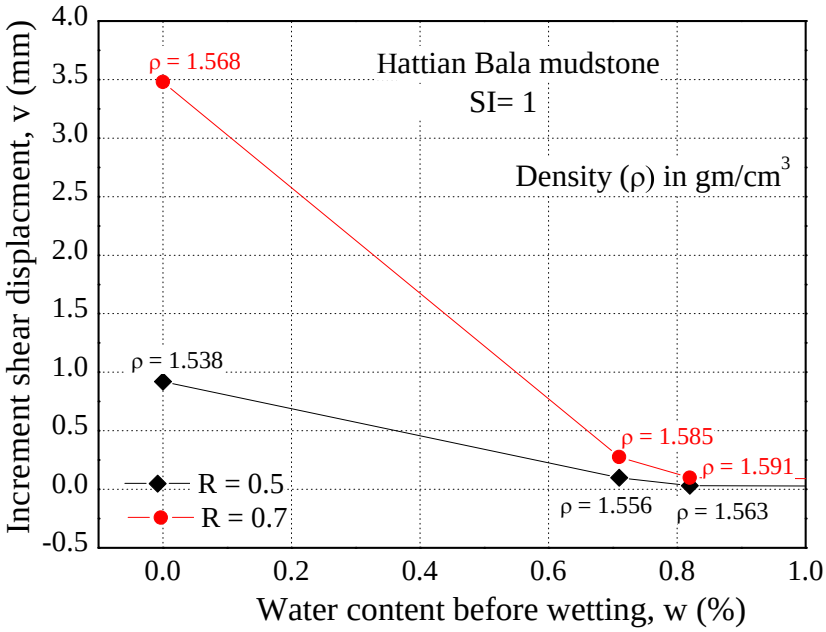

Fig. 6.6 Relationship between water content before wetting and increment creep shear displacement

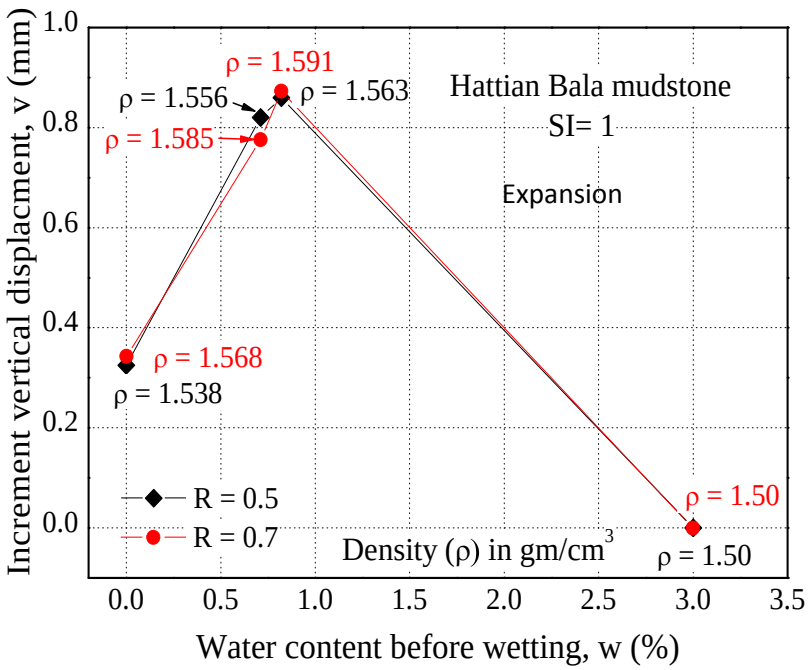

Fig. 6.7 Relationship between water content before wetting and increment creep vertical displacement

6.4 Effect of slaking index (SI)

Figure 6.8 shows the increment shear displacement of various tested materials due to saturation under same anisotropic stress condition i.e. under stress ratio 0.3 and 0.5. The shear displacement of Hattian Bala mudstone specimens having slaking index as level 1 was about 4 mm under R = 0.5 while, the Ishikawa mudstone having slaking index as level 3 specimens led to creep failure during wetting (Fig. 6.8). From the Fig. 6.8, it is seen that the Ishikawa mudstone (SI = 3) specimens showed highest shear displacement during wetting. Similarly, the Hattian Bala mudstone (SI = 1) specimen also showed considerable shear displacement under same condition while other materials such as Chiba gravel and Glass beads (SI = 0) did not show significant shear displacement during wetting.

Large amount of particles crushing as compared to other specimens (Fig. 6.9) during wetting is also responsible for excessive shear displacement for the Ishikawa mudstone specimens. The shear displacement of Hattian Bala mudstone specimen is about one tenth of Ishikawa mudstone specimen because of consisting relatively strong grains. This argument can be justified by comparing Degradation index (I_D) and Slaking ratio (SI) of the tested specimens. The Chiba gravel, Toyoura sand and Glass beads consist of strong grain which can not deteriorate by slaking. That's why; the shear displacement during wetting is negligible as compared to mudstones specimens. Finally, it is inferred that slaking induced deformation and deterioration of soil grains which ultimately leads to enormous shear displacement upon sustained loading can be critical progressive slope failures.

The drying induced shear displacement of Ishikawa mudstone is also higher than that of Hattian Bala mudstones specimen during first drying process (Fig. 6.1a and 6.4a), even the water content of Ishikawa mudstone specimen is higher than Hattian Bala mudstone specimen at the end of drying process and stress ratio lower than Hattian Bala specimen. As already described in previous sections, the deterioration of the particle begin from the surface of the particle during drying process (Moropoulou et al., 2004; Karoglou et al., 2005; Soe et al., 2010). Higher void ratios increase the exposed area of individual particles which lead to easily deterioration of particles. The tensile failure of the weakly crystalline bonded granular materials due to drying induced pore water suctions is also another cause of drying induced slaking (Czerewko and Cripps, 2001). So, higher void ratios of Ishikawa mudstone specimen also lead to higher shear displacement during drying phase as in wetting phase.

Finally, it is quite clear that with the increase in Slaking index (SI) there is drastic increase in shear displacement upon wetting and drying as well. The relationship between Slaking index (SI) and increment shear displacement during wetting could become very important for the practical application.

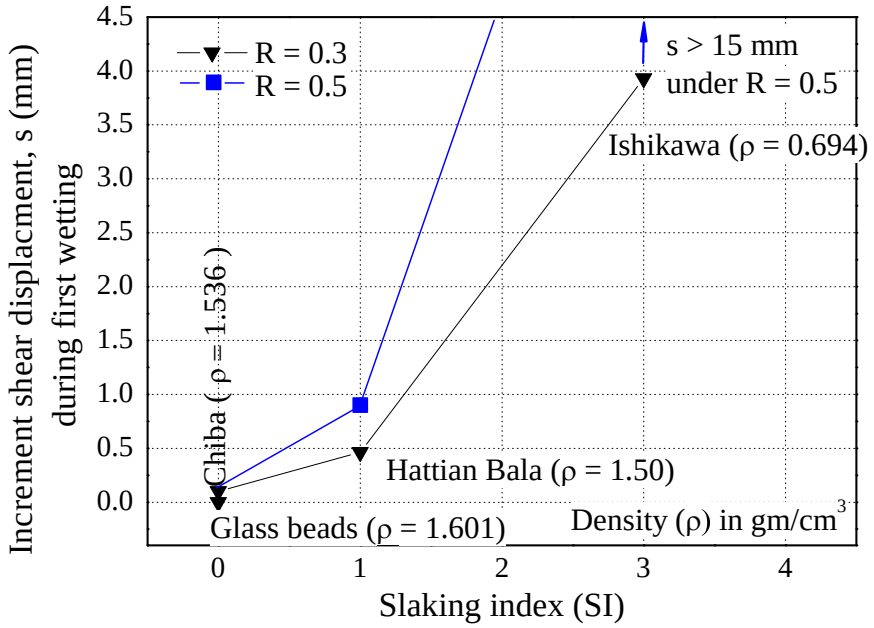

Fig. 6.8 Relationship between Slaking index (SI) and increment shear displacement during wetting

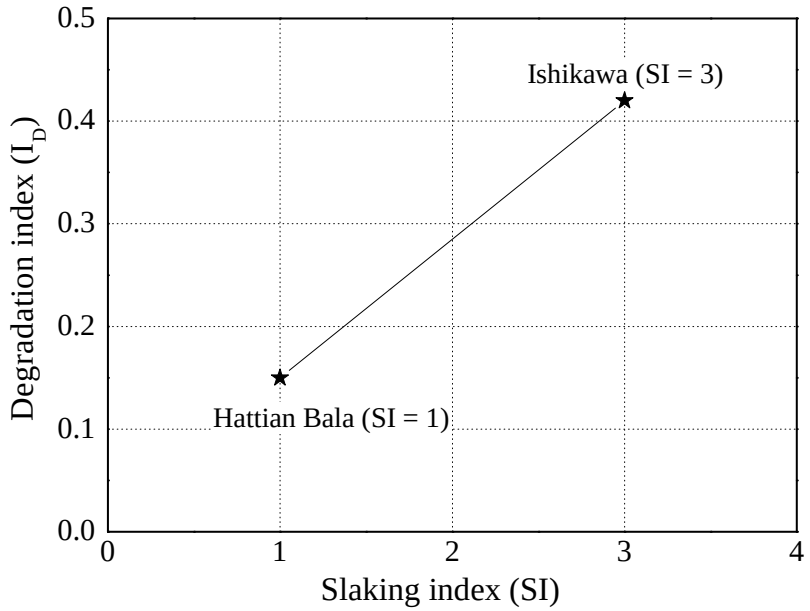

Fig. 6.9 Relationship between Slaking index (SI) and degradation index (ID)

The specimens of Ishikawa mudstone (SI=3) showed vertical compression during first wetting, which is attributed to the sensitivity of material to slaking induced deterioration (Fig. 6.10). In contrast the crushed mudstones having slaking index as level 1 from Hattian Bala, Pakistan showed vertical expansion during saturation probably to presence of expansive clay minerals. Expansion of clay minerals also cause cracking in the grains which ultimately lead to disintegration. Cardoso and Alonso, 2009 also explained swelling induced particles disintegration in mudstones. However, expansive clay mineral montmorillonite of smectite group was not found clearly from X-ray diffraction (XRD) analysis of two geomaterials such as Ishikawa and Hattian Bala mudstones. In addition, Chiba gravel, Toyoura sand and Glass beads specimens having slaking index as level 0 have shown relatively very small vertical settlement during wetting being an indicative of durable soil grains against the slaking.

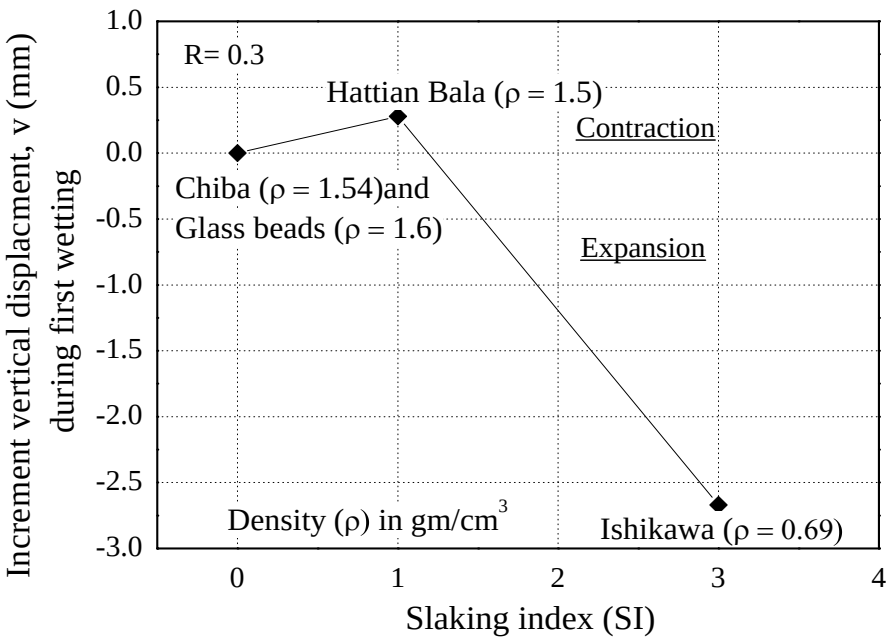

Fig. 6.10 Relationship between Slaking index (SI) and vertical displacement during wetting

As already discussed, the vertical displacement of Ishikawa mudstone having slaking index level 3 during saturation being positive (contraction) is indicative of slaking induced disintegration of soil particles as well as collapse of relatively open structure of these materials having high initial void ratios. So, relatively denser packing was achieved in the specimen after first wetting. These observations are in strong agreement with a study by Neves and Pinto (1988) on prediction of collapse settlement due to saturation rock-fill,

mainly in embankment dams. Therefore, it is inferred that slaking induced deterioration of mudstone stones having higher degree of slaking index (SI) which ultimately leads to enormous compression upon sustained loading can be critical for the embankments constructed with crushed mudstones, for soil structure interaction of foundation placed on such soils as well as progressive slope failures. It is also concluded that the mudstone specimen with smaller slaking index (SI) exhibits expansive behaviour during first wetting while the mudstone specimens with higher slaking index (SI) shows the contractive behaviour.

The reduction in peak angle of internal friction (φ_p) of Ishikawa mudstone (SI = 3) specimens during wetting is higher than the reduction in peak shear strength of Hattian Bala (SI= 1) mudstone specimen. The reduction in peak angle of internal friction (φ_p) is insignificant in the case of that specimen having slaking index level 0 (Chiba gravel and Glass beads). Relatively large inherent void ratios, e (2.3) and slaking induced disintegration during wetting cause the large reduction in peak strength of Ishikawa as compare to Hattian Bala mudstone specimens. Similarly, it is seemed that the potential to disintegrate due to slaking (reduction in strength parameter) is dependent of slaking index of specimen. It is concluded that with the increase in Slaking index (SI), there is tremendous reduction in the mechanical properties of crushed mudstones.

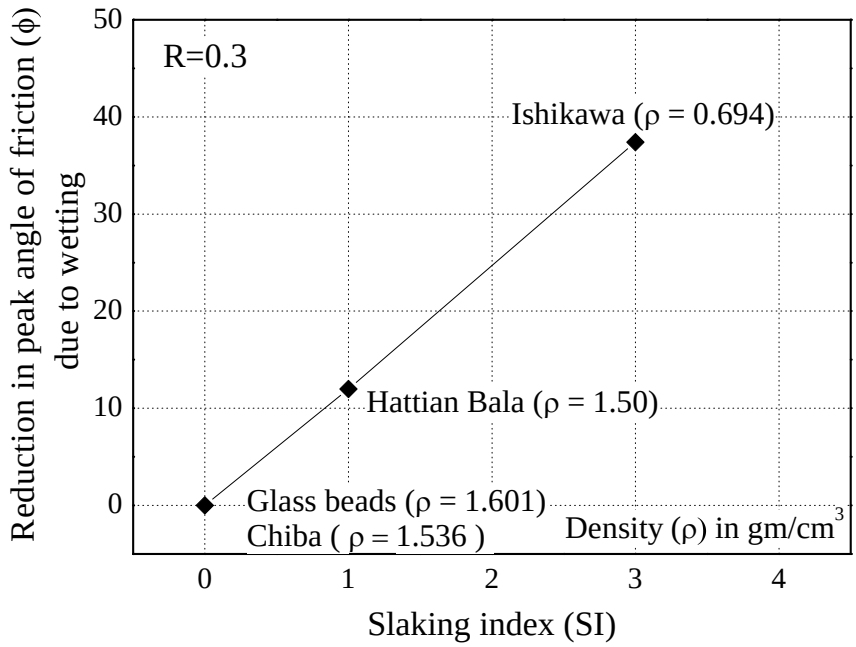

Fig. 6.9 Relationship between Slaking index (SI) and reduction in peak angle of friction (φ_p) due to wetting

6.5 Effect of density (ρ)

The specimens prepared at high initial density showed smaller shear displacement during wetting. The shear displacement of the specimen with initial density of about 1.50 gm/cm^3 was about 0.9 mm while 0.3 mm shear displacement occurred in case of the specimen with initial density of about 1.60 gm/cm^3 under R = 0.5 (Fig. 6.10).

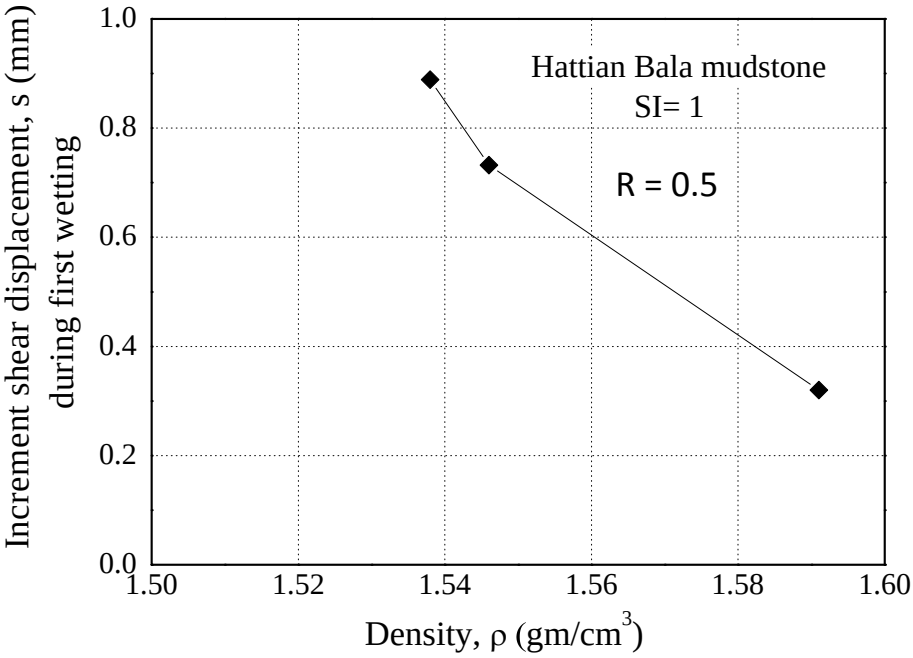

Fig. 6.10 Relationship between density of the specimen and increment shear displacement during first wetting.

From about discussion, it is concluded that the degree of slaking decreases with increase in density of specimen.

6.6 Number of cyclic wetting and drying (N)

The creep shear displacement caused by wetting seems to be decreased with increase in number of wetting and drying cycles of cycle, almost zero during the third wetting (Fig. 6.12). This may be attributed to the specimen densification due to previous wetting and drying processes (Nakano et al., 1998) and higher water content before wetting. Similarly, as already discussed, the higher shear displacement during first wetting also may be due to specimens prepared by oven dried crushed mudstone. Finally, it is concluded that the shear displacement during wetting decreases with increase in number of

Contrary to shear displacement, the vertical displacement was found increasing with increase in number of cyclic wetting and drying.

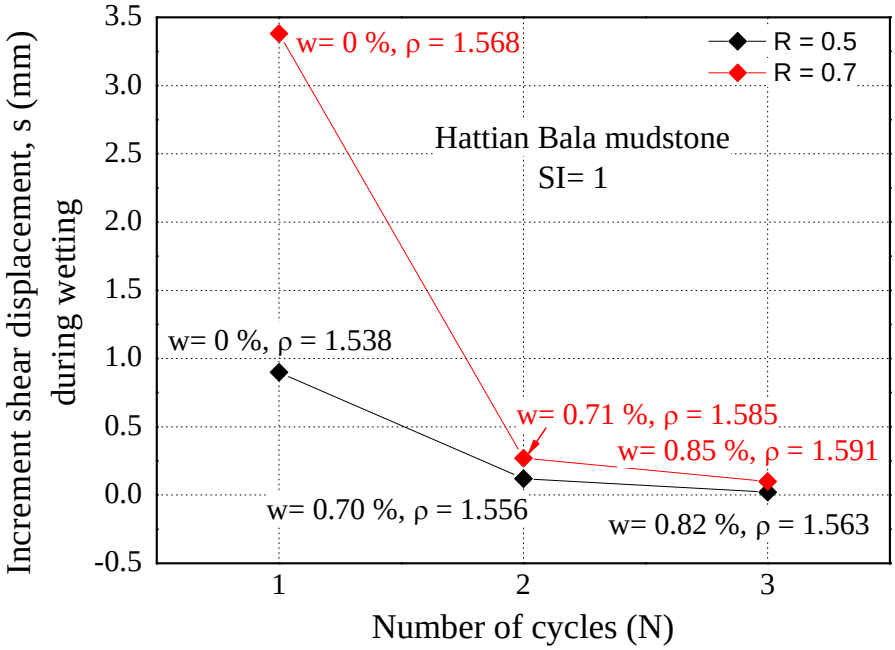

Fig. 6.11 Relationship between number of wetting and drying cycles (N) and increment shear displacement during wetting.

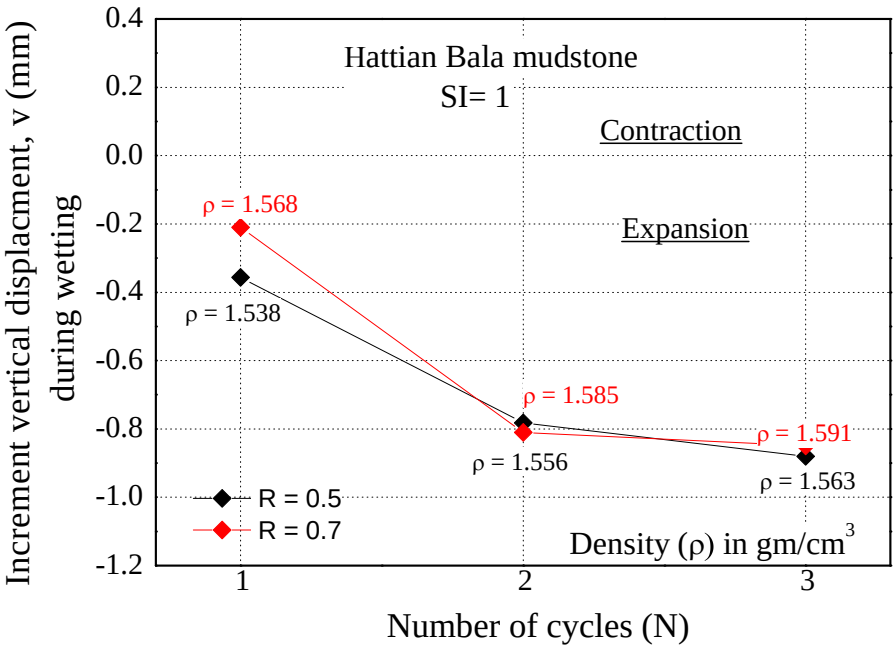

Fig. 6.12 Relationship between number of wetting and drying cycles (N) and increment vertical displacement during wetting.

Figure 6.13 shows the relationship between the number of wetting and drying cycles and peak angle of internal friction (ϕ). The influence of cyclic wetting and drying on peak

angle of friction (ϕ) is seemed insignificant. However, the gradual decrease in peak angle of friction (ϕ) is found on enlarge view of Fig. 6.12 (Fig. 6.13).

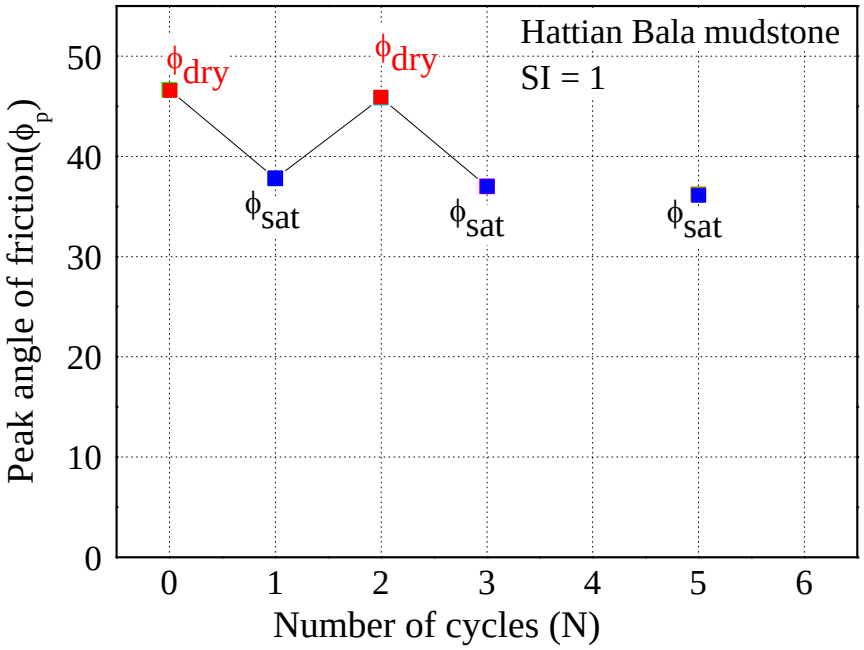

Fig. 6.13 Relationship between number of wetting and drying cycles (N) and increment vertical displacement during wetting.

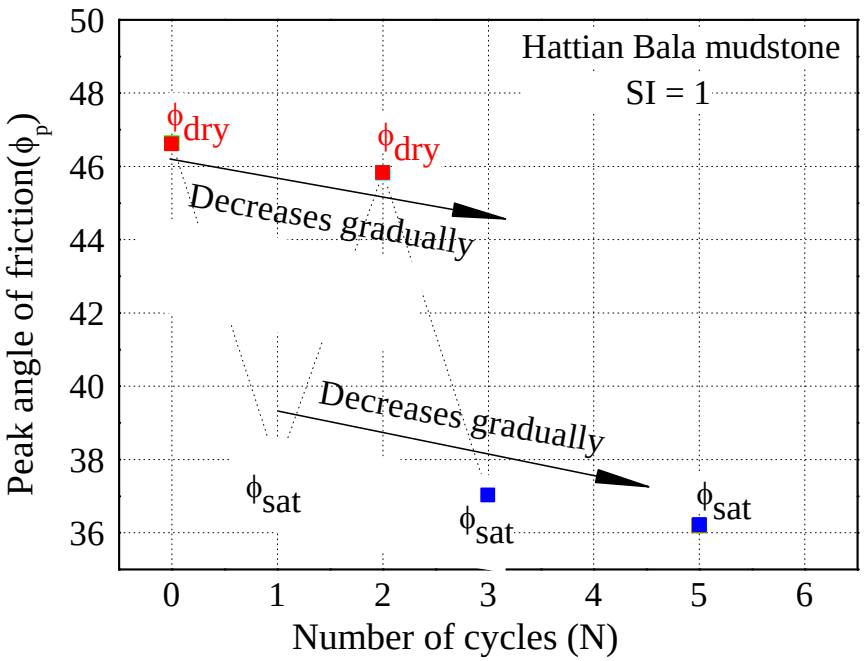

Fig. 6.14 Enlarge view of Figure 6.13

6.7 Summary

The test results obtained from general slaking tests and direct shear tests on various materials were interpreted and anlysed with the with the objectives of examining the factor that influences the slaking behaviour of geomaterials. Along with different types of granular soils, the effects of stress ratio, R, initial water content before wetting, slaking index (SI), density of the specimen (ρ) and number of cyclic wetting and drying (N) on slaking of crushed mudstones were investigated.

From the results, it is seen that the slaking phenomenon is a very complex behaviour which is dependent of various factors such density of specimen, water content before wetting, slaking index (SI) of the specimen, number of cyclic wetting and drying, mineralogical composition etc. The conclusion of this research can be made as following.

$$dS = f(SI, w, \rho, R, N, I_D)$$

Where, dS: Increment shear displacement, SI: Slaking index, *w*= Water content before wetting, R = Stress ratio, N = Number of cyclic wetting and drying and I_D= Disintegration index.

However, the factors inside the functions are also interdependent to each other. Similarly, there are other various factors such as mineral content, stress and deformation histories, drying history etc which influence the increment shear displacement due to slaking. So, the effects of slaking, quantification of deformation and disintegration and its relationships with reduction of strength and deformation characteristics of non-conventional materials from crushed mudstones is still a key concern for researchers.

CHAPTER 7

CONCLUSIONS AND RECOMMENDATIONS

7.1 General

The engineering properties of granular soils are conventionally believed to be unaffected by the cyclic wetting and drying or the presence of water. This is basically due to durable nature of grains of the conventional granular materials such silica sand (Toyoura sand) and sand stone (Chiba gravel) investigated in various geotechnical laboratories. Nonetheless, large scale availability of soft rock deposits in many parts of the world, massive infrastructure developments have been extended to hillsides and mountainous areas because of population growth, economics needs and other constraints. Soft sedimentary rock names mudstone is the most often encountered geomaterials during the major construction works that are undertaken in those areas. Slaking effects on these geomaterials become vital due to their sensitivity to slaking upon distinct seasonal changes. Detailed knowledge of slaking effects on such granular soils is very essential in geotechnical analysis and design for safety over the lifetime of geotechnical structures.

To achieve the proposed objectives of this research, intensive experiments on both conventional (Chiba gravel and Toyoura sand) and non-conventional (Hattian Bala and Ishikawa mudstone) geomaterials by using direct shear apparatus were performed. A series of direct shear tests simulating cyclic wetting and drying under different stress condition were performed. Similarly, about 300 landslide events were studied on basis of precipitation and geology.

7.2 Conclusions

In the beginning of this research, about 300 rainfall induced landslide events were collected and analysed on the basis of precipitation and geology of landslides area. About 50 %

of total rainfall induced landslides in soft sedimentary rock were found to be occurred after moderate rainfall. Similarly, number of rainfall induced landslide followed by drought was found significant. So, the conventional explanation for rainfall induced landslides is insufficient regarding the mechanism of all so called rainfall landslide landslides. Some landslides most probably occur under an unsaturated regime even after light rainfall, resulting only from a decrease in shear strength of the soil especially in soft sedimentary rock formation due to slaking of mudstones. However, detailed field and laboratory investigations of landslide areas are necessary to inspect the subsurface structures and to obtain geotechnical properties of slope materials. Then, real mechanism of land even could be explained precisely

As hypothesized, the strength and deformation characteristics of crushed mudstones under dry, saturated and cyclic wetting and drying condition are not in agreement with usual geotechnical approach towards various standard granular soils such as Silica sand (Toyoura) and sand stone (Chiba gravel). The stress strain behaviour and volume change characteristics of conventional material (Toyoura sand, Chiba gavel and Glass beads) are unaffected by both presence of water and cyclic wetting and drying, where as the mechanical behaviour of non-conventional materials (Hattian Bala and Ishikawa crushed mudstone) is conditioned by the number of cyclic wetting and drying or the presence of water. It is mainly due to the slaking behaviour of mudstones under cyclic wetting and drying or even under single immersion.

The effects of stress ratio (*R)*, initial water content (*w*) before wetting, dry density of the specimens (ρ), slaking index (SI) and number of cyclic wetting and drying (N) on strength, deformation and particles crushing of specimens were investigated.

It is seen that the creep shear displacement during wetting increases with increase in the stress ratio (R), which would indicate high risk of slaking-induced instability at steep slopes. However, there are no significant effects of the stress ratio (R) on the peak shear strength and particles crushing due to slaking.

The shear strength, deformation and disintegration characteristics of crushed mudstone are dependent of initial water content (*w*) before wetting. Higher slaking level is observed as the initial water content (w) of the specimen before wetting became lower.

With the increase in Slaking index (SI) there is drastic increase in the shear displacement upon wetting and drying and decrease in the peak shear strength as well.

The specimens prepared at high initial density (ρ) show smaller shear displacement during wetting.

The creep shear displacement caused by wetting seems to be decreased with increase in number of wetting and drying cycles of cycle, which may be attributed to the specimen densification due to previous wetting and drying processes.

One of the noticeable behaviors observed in these experiments is a quite large creep displacement during the drying processes. The creep displacements during drying increase with the increase in the value of stress ratio (R) and Slaking index (SI). Slaking phenomena cause loss of intra-particles cementation and tensile failure of the weakly crystalline bonded granular materials due to drying induced pore water suctions. Drainage and evaporation of pore water which lead to shrinkage and disaggregation of fabric especially around discontinuities during dry process. Consequently, such an evolution of soil grains produces rounded particles with relatively high sphericity and smooth circumference which sequentially decreases the interlocking behaviour (angle of internal friction) of granular medium. Particles slides on each other during shrinkage causing shear deformation simultaneously.

The strength and stiffness gained during drying process are opposing to the further increase in shear displacement with reduction of pore water which lead to shrinkage and disaggregation of fabric especially around discontinuities. Therefore the drying induced deformation of crushed mudstones is very complex which could be challenging and crucial importance for strategic geotechnical structures.

Finally, it is seen that the slaking phenomenon is a very complex behaviour which is dependent of various factors such density of specimen (ρ), water content (*w*) before wetting, slaking index (SI) of the specimen, number of cyclic wetting and drying (N), mineralogical composition etc. The conclusion of this research can be made as following.

$$dS = f(SI, w, \rho, R, N, I_D)$$

Where, dS: Increment shear displacement, SI: Slaking index, *w*= Water content before wetting, R = Stress ratio, N = Number of cyclic wetting and drying and I_D= Disintegration index.

However, the factors inside the functions are also interdependent to each other. Similarly, there are other various factors such as mineral content, stress and deformation

histories, drying histories etc which influence the increment shear displacement due to slaking. So, the effects of slaking, quantification of deformation and disintegration and its relationships with reduction of strength and deformation characteristics of non-conventional materials from crushed mudstones is still a key concern for researchers

7.3 Recommendations

The author expected large shear deformation with the progress of cyclic wetting and drying and collapse of specimen after certain number of cyclic wetting and drying. However the result observed is contrary to the expectation. This may be attributed to size of crushed mudstone used in the specimen and higher water content before wetting with progress of wetting and drying cycles. The level of slaking is dependent of size of crushed mudstones and initial water content before wetting. It is advised that further tests should be performed on relatively larger crushed mudstones. Similarly, the direct test apparatus should be modified to reduce water content significantly during drying phase and drying duration as well.

Further tests should be performed to investigate the possible effects of slaking index (SI), initial density (ρ), confining stress (σ_v) etc, which enhance analytical description of slaking effects on strength and deformation behaviour of geomaterials. Some simple laboratory tests like oedometer test are recommended to explore possible mechanism of slaking and its effects on strength and deformation.

Large number of rainfall landslide events should be analysed on the basis of precipitation intensity and pattern and geology of landslide area. Drought period should be quantified by using some parameters like DDSLR (Dry Days Since Last Rainfall). Similarly, detailed field and laboratory investigations of landslide areas are recommended to inspect the subsurface structures and to obtain geotechnical properties of slope materials. Then, real mechanism of land even could be explained precisely. Finally, a simple model test of slopes/embankments composed of crushed mudstones under cyclic wetting and drying condition is advised.

REFERENCES

Al-Shamrani, M. A. and Al-Mhaidib, A. I. (1999): Prediction of potential swell of expansive soils using a triaxial stress pathi cel, *Quarterly Journal of Engineering Geology*. **32**, 45-54.

Al-Shamrani, M. A. and Al-Mhaidib, A. I. (2006): Influence of swell on shear strength of expansive soils, *Geotechnical Special Publication, American Society of Civil Engineers, Journal of the Geotechnical Engineering*

Anwar, H. Z., Simada, H., Ichinose, M. and Matsui, K. (2000): Slaking phenomenon of the expandable clay bearing rock, *Proc. of Indonesian Association of Geologists, The 29th Annual Convention*, Bangdung, Indonesia, 21-22 Novemeber, 2000,66-75

Au, S. W. C. (1998): Rain-induced slope instability in Hong Kong, *Engineering Geolology*, **51**(1), 1–36

Aziz, M. (2010): *PhD dissertation*, The University of Tokyo

Barla, M. (1999): Tunnels in Swelling Ground - Simulation of 3D stress paths by triaxial laboratory testing. *Ph.D Thesis*, Politecnico di Torino.

Basma, A. A., Al-Homoud, A. S., Malkawi, A. I. H. and AL-Bashabsheh, M. H. (1996): Swelling–shrinkage behavior of natural expansive clays, *Applied Clay Science*, **11**, 211–227.

Bell, F. G., Entwisle, D. C. and Culshaw M. G. (1997): A geotechnical survey of some British coal measures mudstones, with particular emphasis on durability, *Engineering Geology*, **46,** 115- 29.

Bhasin R., Grimstad, E., Larsen, J. O., Dhawan, A. K., Singh, R., Verma, S. K. and Venkatachalam, K. (2002): Landslide hazards and mitigation measures at Gangtok, Sikkim Himalaya. *Engineering Geology*, **64**(4), 351–368

Bhattarai, P., Marui, H., Tiwari, B., Watanabe, N. and Tuladhar, G. R. (2007): Depth-wise variation of physical and mechanical properties of mustone in relation to weathering-Cases in several landslides in Niigata prefecture. *Journal of the Japan Landslide Society*, **44** (2), 79-89

Botts, M. (1986): The Effects of Slaking on the Engineering Behavior of Clay Shales, *PhD Thesis*, University of Colorado (*http://vast.uah.edu/publications*.)

Botts, M. E. (1998): Effects of Slaking on the Strength of Clay Shales: A Critical State Approach. *Proc. of the 2nd International Symposium on the Geotechnics of Hard Soils / Soft Rocks*, Naples, Italy, October 1998.

Bragg, G. H., Jr., and Zeigler, T. W. (1975*)*: Evaluation and remedial treatment of shale embankments. *Design and construction of compacted shale embankments. Rep. No. FHWA-RD-75-62,* U.S. Federal Highway Administration, Washington, D.C.

Bragg, G. H., Jr., and Zeigler, T. W. (1978): Technical guidelines, Design and construction of compacted shale embankments, *Rep. No.* FHWA-RD-78-141, U.S. Federal Highway Administration, Washington, D.C.

Braudeau, E., Mohtar, R.H. and Chahinian, N. (2004): Estimating soil shrinkage parameters, *Development in Soil Science*, **30**, 225-240.

Canton, Y., Sole-benet, A., Queralt, I. and Pini, R. (2001): Weathering of gypsum-calcareous mudstone under semi-arid environment at Taberanas, SE Spain: Laboratory and field based experimental approach, *Catena*, **44**(2), 111-132

Cao, Y., Huang, R., Feng, T, Zheng, H. and Lv, H. (2006): Study on the slaking characteristics of soft rock engineered slopes at a hydroelectric station in Southwest of China, *The Geological Society of London*, IAEG2006 Paper number, 695

Cetin, H., Laman, H. and Ertunc, A. (200): Settlement and slaking problems in the world's fourth largest rock-fill dam, the Ataturk Dam in Turkey, *Engineering Geology*, **56**(3-4), 225-242.

Chen, F.H. and Ma, G.S. (1987): Swelling and shrinkage behavior of expansive clays, *Proc. of 6th International Conference on Expansive Soils*, New Delhi, India, 127–129.

Chen, W. M. (1997): The influence of water content on the mechanical behaviors of mudstone and its application on fill back engineering. *Master Degree Thesis*, Department of Civil Engineering, National Cheng Kung University.

Chen, X.Q., Lu, Z.W., He, X.F. (1985): Moisture movement and deformation of expansive soils, *Proc. of the 11th International Conference on Soil Mechanics and Foundation Engineering*, San Francisco, USA, 2389–2392.

Chigiraa, M., Wangb,W., Furuyac T. and Kamai, T. (2003): Geological causes and geomorphological precursors of the Tsaoling landslide triggered by the 1999 Chi-Chi earthquake, Taiwan, *Engineering Geology*, **68**, 259–273.

Collison, A., Wade S., Griffiths, J. and Dehn, M. (2000): Modelling the impact of predicted climate change on landslide frequency and magnitude in SE England. *Engineering Geology*, **55**(3), 205–218.

Cui, L. and O'Sullivan, C. (2006): Specimen size and scale effects of direct shear box tests of sands, *Geotechnical Testing Journal*, **29**(6), 507-516.

Czarnomski, N., Moore, M., Pypker, T., Licata, J., and Bond, B. (2005): Precision and accuracy of three alternative instruments for measuring soil water content in two forest soils of the Pacific Northwest, *Canadian Journal of Forest Research*, **35**(8), 1867-1876.

Day, R.W. (1994): Swell–shrink behavior of compacted clay, *Journal of Geotechnical Engineering*, **120**, 618–623.

Dhakal G., Yoneda T., Kato M. and Kaneko, K. (2002): Slake durability and mineralogical properties of some pyroclastic and sedimentary rocks, *Engineering Geology*, **65**, 31-45.

Dick, J. C. and Shakoor, A. (1992): Lithological controls of mudrock durability, *Quarterly Journal of Engineering Geology and Hydrogeology*, **25**, 31-46.

Dick, J. C., Shakoor, A., and Wells, N. A. (1994): A geological approach toward developing a mudrock-durability classification system, *Canadian Geotechnical Journal*, **31**, 17–27.

Doostmohammadi, R., Moosavi, M and Arabi, B. N. (2008): A model for determining cyclic swell-shrink behaviour of argillaceous rock, *Applied clay science*, **42** (1-2), 81-89.

Dunning, S. A., Mitchell, W. A., Rosser, N. J. and Petley D. N. (2007): The Hattian Bala rock avalanche and associated landslides triggered by the Kashmir Earthquake of 8 October 2005, *Engineering Geology*, **93**, 130–144

Duttine, A., Tatsuoka, F., Kongkitkul, W. and Hirakawa, D. (2008): Viscous behavior of unbound granular materials in direct shear, *Soils and Foundations*, **48** (3), 297-318.

Duttine, A., Tatsuoka, F., Lee, J. and Kongkitkul, W. (2009): Viscous properties of Toyoura sand over a wide range of strain rate and its model simulation, *Soils and Foundations*, **49** (2), 221-247.

Editorial (2001): Weathering and geomorphology, *Geomorphology*, **41**, 1-3.

Editorial (2007): Studies in weathering and slope movements-and introduction, **87**, 101-103.

Einav, I. (2007): Breakage mechanics-part I : Theory, *Journal Mechanics and Physics of Solids*, **55**(6), 1274–1297

Einstein, H.H. (1996): Tunnelling in difficult ground-swelling behaviour and identification of swelling rocks, *Rock Mechanics and Rock Engineering*, **28**, 113–124.

Erguler Z. A. and Ulusay R. (2009): Water induced variations in mechanical properties of clay bearing rocks, *International Journal of Rock Mechanics and Mining Sciences*, **46**, 355-370.

Erguler, Z. A. and Shakoor, A. (2009): Quantification of fragment size distribution of clay bearing rocks after slake durability testing, *Environmental and Engineering Geosciences*, **XV** (2), 81-89.

Folk, R. L., Andrew, P. B., and Lewis, D. W. (1970): Detrital sedimentary rock classification and nomenclature for use in New Zealand, *New Zealand Journal of Geology and Geophysics*, **13**(4), 937-968.

Franklin J. A. and Chandra, R. (1972): The slake durability test, *International Journal of Rock Mechanics, Mineral Sciences and Geomechanics*, **9**, 325-341.

Gemici, U. (2001): Durability of shale in Narldere, Izmir, Turkey, with an emphasis on the impact of water on the slaking behaviour, *Environmental Geology*, **41**, 430-439.

Gillott, J. E. (1970): Fabric of Leda clay investigated by optical, electron-optical and X-ray diffraction methods, *Engineering Geology*, **4**, 133-153.

Gokceoglu C., Ulusay, R. and Sonmez, H. (2000): Factors affecting the durability of selected weak and clay bearing rocks from Turkey, with particular

emphasis on the influence of the number of drying and wetting cycles. *Engineering Geology*, **57**, 215-237.

Gonzalez, I. J. and Scherer, G. (2006): Evaluating potential damage to stones from wetting and drying cycle, *Measuring, Monitoring and Modeling Concrete Properties*, **7**, 685-693.

Goto, S. (1986): Strength and deformation characteristics of granular materials in triaxial tests, Ph. D. thesis, University of Tokyo, Japan (in Japanese)

Grainger, P. (1984): The classification of mudrocks for engineering purposes, *Quaternary Journal and Engineering Geology*, **17**(4), 381-387.

Grim, R. (1969): Clay mineralogy: McGraw-Hill Book Company, 596.

Gysel, M. (1987): Design of tunnels in swelling rock. *Rock Mechanics and Rock Engineering*, **20**, 219–242.

Hachinohe, S., Hiraki, N. and Suzuki, T. (1999): Rates of weathering and temporal changes in strength of bedrocks in marine terrace in Boso, Peninsula, Japan, *Engineering Geology*, **55**, 29-43.

Hall, K. and Hall, A. (1996): Weathering by wetting and drying: some experimental results, *Earth surface process and landforms*, **21**: 364-376.

Hanzawa, H. (1992): A new approach to determine soil parameters free from regional variation in soil behavior and technical quality, *Soil and foundations*, **32** (1), 71-84.

Hawlader, B. C., Lee, Y. N. and Lo, K. Y. (2003): Three-dimensional stress effects on time-dependent swelling behaviour of shaly rocks, *Canadian Geotechnical Journal*, **40**(3), 512-535

Hawlader, B. C., Lo, K.Y., Moore, I. D. (2005): Analysis of tunnels in shaly rock considering three-dimensional stress effects on swelling, *Canadian Geotechnical Journal*, **42**, 1–12.

Holtz, R.D. and Kovacs, W.D. (2003): An Introduction to Geotechnical Engineering, *Civil Engineering and Engineering Mechanics Series*. Pearson Education Taiwan Ldt., 733.

Huang, R. and le, W. (2011): Formation, distribution and risk control of landslides in China. *Journal of Rock Mechanics and Geotechnical Engineering*, **3** (2), 97–116.

Huang, S. L., Speck, R. C. and Wang, Z. (1995): The temperature effect on swelling of shales under cyclic wetting and drying, *International Journal of Rock Mechanics and Mining Sciences & Geomechanics Abstract*, **32** (3), 227-236.

Hugett, R. J. (2003): *Fundamentals of geomorphology*, Routledge, London.

Huppert F. (1988): Influence of microfabric on geomechanical behavior of Tertiary fine grained sedimentary rocks from Central North Island, New Zealand. *Bulletin of the International Association of Engineering Geology*, **38,** 83-94.

Ibanez, D. W. and Kronenberg, K. A. (1993): Experimental deformation of shale: Mechanical properties and microstructural indicators of mechanisms, *International Journal of Rock Mechanics and Mining Sciences & Geomechanics Abstracts*, **30**(7), 723-734.

Igwe, O., Sassa, K. and Wang F. (2007): The influence of grading on the shear strength of loose sands in stress-controlled ring shear tests. *Landslides*, **4**, 43-51.

ISRM (1983): Characterisation of swelling rock, *Commission on Swelling Rock.* Pergamon Press, Oxford, UK.

Iwasaki, T. and Tatsuoka, F. (1997): Effects of grain size and grading on dynamic shear moduli of sands, *Soil and Foundations*, **17**(3), 19-25.

Jakobsen, M. and Johansen, T. A. (2000): Anisotropic approximations for mudrocks: A seismic laboratory study. *Geophysics*, **65** (6), 1711-1725

Jewell, R. A. and Worth, C. P. (1987): Direct shear tests on reinforced sand, *Geotechnique*, **37**(1), 53-68.

Jongpradist, P. and Horii, H. (2007): Influence of water content on and relationship between strength and creep behaviors of soft rock – experimental characterization. Rock Mechanics, *Fuenkajorn & Phien-wej (eds*) © 2007. ISBN 978 974 533 613 1

Kanyaya, J. I. and Trenhaile, A. S. (2005): Tidal wetting and drying on shore platforms: An experimental assessment: *Geomophology*, **70**, 129-144.

Kirschbaum, D. B., R. Adler, Y. Hong, S. Hill and Lerner-Lam, A. L. (2009): A global landslide catalog for hazard applications – Method, Results and Limitations, *Journal of Natural Hazards DOI: 10.1007/s11069-009-9401-4.*

Kiyota, T., Konagai, K., Sattar, A., Kazmi, Z. A., Okuno, D. and Ikeda, T. (2011): Breaching failure of a huge landslide dam formed by 2005 Kashmir earthquake, *Soils and Foundations*, **51**(6), 1179-1190.

Koncagul, E.C. and Santi, P. M. (1999): Predicting the unconfined compressive strength of the Breathitt shale using slake durability, shore hardness and rock structural properties, *International Journal of Rock Mechanics and Mining Sciences*, **36**, 139–53.

Ladd, C. C. (1960): Mechanisms of swelling by compacted clay. *Highway Research Board Bulletin, abstract,* **245**, 10–26.

Lashkaripour G.R. and Boomeri M. (2002): The role of mineralogy on durability of weak rocks, *Pakistan Journal of Applied Sciences*, **2**(6), 698-701.

Lashkaripour, G. R. and Ghafoori, M. (2002): Minelalogical controls of mudrock durability. *Engineering Geology for Developing Countries - Proceedings of 9th Congress of the International Association for Engineering Geology and the Environment*. Durban, South Africa, 20 September, 2002

Lings, M. L. and Dietz, M. S. (2004): An improved direct shear apparatus for sand, Geotechnique, 54(4), 245-256.

Lutton, R. J. (1977): Slaking indexes for design. Design and construction of compacted shale embankments. *Rep. No. FHWA-RD-77-1*, U.S. Federal Highway Administration, Washington, D.C.

Malla, S., Wieland, M. and Straubhaar, R. (2007): Assessment of Long-Term Behaviour of Ataturk Dam, Proceeding *othe the 1st national symposium and exposition on dam safety*, Turkey, 28-30 May, 2007.

Matsukura, Y. and Mizuno, K. (1986): The influence of weathering of the geotechnical properties and slope angles of mudstone in the Mineoka earth-slide area, Japan, *Earth surface professes and landforms*, **11**, 263-273.

Matsukura, Y. and Yatsu, E. (1982): Wet-dry slaking of Tertiary shale and tuff. *Transaction, Japanese Geomorphological Union*, **3**(1), 25–39.

Mauritsch H. J., Seiberl, W., Arndt, R., Romer, A., Schneiderbauer, K. and Sendlhofer, G. P. (2000): Geophysical investigations of large landslides in the Carnic Region of southern Austria. *Engineering Geology*, **56**(3–4), 373–388

Means, R. E. and Parcher, J. V. (1963): Physical properties of Soils, Charles E. Merril Books Inc, Columbus, Ohio.

Mirza, M. A. (1996): Geological map of Azad Jammu and Kashmir, Geological Survey of Pakistan (GSP).

Mochizuki, A., Mikasa, M., and Kawamoto, S. (1985): Investigation of settlement of clay fill at a housing development site.'' *Tsuchi-To-Kiso*, **33**(4), 25–32 (in Japanese)

Moon V.G., Beattie A.G. (1995): Textural and micro-structural influences on the durability of Waikato Coal Measures mudrocks. *Quarterly Journal of Engineering Geology*, **28**, 303-312.

Moosavi, M., Yazdanpanah, M. J. and Doostmohammadi, R. (2006): Modeling the cyclic swelling pressure of mudrock using artificial neural network., *Engineering Geology*, **87**, 178–194.

Morgenstern, N. R., Eigenbrod, K. D. (1974): Classification of argillaceous soils and rocks, *Journal of the Geotechnical Engineering Division*, ASCE, **100** (10), 1137-1156

Moriwaki, Y. (1974): Causes of slaking of argillaceous materials. *Ph. D dissertation*, Department of Civil Engineering, University of California, Berkeley.

Nakano, M., Asaoka, A. and Constantinscu, T. D. (1998): Delayed compression and progressive failure of the assembly of crushed mudstones due to slaking, *Soil and Foundations*, ***38***(4), 183-198

Nakano, R. (1967): On weathering and changes of properties of tertiary mudstone related to landslide. Soils and Foundation, **3**, 1-14.

Noda, T. and Nishi, M. (1988): A study of soft-rock embankment deformation due to water increase, *Proc., JSCE*, **391**(8), 77–86 (in Japanese).

Okamoto, R., Kojima, K. and Yoshinaka, R. (1981): Distribution and engineering properties of weak rocks in Japan. *Weak Rock*, **2**, p.1269–1283.

Osipov, V. I., Bik, N. N. and Rumjantseva, N. A. (1987): Cyclic swelling of clays, *Applied Clay Science*, **2**, 363–374.

Panabokke, C. R. and Quirk, J.P. (1987): Effect of initial water content on stability of soil aggregates in water, *Soil Science*, **83**(3), 185-196.

Parise, M, and Wasowski, J. (1999): Landslide Activity Maps for Landslide Hazard Evaluation: three case studies from Southern Italy, *Natural Hazards* **20**(2–3), 159–183.

Pejon, O. J. and Zuquette, L. V. (2002): Analysis of cyclic swelling of mudrocks, Engineering Geology, **67**, 97-108.

Pradini, G., Vigna, G., Pini, R., Regues, D. and Gallart, F. (1996): Structure and porosity of smectitic mudrocks as affected by experimental wetting-drying cycles and freezing-thawing cycles, *Catena*, **27** (3/4), 149-165

Qiu, J. Y., Tatsuoka, F. and Uchimura, T., (2000): Constant pressure and constant volume direct shear tests on reinforced sand, *Soils and Foundations*, **40** (4), 1-17.

Qureshi, M. U., Towhata, I. Yamada, S. and Aziz M. (2009): Field and laboratory tests on risk of slope failure due to weathering of rock materials. *Geophysical Research Abstracts11*, EGU2009-7133 , **11**

Regues, D., Pardini, G. and Gallart, F.(1995): Regolith behavior and physical weathering of clayey mudrock as dependent on seasonal weather conditions in a badland area at Vallcebre, Eastern Pyrenees, *Elsevier Science,***25**, 199-212.

Runqiu, H. (2009): Some catastrophic landslides since the twentieth century in the southwest of China, *Landslides*, **6**, 69–81.

Sadisun, I. A., Bandono, Shimada, H., Ichinose, M. and Mastui, K. (2003): Slope instability of road cuts due to rock slaking. *Proc. of 12th Asian regional conference on soil mechanics and geotechnical engineering*, 747-750.

Sadisun, I. A., Shimada, H., Ichinose, M. and Mastui, K. (2004): Textural and mineralogical properties of argillaceous rocks in relation to their propensity of slaking, *engineering geology for sustainable development in mountainous area*, 168-172.

Sadisun, I. A., Shimada, H., Ichinose, M. and Mastui, K. (2005): Study on the physical disintegration characteristics of Subang claystone subjected to a modified slaking index test, *Geotechnical and Geological Engineering*, **23**, 199–218.

Sadisun, I.A., Shimada, H. and Ichinose, M. (2002): Improved procedures for evaluating physical deterioration of argillaceous rocks, In: Y. Lim, C. Tang, X. Feng and S. Wang (eds.), *Proceedings of 2nd Intl. Conf on New Development in Rock Mech. and Rock Eng.*, P. R. China, Rinton Press, 36–39.

Safaei, M., Omar, H., Huat, K. B. and Yousof, B. M. Z. (2002): Relationship between Lithology Factor and landslide occurrence based on Information Value (IV) and Frequency Ratio (FR) approaches-Case study in North of Iran. *Geotechnical Engineering Electronic Journal*, **17**, 79-90.

Saffet, Y. (2011): Correlation between slake durability and rock properties for some carbonate rocks. *Bull Eng Geol Environ* (2011), **70**:377–383, DOI 10.1007/s10064-010-0317-8

Santi P.M. and Koncagul, E. C. (1996): Predicting the mode, susceptibility and rate of weathering of shales. *In*: Matheson G., ed., Design with residual materials - geotechnical and construction considerations. *ASCE Geotechnical Special Publication*, **63**, 12-26.

Santi, P.M. (1998): Improving of jar slake, slake index, and slake durability tests for shales, *Environmental & Engineering Geoscience*, **6**(3), 385–396.

Sattar, A., Konagai, K., Kiyota, T., Ikeda, T. and Johansson, J. (2010): Measurement of debris mass changes and assessment of the dam-break flood potential of earthquake-triggered Hattian landslide dam, *Landslides*, DOI: 10.1007/s10346-010-0241-9.

Scherer, G. (2006): Internal stress and cracking in stone and masonry. In: MS Konsta-Gdoutos (Editor), measuring, monitoring and concrete properties, *ed. M.S. Konsta-Gdoutos* (Springer, Dordrecht, Netherlands), 633-641

Seedsman, R. W. (1986): The behavior of clay shales in water, *Canadian Geotechnical Journa*, **23**, 18–22.

Seedsman, R.W. (1993): Comprehensive rock engineering, *Characterizing clay shales*, Pragamon press Oxford, **3**,151–164.

Shamburger, J. H., Patrick, D. M., and Lutton, R. J. (1975): Survey of problem areas and current practices. Design and construction of compacted shale embankments, *Rep. No. FHWA-RD-75-61*, U.S. Federal Highway Administration, Washington, D.C.

Shibuya, S., Mitachi T., and Tamate, S. (1997): Interpretations of direct shear box testing of sands as quasi-simple shear, *Geotechnique*, **47** (4), 769-790.

Singh, T. N., Verma, A. K., Singh, V. and Sahu, A. (2005): Slake durability study of shaly rock and its predictions, *Environmental Geology*, **47**, 246–253.

Soralump, S. (2010): Corporative of geotechnical approach for landslide susceptibility mapping in Thailand, *Proc. of International conference on slope 2010: Geotechnique and Geosythentics for slope*, 27-30, July, Chiangmi, Thailand

Spears, D. A. and Taylor, R. K. (1971): The influence of weathering of the composition and engineering properties of in situ coal measures rocks. *Intenrational Journal of Rock mechanics and mineral Science,* **9**, 729-756

Sri-in, T. and Fuenkajorn, K. (2007): Slake durability index and strength testing of some rocks in Thailand, *Rock Mechanics*, Fuenkajorn & Phien-wej (eds), 145-159

Starr, J. L., and Paltineanu, I. C. (2002): Methods for Measurement of Soil Water Content: Capacitance Devices. *In J.H.Dane, and G.C.Topp (ed.)* Soil Science Society of America, Inc., 463-474.

Strohm, W. E., (1978): Field and laboratory investigations, Phase III. Design and construction of compacted shale embankments. Rep. No. FHWA-RD-78-140, U.S. Federal Highway Administration, Washington, D.C.

Subba Rao, K.S. and Satyadas, G. G. (1987): Swelling potential with cycles of swelling and partial shrinkage. *6th International Conference on Expansive Soils,* New Delhi, India, 137–142.

Surendra, M., Lovell, C. W. and Wood, L. E. (1981): Laboratory studies of the stabilization of non-durable shale. *Transportation Research Record*, **79**, 33-40.

Taheria, A., Sasakia, Y., Tatsuokaa, F. and Watanabe, K. (2012): Strength and deformation characteristics of cement-mixed gravelly soil in multiple-step triaxial compression, *Soils and Foundations,* **52** (1), 126–145..

Takagi, M., Yokata, S., Suga K., Yasoda S. and Ota H. (2010): The actual situation of the slope of earthfill that collapsed by an earthquake disaster in the Tomei Expressway Makinohara district, 193-196

Tatsuoka, F., Sakamoto, M., Kawamura, T. and Fukushima, S. (1986): Strength and deformation characteristics of sand in plane strain compression at extremely low pressures, *Soil and Foundation*, **26**-1, 65-8

Taylor, R. K. (1988): Coal Measures mudrocks: composition, classification and weathering processes. *Quarterly Journal of Engineering Geology and Hydrogeology*, **21**, 85-99.

Taylor, R. K. and Spears, D. A. (1970): The breakdown of British coal measures rocks. *Int J Rock Mech Min Sci*, **7**, 481–501.

Terzaghi K. (1936): Stability of slopes in natural clay. *Proc. Int. Conf. Soil Mech.*, Harvard, **1**, 161-165.

Terzaghi, K., and Peck, R. B. (1948): *Soil mechanics in engineering practice*, Wiley, New York, 300–302.

Tovar, R. D. and Colmenares, J.E. (2011): Effect of drying and wetting cycles on the shear strength of argillaceous rocks. *Unsaturated Soils* – Alonso & Gens (eds), Taylor & Francis Group, London, ISBN 978-0-415-60428-**4**, 1471-1476.

Towhata, I., Yamazaki, H., Kanatani, M., Lin, C.E. (2002): Direct shear tests on rock specimens of Tsaoling earthquake-induced landslide site and simple stability analysis. *In: Sassa, K. (Ed.), Proc. Int'l. Symp. Landslide risk mitigation and protection of cultural and natural heritage,* Kyoto, 123– 138.

Tucker, M. E. (1981): *Sedimentary Petrology: An Introduction*. (59), 986-996.

U.S. Geological Survey (2000): Landslide hazards. *USGS Fact Sheet Fs-071-00.*

Ulusay, R., Arikan, F., Yoleri, M.F. and Caglayan, D. (1995) Engineering geological characterization of coal mine waste material and evaluation in the context of back analysis of spoil pile instabilities in a strip mine SW Turkey, *Engineering Geology*, **40**, 77–101.

USBR (2006): *Engineering geology field manual*, Technical Service Center, U. S. Department of Interior Bureau of Reclamation.

Vallejo, L. E., Wlesh, R. A., Lovell, C.W. and Robinson, M. K. (1993): The influence of fabric and composition on the durability of shale. In: Rock for Erosion Control, *ASTM STP* **1117**:15-70.

Wells, T., Binning, P. and Willgoose, G. (2005): The role of moisture cyclic in the weathering of quartz chlorite schist in a tropical environment: finding of a laboratory simulation, *Earth surface process and landforms*, **30**, 413-428.

Wood, D. M. and Maeda, K. (2008): Changing grading of soil: effect on critical states, *Acta Geotechnica*, **3**, 3-14.

Wu, P. K., Matsushima, K. and Tatsuoka, F. (2008): Effects of specimen size and some other factors on the strength and deformation of granular soil in direct shear tests, *Geotechnical Testing Journal*, ASTM , **31** (1), 45-64.

Yagiz, S. (2010): Correlation between slake durability and rock properties for some carbonate rocks, *Bull Eng Geol Environ, DOI 10.1007/s10064-010-0317-8.*

Yamagishi, H (2000): Recent Landslides in Western Hokkaido, Japan. *Pure Applied Geophysics*, **157**(6–8), 1115–1134.

Yamaguchi, H., Yoshida, K. Kuroshima, I. and Fukuda, M. (1988): Slaking and shear properties of mudstones. *Rock mechanics and power plants*, Ramana (ed.), 133-144

Yatshu, E. (1988): The Nature of weathering: An introduction. Sozosha, Tokyo

Yilmaz, I. and Karacan, E. (2005): Slake durability and its effect on the dolomite formation in the gypsum, *Environmental Geology*, **47**, 1010-1017

Yoshida, N. Asce, M. and Hosokawa, K. (2004): Compression and shear behavior of mudstones aggregates. *Journal of Geotechnical and Geo-environmental engineering*, **130** (5), 519-525

Yoshida, N., Enami, K. and Hosokawa, K. (2002): Staged compression-immersion direct shear test on compacted mudstone, J. Test. Eval., **30** (3), 239-244.

Yoshida, N., Morgenstern, N. R., and Chan, D. H. (1991): Finite element analysis of softening effects in fissured, over consolidated clays and mudstones, *Canadian Geotechnical Journal*, **28**, 51–61.

Yoshida, N., Nishil, M. Kitamural, M. and Adachi, T. (1997): Analysis of mudstone deterioration and its effect on tunnel performance. *International Journal of Rock Mechanics and mineral Science*, **34**, 3-4, Paper No. 353.

Youn, H. and Tonon, F. (2010): Effect of air-drying duration on the engineering properties of four clay-bearing rocks in Texas, *Engineering Geology*, doi: 10.1016/j.enggeo.2010.06.012.

Zhang, C. L., Wieczorek, K. M. and Xie, L. (2010): Swelling experiments on mudstones, *Journal of Rock Mechanics and Geotechnical Engineering*, **2** (1): 44–51

APPENDIX I

List of Landslides

S.N.	Name	Date	Location	Provinance	Longitude	Lattitude
1	Shuangliu landslide	6/6/2000	Gulin	Sichuan, China	106.175 7	27.929 8
2	Yingjiang landslide	8/14/2000	Yingjiang	Yunnan, China	97.982 2	24.759 1
3	Qianjiangping landslide	7/13/2003	Zigui	Hubei, China	110.602 3	30.975 7
4	Ganchuanxiang landslide	5/13/2003	Xiushan	Chongqing, China	109.102 1	28.574 6
5	Tiantaixiang landslide	9/5/2004	Xuanhan	Sichuan, China	108.057 1	31.435 5
6	Yingpancun landslide	9/1/2004	Shuicheng	Guizhou, China	105.014 3	26.731 2
7	Lianglongxiang landslide	6/30/2004	Xingwen	Sichuan, China	105.081 8	28.282 6
8	Luotancun landslide	7/20/2004	Tongdao	Hunan, China	109.491 9	26.076 8
9	Yanjiao rockfall	12/3/2004	Nayong	Guizhou, China	105.248 4	26.697 4
10	Shuidonggou rockfall	5/9/2005	Jixian	Shanxi, China	110.679 0	36.090 1
11	Qixingjie landslide	6/23/2005	Jian’ou	Fujian, China	118.305 7	27.019 6
12	Fenglongcun debris flow	9/1/2005	Wencheng	Zhejiang, China	119.882 5	27.848 7
13	Qingshan’ao debris flow	6/25/2006	Longhui	Hunan, China	110.747 1	27.580 2
14	Shimoxia debris flow	8/11/2006	Qingyuan	Zhejiang, China	119.318 5	27.560 4
15	Pingtoucun debris flow	8/11/2006	Qingyuan	Zhejiang, China	119.307 5	27.540 4
16	Zhangjia landslide	7/15/2006	Yongxing	Hunan, China	113.185 8	26.359 7
17	Luomapu debris flow	7/14/2006	Yanting	Sichuan, China	101.883 6	27.6851
18	Shiqiaotou rockfall	6/18/2006	Kangding	Sichuan, China	102.186 3	30.114 4
19	Hesancun debris flow	7/14/2006	Longhai	Fujian, China	117.554 4	24.384 0
20	Zhongxilinchang landslide	7/14/2006	Zhangpu	Fujian, China	117.559 4	24.284 7
21	Xianwukuang debris flow	7/15/2006	Yizhang	Hunan, China	113.318 7	25.646 3
22	Gaoloucun landslide	10/6/2006	Huaxian	Shannxi, China	109.663 6	34.448 4

S.N.	Name	Date	Location	Provinance	Longitude	Lattitude
23	Qiantuocun landslide	5/10/2007	Leibo	Sichuan, China	103.332 9	28.065 0
24	Miaozigou debris flow	5/24/2007	Jiulong	Sichuan, China	101.679 2	28.610 0
25	Fenglexiang rockfall	5/25/2007	Shimian	Sichuan, China	102.544 3	29.324 9
26	Sujiahedianzhan andslide	7/19/2007	Tengchong	Yunnan, China	98.257 8	25.339 2
27	Tianwanhe debris flow	8/10/2007	Shimian	Sichuan, China	102.119 3	29.396 3
28	Taipingzhen landslide	6/15/2007	Badong	Hubei, China	110.330 4	29.911 9
29	Gaoyangzhai landslide	11/20/2007	Badong	Hubei, China	110.328 8	30.622 7
30	Shang’ancun rockfall	6/13/2008	Lvliang	Shanxi, China	111.150 4	37.578 7
31	Huashitou landslide	8/9/2008	Maguan	Yunnan,China	104.532 5	22.909 7
32	Renjiaping debris flow	9/24/2008	Beichuan	Sichuan, China	104.442 6	31.810 0
33	Banpocun landslide	4/22/2008	Yuncheng	Shanxi, China	110.616 4	35.750 9
34	Yangtiyan landslide	4/26/2009	Zhaotong	Yunnan,China	105.054 0	27.859
35	Jiuzhou landslide	5/16/2009	Lanzhou	Gansu, China	103.801 9	36.083 4
36	Jiweishan landslide	6/5/2009	Wulong	Chongqing, China	107.432 9	29.232 2
37	Minluocun landslide	6/8/2009	Liping	Guizhou, China	108.759 1	26.082 8
38	Santuancun landslide	6/10/2009	Liping	Guizhou, China	109.420 6	26.114 7
39	Huoshicun landslide	6/20/2009	Tongzi	Guizhou, China	106.649 6	28.074 0
40	Chang'anzhen rockfall	7/3/2009	Rong'an	Guangxi, China	109.385 4	25.265 1
41	Dafengtan landslide	7/12/2009	Xuanhan	Sichuan, China	108.251 8	31.627 3
42	Xinguan debris flow	7/17/2009	Wenxian	Gansu, China	104.427 8	33.026 2
43	Mushurexi debris flow	7/17/2009	Xiaojin	Sichuan, China	102.233 1	30.792 8
44	Xiaowan landslide	7/20/2009	Fengqing	Yunnan, China	100.031 2	24.729 2
45	Xiangshuigou debris flow	7/23/2009	Kangding	Sichuan, China	102.179 0	30.180 7
46	Tiexijingguansuo landslide	7/25/2009	Huaihua	Hunan, China	109.977 3	27.086 5
47	Nanyueshan landslide	7/25/2009	Huaihua	Hunan, China	110.015 7	27.111 6
48	Liaojiaolou landslide	7/25/2009	Huaihua	Hunan, China	110.022 4	27.102 7
49	Tianduan landslide	7/25/2009	Huaihua	Hunan, China	110.000 1	27.072 9
50	Sanchaxi landslide	7/25/2009	Huaihua	Hunan, China	110.023 9	27.098 5

S.N.	Name	Date	Location	Provinance	Longitude	Lattitude
51	Xinhua landslide	7/25/2009	Huaihua	Hunan, China	110.0117	27.099 0
52	Shuping landslide	7/25/2009	Hongjiang	Hunan, China	110.1686	29.190 1
53	Shanghengling landslide	7/25/2009	Hongjiang	Hunan, China	110.028 5	27.126 9
54	Houziyan landslide	8/6/2009	Hanyuan	Sichuan, China	102.781 9	29.313 1
55	Huangbi landslide	8/9/2009	Qianshan	Jiangxi, China	117.693 8	27.899 4
56	Qingliangfeng landslide	8/13/2009	Lin'an	Zhejiang, China	119.003 7	30.086 9
57	Sanjiezhen landslide	8/15/2009	Chengzhou	Zhejiang, China	120.841	7 29.718 9
58	Maoniugou debris	8/15/2009	Luding	Sichuan, China	102.178 1	30.0284
59	Qianwukeng debris	8/16/2009	Quzhou	Zhejiang, China	118.753 5	29.125 4
60	Zuobie debris flow	8/16/2009	Nimu	Tibet, China	90.080 9	29.339 8
61	Wenquanxiang debris	8/17/2009	Yanbian	Sichuan, China	101.867 3	26.687 6
62	Machi landslide	9/5/2009	Huating	Gansu, China	106.620 0	35.276 3
63	Longdagou debris flow	9/12/2009	Luding	Sichuan, China	102.162 8	29.5553
64	Xiaogou landslide	9/14/2009	Kangxian	Gansu, China	105.564 7	33.206 7
65	Zhangjiazui rockfall	11/16/2009	Zhongyang	Shanxi, China	111.200 0	37.446 0
66	Guoguang landslide	11/28/2009	Hengshan	Hunan, China	112.652 8	27.411 1
67	Dengfushan landslide	1/8/2010	Nanjing	Jiangsu, China	118.769 9	31.992 7
68	Yangyandi landslide	1/18/2010	Dejiang	Guizhou, China	108.144 0	28.546 3
69	Dengcun rockfall	2/26/2010	Sihui	Guangxi, China	112.589 7	23.334 9
70	Shuanghuyu rockfall	3/10/2010	Zizhou	Shannxi, China	110.027 8	37.614 5
71	Pingzhai rockfall	3/29/2010	Zhijin	Guizhou, China	105.779 0	26.674 2
72	Hongtaoshan rockfall	4/12/2010	Nanping	Fujian, China	118.199 4	26.638 8
73	Zengchong landslide	4/23/2010	Qichun	Hubei, China	115.585 0	30.297 5
74	Huangni'ao debris flow	5/6/2010	Liling	Hunan, China	113.475 9	27.667 3
75	Yanyacun landslide	5/17/2010	Baokang	Hubei, China	110.953 8	31.749 7
76	Hefang landslide	5/23/2010	Dongxiang	Jiangxi, China	116.629 6	28.221 8
77	Anshancun landslide	6/1/2010	Qianshan	Jiangxi, China	117.826 0	28.171 1
78	Chencun landslide	6/2/2010	Rongxian	Guanxi, China	110.745 1	22.7933
79	Jili landslide	6/3/2010	Laibing	Guangxi, China	109.189 2	23.642 2
80	Dayetiekuang landslide	6/12/2010	Huangshi	Hubei, China	114.892 4	30.223 4
81	Shuangjigou landslide	6/14/2010	Kangding	Sichuan, China	102.289 4	30.435 4
82	Yanta landslide	6/14/2010	Nanping	Fujian, China	118.185 4	26.644 7

S.N.	Name	Date	Location	Provinance	Longitude	Lattitude
83	Chenjiawan debris flow	6/16/2010	Jiulong	Sichuan, China	101.703 5	28.381 8
84	Gaotangling debris flow	6/20/2010	Guiyang	Hunan, China	112.729 4	25.614 7
85	Guixi landslide	6/20/2010	Guixi	Jiangxi, China	117.360 9	28.303 6 0
86	Guanling landslide	6/28/2010	Guanling	Guizhou, China	105.330 2	25.956 4
87	Shenhe landslide	7/6/2010	Zhushan	Hubei, China	110.223	1 32.108 6
88	Toutang landslide	7/13/2010	Xuyong	Sichuan, China	105.413 3	28.219 2
89	Mingshuiquan landslide	7/14/2010	Xianning	Hubei, China	114.338 4	29.715 4
90	Dalingtou rockfall	7/15/2010	Poyang	Jiangxi, China	117.012 8	29.6228
91	Damucun landslide	7/15/2010	Xianning	Hubei, China	114.616 0	29.821 8
92	Guojiaba landslide	7/16/2010	Zigui	Hubei, China	110.684 5	30.912 7
93	Muchenggou debris flow	7/16/2010	Litang	Sichuan, China	102.990 3	31.516 8
94	Niumachang landslide	7/7/2010	Nanjiang	Sichuan, China	106.614 6	31.874 3
95	Wangshuiyan landslide	7/17/2010	Suining	Sichuan, China	105.681 8	30.428 1
96	Huagongchang debris flow	7/17/2010	Hanyuan	Sichuan, China	102.680 7	29.353 5
97	Muzhucun landslide	7/18/2010	Ankang	Shannxi, China	108.875 9	32.275 6
98	Qiyan landslide	7/18/2010	Ankang	Shannxi, China	108.725 7	32.562 2
99	Chengnancun rockfall	7/18/2010	Tongjiang	Sichuan, China	107.258 2	31.907 4
100	Fenghuangjie landslide	7/19/2010	Pingchang	Sichuan, China	107.148 2	31.442 9
101	Weiganba landslide	7/19/2010	Wanyuan	Sichuan, China	107.836 2	31.763 3
102	Jinshaba landslide	7/20/2010	Mianning	Sichuan, China	101.873 2	28.452 9
103	Xinqiaocun landslide	7/20/2010	Longping	Sichuan, China	105.263 2	29.200 5
104	Qinlingcun landslide	7/23/2010	Guangyuan	China	105.849 0	32.568 4
105	Qiao’ergou landslide	7/24/2010	Shanyang	Shannxi, China	110.055 1	33.486 2
106	Diangoucun rockfall	7/24/2010	Huangting	Gansu, China	106.636 4	35.218 8
107	Tei'amocun debris flow	7/24/2010	Ganluo	Sichuan, China	102.788 1	29.198 2
108	Hutang landslide	7/25/2010	Loudi	Hunan, China	112.240 5	27.617 2
109	Mugudianzhan debris	7/26/2010	Gongshan	Yunnan, China	98.78	2 27.596 4

S.N.	Name	Date	Location	Provinance	Longitude	Lattitude
110	Ermanshan landslide	7/27/2010	Hanyuan	Sichuan, China	102.743 9	29.322 5
111	Yingjunzhen landslide	8/4/2010	Changchun	Jilin, China	125.474 7	43.873 3
112	Zhouqu debris flow	8/8/2010	Zhouqu	Gansu, China	104.371 8	33.789 3
113	Nanyugou debris flow	8/10/2010	Zhouqu	Gansu, China	104.410 7	33.723 8
114	Chenjiawan landslide	8/11/2010	Tianshui	Gansu, China	105.722 4	34.576 4
115	Mashicun debris flow	8/12/2010	Chengxian	Gansu, China	105.656 4	33.990 2
116	Zhuanghecun landslide	8/12/2010	Zhangchuan	Gansu, China	106.139 3	35.023 0
117	Pingwangcun landslide	8/12/2010	Zhangchuan	Gansu, China	106.140 6	35.021 5
118	Wenjiagou debris flow	8/13/2010	Mianning	Sichuan, China	104.117 1	31.551 7
119	Sanhecun debris flow	8/13/2010	Jiuzhaigou	Sichuan, China	104.213 4	33.189 0
120	Shenxigou debris flow	8/13/2010	Dujiangyan	Sichuan, China	103.628 7	31.092 6
121	Sezucun debris flow	8/13/2010	Danba	Sichuan, China	101.880 3	31.108 7
122	Yazhacun-1 debris	8/14/2010	Jiuzhaigou	Sichuan, China	103.933 7	33.314 5
123	Dangduocun debris	8/14/2010	Baiyu	Sichuan, China	99.113 2	31.380 7
124	Long’andianzhan rockfall	8/17/2010	Songpan	Sichuan, China	103.713 2	32.401 3
125	Yazhacun-2 debris	8/18/2010	Jiuzhaigou	Sichuan, China	103.932 7	33.312 1
126	Yatungou debris flow	8/18/2010	Jiuzhaigou	Sichuan, China	103.861 9	33.295 0
127	Dongyuegu debris	8/18/2010	Gongshan	Yunnan, China	98.775 0	27.601 8
128	Zhangjiagou landslide	8/20/2010	Jianyang	Sichuan, China	104.244 5	30.312 7
129	Pan’angou debris flow	8/23/2010	Xiaojin	Sichuan, China	102.085 5	30.755 3
130	Huayang debris flow	8/24/2010	Huayin	Shannxi, China	109.999 9	34.413 1 0
131	Dashifang landslide	9/1/2010	Baoshan	China	98.986 3	25.574 4
132	Songraocun debris	9/6/2010	Bomi	Tibet, China	95.471 2	29.911 9
133	Rangyuhe landslide	9/15/2010	Fangxian	Hubei, China	111.043 7	32.038 0
134	Guomaricun debris	9/20/2010	Tongren	Qinghai, China	102.043 5	35.570 0
135	Lingtoucun debris	9/21/2010	Yangcun	Guangdong, China	111.359 7	22.103 2
136	Maliuwa debris flow	9/21/2010	Beichuan	Sichuan, China	104.436 9	31.751 0
137	Patal Landslide	8/26/2006	Achham	Nepal	81.3005	29.005
138	Baglung landslide	7/12/2006	Baglung	Nepal	83.6659	28.2135
139	Barangay 97 Landslide	3/16/2011	Tacloban City	Phillipines	124.9693	11.2196
140	Chittagong landslide	6/11/2007	Chittagong	Bangaladesh	91.7951	23.3713

S.N.	Name	Date	Location	Provinance	Longitude	Lattitude
141	Cocuta landslide	3/27/2011	North Columbia	USA	-72.877	7.4319
142	Mastamandu landslide	6/8/2009	Dadeldhula	Nepal	81.3005	29.2269
143	Dharla landslide	8/15/2007	Himanchal	India	77.072	30.906
144	Doba Syedan landslide	3/21/2007	Jhelum	Pakistan	73.4432	34.338
145	Eungella landslide		Mackay	Austrailia	148.4822	-21.0979
146	Ramche landslide	8/16/2006	Rasuwa	Nepal	85.1786	28.021
147	Attabad landslide	1/4/2010	Attabad	Pakistan	74.64941	36.31507
148	La Paz landslide	2/27/2011	La Paz	Bolivia	-68.1466	-16.4988
149	Dana point landslide	1/11/2011	California	USA	-117.69412	33.4671
150	Gulmi landslide	8/20/2003	Gullmi	Nepal	83.26752	28.08387
151	Oas landslide	1/20/2011	Albay	Phillipines	123.4949	13.2584
152	Pasco landslide	1/10/2011	Pasco	Peru	-72.6931	-12.8576
153	Taplejung landslide	8/8/2002	Taplejung	Nepal	87.6666	27.35
154	Ayuttaha landslide	Aug-11	Ayuttaha	Thailand	100.5235	14.316284
155	Krabi Lanslide	3/29/2011	Krabi	Thailand	99.1026	8.124038
157	Mae hong son landslide	3/31/2011	Mae hong son	Thailand	87.89	18.73817
158	NW Oregon highway	1/18/2011	Tillamook	USA	-123.8245	45.4114
159	Bududa landslide	1/10/2010	Bududa	Uganda	34.3317	1.0099
160	Darchula landslide	2/5/2010	Darchula	Nepal	80.545	28.844
161	Mount Elegon landslide	5/4/2010	Bumwalukani	Kenya	37.5152	0.5123
162	Kilimanjaro landslide	11/11/2009	Kilimanjaro	Tanzania	37.8088	4.13287
163	Tawang landslide	11/28/2010	Arunanchal	India	91.99012	27.5514
164	Gurdi lanslides	9/9/2006	Tanahu	Nepal	84.2279	27.9134
165	Hallar Bridge landslide	1/5/2007	Kotli	Pakistan	73.70622	33.545227
166	Sungai Sariak landslide	1/8/2007	Sumatra	Indonesia	100.9833	0.0667
167	Bandar Seri, landslide	1/8/2007	Begawan	Brunei	114.917	4.98333
168	Nuwara Eliya	1/13/2007	Nuwara Eliya	Sri Lanka	80.757715	6.965843
169	Sangihe island	1/15/2007	Jakarta	Indonesia	125.540125	3.542435
170	Dongala landslide	1/31/2007	Central Sulawesi	Indonesia	119.762	-0.6811
171	Banten landslide	2/6/2007	Cadasari	Indonesia	106.1	-6.25
172	Semarang landslide	2/19/2007	Central Java	Indonesia	110.141	-7.28
173	Rawalakot landslide	2/25/2007	Kashmir	Pakistan	73.7666	33.8666
174	Doba landslide	3/19/2007	Kashmir	India	74.3333	33.8778
175	Muzaffarabad landslide	3/20/2007	Kashmir	Pakistan	73.494	33.5708
176	Islamabad lanslide	3/21/2007	Kashmir	Pakistan	73.038023	33.703333
177	Salyana landslide	3/21/2007	Salyana	Nepal	81.28859	27.608918
178	Badakhshan landslide	3/28/2007	Bamyan	Afaghanistan	69.169616	34.535309
179	Galle landslide	5/4/2007	Galle	Sri Lanka	80.217393	6.032751
180	Samarouli landslide	5/8/2007	Jambu-Kashmir	India	75.231	33.242
181	Rangmati	6/11/2007	Rangamati	Bangaladesh	92.145249	22.63678
182	Indira Bypass	6/13/2007	Amdo Golai	India	88.408898	26.732372
183	Sevoke	6/15/2007	Sevoke	India	88.526	26.8096

S.N.	Name	Date	Location	Provinance	Longitude	Lattitude
184	Chiayi landslide	6/24/2007	Chiayi County	Taiwan	120.4256	23.4535
185	Ratnagiri landslide	6/25/2007	Ratnagiri	India	73.5189	16.9648
186	Kozhikode landslide	6/25/2007	Kozhikode	India	75.8275	11.2738
187	Wayanad landslide	6/25/2007	Wayanad	India	76.074	11.7095
188	Kurnool landslide	6/25/2007	Kurnool	India	78.0501	15.8294
189	Cuddappa landslide	6/25/2007	Cuddappa	India	78.8205	14.4702
190	Prakasam landslide	6/25/2007	Prakasam	India	80.6128	16.6252
191	Karimnagar landslide	6/25/2007	Karimnagar	India	79.1492	18.431
192	Vasco landslide	7/30/2007	Vasco	India	73.8277	15.4014
193	Lawngtlai landslide	7/30/2007	Lawngtlai	India	92.899	22.533
194	Saiha landslide	7/30/2007	Saiha	India	92.967	22.479
195	Joshimath landslide	7/30/2007	Joshimath	India	79.56	30.557
196	Chamoli landslide	7/30/2007	Chamoli	India	79.349	30.4
197	Uttarkashi landslide	7/30/2007	Uttarkashi district	India	78.439	30.733
198	Dhading landslide	8/10/2007	Dhading	Nepal	84.914	27.863
199	Khotang landslide	8/10/2007	Khotang	Nepal	86.85	27.016
200	Surkhet slide	8/10/2007	Surkhet	Nepal	81.601	28.601
201	Vernon County lanslide	8/18/2007	WI	USA	-91.225567	43.59595
202	Cody landslide	8/18/2007	WY	USA	-109.8661	44.465862
203	Rochester landslide	8/18/2007	MN	USA	-92.4671	44.0304
204	LaCrosse landslide	8/19/2007	WI, hwy 35	USA	-91.219367	43.6796
205	Brownsville landslide	8/19/2007	Minnesota	USA	-91.280567	43.68896
206	Duli Village landslide	8/24/2007	Rukum	Nepal	82.616667	28.616667
207	Neta landslide	8/24/2007	Gulmi	Nepal	83.097064	28.087699
208	Argha landslide	8/24/2007	Pyuthan	Nepal	83.083333	27.916667
209	Hattisurey landslide	8/24/2007	Kalimpong	India	88.430782	27.071335
210	Kabilas landslide	7/31/2003	Chitwan	Nepal	84.3500	27.6300
211	Koteswora landslide	7/30/2003	Nuwakot	Nepal	84.3083	27.7061
212	Jalbhir landslide	7/30/2003	Chitwan	Nepal	84.2578	27.7009
213	Baijnath landslide	7/30/2003	Far western	India	79.6082	29.9262
214	Chhip Chhipe landslide	7/30/2003	Tanahu	Nepal	84.2500	27.9167
215	Rupendehi landslide	7/30/2003	Rupendehi	Nepal	83.4167	27.6667
216	Bara landslide	7/30/2003	Bara	Nepal	85.0000	27.0333
217	Siraha landslide	7/30/2003	Siraha	Nepal	86.2000	26.6500
218	Krishna Bhir lanslide	7/30/2003	Chitwan	Nepal	84.7931	27.7922
219	Gaidakot landslide	7/30/2003	Nawalparasi	Nepal	83.6741	27.5352
220	Ratanpur landslide	7/30/2003	Nawalparasi	Nepal	83.7062	27.5060
221	Bhagar Village landslide	7/30/2003	Nawaparasi	Nepal	83.7623	27.6143
222	Damauli landslide	8/1/2003	Tanahu	Nepal	84.2693	27.9684
223	Hadikhola landslide	8/1/2003	Makwanpur	Nepal	84.8400	27.5947
224	Manakamana landslide	8/1/2003	Gorkha	Nepal	84.4720	28.0381
225	Tigray landslide	9/11/2003	Tigray	Ethiopia	39.5000	13.5000

S.N.	Name	Date	Location	Provinance	Longitude	Lattitude
226	Painreman landslide	1/10/2003	West Kalimantan	Indonesia	109.331	-0.023
227	Petropolis landslide	1/11/2003	Rio de Janeiro	Brazil	-43.1823	-22.5046
228	Borneo landslide	1/11/2003	Borneo	Indonesia	109.1489	0.2424
229	Minas Gerais landslide	1/17/2003	Minas Gerais	Brazil	-43.1756	-22.9100
230	Garut landslide	1/29/2003	Java	Indonesia	107.8918	-7.2250
231	Cantilan	1/31/2003	West Java	Indonesia	108.4330	-7.1000
232	Sarawak	2/10/2003	Sarawak	Malaysia	114.9442	4.0188
233	Dasu landslide	2/18/2003	Kohistan	Pakistan	75.3167	35.6167
234	Ghorvodor landslide	2/19/2003	Khatlon	Tajikistan	69.0595	37.8644
235	Neelum Valley landslide	2/26/2003	Neelum Valley	Pakistan	73.5750	34.4588
236	Tolti landslide	3/4/2003	Skardu	Pakistan	76.1000	35.0333
237	Doda Landslide	3/6/2003	Jammu	India	75.5464	33.1517
238	Bawngkawn	5/4/2003	Bawngkawn	India	92.7084	23.7417
239	Noabadi landslide	5/5/2003	Akhaura	Bangladesh	91.2189	23.8617
240	Lawngtlai landslide	5/5/2003	Lawngtlai	India	92.9000	22.5330
241	Baotou landslide	5/11/2003	Guizhou	China	104.6750	25.4000
242	Gatara landslide	5/15/2003	Muranga	Kenya	37.1500	0.7060
243	Mbarara landslide	5/16/2003	Mbarara	Uganda	30.7500	-0.4167
244	Xiangjiang landslide	5/17/2003	Hunan	China	112.9500	27.1012
245	Dothupitiya landslide	5/17/2003	Ratnapura	Sri Lanka	80.6000	6.6855
246	Gandoh landslide	1/6/2008	Doda, Kashimir	India	75.5464	33.1517
247	Gedangan landslide	1/6/2008	Malang	Indonesia	112.6278	-7.9720
248	Karnataka landslide	8/9/2008	Karnataka	India	74.1100	15.1500
249	Edakumeri, landslide	8/10/2008	Subrahmanya	India	75.6050	12.6445
250	Monkey Hill landslide	8/10/2008	Maharashtra	India	73.4700	18.7200
251	Gaiparnath landslide	8/10/2008	Chambal ravines	India	75.7200	25.0800
252	Hamang landslide	8/10/2008	Ilam	Nepal	87.9190	26.9122
253	Hualoy landslide	8/11/2008	West Seram	Indonesia	128.4000	-3.3000
254	Yedakumeri landslide	8/12/2008	Hassan-Mangalore	India	75.6600	12.8450
255	Ayanur landslide	8/12/2008	Karnataka	India	75.4520	13.9860
256	Jog falls landslide	8/12/2008	Karnataka	India	74.8122	14.2290
257	Myawaddy landslide	8/13/2008	Karen State	Burma	97.9380	16.6240
258	Papum Pare landslide	8/14/2008	Arunachal	India	94.0000	27.1630
259	Shimla landslide	8/14/2008	Shimla, Mandi	India	77.1200	31.0000
260	Chandibhanjyag landslide	8/14/2008	Chitwan	Nepal	84.4320	27.7950
261	Riasi landslide	8/15/2008	Jammu and Kashmir	India	74.9277	33.0000
262	Luang Prabang landslide	8/15/2008	Luang Prabang	Laos	102.5160	18.0900
263	Bharta landslide	8/15/2008	Kalikot	Nepal	81.7557	29.1964
264	Bobadan landslide	8/16/2008	Mogoke	Burma	96.4800	22.9000
265	Portarlington landslide	8/16/2008	Portarlington	Ireland	-7.2068	53.1468

S.N.	Name	Date	Location	Provinance	Longitude	Lattitude
266	Sadi landslide	8/16/2008	Pyuthan	Nepal	82.8332	28.0993
267	Dong Thap landslide	8/16/2008	Dong Thap	Vietnam	105.5740	10.5780
268	Gathaithi landslide	11/3/2009	Murang	Kenya	37.2000	-0.4333
269	Gikingo landslide	11/3/2009	Imenti	Kenya	37.6561	0.0571
270	Kangema landslide	11/3/2009	Murang'a	Kenya	36.9667	-0.6833
271	Rawang landslide	11/3/2009	Kuala Lumpur	Malaysia	101.6352	3.2909
272	Templer's Park landslide	11/3/2009	Jalan Ipoh	Malaysia	101.6314	3.2971
273	Bukhel landslide	11/5/2009	Lalitpur	Nepal	85.3500	27.5000
274	Bac Tra My landslide	11/5/2009	Quang Nam	Vietnam	108.4671	15.5721
275	St Cyrus landslide	11/6/2009	Aberdeenshire	Scotland	-2.4170	56.7709
276	Sakhon landslide	11/6/2009	Narathiwat	Thailand	101.5081	6.1700
277	Jalan landslide	11/7/2009	Batu Caves	Malaysia	101.6826	3.2711
278	Moo 6 landslide	11/7/2009	Yala	Thailand	100.9417	6.8241
279	Kawthoung	10/2/2009	Tanintharyi	Myanmar	98.5465	9.9988
280	Puddipadi	10/3/2009	Kerala	India	75.9957	11.4816
281	Balussery	10/3/2009	Kerala	India	75.8289	11.4477
282	Kawthaung	10/3/2009	Tanintharyi	Myanmar	98.5465	9.9988
283	Benguet	10/3/2009	Benguet	Philippines	120.8512	16.5364
284	Ampukao	10/3/2009	Benguet	Philippines	120.6890	16.3452
285	Kyokyezo	10/3/2009	Kabale	Uganda	29.9821	-1.2509
286	Pardawaras	10/4/2009	Sedayu	Indonesia	104.4480	-5.5208
287	Sedayu	10/4/2009	Semaka	Indonesia	104.4842	-5.4721
288	Way Kerap	10/4/2009	Tanggamus	Indonesia	104.7608	-5.5160
289	Beckel	10/4/2009	Benguet	Philippines	120.5855	16.4564
290	Chhinga Veng	10/5/2009	Aizawl	India	92.7173	23.7374
291	Lower Kitma	10/5/2009	Baguio City	Philippines	120.5970	16.4020
292	Su-hua Highway	10/5/2009	Yilan	Taiwan	121.7195	24.6929
293	western Bhutan	10/6/2009	Western Bhutan	Bhutan	90.4997	27.0524
294	Dadeldhura	10/6/2009	Dadeldhura	Nepal	80.6750	29.2833
295	Shera	7/1/2009	Mugu	Nepal	82.5068	29.7225
296	Dhapade	7/2/2009	Tanahun	Nepal	84.2279	27.9447
297	Damauli	7/2/2009	Tanahun	Nepal	84.2805	27.9586
298	Deurali	7/2/2009	Kaski	Nepal	83.9806	28.2039
299	Umlazi	2/6/2009	Durban	South Africa	30.8660	-29.9540
300	Abidjan	6/12/2009	Abidjan	Ivory Coast	-4.0276	5.3363